EVALUATION OF PRESENT LEGISLATION AND REGULATIONS ON TIRE SIZES, CONFIGURATIONS AND LOAD LIMITS

59.1

Final Draft

by

Jatinder Sharma
John Hallin
and
Joe P. Mahoney

Prepared by the
University of Washington

for the

Washington State Transportation Commission
Department of Transportation
and in Cooperation with
U.S. Department of Transportation
Federal Highway Administration

WSDOT Contract Agreement Y-2292

July 1983

TECHNICAL REPORT STANDARD TITLE PAGE

1. Report No.	2. Government Accession No.	3. Recipient's Catalog No.

4. Title and Subtitle
Evaluation of Present Legislation and Regulations on Tire Sizes, Configurations and Load Limits

5. Report Date
July 1983

6. Performing Organization Code

7. Author(s)
Jatinder Sharma, John Hallin and Joe P. Mahoney

8. Performing Organization Report No.

9. Performing Organization Name and Address
University of Washington
Department of Civil Engineering
Seattle, WA 98195

10. Work Unit No.

11. Contract or Grant No.
WSDOT Y-2292

12. Sponsoring Agency Name and Address
Washington State Department of Transportation
Highway Administration Building
Olympia, WA 98504

13. Type of Report and Period Covered
Final Report

14. Sponsoring Agency Code

15. Supplementary Notes
WSDOT Contract Manager - Mr. Art Peters

16. Abstract

This report describes the techniques used to evaluate the effects of various axle configurations with dual and single tires on pavement performance and the current State of Washington Regulation RCW 46.44.042. Equivalent wheel load factors were developed for various widths of single tires on both rigid and flexible pavements. Single tires with widths 10 to 18 inches were analyzed and it was found that by equivalent axle loads the predicted damage to pavements was greater for axles with single tires than those with dual tires.

To verify the theoretical analyses, two field experiments were conducted. First, extensometers were placed in the outer wheelpath of the pavement ramp at the Fife I-5 weigh station. Truck induced pavement surface deflections were measured after the vehicles were weighed on the scale. A comparison of measured and calculated deflections revealed good agreement thus in part verifying the theoretically based calculations. Second, a field site near Edmondton, Alberta was also used in the verification process by use of the WSDOT Falling Weight Deflectometer. Again the theoretical approach was further verified.

17. Key Words	18. Distribution Statement
Regulation, Tire, Axle, Single Tires, Dual Tires, Single Axle, Tandem Axle, Tire Width	No restrictions. This document is available to the public through the National Technical Information Service, Springfield, Virginia 22161.

19. Security Classif. (of this report)	20. Security Classif. (of this page)	21. No. of Pages	22. Price

Form DOT F 1700.7 (8--69)
HWY FORM 341-004 6/72

TABLE OF CONTENTS

TABLE OF CONTENTS (Cont.)

ACKNOWLEDGMENTS

We would like to express our appreciation to Messrs Newt Jackson, Art Peters, Carl Toney and Joe Bell of the Materials and Research Offices of the Washington State Department of Transportation for their continual support and assistance in the completion of this study.

We would also like to thank the Alberta Research Council for their assistance in allowing us to use their data and in allowing us to test their test sections with the Falling Weight Deflectometer.

LIST OF FIGURES

LIST OF FIGURES (Cont.)

LIST OF FIGURES (Cont.)

LIST OF FIGURES (Cont.)

LIST OF FIGURES (Cont.)

LIST OF FIGURES (Cont.)

LIST OF TABLES

LIST OF TABLES (Cont.)

LIST OF TABLES (Cont.)

TABLE OF CONTENTS (Cont.)

The contents of this report reflect the views of the authors who are responsible for the facts and the accuracy of the data presented herein. The contents do not necessarily reflect the official views or policies of the Washington State Transportation Commission, Department of Transportation or the Federal Highway Administration. This report does not constitute a standard, specification, or regulation.

INTRODUCTION

The increased use of single tires in lieu of dual tires has led to a concern over whether current Washington Department of Transportation regulations accurately consider the relative effects of single and dual tires on pavement performance. This report describes both analytical and field studies which were used to compare the damaging effects of axles with various widths of single tires and axles with dual tires.

The objective of the study was to develop techniques for evaluating the effects of various axle configurations with dual and single tires on pavement performance. By use of the techniques developed, evaluate current State of Washington regulations pertaining to tire sizes, configurations, and recommend changes, if required. The principle regulation evaluated was The Revised Code of Washington (RCW) 46.44.042: "Maximum gross weights - tire factor ... it is unlawful to operate any vehicle upon the public highways with a gross weight, including load, upon any tire concentrated upon the surface of the highway in excess of 550 lbs per inch width of such tire, up to a maximum width of 12 inches and for a tire having a width of 12 inches of more there shall be allowed a 20 percent tolerance above 550 lbs per inch width of such tire".

Study Approach

A separate analysis was made for rigid and flexible pavements using existing finite element and elastic layer computer programs to calculate stresses and strains in the pavement sections under various tire loads. The calculated stresses and strains were then used to determine the fatigue life of the pavement under these loads. Dual tires with a width of ten inches and a center to center spacing of 15 inches and single tires with widths of 10, 12, 14, 16, and 18 inches were used in the analysis.

Equivalency relationships were developed between single and dual tires based on their relative fatigue lives. The equivalency relationships between single and dual tires were then compared with RCW 46.44.042 to determine if the regulation adequately considered the relative damage effect of single tires. The study approach is outlined in Figure 1.

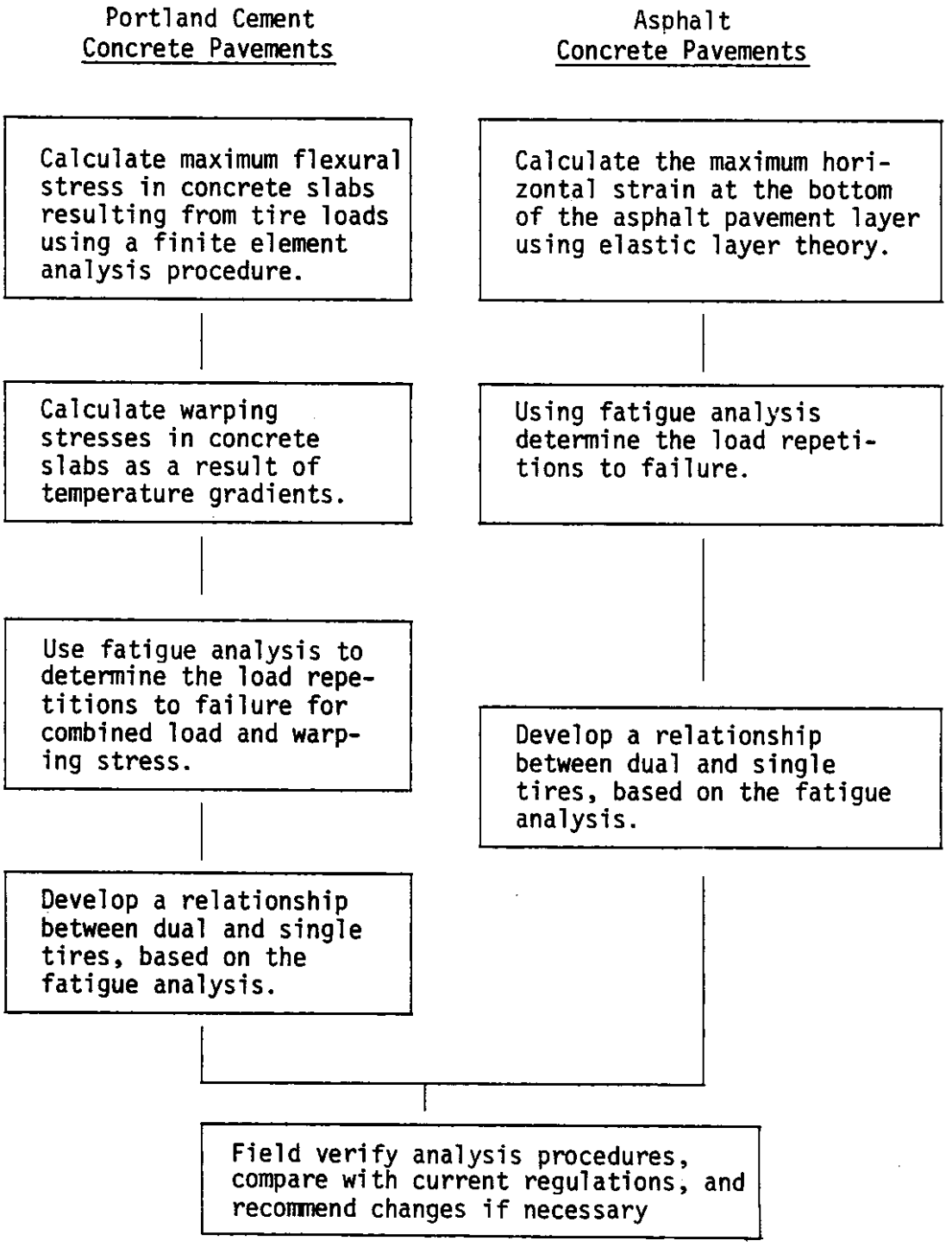

Figure 1. Study Approach

Report Organization

The report contains four chapters and a series of appendices. Chapter 1 overviews the theoretical analysis of portland cement concrete pavements, Chapter 2 is a similar treatment for asphalt concrete pavements, Chapter 3 is used to discuss the two field sites used in the verification process, and Chapter 4 the study conclusions and recommendations.

CHAPTER 1

PORTLAND CEMENT CONCRETE PAVEMENTS

General

This chapter describes the development of a load equivalency relationship between axles with single and dual tires, for concrete pavements. The relationship is based on a comparison of the fatigue damage which results from repetitions of predicted tensile stresses occurring in the pavement. Stresses in concrete pavements result primarily from two sources, traffic loads and temperature gradients within the pavement. The magnitude of these stresses is a function of the pavement section, material properties of the concrete, joint design, and subgrade support. Load and temperature stresses were calculated for the range of conditions generally expected to occur in the State of Washington.

Pavement Design Standards

In Washington nearly all recently constructed portland cement concrete (PCC) pavements on the State system are nine inches thick. The concrete is placed on a subbase of gravel or asphalt treated base four inches or more in thickness. Increased truck volumes on Interstates 5 and 90 may necessitate the use of thicker pavement sections for future construction on these routes. Also, with the increases in asphalt cement prices in recent years, concrete has become increasingly more competitive for lower volume primary routes. Slabs with thicknesses ranging from 7 inches to 11 inches have been used by adjacent states. Therefore, for this study pavement thicknesses of 7 to 12 inches were considered.

Washington does not place reinforcing steel in PCC pavement and dowels are not used in transverse contraction joints. Aggregate interlock is assumed to provide load transfer acress the joints. The transverse contraction joints are skewed counterclockwise at a ratio of 2:12, with a random spacing of 9, 10, 14 and 13 feet. A joint spacing of 13 feet, with aggregate interlock was used for this study.

Material Properties

Concrete for PCC pavements is designed to have a modulus of rupture

of at least 650 psi when opened to traffic. The modulus of rupture, as determined by the use of a simple beam with center-point loading, is generally in excess of 700 psi. For analysis purposes, a modulus of rupture of 750 psi was used. This value was selected to account for the initial test values plus the increase of strength expected during the design life of the pavement. The concrete was assumed to have a modulus of elasticity of 4.5×10^6 psi and a Poisson's ratio of 0.15.

The support given to concrete pavements by the subgrade and subbase is generally estimated in terms of the modulus of subgrade reaction (K). In the original development of the theoretical stress determination in PCC slabs, it was assumed that the reactions of the subgrade were vertical only and proportional to the deflections of the slab, the reaction per unit area at a given point being the product of the deflection at that point and a coefficient of subgrade stiffness, which was termed the modulus of subgrade reaction. This modulus is normally expressed in pounds per square inch per inch of deflection [22]. The test procedure for determining the modulus of subgrade reaction calls for applying a load to a 30 inch diameter plate and measuring the deflection. The modulus of subgrade reaction is equal to the load in pounds per square inch divided by the deflection of the plate in inches. Since the direct measurement of the modulus of subgrade reaction is expensive and time consuming, approximate values are generally used, which are a function of other test procedures. Washington estimates the modulus of subgrade reaction from stabilometer R-values using Figure 2. Figures 3 and 4 are then used to adjust the subgrade K for subbase to arrive at a K-value for use in pavement design. K-values of 100 pci and 300 pci were selected for the analysis, as being representative of the range of values generally expected in Washington.

Analysis of Load Stresses

Load related stresses in concrete pavements were determined using the ILLI-SLAB finite element computer program [18]. The analysis procedure in this program is based on the theory of a medium thick elastic plate on a Winkler foundation. This program can be used to analyze PCC pavements having joints or cracks with various types of load transfer

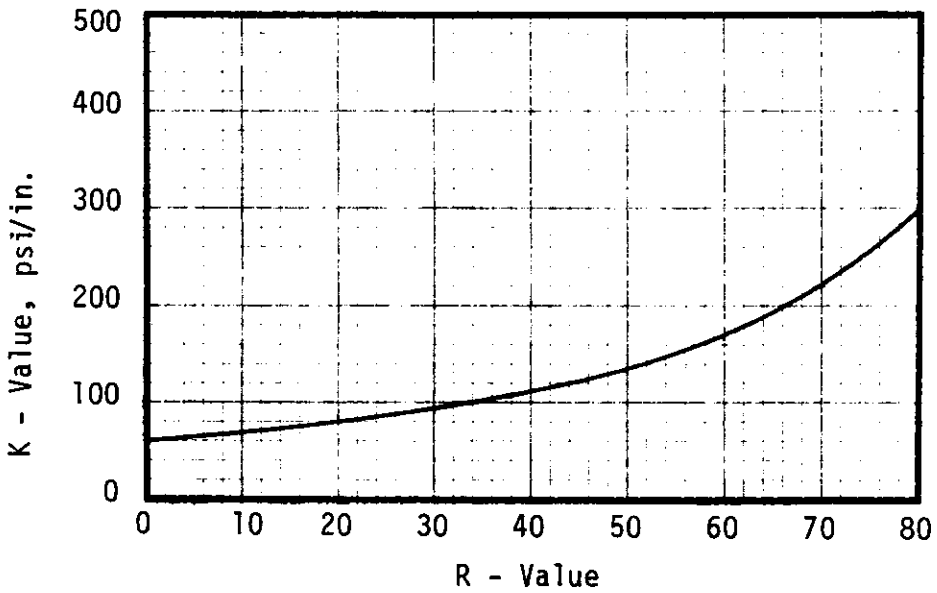

Figure 2. Approximate Relationship Between the Modulus of Subgrade Reaction (K) and Stabilometer R - Value [14]

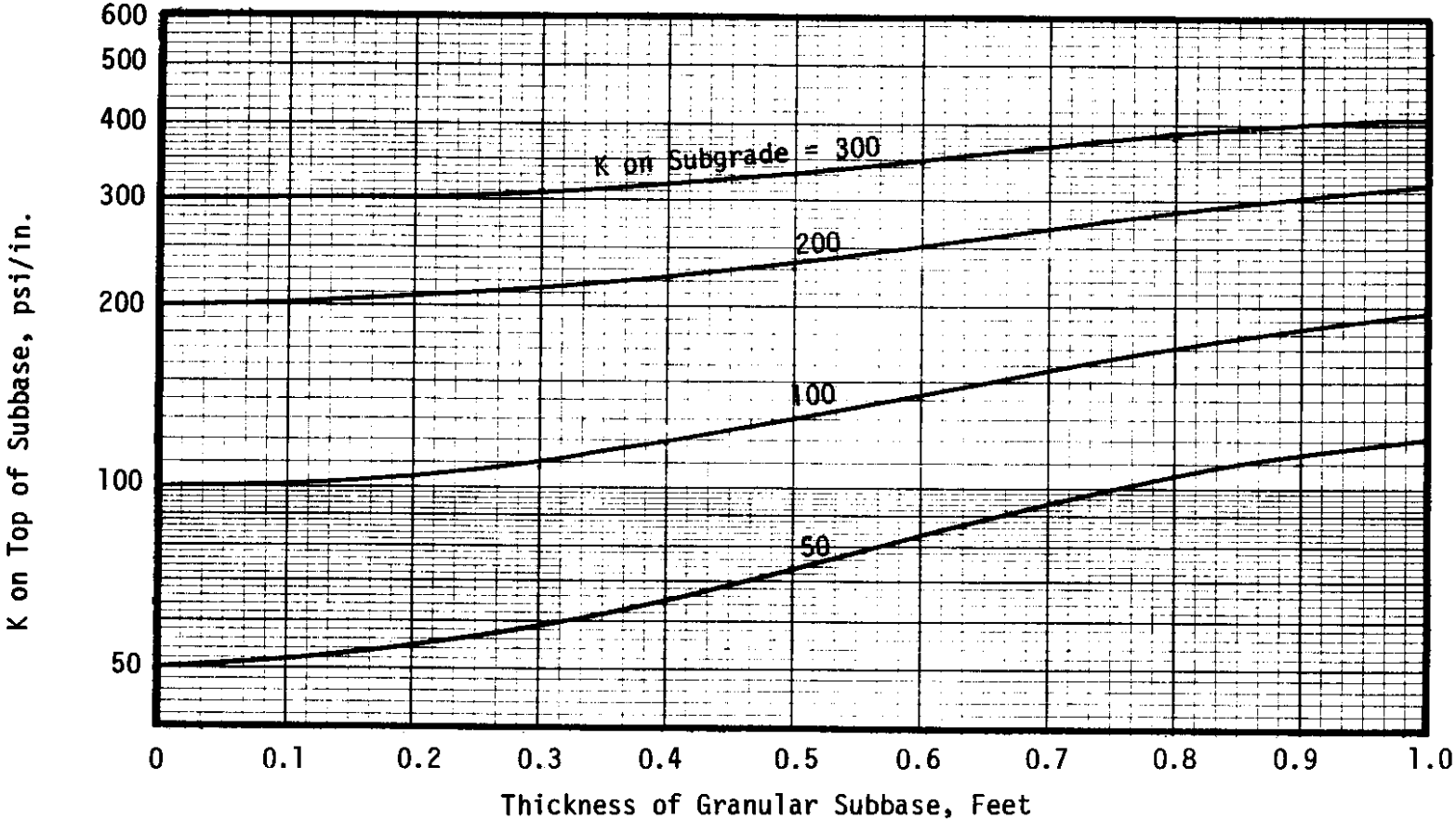

Figure 3. Estimated Modulus of Subgrade Reaction (K) at the Top of a Granular Subbase [4]

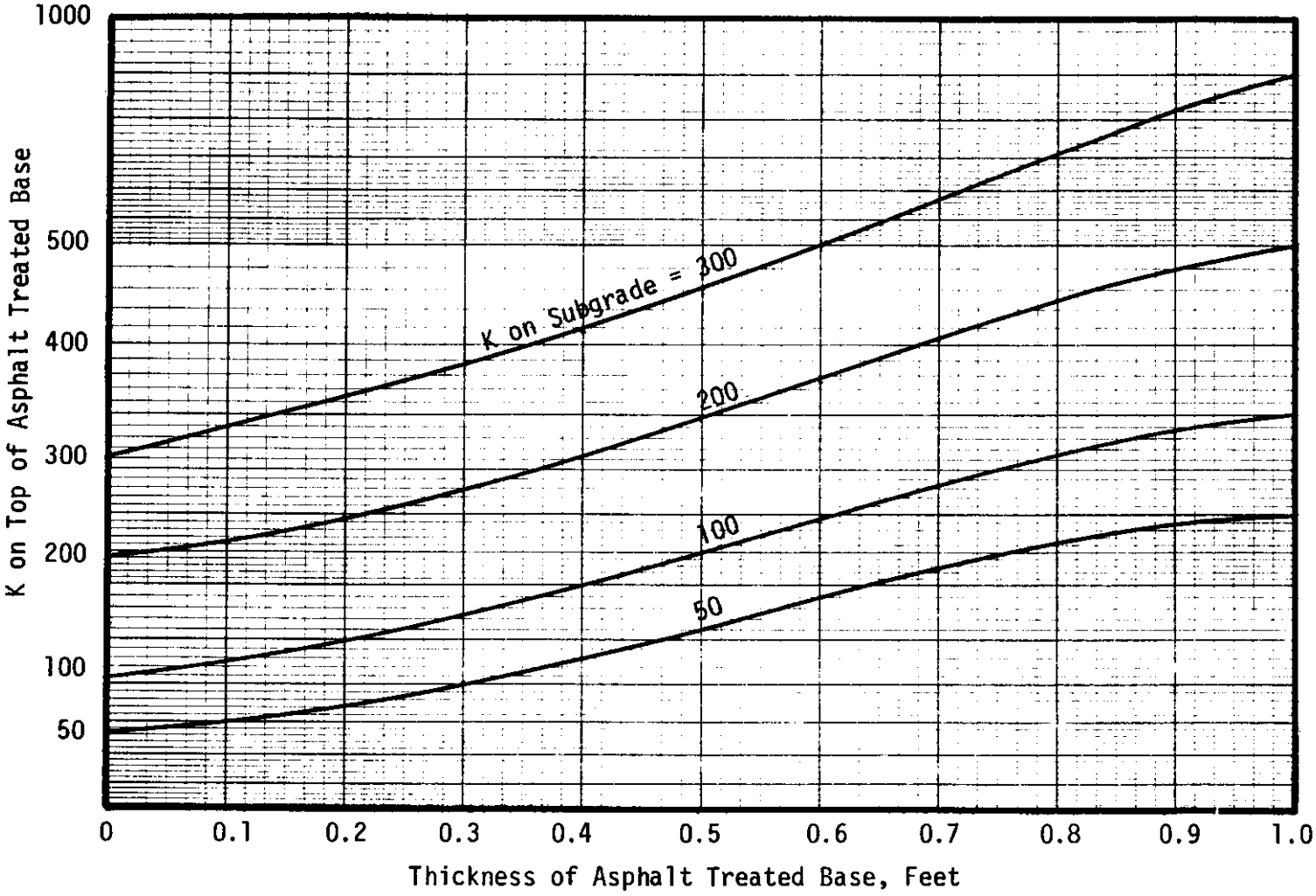

Figure 4. Estimated Modulus of Subgrade Reaction (K) at the Top of an Asphalt Treated Base [14]

systems, such as dowel bars, reinforcement steel, aggregate interlock, or key ways.

The concrete pavement to be analyzed can consist of 1, 2, 3, 4 or 6 slabs with a maximum of one longitudinal and two transverse joints. Wheel loads are applied through uniformly loaded rectangles. The following are input into the program: slab sizes, factor for bond or lack of bond with the base, modulus of subgrade reaction, pavement thickness, modulus of elasticity of the concrete, Poisson's ratio of the concrete, location of the tire load, dimensions of load contact area, contact pressure, and type of load transfer at the joints.

Tabatabaie and Barenberg [17] compared the solutions obtained using the ILLI-SLAB program with results of theoretical solutions and experimental studies. These included Westergaard's equations, Pickett's and Ray's influence charts, AASHTO road test data and Teller and Sutherland's work at the Arlington Test Farm. These comparisons show the ILLI-SLAB program solutions agree closely with both the theoretical and experimental results.

There are a large number of variables which affect the stresses in concrete pavement. As a first step in the study, the variables which had the greatest effect on tensile stresses in the pavement slab were indentified. This analysis was made using the maximum legal axle loads of 20,000 lbs for single axles and 34,000 lbs for tandem axles. Tire widths were based on the regulatory requirement of a maximum tire load of 550 lb per inch of width for tires less than 12 inches wide and 660 lb per inch of width for tires 12 inches or greater in width.

Since the loaded area is a rectangle, the transverse dimension was the tire width and the longitudinal dimension varied depending on the axle load. The tire contact pressure was 80 psi.

The initial phase of the analysis consisted of determining the magnitude of the horizontal stresses in the concrete pavement for single and tandem axles at four separate load positions. The axle configurations examined were: Case I, a single axle with dual 10-inch tires; Case II, a single axle with single 16-inch tires; Case III, tandem axles with 10-inch dual tires; and Case IV, tandem axles with single 13-inch tires.

Four load positions were analyzed: (A) at the joint with the vehicle centered in the lane; (B) at the joint with the right wheel at the pavement edge; (C) at the midpoint of the slab with the right wheel at the pavement edge; and (D) at the midpoint of the slab with the right wheel 12 inches from the pavement edge. Since the program did not permit skewed joints, the loads were offset to simulate skewed joints for A and B. The Cases are shown in Figures 5 through 8. The results clearly showed that the mid-panel edge loadings were the most critical cases. For single axles, the maximum tensile stresses for positions A, B and D were approximately 30, 40 and 75 percent of position C, respectively. While for tandem axles, the maximum tensile stresses for positions A and B were approximately 40 and 65 percent of position C, respectively. The maximum tensile stress for the critical cases were located at the bottom of the mid-panel edge of the slab.

The sensitivity of load related stresses to variations in tire pressure, single tire width, and joint spacing were analyzed. This analysis was made using a single axle, mid-panel edge load, 9-inch pavement and a modulus of subgrade reaction equal to 100.

Tire pressures of 70, 80, 90 and 100 psi were analyzed for both 10-inch dual tires and 16-inch single tires. The results, shown in Figure 9, indicate that the variation in edge stress is about one percent for pressures between 70 and 100 psi. Therefore, within the range of tire pressures normally encountered there is a negligible effect on the resulting pavement stresses.

The effects of tire width were analyzed using a 20 kip axle load with 10, 12, 14, 16 and 18 inch wide single tires. The results, shown in Figure 10, indicate a definite relationship between tire width and pavement stresses.

Joint spacings of 13, 15 and 20 feet were analyzed to determine the effect of joint spacing on pavement edge stress. The results, presented in Figure 11, indicate a maximum variation in calculated maximum edge stress of less than three percent.

Based on the preceding analysis, the following decisions were made relative to the computation of wheel load stresses:

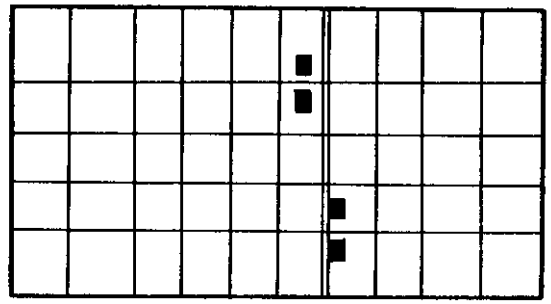

Position A

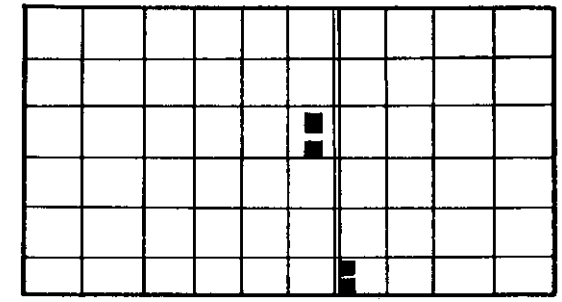

Position B

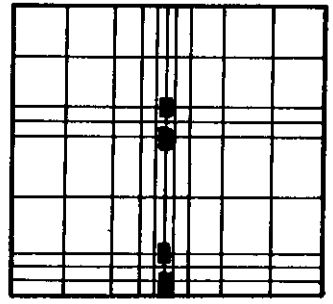

Position C

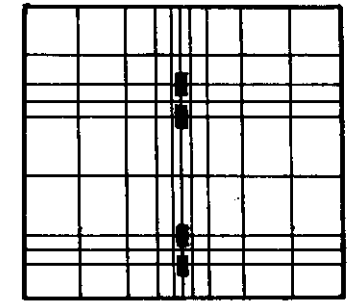

Position D

Figure 5. Loading Case I, Single Axle with Dual 10-inch Tires

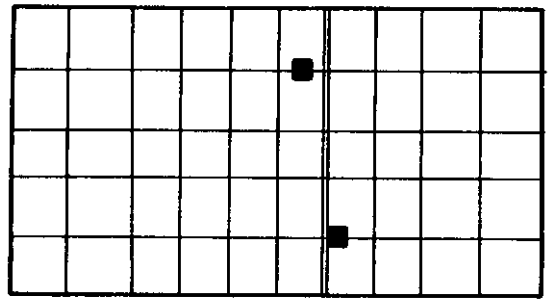

Position A

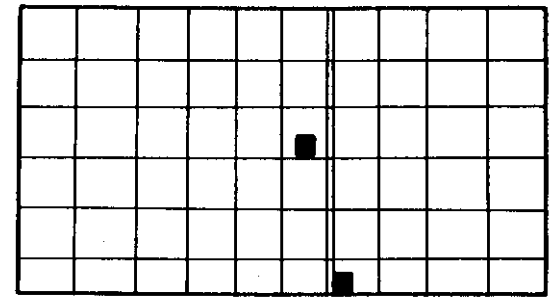

Position B

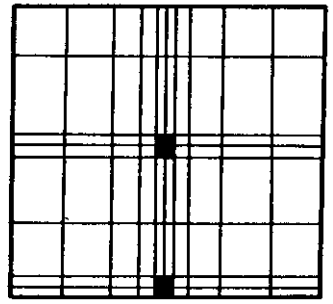

Position C

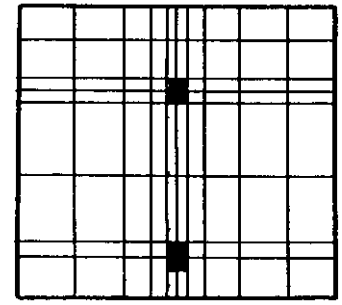

Position D

Figure 6. Loading Case II, Single Axle with Single Tires

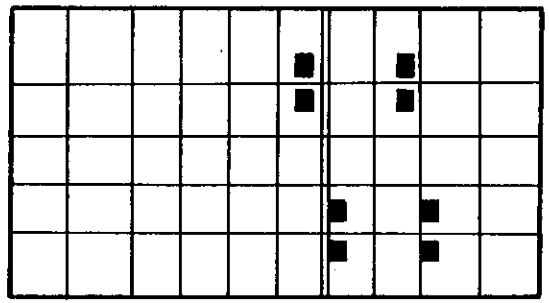

Position A

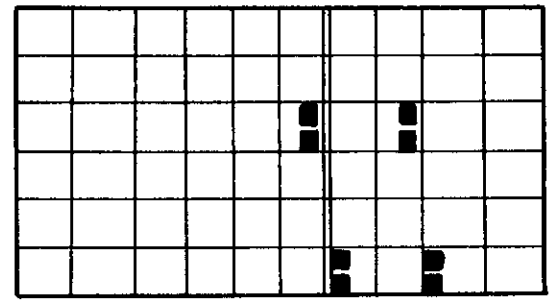

Position B

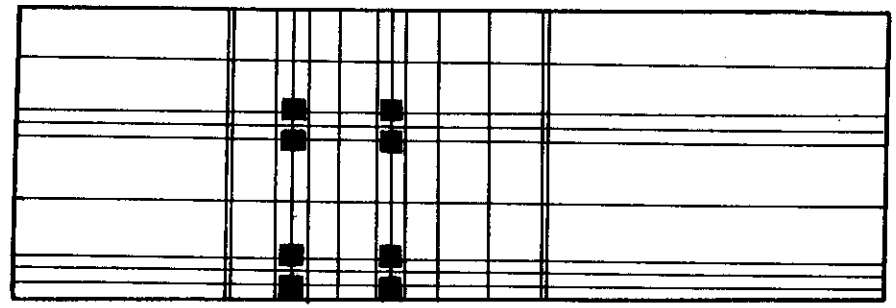

Position C

Figure 7. Loading Case III, Tandem Axle with Dual 10-inch Tires

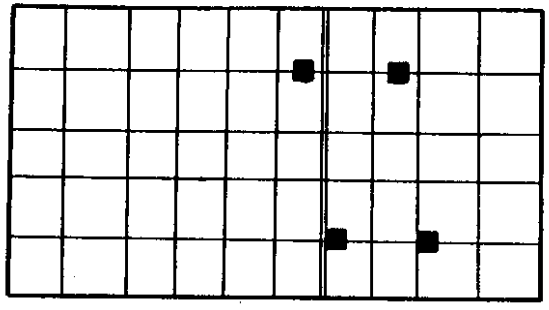

Position A

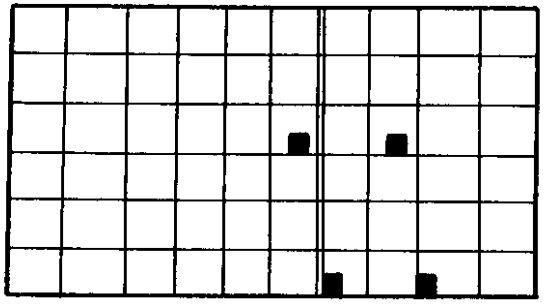

Position B

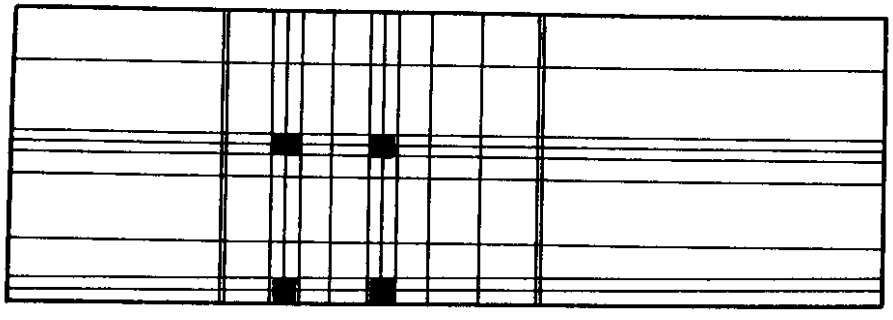

Position C

Figure 8. Loading Case IV, Tandem Axle with Single Tires

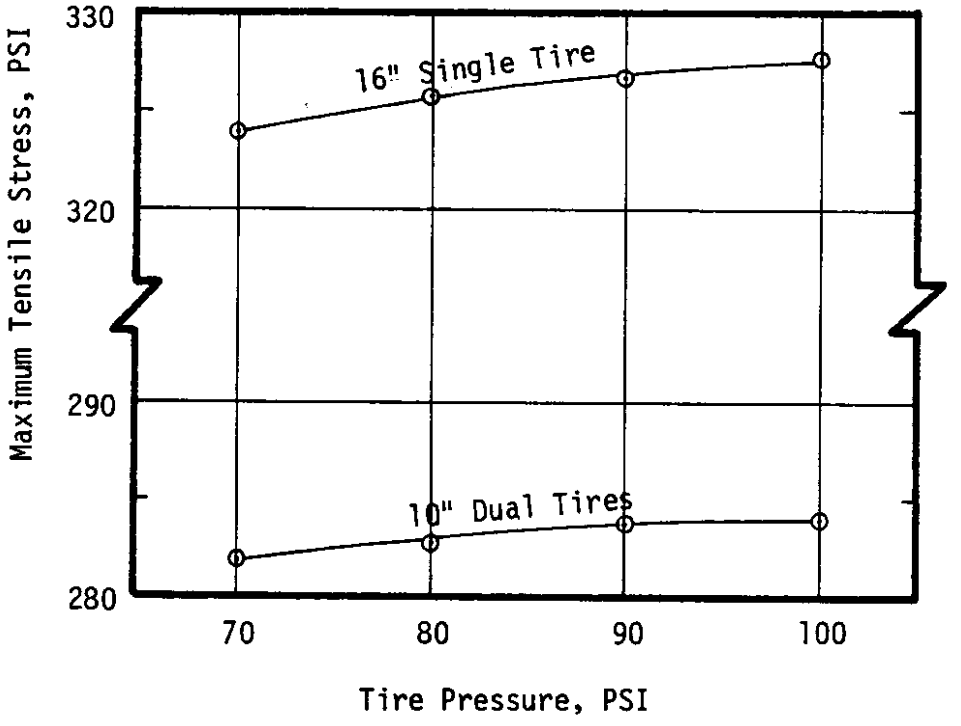

Figure 9. Effect of Variations in Tire Pressure on Edge Stress

Figure 10. Effect of the Width of a Single Tire on Edge Stress (20,000 lb. axle load)

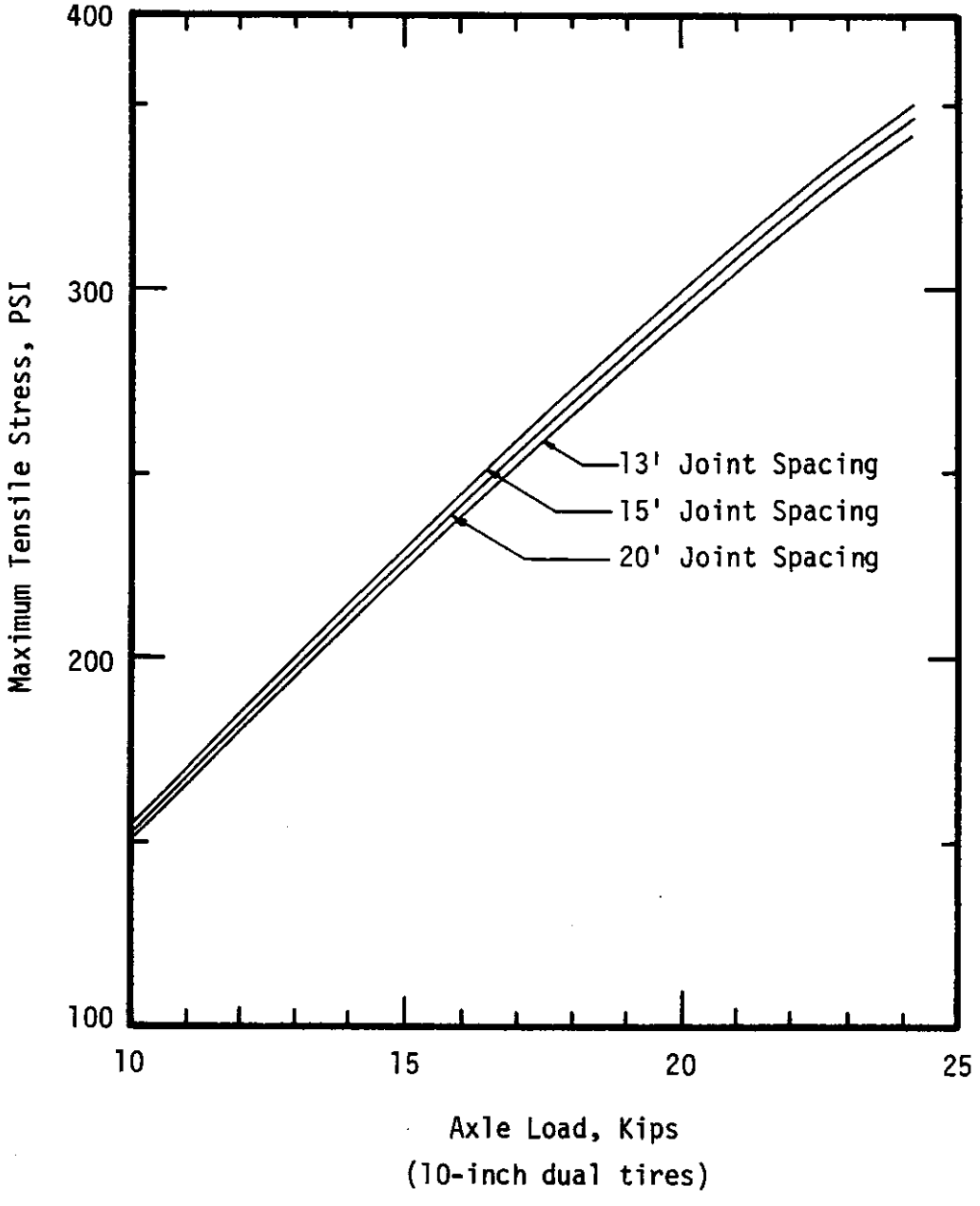

Figure 11. Effect of Joint Spacing on Load-Related Edge Stresses

1. Mid-panel edge loadings, Cases IC, IIC, IIIC and IVC are the most critical and were selected for used in this analysis. For purposes of analysis, selection of the most critical condition was considered reasonable. Darter reported [5] that there are a significant portion of the loads near the pavement edge.

2. A constant contact tire pressure of 80 psi would be used.

3. The effects of 10, 12, 14, 16 and 18 inch wide single tires would be considered.

4. All load stress computations would be made using a joint spacing of 13 feet.

Figures 12 through 17 are plots of the maximum edge stresses for single and tandem axles on 7, 9 and 12 inch thick concrete pavements. Figure 18 shows the maximum stresses when the wheel is offset 12 inches from the edge.

Analysis of Warping Stresses in Concrete Pavement

Differences in temperature between the top and bottom surfaces of a concrete slab will cause the slab to warp. If the slab was free to move, no stresses would develop. However, the weight of the slab and its intimate contact with the subbase restrict its movement and stresses are developed.

Measurements by Teller and Southerland of the Bureau of Public Roads [20] show that the maximum temperature differential that causes warping is much larger during the day than during the night. Furthermore, during the daytime the upper surface of the pavement is at a higher temperature than the bottom of the pavement putting tensile stresses at the bottom of the slab. This is important because the maximum load related tensile stresses also occur at the bottom of the pavement slab.

To evaluate the tensile stresses which develop in the concrete slab during the daytime, the temperatures at the top and bottom of the slab must be computed. A procedure which is commonly used is to calculate the mean monthly daytime gradient using Weather Bureau data [5, 11].

The pavement temperature calculations for this study were made using a procedure developed by Barber [2]. The procedure uses the following

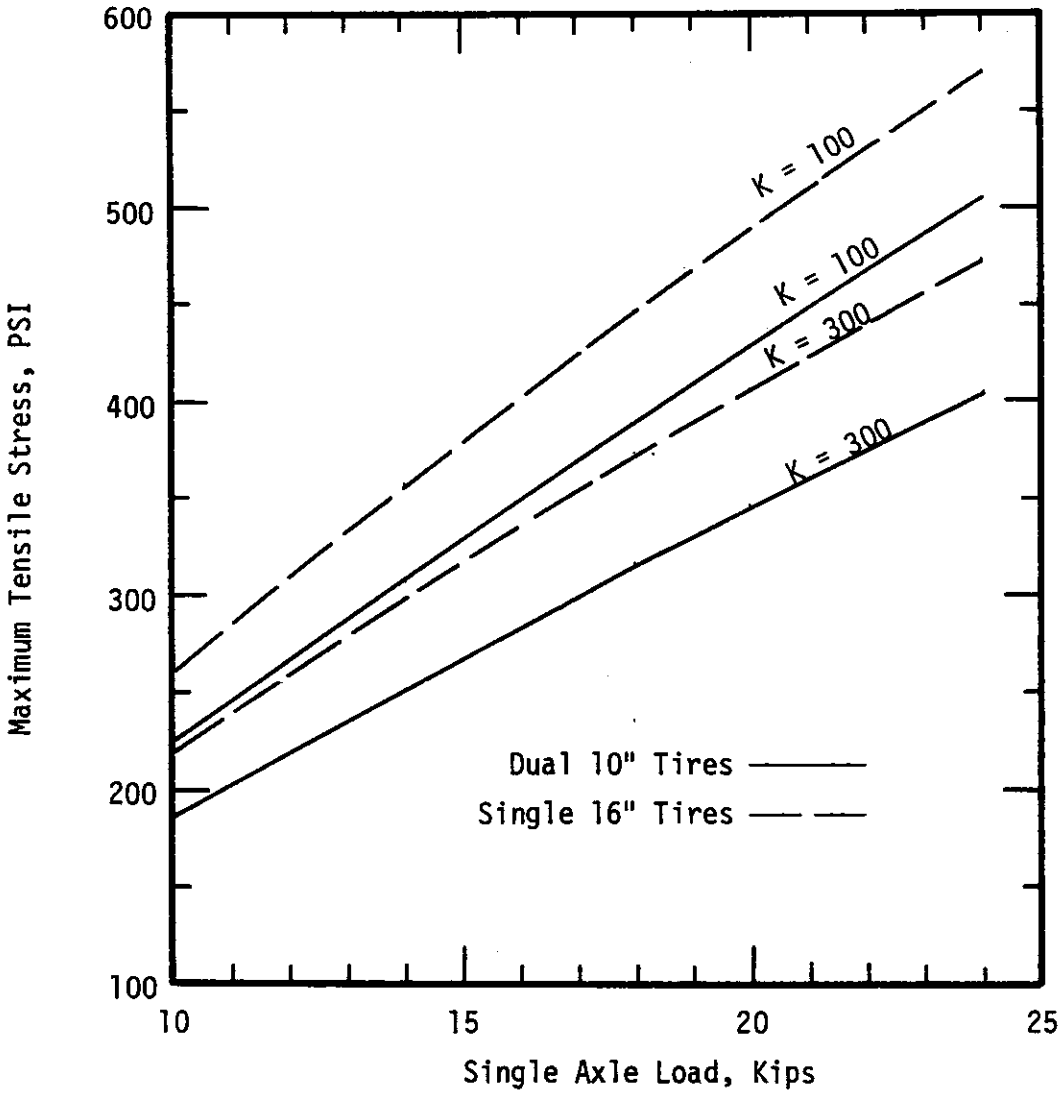

Figure 12. Edge Stress Versus Single Axle Load for 7-inch Pavements, Loading Cases I-C and II-C

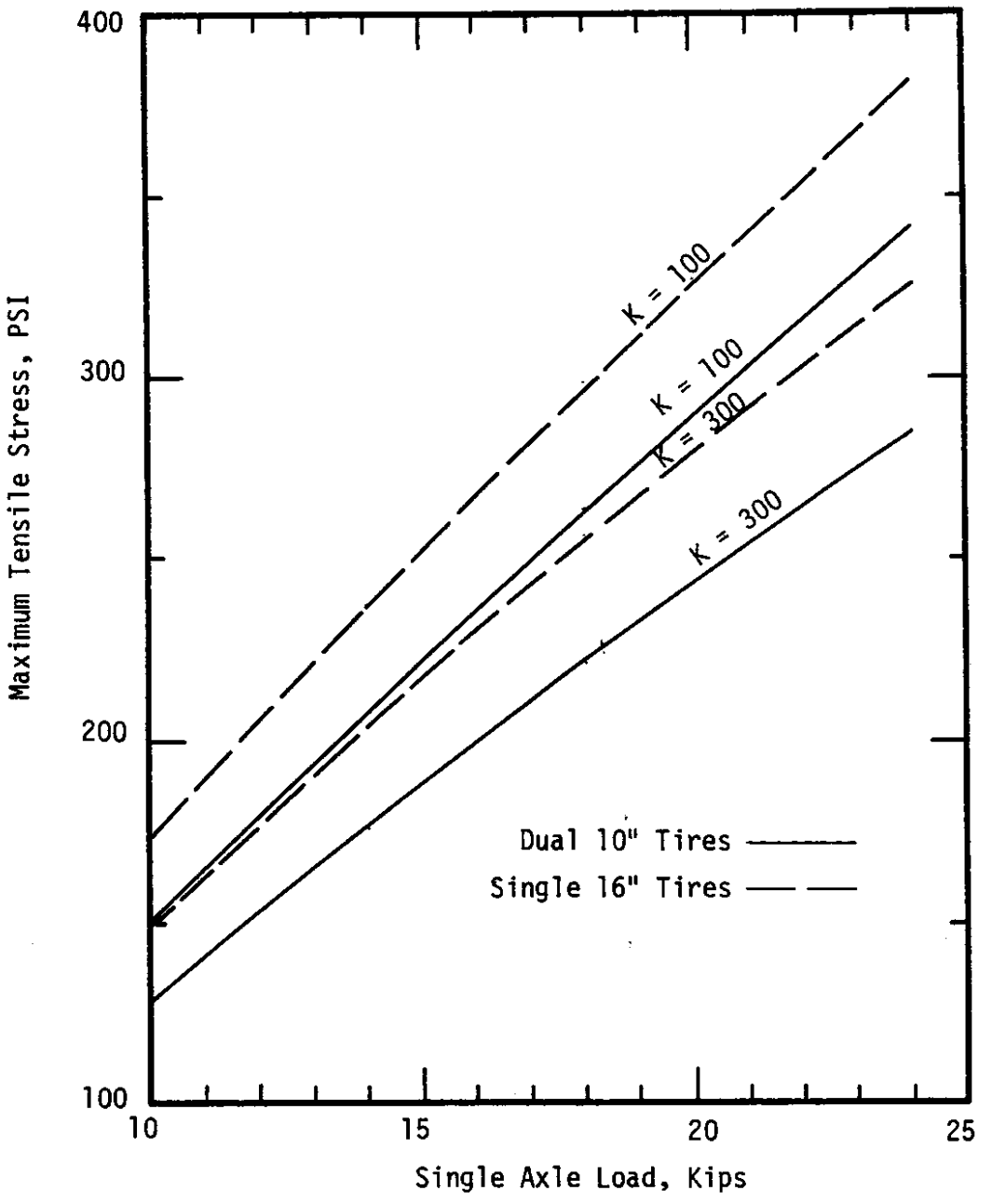

Figure 13. Edge Stress Versus Single Axle Load for 9-inch Pavements, Loading Cases I-C and II-C

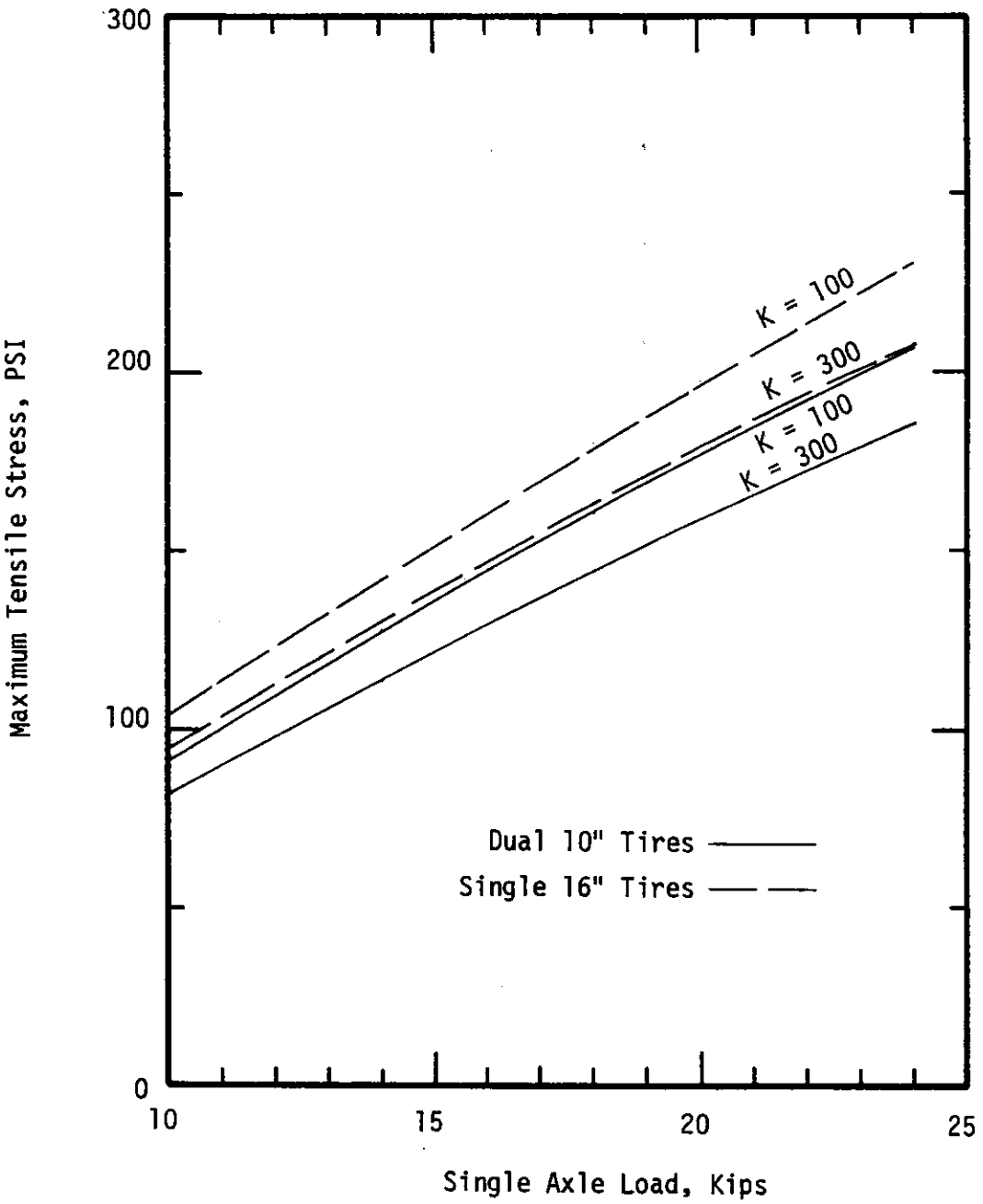

Figure 14. Edge Stress Versus Single Axle Load for 12-inch Pavements, Loading Cases I-C and II-C

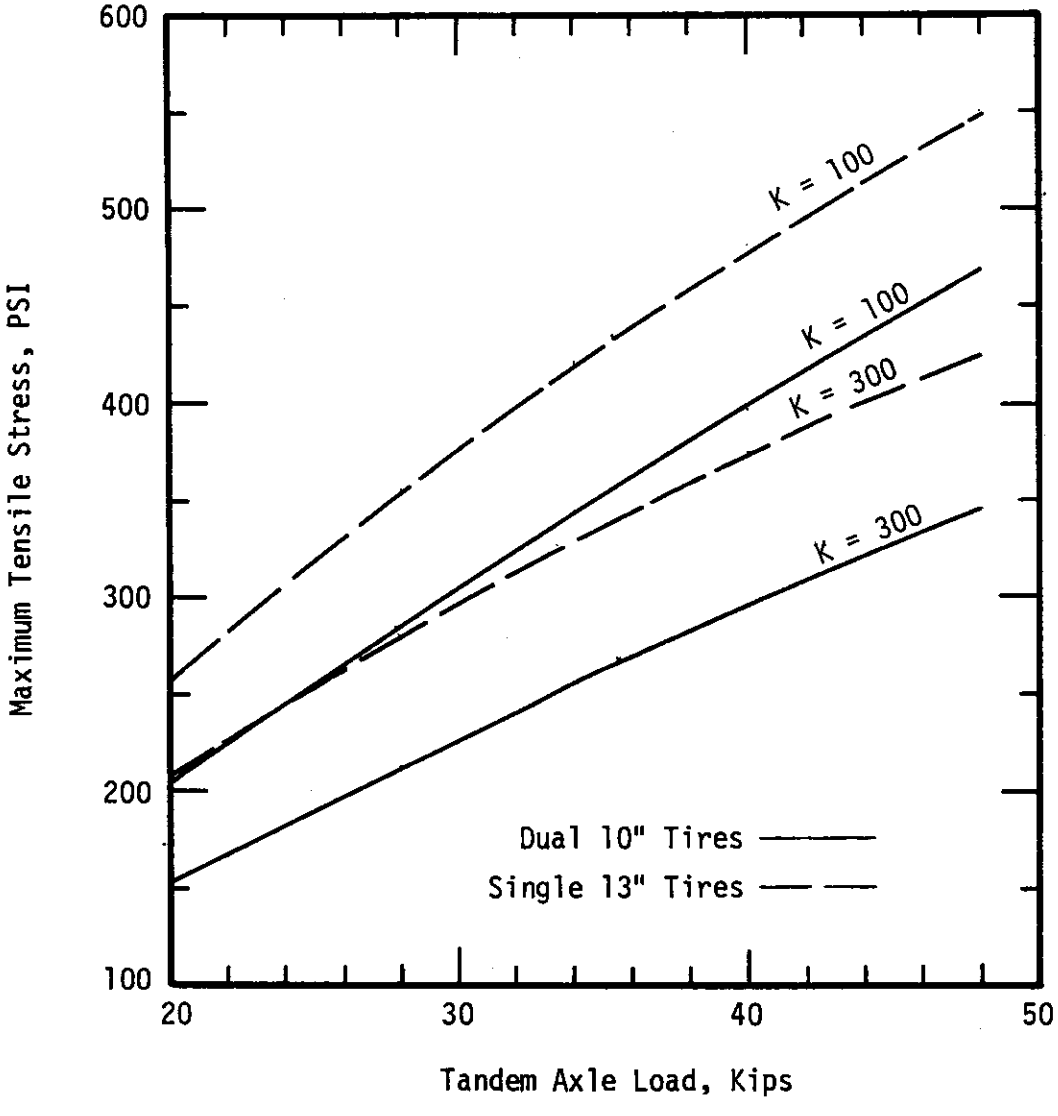

Figure 15. Edge Stress Versus Tandem Axle Load for 7-inch Pavements, Loading Cases III-C and IV-C

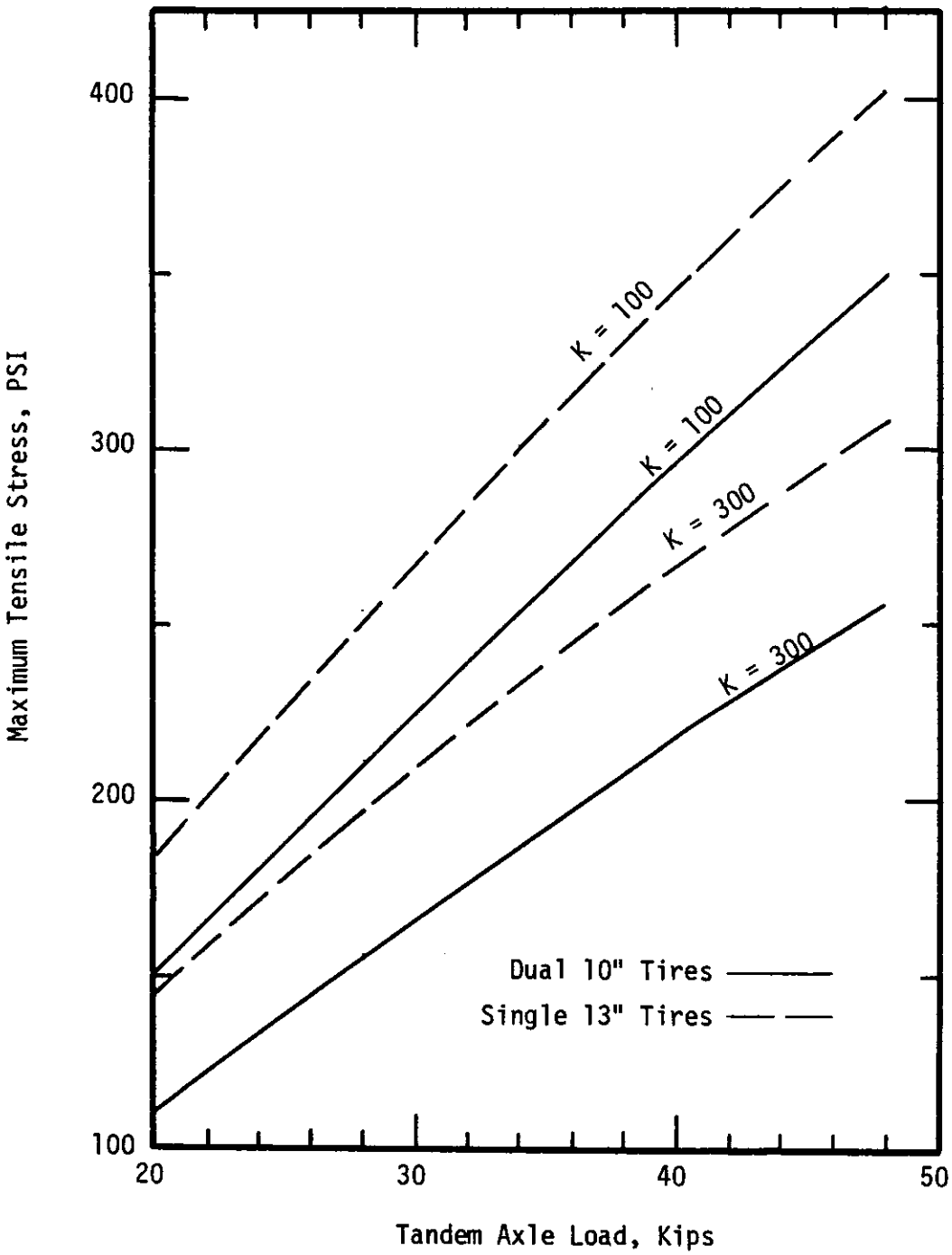

Figure 16. Edge Stress Versus Tandem Axle Load for 9-inch Pavements, Loading Cases III-C and IV-C

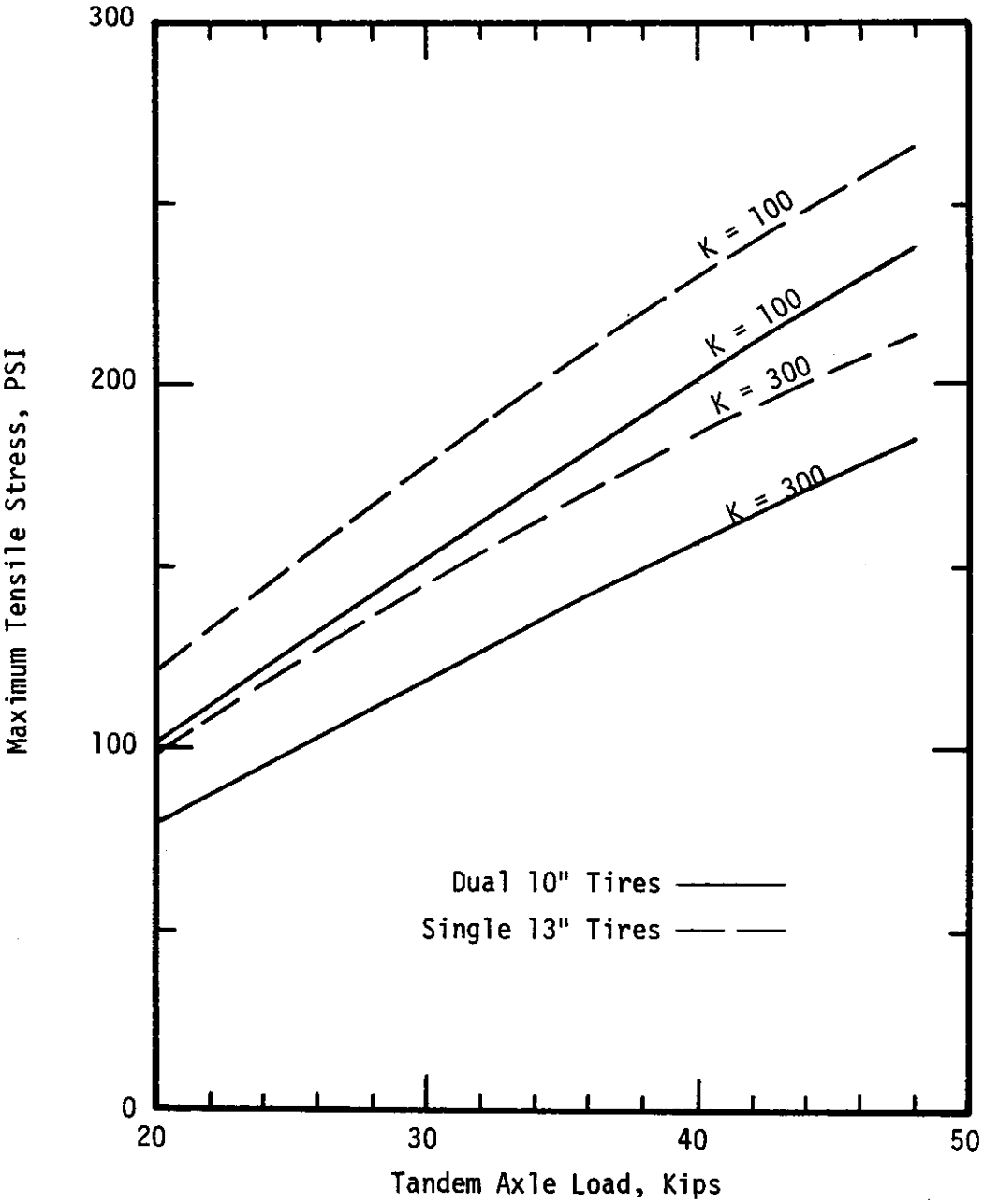

Figure 17. Edge Stress Versus Tandem Axle Load for 12-inch Pavements, Loading Cases III-C and IV-C

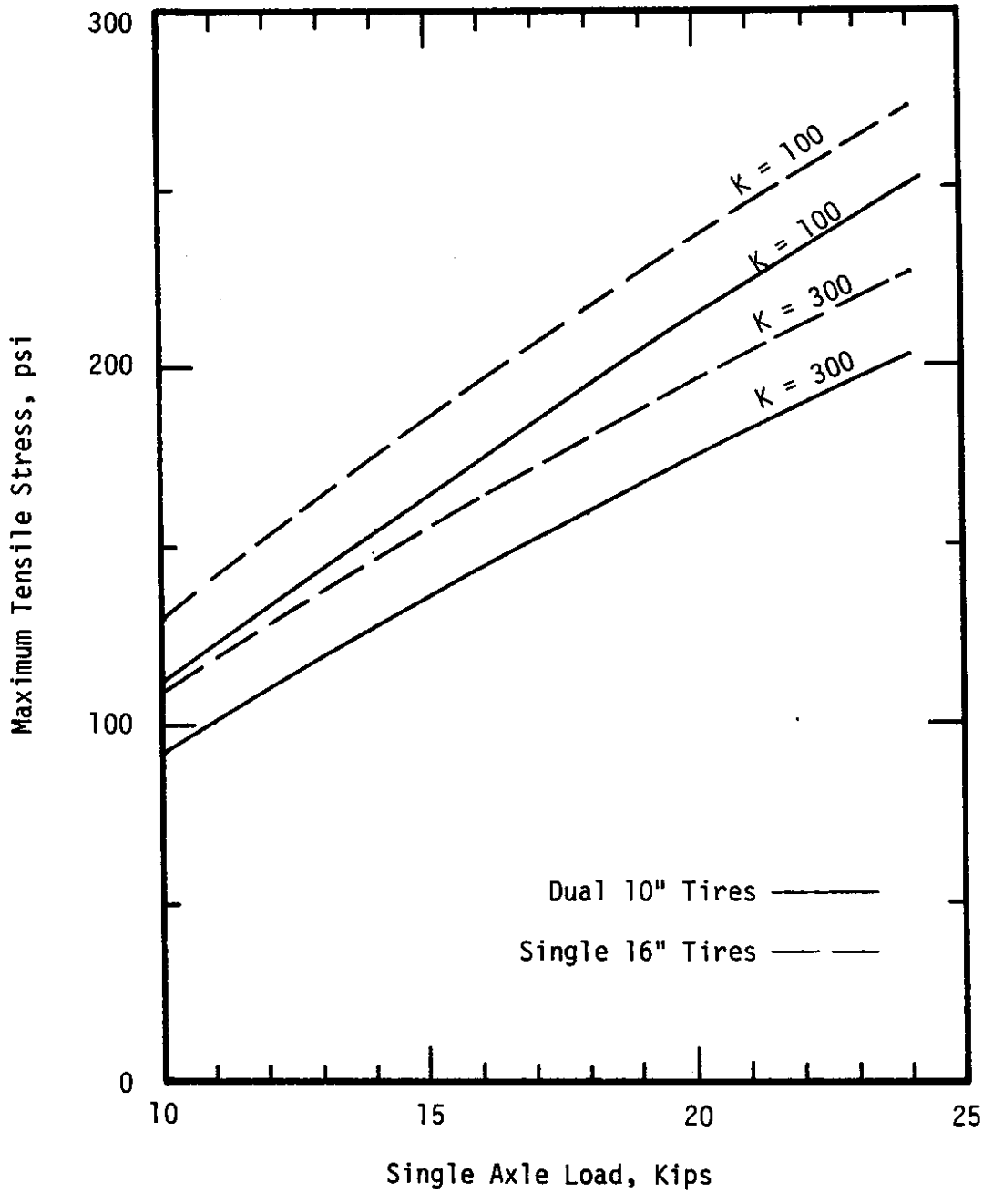

Figure 18. Edge Stress Versus Single Axle Load for 9-inch Pavements, Loading Cases I-D and II-D (load 12-inches from the pavement edge)

relationship between pavement temperature and wind, precipitation, air temperature, and solar radiation, as controlled by the thermal properties of the pavement.

$$T = T_A + R + \frac{He^{-Xc}}{[(H + C)^2 + C^2]^{\frac{1}{2}}} (0.5\ T_R + 3R) \quad \text{.....(1)}$$

where T = temperature of the pavement at a specified depth, °F

T_A = average air temperature, °F

R = average contribution to effective air temperature by solar radiation

$R = 0.67\ (b)(\frac{D}{24 \times h})$

b = absorptivity of surface to solar radiation

b ≃ 0.65 for portland cement concrete

b ≃ 0.95 for black surface

D = mean daily solar radiation, BTU/sq. ft.

h = surface coefficient, BTU per sq. ft. per hour, °F

h ≃ 4.4 for exposed area

H = h/k

k = conductivity, BTU per sq. ft. per hour, °F per ft.

k ≃ 0.9 for portland cement concrete

k ≃ 0.7 for asphalt cement concrete

X = depth below surface in <u>feet</u>

$C = (0.131/c)^{\frac{1}{2}}$

c = diffusivity, ft. sq. per hour = $\frac{K}{sw}$

s = specific heat, BTU per pound °F

s ≃ 0.2 portland cement concrete

s ≃ 0.22 dry stone plus asphalt

w = density of material, pounds per cu. ft.

T_R = daily temperature range

Maximum pavement temperatures at the top and bottom surfaces of concrete slabs were calculated for 7, 9, 10 and 12 inch slabs for two locations in Washington State, for the mean day each month. Normal maximum, minimum and average temperatures over a 30 year period were obtained from weather data [15]. Solar radiation data was also obtained from

data compiled by the National Oceanic and Atmospheric Administration [10].

For calculation of pavement temperatures in Eastern Washington temperature and solar radiation data gathered at Spokane Internation Airport was used. Western Washington pavement temperatures were calculated using temperatures gathered at Olympia Airport and solar radiation data collected at Seattle-Tacoma International Airport. It was felt the temperatures at Olympia would be more representative of the I-5 corridor than Seattle, which is more subject to a marine climate. However, the only radiation data available on the west side was for Seattle. Table 1 gives the weather data used to compute the maximum pavement temperatures for the mean day of each month. The temperatures calculated for the pavement surface and at the bottom of 7, 9, 10 and 12 inch slabs are listed in Table 2.

Temperature gradients were calculated using the following relationship:

$$G = \frac{T_s - T_b}{H} \quad \text{.....(2)}$$

where G = thermal gradient, °F/in.

T_s = temperature at the surface of the slab, °F

T_b = temperature at the bottom of the slab, °F

H = PCC slab thickness, inches

The maximum positive gradients for the mean day of each month are shown in Table 3.

The computed pavement temperatures compare quite favorably with measurements made by Teller and Southerland [20] at Arlington, Virginia. They found that during the summer when the effect of solar radiation is greatest, the surface of the slab will be approximately 20°F higher than the air temperature. The computed surface temperatures for July were 25°F and 19°F higher than the average air temperature for Eastern and Western Washington, respectively. The maximum temperature differential between the top and bottom surfaces measured by Teller and Southerland for a nine inch slab was 31°F. This compares with 23°F and 21°F calculated for Eastern and Western Washington, respectively.

Since the climates in Virginia and Washington State are different,

Table 1. Climatic Data Used to Calculate Temperature Gradients in Concrete Pavements

Eastern Washington

Month	Average Air Temperature for Normal Days: Daily Maximum °F	Daily Minimum °F	Monthly Average °F	Average Solar Radiation BTU/Sq. Ft.
January	31.1	19.6	25.4	315.0
February	39.0	25.3	32.2	605.6
March	46.2	28.8	37.5	1040.6
April	57.0	35.2	46.1	1493.0
May	66.5	42.8	54.7	1917.9
June	73.6	49.4	61.5	2082.8
July	84.3	55.1	69.7	2357.5
August	81.9	54.0	68.0	1942.0
September	72.5	46.7	59.6	1435.3
October	58.1	37.5	47.8	840.9
November	41.8	29.2	35.5	397.7
December	33.9	24.0	29.0	255.2

Western Washington

Month	Average Air Temperature for Normal Days: Daily Maximum °F	Daily Minimum °F	Monthly Average °F	Average Solar Radiation BTU/Sq. Ft.
January	45.1	31.1	38.1	262.4
February	49.6	32.2	40.9	494.5
March	54.4	34.0	44.2	854.2
April	62.3	37.6	50.0	1295.3
May	68.6	41.6	55.1	1720.1
June	72.6	45.5	59.1	1797.4
July	79.7	48.0	63.9	1980.4
August	78.9	47.8	63.4	1607.3
September	72.6	44.4	58.5	1154.1
October	62.3	40.5	51.4	650.8
November	52.4	35.2	43.8	338.4
December	47.5	33.9	40.7	212.6

Table 2. Calculated Maximum Temperatures °F for the Mean Day of Each Month.

Month	EASTERN WASHINGTON					WESTERN WASHINGTON				
		Bottom of Slab Slab Thickness					Bottom of Slab Slab Thickness			
	Surface	7"	9"	10"	12"	Surface	7"	9"	10"	12"
January	33	29	28	28	27	46	41	41	40	40
February	44	38	37	36	36	53	46	45	45	44
March	56	46	45	44	44	62	52	51	50	49
April	72	58	56	56	55	74	61	59	59	58
May	86	70	68	67	66	85	69	67	66	65
June	96	78	75	75	73	91	74	72	71	69
July	109	88	86	85	83	99	80	78	77	75
August	101	84	81	81	79	93	77	75	74	73
September	86	72	70	69	68	82	69	67	67	66
October	65	55	54	54	53	67	58	57	56	56
November	45	39	39	38	38	53	48	47	47	46
December	35	32	31	31	31	48	43	43	43	42

Table 3. Maximum Positive Thermal Gradients (°F/inch) for the Mean Day of Each Month in Washington State.

MONTH	7" Pavement		9" Pavement		10" Pavement		12" Pavement	
	Eastside	Westside	Eastside	Westside	Eastside	Westside	Eastside	Westside
January	.65	.71	.57	0.56	.53	0.60	.47	0.50
February	.97	1.00	.85	0.89	.79	0.80	.70	0.75
March	1.45	1.43	1.27	1.22	1.19	1.20	1.06	1.08
April	1.98	1.86	1.73	1.67	1.61	1.50	1.44	1.33
May	2.40	2.29	2.10	2.00	1.97	1.90	1.74	1.67
June	2.55	2.43	2.24	2.11	2.09	2.00	1.85	1.83
July	2.95	2.71	2.58	2.44	2.42	2.20	2.14	2.00
August	2.56	2.29	2.24	2.00	2.10	1.90	1.86	1.67
September	2.06	1.86	1.81	1.67	1.69	1.50	1.50	1.25
October	1.39	1.29	1.22	1.11	1.14	1.10	1.01	0.92
November	.76	0.71	.66	0.67	.62	0.60	.55	0.58
December	.55	0.71	.47	0.55	.45	0.50	.40	0.50

direct comparisons are not appropriate, however, the comparison does give an indication that the calculated pavement temperatures are reasonable.

A review of Table 3 indicates the average differences in the thermal gradients between Western and Eastern Washington were approximately five percent. Therefore, to reduce the amount of computations it was decided to use only the Western Washington pavement temperatures for analysis.

To determine the maximum combined load and warping tensile stresses, the warping stresses were calculated at the center and the bottom of the longitudinal pavement edge. This was the location where the maximum load related edge stresses were found. Two methods for computing warping stress were considered. The first method was an analysis procedure presented by Bradbury [4] which is based on the analysis of temperature stresses in concrete pavements developed by Westergaard [28]. The maximum edge stress for the Bradbury analysis is expressed by the general formula:

$$S_t = \frac{CEe\Delta t}{2} \quad \text{.....(3)}$$

where S_t = warping stress, psi

E = modulus of elasticity of the concrete, psi

e = thermal coefficient of concrete, 0.000005 per degree F

Δt = temperature differential between top and bottom slab, °F

C = a coefficient, the value of which depends upon slab length and the radius of relative stiffness

A second method of analysis is a set of regression equations developed by Darter [5] using data developed from a finite element analysis. The first equation determines the edge warping stress (STRC). His results indicated that the curl stresses could not be added directly to the load stress to obtain the combined stress. Therefore, the second equation provides an adjustment factor (R) to adjust the warping stress so that it could be added directly to the load stress. R ranges from about 0.8 to 1.5 depending on slab/foundation conditions. The following

are the two regression equations:

Curl stress:

$$STRC = [(G)(ET)/(5 \times 10^{-6})][0.006712k + 79.07391 \log_{10}k + 11.72690L - 0.00720kL - 3.22139L \log_{10}k - 0.06883LES - 0.59539ES \log_{10}k - 204.39477H/K - 38.08854L/H - 8.36842H \log_{10}k + 0.07151ESH + 0.95691LES \log_{10}k + 0.20845LH \log_{10}k + 0.00058LHk - 0.00201LES \log_{10}k] \quad \ldots\ldots(4)$$

R adjustment factor:

$$R = 0.48039 + 0.01401H - 0.00427ES - 0.27278G - 0.00403L \quad \ldots\ldots(5)$$
$$+ 0.19508 \log_{10}k + 0.45187G \log_{10}H - 0.00532G^2 + 0.01246GL - 0.00622GL \log_{10}k + 8.7872 \log_{10} (H^3/k)/H^2 + 0.00104GES - 0.11846G \log_{10} (H^3/k) + 0.07001 \log_{10} (ES + 1.0) - 0.01331G$$

where H = PCC slab thickness, inches
G = thermal gradient through slab, °F/in.
k = modulus of foundation support (top of subbase, pci)
L = slab length, ft.
ES = erodability of support along slab edge, inches
ET = thermal coefficient of contraction of PCC/°F

$$\text{Adjusted Curl Stress} = R \times STRC \quad \ldots\ldots(6)$$

To compare the two methods of analysis, the calculated pavement temperatures for Western Washington in July were used. July was chosen because this month had the highest average thermal gradient and therefore, the highest predicted warping stresses. The following variables were used in the analysis: modulus of subgrade reaction 50, 100, 200, 300; pavement thicknesses 7, 9 and 12 inches. In the Darter equations an erodability factor of zero was selected because very little pavement pumping is observed in Washington. The stresses calculated by each method are plotted in Figures 19 through 21. These figures indicate that with higher values of modulus of subgrade reaction and greater pavement depths, the Bradbury analysis gives much higher stresses than the Darter equations. The warping stresses calculated by the Bradbury procedure are generally considered to be higher than measured stress because the effect of a moisture gradient through the slab causes

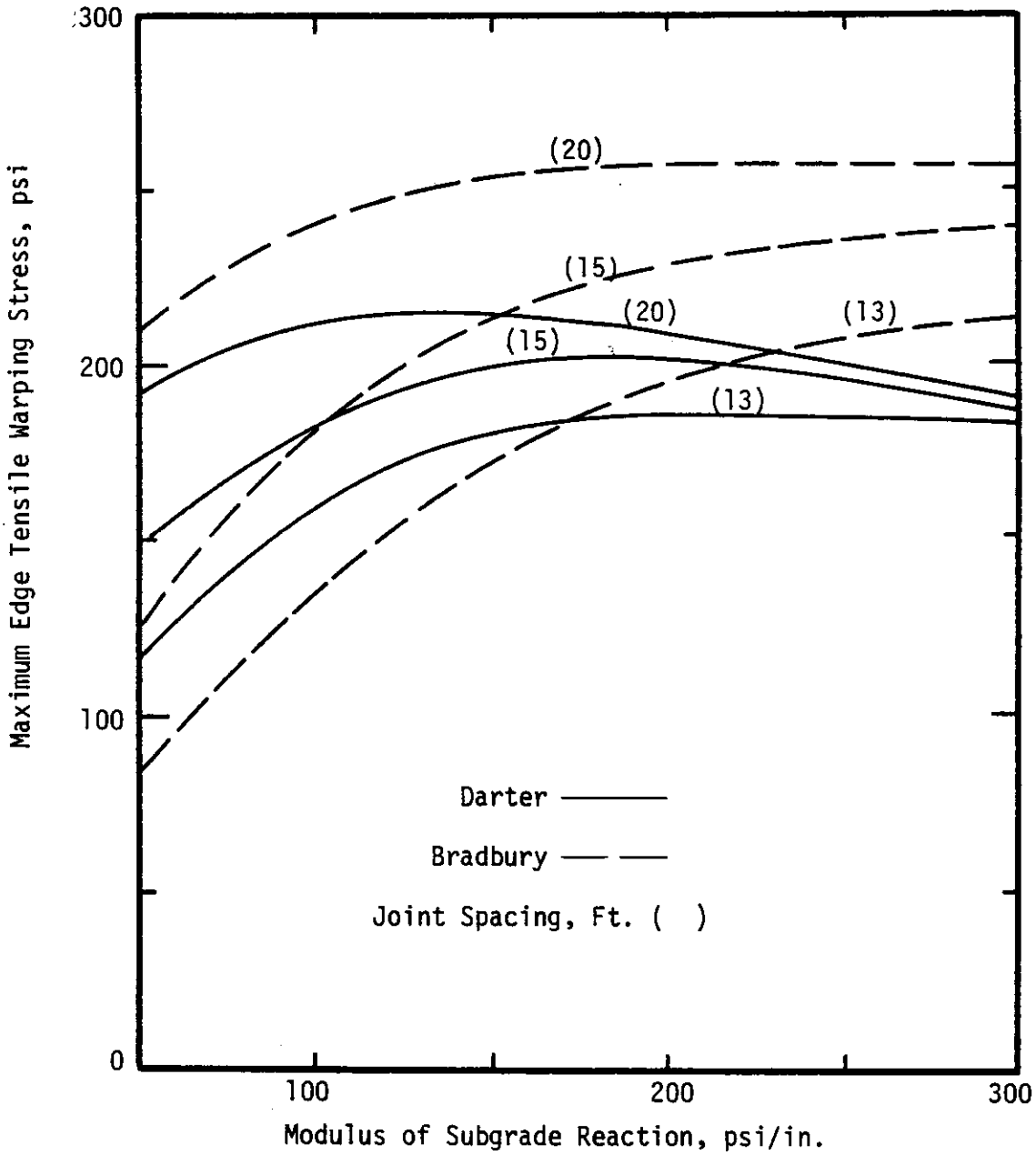

Figure 19. Warping Edge Stress for 7-inch Pavements Located in Western Washington, During July

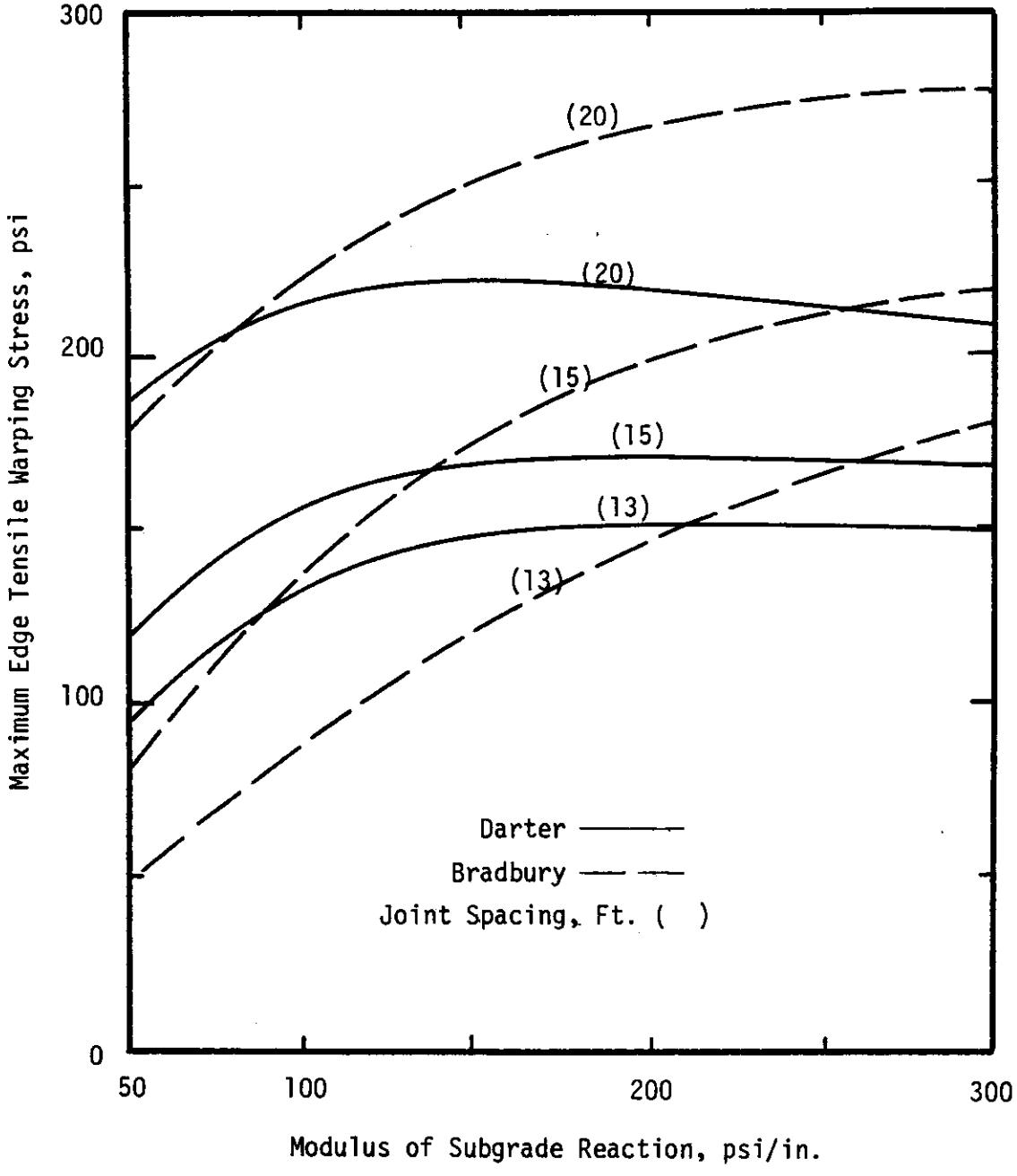

Figure 20. Warping Edge Stress for 9-inch Pavements Located in Western Washington, During July

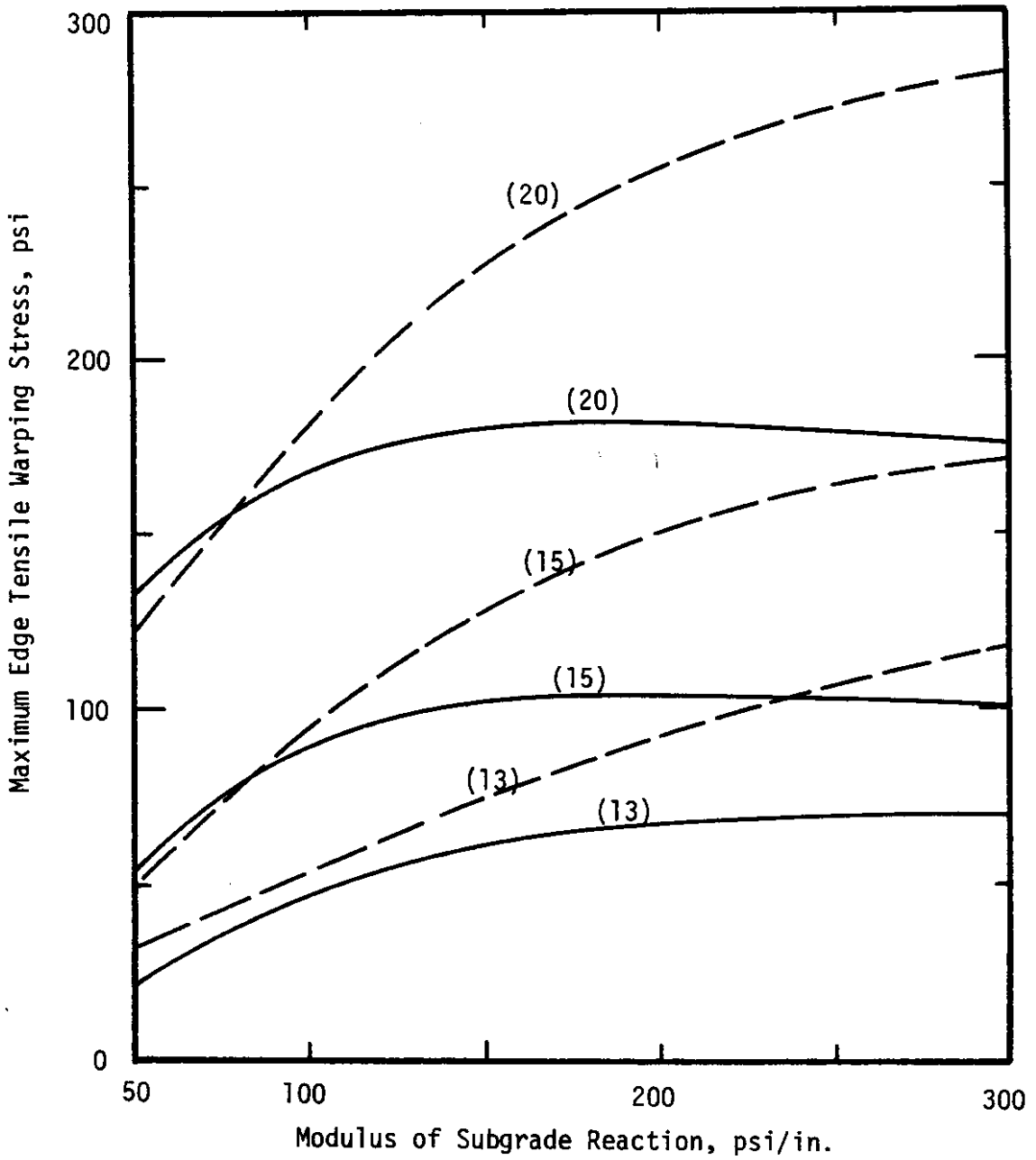

Figure 21. Warping Edge Stress for 12-inch Pavements Located in Western Washington, During July

stresses of an opposite sign to thermal curl stress. Also, slab settlement will reduce the warping stress [5]. Macleod and Monismith [11] reduced stresses calculated using the Bradbury procedure by 33 percent to account for these factors.

Darter [5] states "The computation of curling stresses using the finite element (FE) program provides a much more realistic analysis than the Westergaard/Bradbury analysis. The FE program allows the slab to curl in a weightless condition, and then the restraining weight of the slab is added. Hence, the slab is restrained by its weight. The Bradbury model assumes full restraint of the slab which should give higher stresses."

Based on the comparison of the two procedures and a review of previous work, the Darter procedure was selected to compute edge warping stresses for this analysis. However, it was noted that above a modulus of subgrade reaction of approximately 200 psi per inch the warping stress tended to decrease. This decrease is most evident with decreasing pavement thickness and increased joint spacing. Traditionally, it is believed that warping stresses increase as the modulus of subgrade reaction increases, because stiff subgrades do not yield [29]. Majidzadeh, Ilves, and McComb reported [12] that when analyzing warping stresses using a coupled finite element-elastic multilayer subgrade program (RIGMUL), no appreciable differences in warping stresses were noted for changes in subgrade support conditions. For this study it was decided to use the warping stresses computed using the Darter equation for modulus of subgrade reactions of 200 and below. For modulus values above 200 the warping stress versus modulus curve was kept flat. This assumed, that for very weak subgrades, the subgrade yields as the slab warps. This provides uniform support over the length of the slab reducing stresses.

The mid-panel edge warping stresses calculated using Darter's equations are given in Appendix A.

Analysis of the calculated edge warping stresses reveals, that decreasing the pavement thickness and/or increasing the joint spacing can result in a significant increase in warping stress. For a 9 inch

pavement with a K-value for the subgrade of 100, increasing the joint spacing from 13 feet to 20 feet results in a 60 percent increase in warping stress. A 7 inch pavement with a K-value for the subgrade of 100 will have a 25 percent higher warping stress than a 9 inch pavement on the same subgrade.

Fatigue Analysis

There have been numerous studies which show that plain concrete beams experience fatigue failure when subjected to high repetitive flexural stresses. However, no correlation has been performed between laboratory and field fatigue results [5]. Vesic and Saxena [26] computed stresses for all rigid pavement slabs of the AASHTO Road Test, for which the serviceability data was available. They found that if the critical stresses for each loading case and slab were plotted versus the number of load repetitions needed to reduce the serviceability index to 2.5 the following relationship resulted:

$$N_{2.5} = 225{,}000 \left(^{fc}/_{\sigma}\right)^4 \quad \text{.....(7)}$$

where:

$N_{2.5}$ = load repetitions to a serviceability index of 2.5
fc = tensile strength of concrete, psi
σ = tensile stress, psi

MacLeod and Monismith [11] found, after detailed traffic analyses of 600 lane miles of pavement in the San Francisco Bay Area, a common fatigue relationship for PCC pavements when Equation (7) is used. In their analysis, fc was the modulus of rupture of the concrete and σ was the combined effects of load and thermal stresses.

Equation (7) was selected for use in this study. The tensile stress used in the equation was the combined load and adjusted warping stress. The tensile strength was assumed to be 750 psi. The fatigue analysis was made by assuming that the load repetitions occurred during the daytime, which was also the period of maximum warping stress. The load stress was combined with the mean adjusted warping stress for each month and the allowable axle repetitions to a serviceability level of

2.5 calculated. Allowable repetitions for a specific axle load and pavement section was based on the following relationship:

$$\sum_{i=1}^{12} \frac{n}{Ni} = 1 \quad \text{.....(8)}$$

n = 1/12 of the total load applications

Ni = the allowable number of load applications for each month

Axle load versus repetitions to a serviceability index of 2.5 were developed for single axles with dual tires and 10, 12, 14, 16 and 18 inch wide single tires. Pavement thicknesses of 7, 9 and 12 inches with moduli of subgrade reaction of 100 and 300 were used to develop these fatigue relationships. Figures 22 through 24 are the fatigue curves developed. Fatigue curves were also developed for tandem axles with dual tires and 13 inch wide single tires (Figures 25 through 27).

Equivalent Wheel Load Factors

Single Axles

The fatigue curves were used to determine the percent of a dual tire axle load an axle with a specific width of single tires could carry and have an equivalent number of repetitions to a serviceability index of 2.5. It was found that each pavement depth and modulus of subgrade reaction had an individual relationship. These are shown in Figure 28. This equivalency can also be modeled by the following regression equation:

$$PDL = 54.2 + 1.77\ (STW) - 0.0116\ (k) + .618\ (D) \quad \text{.....(9)}$$

where PDL = percent of dual tire axle load on an axle with single tires which gives equivalent fatigue life

STW = width of single tire, inches

k = modulus of subgrade reaction, psi/in.

D = thickness of pavement slab, inches

R^2 = .987

σ^2 = .377

n = 150

Equivalent wheel load factors were developed for dual tires on

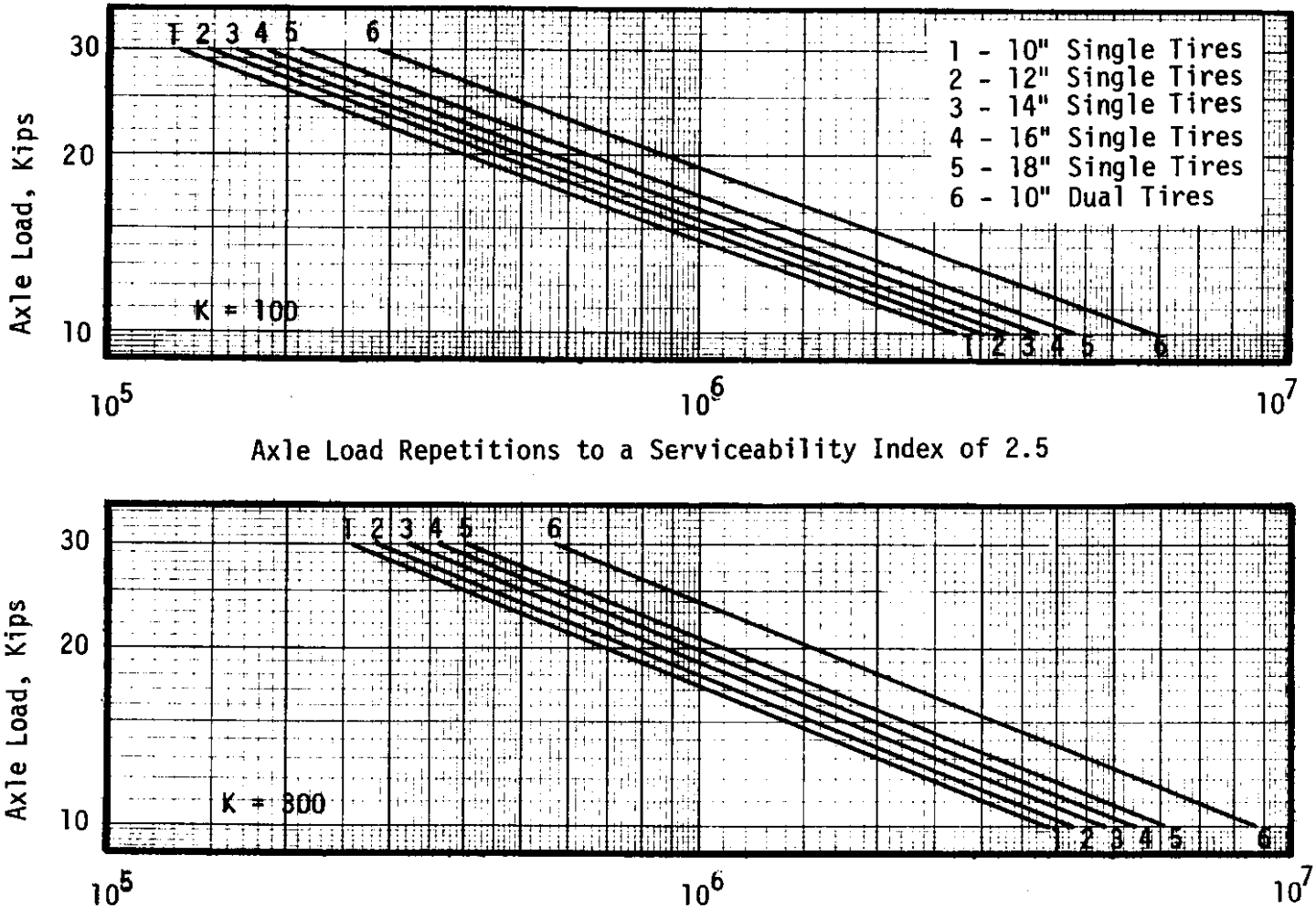

Figure 22. Axle Load Repetitions to a Serviceability Index of 2.5 for Single Axle, Edge Loading (cases I-C, II-C) on a 7-inch Pavement

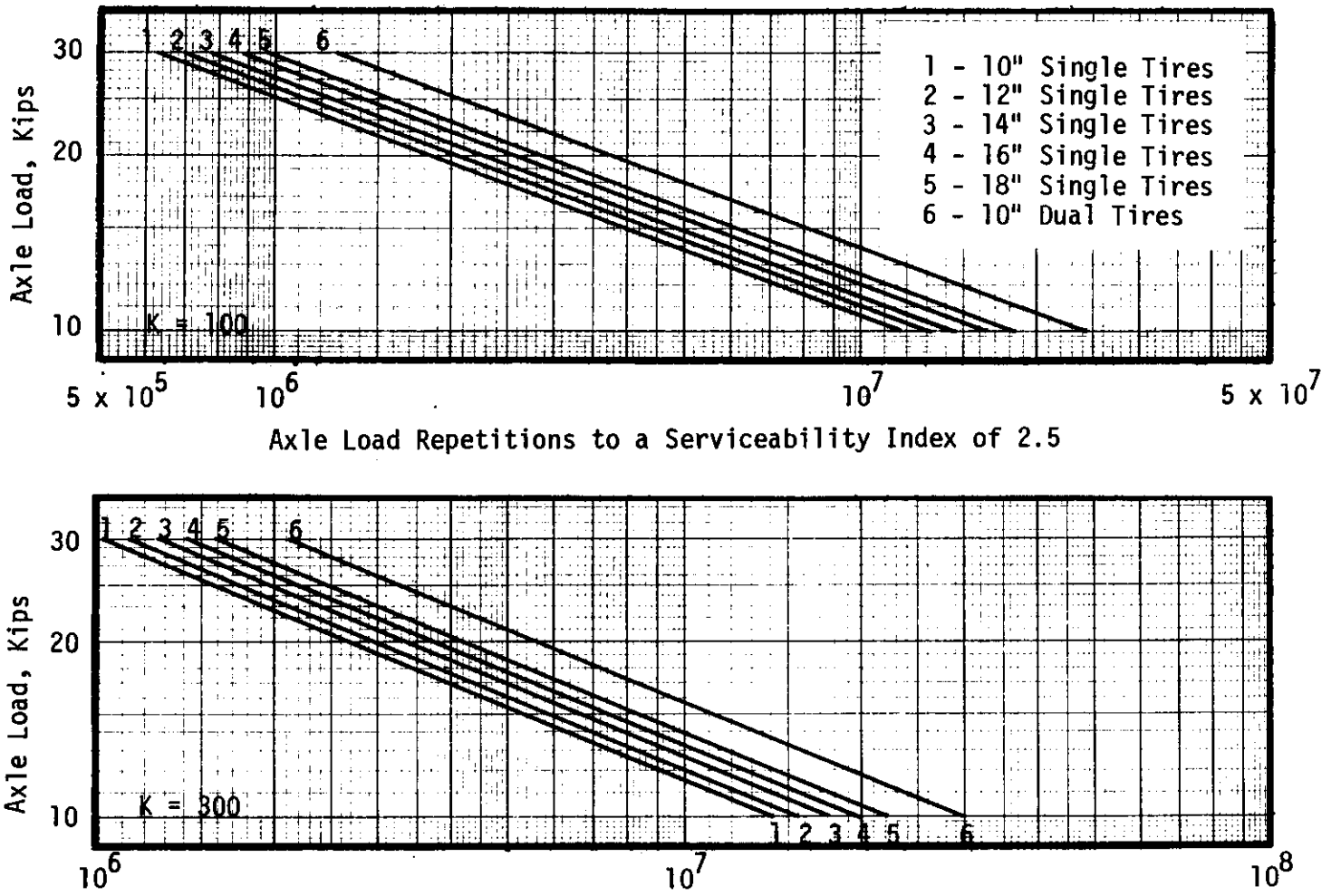

Figure 23. Axle Load Repetitions to a Serviceability Index of 2.5 for Single Axle, Edge Loading (cases I-C, II-C) on a 9-inch Pavement

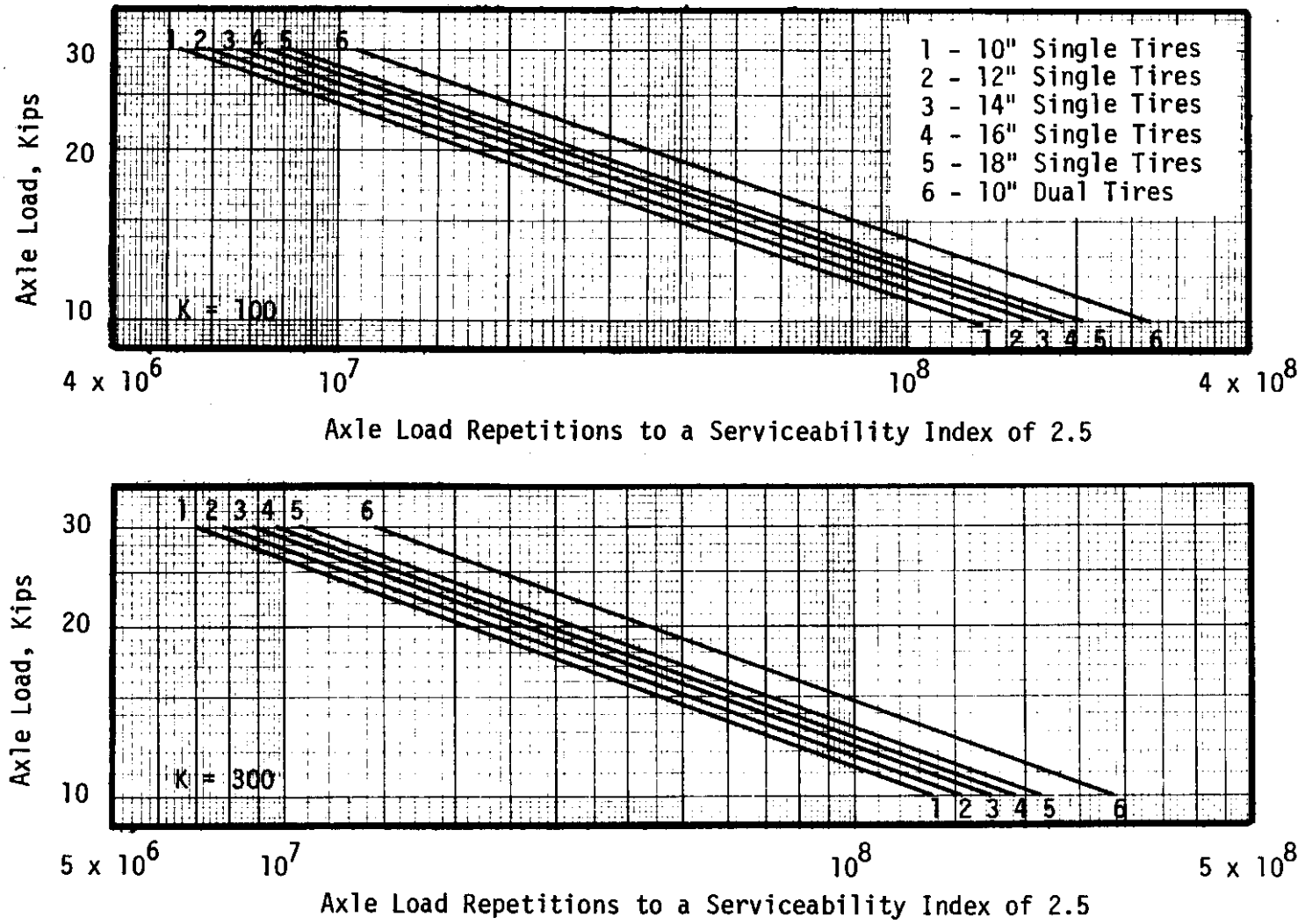

Figure 24. Axle Load Repetitions to a Serviceability Index of 2.5 for Single Axle, Edge Loading (cases I-C, II-C) on a 12-inch Pavement

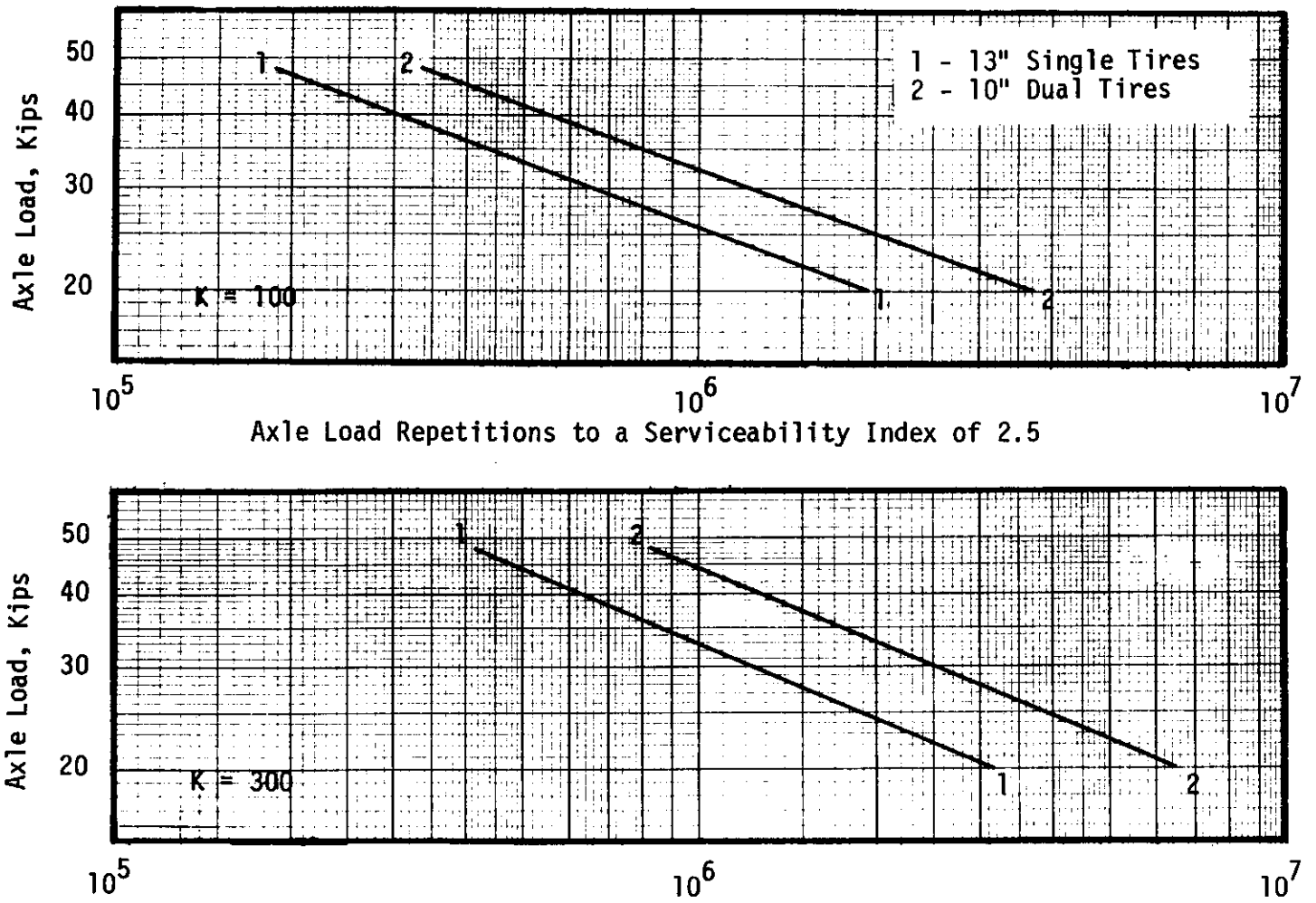

Figure 25. Axle Load Repetitions to a Serviceability Index of 2.5 for Tandem Axle Edge Loadings (cases III-C, IV-C) on a 7-inch Pavement

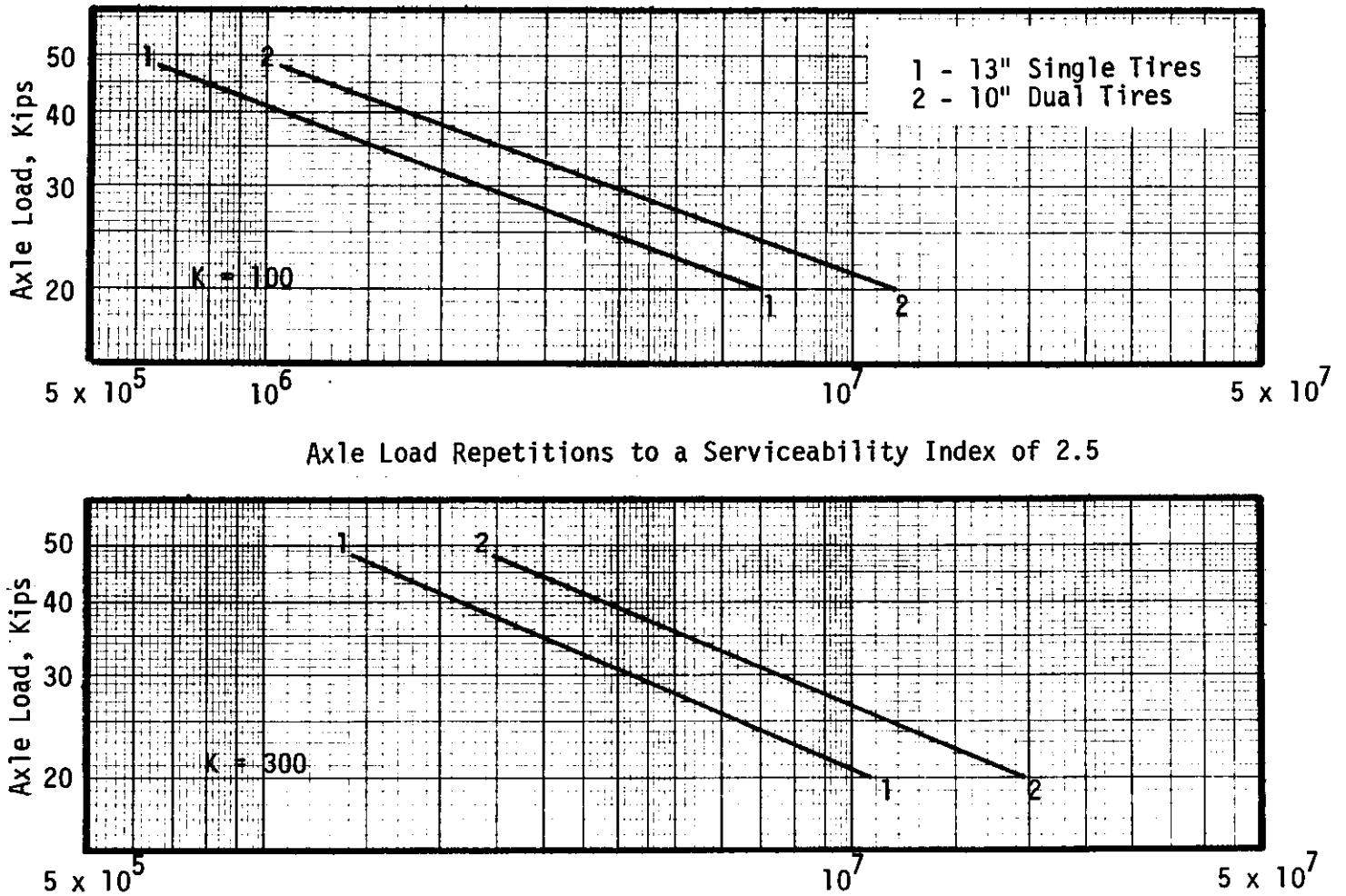

Figure 26. Axle Load Repetitions to a Serviceability Index of 2.5 for Tandem Axle, Edge Loading (cases III-C, IV-C) on a 9-inch Pavement

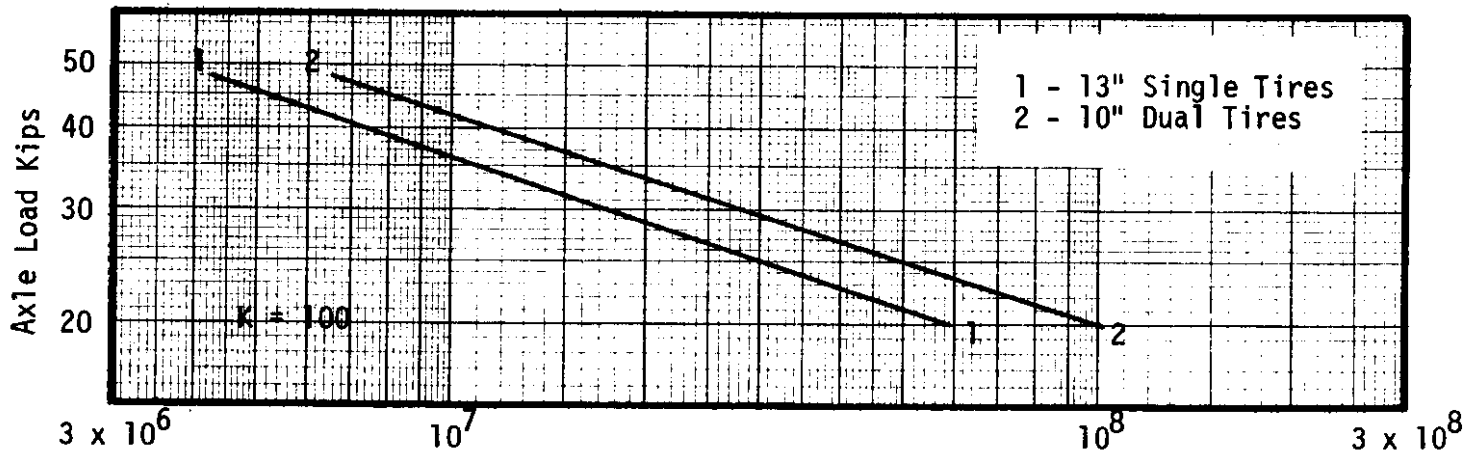

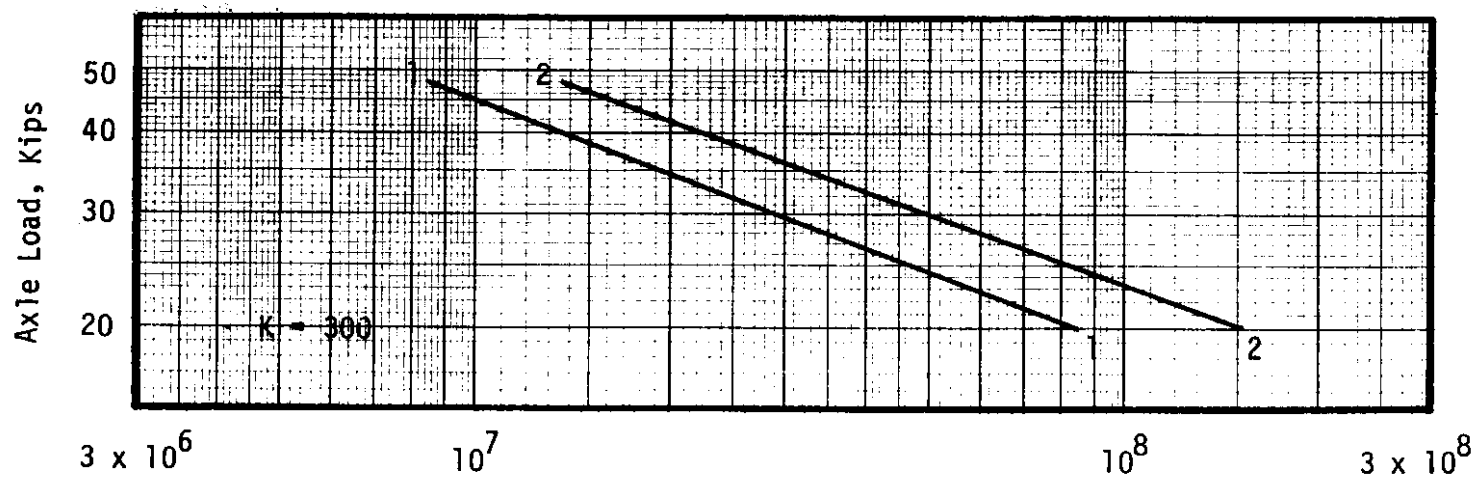

Figure 27. Axle Load Repetitions to a Serviceability Index of 2.5 for Tandem Axle, Edge Loading (Cases III-C, IV-C) on a 12-inch Pavement

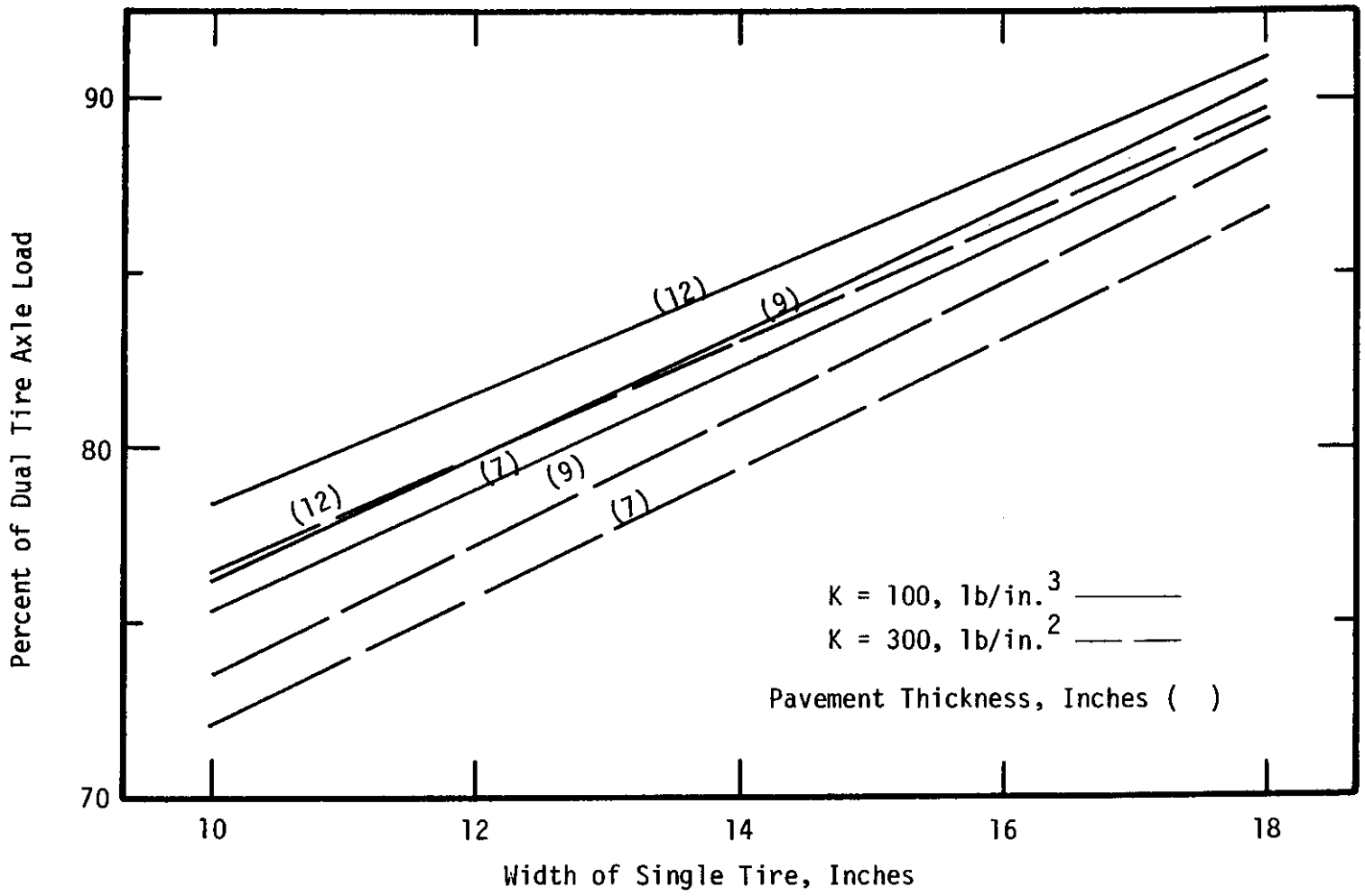

Figure 28. Percent of Dual Tire Axle Loads which an Axle with Single Tires Can Carry for Equivalent Pavement Life

single axles and 10, 12, 14, 16 and 18 inch wide single tires on single axles. The factors were developed for 7, 9 and 12 inch pavements with moduli of subgrade reactions of 100 and 300 psi/in. These factors are the equivalent 18-kip dual tire single axle loads for the load being evaluated. The factors were developed using the following equation:

$$F_i = \frac{N_{18}}{Ni} \quad \text{.....(10)}$$

F_i = equivalency factor

N_{18} = repetitions to a serviceability index of 2.5 for an 18-kip dual tire single axle load

N_i = repetitions to a serviceability index of 2.5 for the axle load being evaluated

The equivalency factors for single axles are given in Table 4 - 10.

Tandem Axles

Equivalency relationships were developed between 13 inch wide single tires and dual tires on tandem axles. The percent of a dual tire tandem axle load which can be carried on a tandem axle with 13 inch single tires and give equivalent fatigue life are given in Table 11. These equivalencies were developed using fatigue curves (Figures 25 through 27).

Equivalent wheel load factors were developed for tandem axles with dual tires and tandem axles with 13 inch wide single tires. These factors are the equivalent 18-kip dual tire single axle loads and were developed using Equation (10). The factors for tandems with dual tires are given in Table 12 and tandems with 13 inch wide single tires are given in Table 13.

Equivalent wheel load factor tables were not developed for widths of single tires on a tandem axle other than 13 inches. However, the equivalency tables for dual and single 13 inch wide tandem axles and the appropriate equivalency tables for single axles were used to develop factors for converting tandem axles to single axles. These factors are presented in Table 14 and are used as follows: From Table 14 determine the appropriate factor based on pavement thickness and subgrade modulus. Divide the tandem axle load by two, find the equivalence factor for a single axle in the appropriate Table 4 - 10. Multiply the single axle equivalence factor by the factor from Table 14 to

Table 4. Traffic Equivalence Factors, Rigid Pavements
Dual Tires, Single Axle Load.

Equivalent 18-Kip Dual Tire Single Axle Loads

Axle Load	SLAB THICKNESS 7	7	9	9	12	12
	MODULUS OF SUBGRADE REACTION					
	100	300	100	300	100	300
10.	.19839	.23476	.20768	.24480	.1794	.20379
12.	.32765	.36800	.33816	.37879	.3057	.33378
14.	.50078	.53815	.51067	.54787	.4797	.50656
16.	.72316	.74797	.72982	.75427	.7087	.72706
18.	1.00000	1.00000	1.00000	1.00000	1.0000	1.00000
20.	1.33635	1.29663	1.32543	1.28693	1.3607	1.32993
22.	1.73711	1.64009	1.71018	1.61681	1.7978	1.72126
24.	2.20708	2.03252	2.15819	1.99129	2.3184	2.17826
26.	2.75093	2.47594	2.67328	2.41192	2.9296	2.70509
28.	3.37324	2.97229	3.25917	2.88020	3.6381	3.30583
30.	4.07853	3.52343	3.91950	3.39752	4.4510	3.98444
32.	4.87119	4.13114	4.65779	3.96524	5.3751	4.74481
34.	5.75559	4.79716	5.47752	4.58466	6.4172	5.59075
36.	6.73599	5.52315	6.38209	5.25704	7.5842	6.52600
38.	7.81662	6.31072	7.37484	5.98357	8.8827	7.55426
40.	9.00163	7.16145	8.45902	6.76544	10.3194	8.67913

Table 5. Traffic Equivalence Factors, Rigid Pavements Seven Inches Thick, Modulus of Subgrade Reaction = 100, Single Tires, Single Axles.

Equivalent 18-Kip Dual Tire Single Axle Loads

Axle Load	Single Tire Width 10"	12"	14"	16"	18"
10.	.4315	.3835	.3391	.3034	.2700
12.	.7127	.6334	.5600	.5010	.4460
14.	1.0892	.9681	.8560	.7657	.6816
16.	1.5729	1.3980	1.2361	1.1058	.9843
18.	2.1750	1.9332	1.7093	1.5291	1.3612
20.	2.9066	2.5834	2.2842	2.0434	1.8190
22.	3.7782	3.3581	2.9692	2.6562	2.3645
24.	4.8004	4.2666	3.7725	3.3748	3.0042
26.	5.9833	5.3180	4.7021	4.2064	3.7445
28.	7.3368	6.5210	5.7658	5.1580	4.5916
30.	8.8708	7.8844	6.9713	6.2364	5.5516
32.	10.5949	9.4168	8.3262	7.4484	6.6305
34.	12.5184	11.1264	9.8378	8.8007	7.8344
36.	14.6508	13.0217	11.5136	10.2998	9.1689
38.	17.0012	15.1107	13.3607	11.9522	10.6398
40.	19.5786	17.4015	15.3862	13.7642	12.2528

Table 6. Traffic Equivalence Factors, Rigid Pavements Seven Inches Thick, Modulus of Subgrade Reaction = 300, Single Tires, Single Axles

Equivalent 18-Kip Dual Tire Single Axle Loads

Axle Load	Single Tire Width 10"	12"	14"	16"	18"
10.	.5205	.4740	.4185	.3684	.3319
12.	.8159	.7431	.6560	.5774	.5202
14.	1.1932	1.0866	.9593	.8444	.7608
16.	1.6584	1.5103	1.3333	1.1736	1.0574
18.	2.2172	2.0192	1.7826	1.5691	1.4137
20.	2.8749	2.6182	2.3113	2.0345	1.8330
22.	3.6365	3.3117	2.9236	2.5735	2.3185
24.	4.5066	4.1041	3.6231	3.1892	2.8733
26.	5.4898	4.9995	4.4135	3.8850	3.5002
28.	6.5903	6.0017	5.2983	4.6638	4.2018
30.	7.8123	7.1146	6.2807	5.5286	4.9809
32.	9.1597	8.3417	7.3640	6.4822	5.8400
34.	10.6365	9.6865	8.5512	7.5272	6.7816
36.	12.2462	11.1524	9.8454	8.6663	7.8079
38.	13.9924	12.7427	11.2493	9.9021	8.9212
40.	15.8787	14.4605	12.7657	11.3270	10.1239

Table 7. Traffic Equivalence Factors, Rigid Pavements Nine Inches Thick, Modulus of Subgrade Reaction = 100, Single Tires, Single Axles

Equivalent 18-Kip Dual Tire Single Axle Loads

Axle Load	Single Tire Width 10"	12"	14"	16"	18"
10.	.4251	.3848	.3407	.2950	.2728
12.	.6922	.6266	.5548	.4803	.4442
14.	1.0453	.9463	.8378	.7254	.6709
16.	1.4939	1.3524	1.1973	1.0367	.9589
18.	2.0469	1.8530	1.6405	1.4204	1.3137
20.	2.7130	2.4561	2.1744	1.8827	1.7412
22.	3.5005	3.1690	2.8056	2.4292	2.2466
24.	4.4176	3.9992	3.5406	3.0656	2.8352
26.	5.4719	4.9537	4.3857	3.7972	3.5119
28.	6.6711	6.0394	5.3468	4.6294	4.2815
30.	8.0227	7.2630	6.4301	5.5674	5.1490
32.	9.5339	8.6310	7.6413	6.6161	6.1189
34.	11.2118	10.1500	8.9861	7.7805	7.1958
36.	13.0634	11.8262	10.4701	9.0653	8.3841
38.	15.0954	13.6658	12.0988	10.4755	9.6882
40.	17.3146	15.6748	13.8774	12.0155	11.1125

Table 8. Traffic Equivalence Factors, Rigid Pavements Nine Inches Thick, Modulus of Subgrade Reaction = 300, Single Tires, Single Axle

Equivalent 18-Kip Dual Tire Single Axle Loads

Axle Load	Single Tire Width 10"	12"	14"	16"	18"
10.	.5034	.4620	.4054	.3633	.32533
12.	.7789	.7149	.6273	.5621	.50339
14.	1.1266	1.0340	.9074	.8131	.72810
16.	1.5510	1.4235	1.2492	1.1194	1.00240
18.	2.0563	1.8872	1.6562	1.4840	1.32896
20.	2.6463	2.4288	2.1314	1.9098	1.71028
22.	3.3247	3.0513	2.6777	2.3994	2.14868
24.	4.0947	3.7581	3.2980	2.9551	2.64635
26.	4.9597	4.5519	3.9946	3.5793	3.20535
28.	5.9226	5.4356	4.7701	4.2743	3.82767
30.	6.9864	6.4119	5.6269	5.0420	4.51517
32.	8.1538	7.4834	6.5672	5.8845	5.26965
34.	9.4276	8.6524	7.5931	6.8037	6.09284
36.	10.8102	9.9213	8.7066	7.8015	6.98640
38.	12.3042	11.2925	9.9099	8.8797	7.95194
40.	13.9119	12.7681	11.2048	10.0400	8.99100

Table 9. Traffic Equivalence Factors, Rigid Pavements 12 Inches Thick, Modulus of Subgrade Reaction = 100, Single Tires, Single Axle

Equivalent 18-Kip Dual Tire Singel Axle Loads

Axle Load	Single Tire Width 10"	12"	14"	16"	18"
10.	.3640	.3274	.2895	.2598	.2356
12.	.6203	.5579	.4933	.4427	.4014
14.	.9733	.8754	.7741	.6947	.6299
16.	1.4381	1.2934	1.1436	1.0264	.9307
18.	2.0291	1.8249	1.6136	1.4482	1.3132
20.	2.7609	2.4831	2.1956	1.9705	1.7868
22.	3.6478	3.2808	2.9010	2.6036	2.3608
24.	4.7042	4.2310	3.7411	3.3576	3.0445
26.	5.9443	5.3462	4.7227	4.2477	3.8471
28.	7.3820	6.6393	5.8706	5.2688	4.7776
30.	9.0314	8.1228	7.1823	6.4461	5.8451
32.	10.9065	9.8092	8.6734	7.7844	7.0586
34.	13.0210	11.7110	10.3550	9.2936	8.4271
36.	15.3887	13.8405	12.2380	10.9835	9.9594
38.	18.0234	16.2101	14.3333	12.8640	11.6646
40.	20.9388	18.8322	16.6517	14.9448	13.5514

Table 10. Traffic Equivalence Factors, Rigid Pavement 12 Inches Thick, Modulus of Subgrade Reaction = 300, Single Tires, Single Axle

Equivalent 18-Kip Dual Tire Single Axle Loads

Axle Load	Single Tire Width 10"	12"	14"	16"	18"
10.	.4222	.3791	.3341	.3036	.2743
12.	.6916	.6210	.5473	.4973	.4493
14.	1.0496	.9425	.8306	.7547	.6819
16.	1.5064	1.3527	1.1921	1.0833	.9787
18.	2.0719	1.8605	1.6396	1.4899	1.3461
20.	2.7555	2.4743	2.1806	1.9815	1.7902
22.	3.5663	3.2024	2.8223	2.5646	2.3169
24.	4.5132	4.0526	3.5716	3.2455	2.9321
26.	5.6047	5.0328	4.4354	4.0304	3.6412
28.	6.8494	6.1505	5.4204	4.9255	4.4498
30.	8.2554	7.4130	6.5331	5.9366	5.3633
32.	9.8309	8.8276	7.7798	7.0695	6.3868
34.	11.5836	10.4015	9.1669	8.3299	7.5255
36.	13.5214	12.1415	10.7003	9.7233	8.7844
38.	15.6518	14.0546	12.3863	11.2554	10.1685
40.	17.9825	16.1474	14.2307	12.9314	11.6826

Table 11. Percent of Dual Tire Tandem Axle Load on 13-Inch Single Tire Tandem Axle for Equivalent Rigid Pavement Performance

Pavement Thickness Inches	*Modulus of Subgrade Reaction psi/in.	Percent of Dual Tire Tandem [1]
7	100	80.0
7	300	75.8
9	100	82.2
9	300	79.0
12	100	85.4
12	300	82.0

[1] Percent of a dual tired tandem axle load which can be carried on a tandem axle with 13-inch wide single tires and give equivalent fatigue life.

Table 12. Traffic Equivalence Factors, Rigid Pavement, Dual Tires, Tandem Axles

Equivalent 18-Kip Dual Tire Single Axle Loads

Axle Load	SLAB THICKNESS 7	7	9	9	12	12
	MODULUS OF SUBGRADE REACTION, PCI					
	100	300	100	300	100	300
20.	.31317	.31042	.42403	.36784	.48031	.38074
22.	.40698	.38948	.55133	.46028	.64622	.49490
24.	.51697	.47911	.70065	.56480	.84728	.62876
26.	.64423	.57968	.87348	.68180	1.08704	.78366
28.	.78981	.69152	1.07128	.81162	1.36913	.96090
30.	.95477	.81495	1.29549	.95461	1.69717	1.16176
32.	1.14014	.95028	1.54753	1.11108	2.07484	1.38749
34.	1.34692	1.09781	1.82878	1.28136	2.50583	1.63934
36.	1.57612	1.25782	2.14061	1.46573	2.99386	1.91853
38.	1.82871	1.43059	2.48436	1.66449	3.54269	2.22624
40.	2.10566	1.61638	2.86137	1.87791	4.15608	2.56366
42.	2.40792	1.81545	3.27295	2.10626	4.83783	2.93197
44.	2.73645	2.02805	3.72039	2.34979	5.59175	3.33231
46.	3.09216	2.25441	4.20498	2.60876	6.42168	3.76583
48.	3.47598	2.49478	4.72798	2.88341	7.33147	4.23364

Table 13. Traffic Equivalence Factors, Rigid Pavement, 13 Inch Wide Single Tires Tandem Axles

Equivalent 18-Kip Dual Tire Single Axle Loads

Axle Load	SLAB THICKNESS 7	7	9	9	12	12
	MODULUS OF SUBGRADE REACTION, PCI					
	100	300	100	300	100	300
20.	.60029	.63487	.73183	.66559	.8193	.67744
22.	.77401	.79230	.94501	.82966	1.0907	.87416
24.	.97616	.96989	1.19343	1.01453	1.4163	1.10324
26.	1.20843	1.16820	1.47925	1.22075	1.8011	1.36664
28.	1.47249	1.38778	1.80455	1.44889	2.2498	1.66626
30.	1.76995	1.62916	2.17140	1.69944	2.7676	2.00397
32.	2.10236	1.89281	2.58179	1.97290	3.3593	2.38158
34.	2.47128	2.17923	3.03769	2.26973	4.0299	2.80086
36.	2.87820	2.48885	3.54101	2.59038	4.7843	3.26356
38.	3.32461	2.82211	4.09365	2.93527	5.6275	3.77138
40.	3.81195	3.17944	4.69746	3.30482	6.5643	4.32600
42.	4.34166	3.56122	5.35425	3.69943	7.5999	4.92908
44.	4.91512	3.96786	6.06583	4.11948	8.7389	5.58222
46.	5.53372	4.39973	6.83396	4.56535	9.9866	6.28704
48.	6.19882	4.85720	7.66038	5.03738	11.3477	7.04509

Table 14. Equivalence Factors Between Tandem Axle Repetitions and Repetitions of One Axle in the Tandem Pair. Rigid Pavements Single or Dual Tires.

Pavement Thickness, Inches	Modulus of Subgrade Reaction (k) psi/in.	Equivalent* Single Axles (Rigid Pavement)
7	100	1.6
7	300	1.3
9	100	2.1
9	300	1.5
12	100	2.9
12	300	1.9

*i.e. for a 9 inch pavement, k = 100 a 40 kip tandem is equivalent to 2.1 20 kip single axles of similar tire configuration.

determine the equivalent 18-kip dual tire axle loads for the tandem axle.

Example: Analysis to determine the 18-kip dual tire, single axle equivalent repetitions for a tandem axle

Given: Tandem axle with a load of 44 kips, single 14 inch wide tires, pavement section - 7 inch PCC, K = 300.

Calculations: Load on each axle of the tandem pair

$$= \frac{\text{tandem axle load}}{2} = \frac{44}{2} = 22 \text{ kips}$$

Equivalent single axle factor from Table 14

= 1.3

18-kip equivalent axle load repetitions for a 22-kip single axle with 14 inch wide single tires, from Table 6

= 2.9236

Equivalent 18-kip dual tire, single axle equivalent repetitions for the tandem axle

= 1.3 x 2.9236 = 3.8007

CHAPTER 2

ASPHALT CONCRETE PAVEMENTS

Overview

The analysis of single versus dual tires on flexible pavements presents an interesting problem if currently available analysis procedures are to be used. This problem results because the various elastic layer analysis and finite element procedures developed for flexible pavements utilize uniform circular loads. As a result, the width of the tire being modeled is a function of tire pressure and load.

There are two previously reported studies where load equivalency factors between single and dual tires were developed. In one study reported by Deacon [6] an elastic layer analysis program developed by Chevron Research Company was used to compute the maximum tensile strains under various single and dual tired axle loads. In his analysis, the modulus of the asphalt pavement was 400,000 psi, which was representative of high-quality asphalt concrete at temperatures of 70°F, with a time of loading between 0.1 and 0.01 seconds. Moduli of 20,000 psi and 6,000 psi were used for the base and subgrade, respectively. Poisson's ratios of 0.35, 0.40 and 0.45 were chosen for the asphalt concrete, granular base and subgrade.

The load equivalency factors developed were based on fatigue distress, where fatigue life was described as:

$$N = K \left[\frac{1}{\varepsilon}\right]^C \quad \text{.....(11)}$$

N = number of load repetitions to failure

ε = maximum principal tensile strain

K and C are constants

The load equivalency factor (F_i) is defined as the ratio of the number of load applications to failure of a standard load (N_b) to the number of applications to failure of the axle load under study (N_i)

$$F_i = \frac{N_b}{N_i} \quad \text{.....(12)}$$

since $N_i = K [\frac{1}{\varepsilon_i}]^C$

$$F_i = [\frac{\varepsilon_i}{\varepsilon_b}]^C \quad \text{.....(13)}$$

where $C = 5.5$

The standard load was an 18,000 pound single axle dual-tired load.

Figure 29 shows the load equivalency between single and dual tires for various pavement structural numbers. Deacon's analysis did not attempt to model the widths of the single tires. Contact pressures were a function of tire loads and the single tires were assumed to be the same size as the tires used on the axles with dual tires.

Terrel and Rimsritong [25] compared the relative destructive effects of various widths of single tires and dual tires. Elastic layer analysis was used to calculate the horizontal tensile strains at the bottom of the asphalt pavement. The maximum radial strain for each tire size and load was used to calculate the load repetitions to failure using the fatigue relationship shown in Figure 30, which was based on work performed by Epps and Monismith. To simulate tire widths for various wheel loads, the contact pressure was varied as shown in Table 15. The relationship developed for repetitions to failure for various pavement sections and tire widths is shown in Figures 31 and 32.

Flexible Pavement Study Approach

The development of flexible pavement equivalency factors for axles with single tires to axles with dual tires is an extension of the earlier study performed by Terrel and Rimsritong [25] for the Washington State Highway Commission. In their study several thicknesses of pavement structures were used: 3, 6 and 9.5 inches of asphalt concrete pavement on 8 inches of crushed aggregate base. These sections represent the range of flexible pavement structures generally constructed in Washington State and were used in the analysis being reported in this report.

The calculation of stresses, strains and deflections in the pavement resulting from various wheel loads was performed using layered elastic theory. Where appropriate the values contained in Terrel and

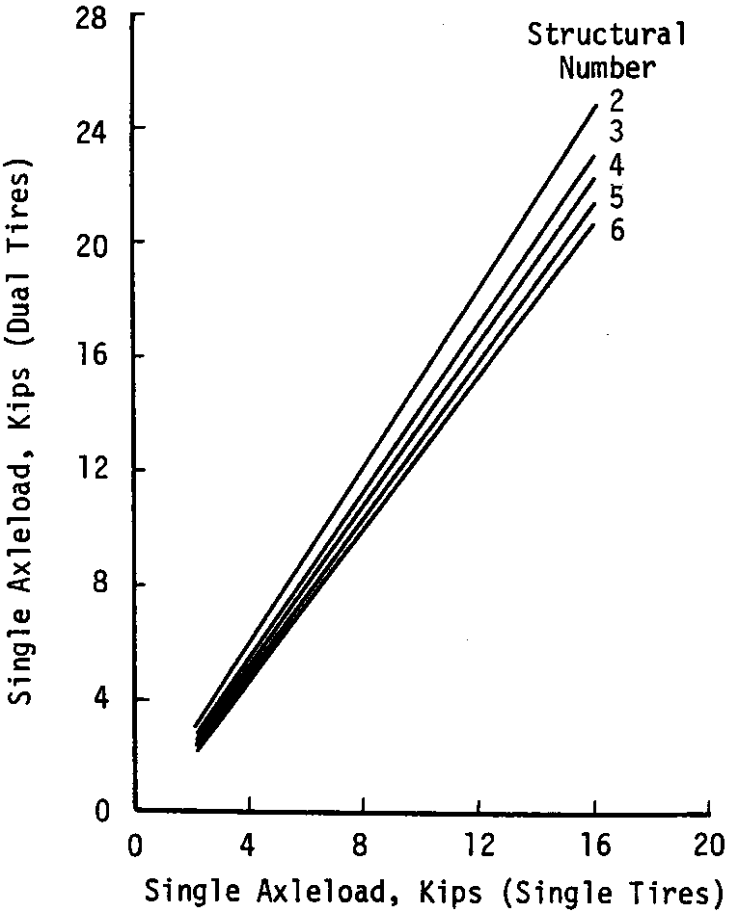

Figure 29. Load Equivalency Between Single and Dual Tires as Developed by Deacon [from Ref. 6]

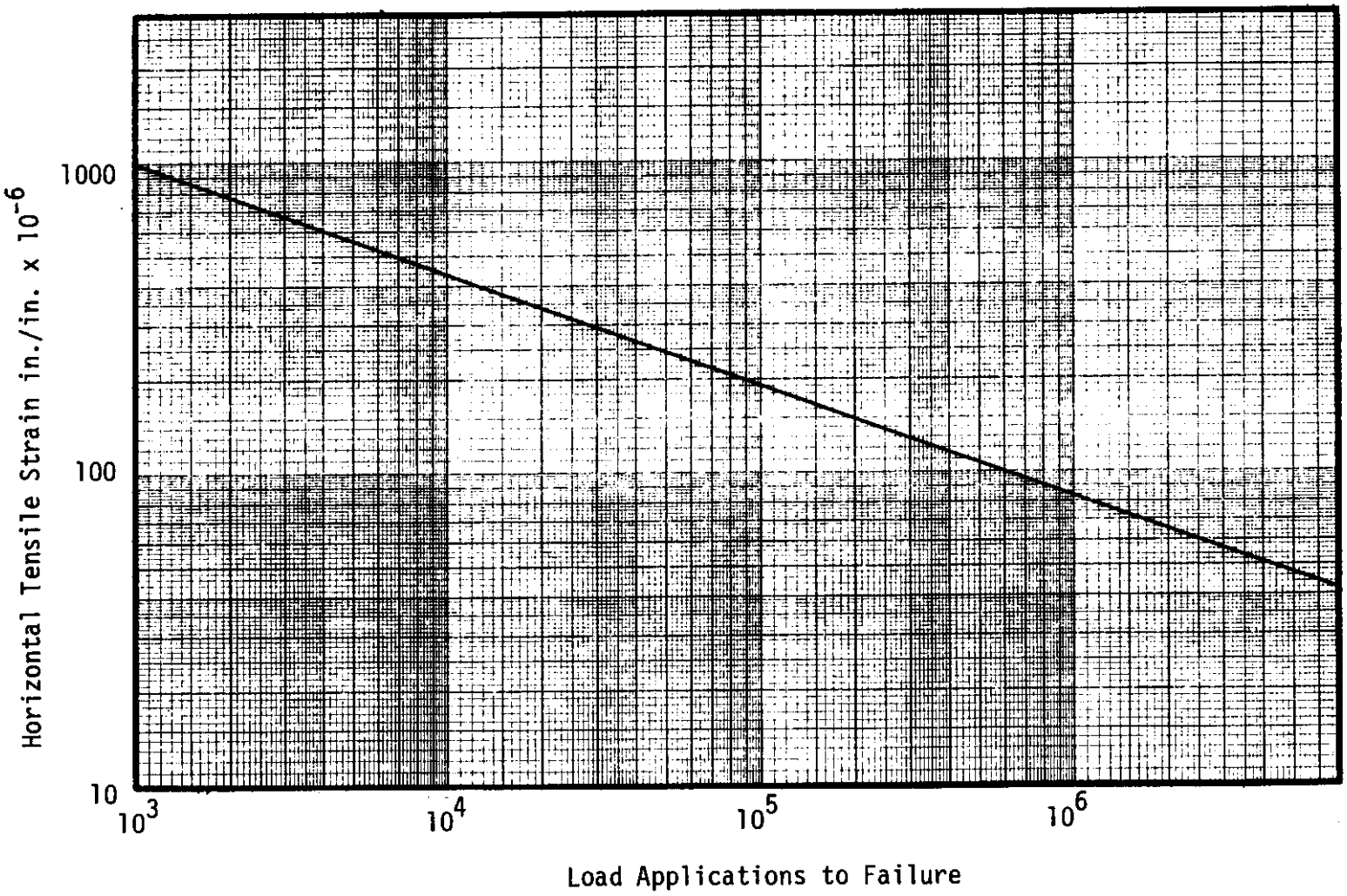

Figure 30. Relationship Between Horizontal Tensile Strain at the Bottom of Asphalt Concrete and Allowable Number of Load Applications used by Terrel and Rimsritong, Based on Work by Epps and Monismith [From Reference 25]

Table 15. Tire Contact Pressures Used by Terrel and Rimsritong to Simulate Tire Widths [From Reference 25]

Tire Width (in.)	Contract Area ($in.^2$)	Wheel Load (lb.)	Contact Pressure (psi)
8	50.27	4,000	79.58
		6,000	119.37
		8,000	159.15
10	78.54	4.000	50.93
		6,000	76.40
		8,000	101.86
		10,000	127.32
15	176.71	6,000	33.95
		8,000	45.27
		10,000	56.59
		12,000	67.59
18.5	268.80	6,000	22.32
		8,000	29.76
		10,000	37.20
		12,000	44.64

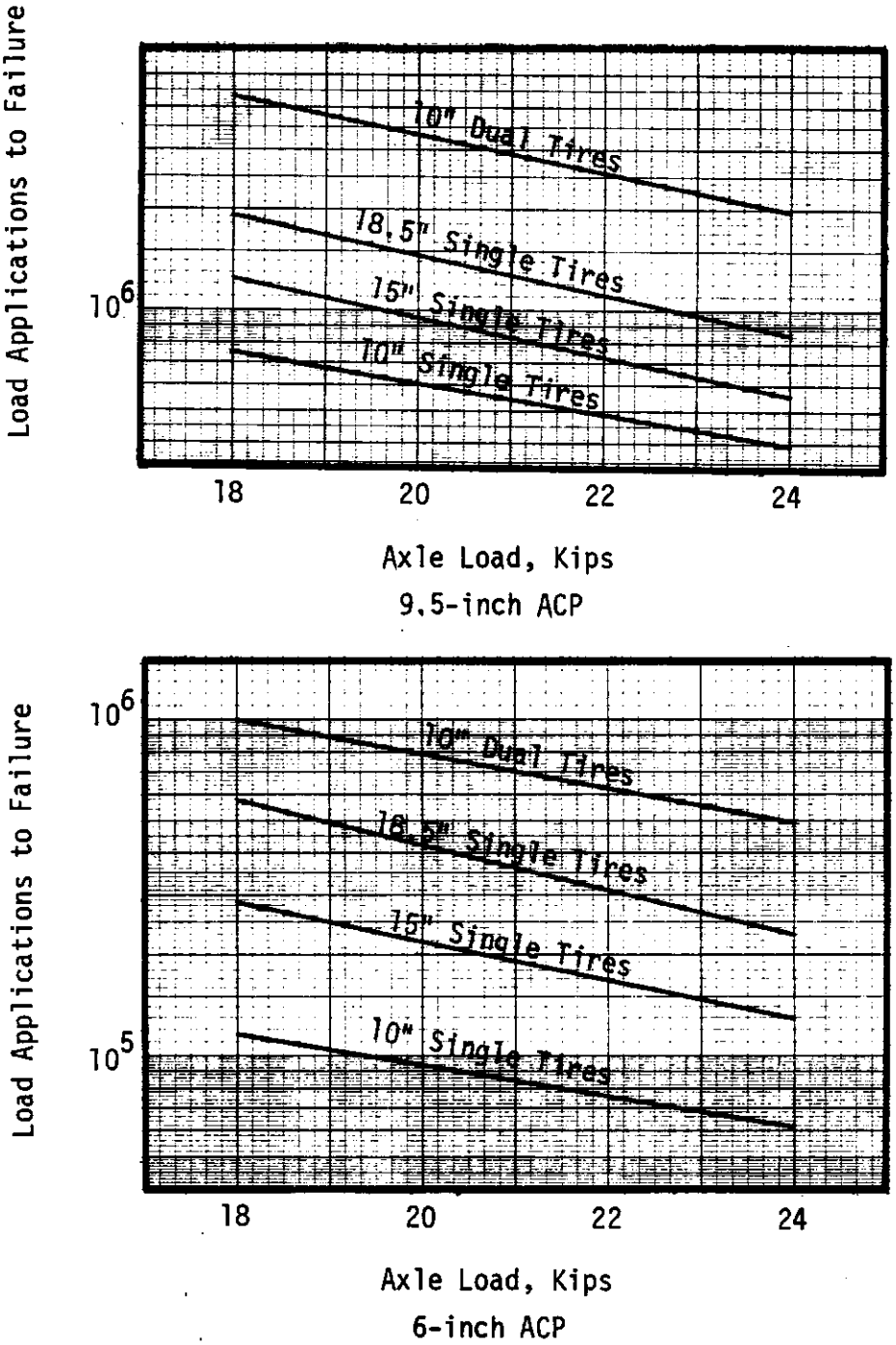

Figure 31. Equivalencies for Fatigue Behavior Developed by Terrel and Rimsritong [25] for 9.5-inch and 6-inch Pavements

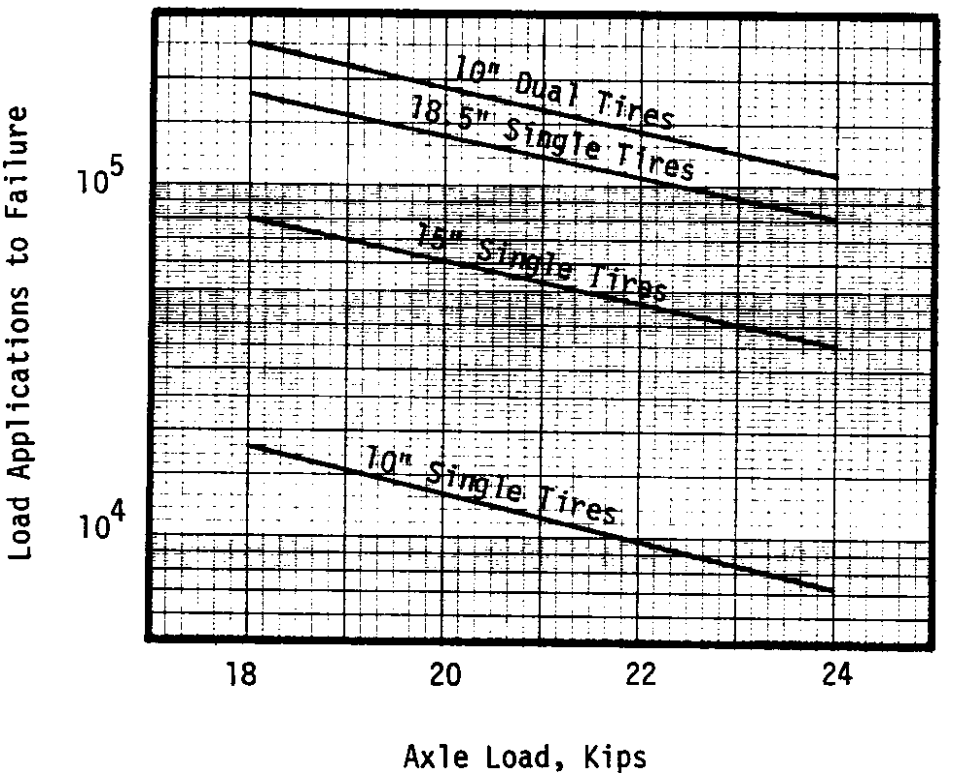

Figure 32. Equivalencies for Fatigue Behavior Developed by Terrel and Rimsritong [25] for 3-inch Asphalt Concrete Pavement

Rimsritong's report [25] were used. For the additional cases analysed in this study, the Multi-Layer Elastic Theory Iterative Method-Dual Wheel Option (PSAD2A) computer program was used to calculate stresses, strains and deflections in the pavement [8]. PSAD2A has the capability of printing stresses and strains due to dual wheel configurations. In addition, for layers with stress dependent resilient modulus values, the modulus can be determined through an iterative process.

Material Properties

The use of an elastic layer program requires that a proper value for the resilient modulus and Poisson's ratio be selected for each layer.

Asphalt Concrete

The resilient modulus of asphalt concrete is a function of its temperature. It is obtained by testing over a range of temperatures from 40°F to 100°F at a time loading of 0.1 second. Resilient modulus versus temperature relationships have been developed for Washington State University Test Track pavements [25]. They are shown in Figure 33. Using an average temperature condition of 68°F a resilient modulus of 400,000 psi was selected. The Poisson's ratio was assumed to be 0.3.

Crushed Aggregate Base

The resilient modulus of untreated aggregates is a function of the confining stress. Repeated load triaxial testing is used to develop the following relationship:

$$M_R = K_1 \theta^{K_2} \quad \text{.....(14)}$$

where

M_R = resilient modulus

θ = bulk stress ($\sigma_1 + 2\sigma_3$ in triaxial test)

K_1, K_2 = constants obtained from triaxial testing

The relationship developed for crushed aggregate base on a project at the Washington State University Test Track was [24]:

$$M_R = 2843\ \theta^{0.6} \quad \text{..... (15)}$$

This relationship and a Poisson's ratio of 0.4 were used for crushed

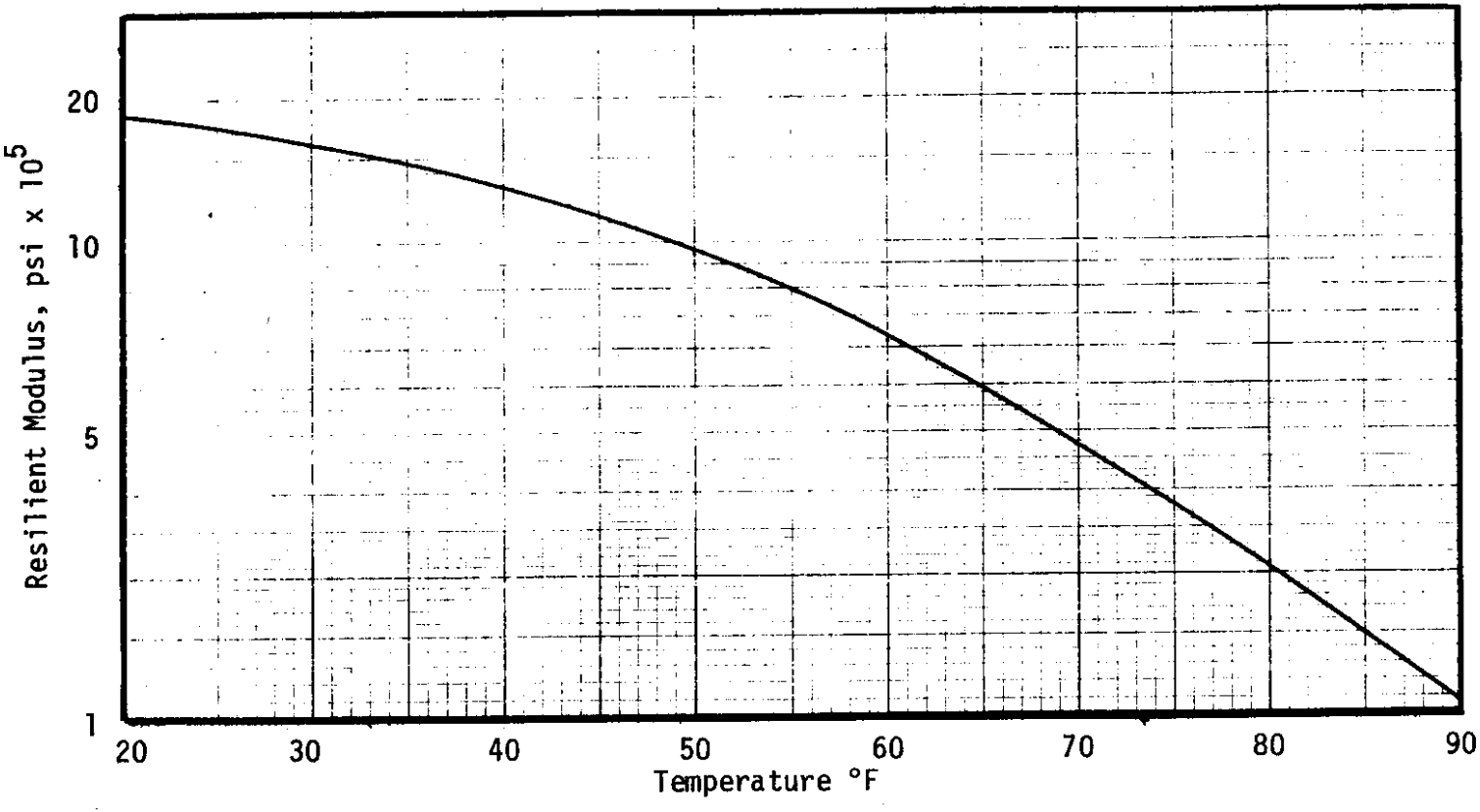

Figure 33. Resilient Modulus vs. Temperature Relationship for Asphalt Concrete Pavement [From Reference 25]

aggregate base in the analysis for this study.

Subgrade

A wide range of modulus values for subgrade materials are encountered on highway construction in the State of Washington. Terrel and Rimsritong [25] used an average value of 6,500 psi in their calculations. For uniformity this value was used in this study. The Poisson's ratio used was 0.45.

Fatigue Analysis

To compare axles with single tires to axles with dual tires, a fatigue distress model was used. Fatigue distress is assumed to be the cracking which results from repeated load applications and is a function of the maximum horizontal strain at the bottom of the asphalt concrete layer. Fatigue analysis was used because cracking is the principal form of asphalt pavement distress in Washington State. [27] The fatigue model used to calculate repetitions to failure was developed by Finn et al. [7] Its development was based on shifting laboratory fatigue curves to conform with field conditions, using AASHO Road Test data. The model used in this analysis predicts repetitions resulting in fatigue cracking equal to of less than 10 percent of the wheel path area is:

$$\log N_f = 15.947 - 3.219 \log (\varepsilon/10^{-6}) - 0.854 \log (|E^*|/10^3) \quad \ldots (16)$$

where N_f = repetitions to failure

ε = maximum tensile strain at the bottom of the asphalt bound layer

$|E^*|$ = resilient modulus in psi

Modeling Techniques Evaluated

Terrel and Rimsritong modeled tire width by adjusting the contact pressure. As shown in Table 15, this resulted in contact pressures which are not representative of contact pressures encountered in the field. Also, a large circle may not be representative of the shape of a wide tire under heavy loading.

To see if contact pressure or shape would have a major effect on the calculated tensile strains at the bottom of the pavement, two alternate modeling techniques were used. One was to model the width of a single tire using two adjacent circles with a constant contact pressure and

fit a fatigue curve. The second method was to model the width of the single tire using a single circle with a constant pressure and fit a fatigue curve. The results of the three techniques were then compared with the limited field data available.

When calculating the fatigue life for dual tires, Terrel and Rimsritong used the maximum horizontal radial strain at the bottom of the pavement. In analysing the strains under dual tires for various pavement sections and wheel loads it was noted that the tangential strain always exceeded the radial strain. For dual tires, these tangential strains are in the longitudinal pavement direction. Based on field experience at a number of test roads, higher tangential strains would be expected. Terrel reported [23] that the initial cracking at the Brampton Test Road, Morro Bay Test Road and the Washington State University Test Track were short transverse cracks. Measurements of horizontal strains at the bottom of the asphalt pavement, reported by Zube and Forsyth [30], also indicated that the maximum was in the longitudinal direction. Therefore, a decision was made to use maximum horizontal tensile strain at the bottom of the asphalt concrete layer to calculate fatigue life, which in all cases was tangential strain for dual tires.

The following is a description of the three analysis techniques used:

Constant Radius - Variable Pressure

This procedure is similar to the one used by Terrel and Rimsritong [25]. Three single tire widths were evaluated, 10, 15 and 18.5 inches. The width of each dual tire was 10 inches. The tire widths were maintained by varying the tire pressures as listed in Table 15. Equation (16) was used to calculate the fatigue life for various axle loads on the three pavement sections being evaluated. The horizontal tensile strains reported by Terrel and Rimsritong [25] were used for the single tires and maximum horizontal strains were calculated for the dual tires. Figures 34, 35 and 36 show the relationship developed between axle loads and repetitions to failure for the three pavement sections.

Double Circle - Constant Pressure

This method and the single circle - constant pressure method, to be discussed next, use the assumption that the axle load versus

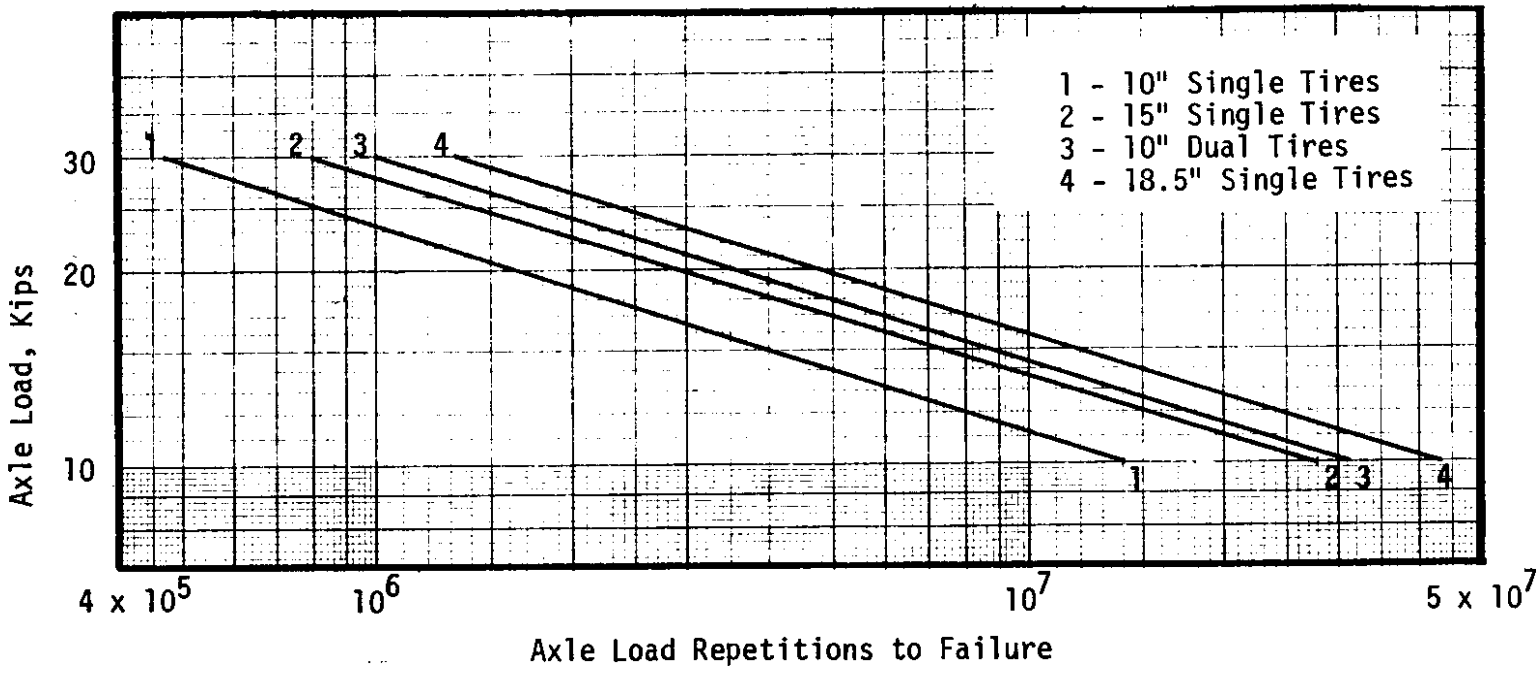

Figure 34. Axle Load Repetitions to Failure for Single Axles on a 9.5-inch Asphalt Concrete Pavement over an 8-inch Crushed Aggregate Base. Constant Radius Method.

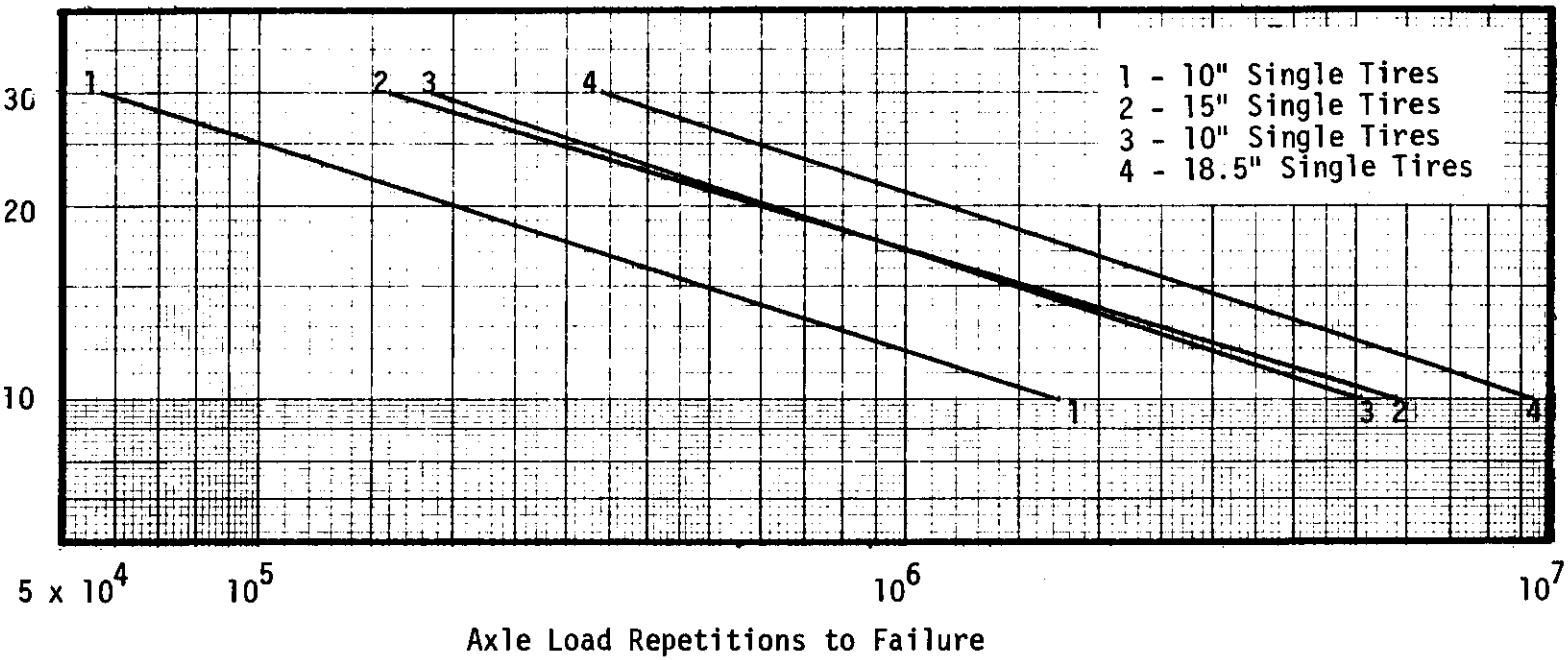

Figure 35. Axle Load Repetitions to Failure for Single Axles on a 6-inch Asphalt Concrete Pavement over an 8-inch Crushed Aggregate Base. Constant Radius Method.

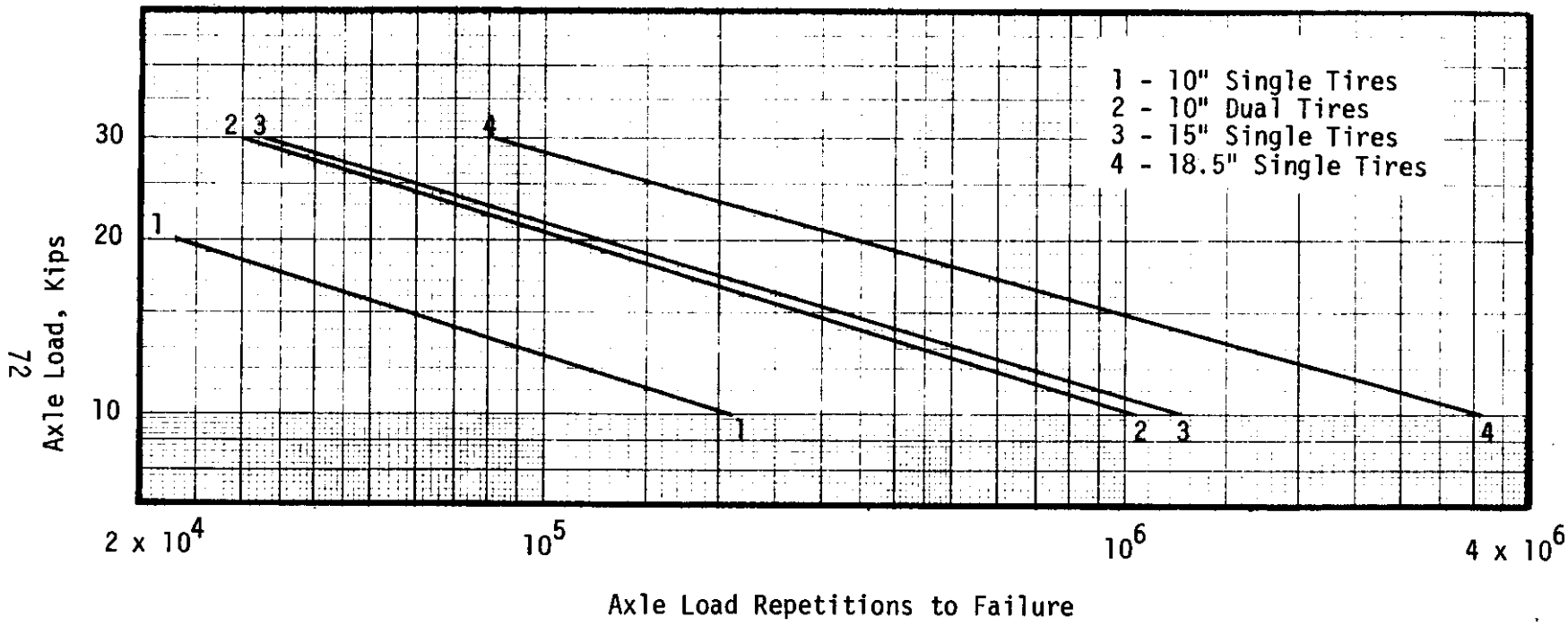

Figure 36. Axle Load Repetitions to Failure for Single Axles on a 3-inch Asphalt Concrete Pavement over an 8-inch Crushed Aggregate Base. Constant Radius Method.

repetitions to failure fatigue curves for various tire widths are parallel for a given pavement section. This assumption appears reasonable based on the analysis of concrete pavements described in this report and the constant radius - variable pressure method for flexible pavements. To determine the slope of the fatigue curves, curves were developed for dual tires. Two methods were used to develop these curves, applying the wheel load through a circle with constant radius and applying the load using a constant contact pressure of 80 psi. The slopes of the two curves were very close for the 9.5 inch asphalt concrete pavement section. The difference in slopes increased as the asphalt pavement section decreased. Figures 37, 38 and 39 show the relationships developed for 9.5, 6 and 3 inch asphalt concrete pavement sections on 8 inches of aggregate base. It was concluded that an average of the slopes of the two curves would be an adequate representation of the slope of the fatigue curve. For dual tires the average curve was fit through the intersection of the constant contact pressure curve and the constant radius curve. It is interesting to note that the constant pressure and the constant radius curves intersected between the 20 kip and 25 kip axle loads. This indicates that, in the load range generally used for elastic layer analysis of dual tire axle loads, the size of the loading circle and contact pressure are close to actual conditions.

To model tire width using the double circle method, two adjacent loading circles were used, with a constant contact pressure of 80 psi. The radius of the circles was chosen so that four times the radius equalled the desired tire width. The total area, of the two circles, was calculated and multiplied by the contact pressure. This represented the simulated load on the single tire and is illustrated in Figure 40.

The maximum horizontal tensile strain was determined using the PSAD2A program and the repetitions to failure calculated using Equation (16). The point representing axle load versus number of repetitions to failure was plotted and a fatigue curve fit through the point. Calculations were made for simulated tire widths of 10, 12, 14, 16 and 18

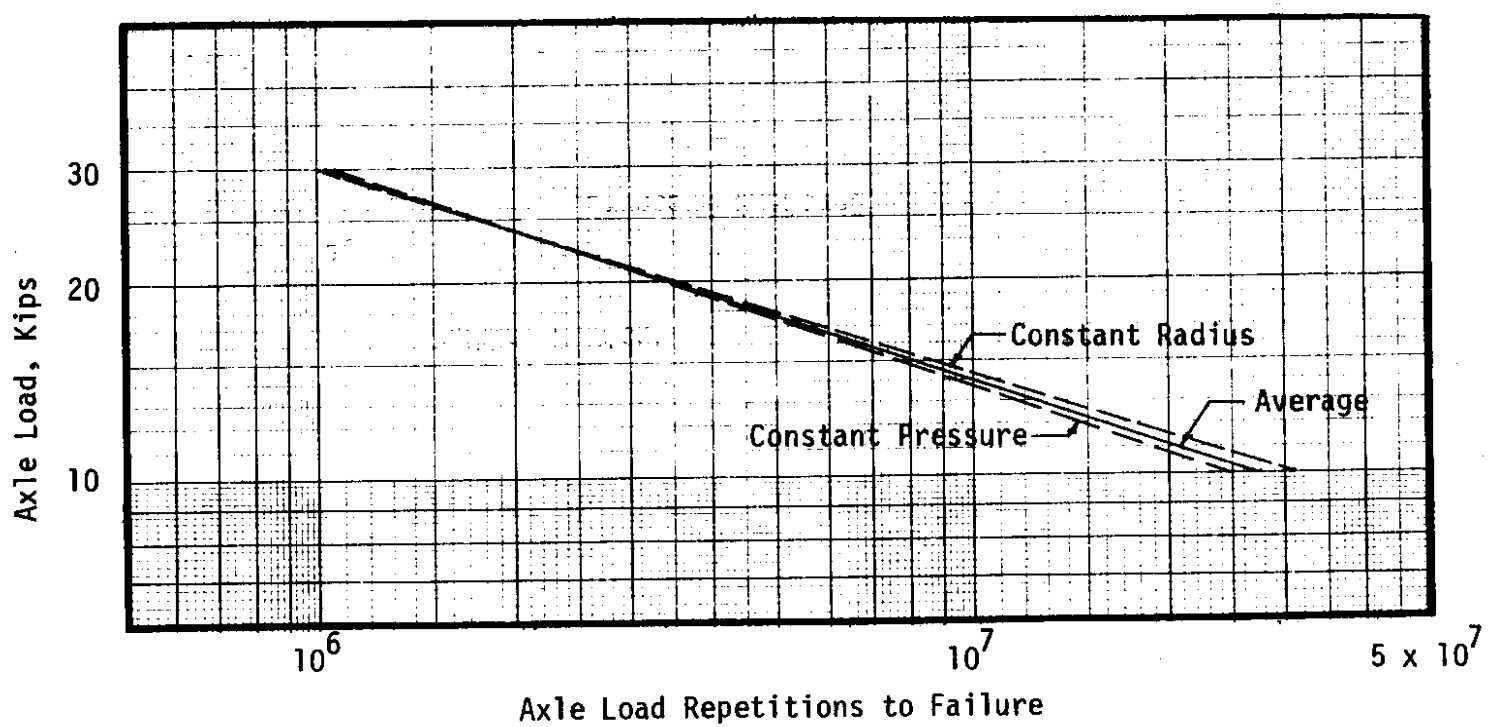

Figure 37. Fatigue Relationship for Single Axles with Dual Tires, 9.5-inch Asphalt Concrete Pavement over 8-inches of Crushed Aggregate Base

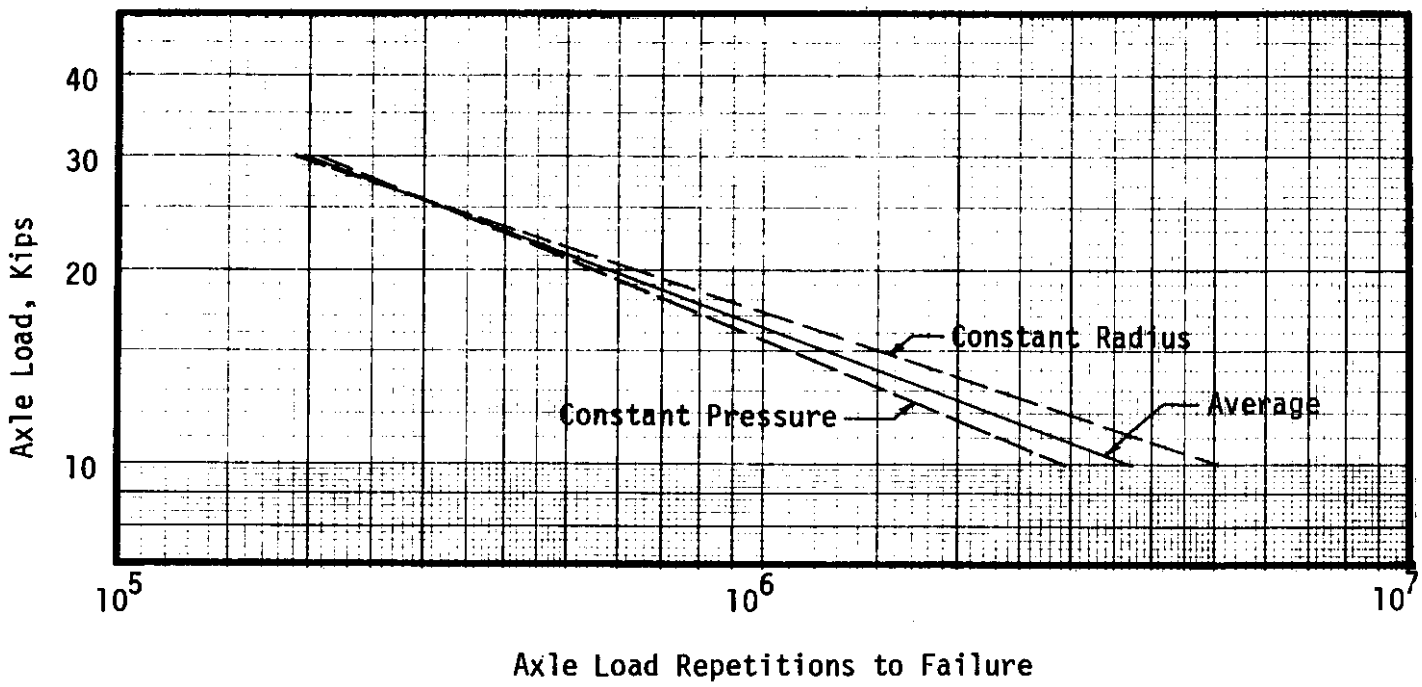

Figure 38. Fatigue Relationship for Single Axles with Dual Tires, 6-inch Asphalt Concrete Pavement over 8-inches of Crushed Aggregate Base

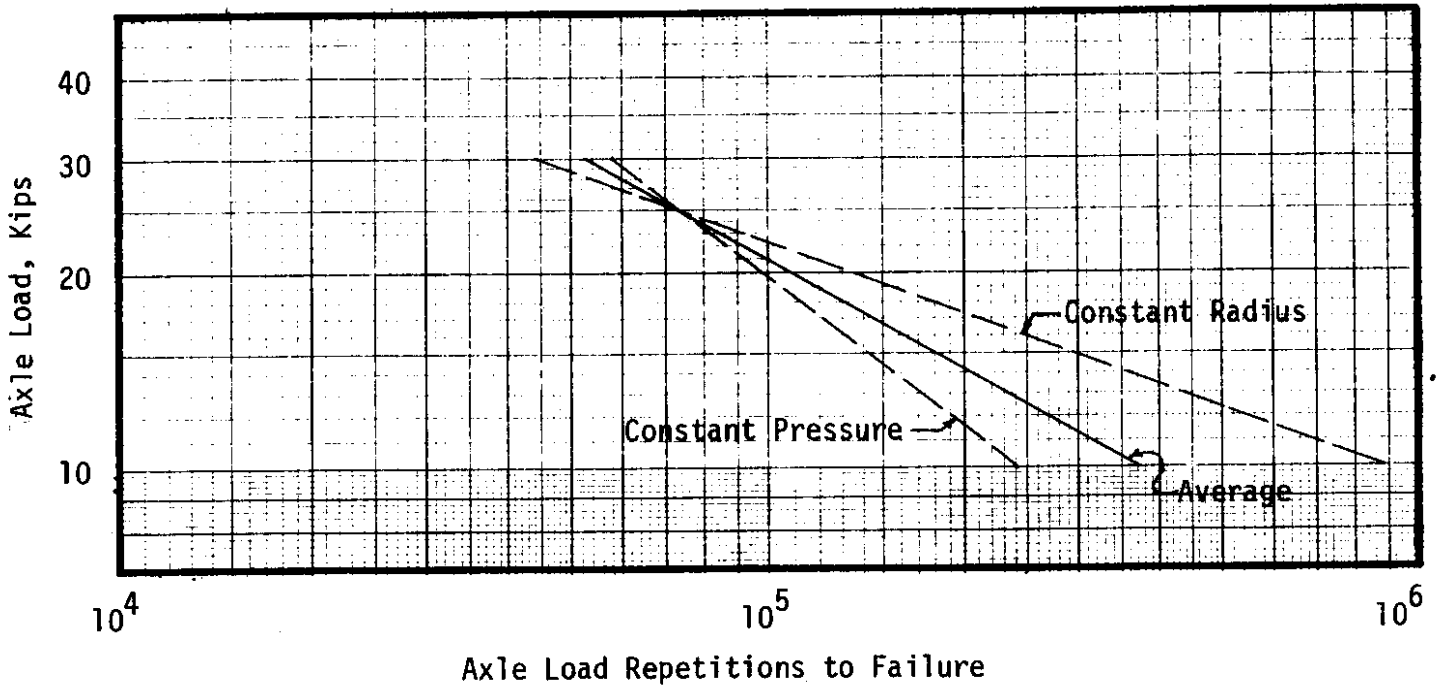

Figure 39. Fatigue Relationship for Single Axles with Dual Tires, 3-inch Asphalt Concrete Pavement over 8-inches of Crushed Aggregate Base

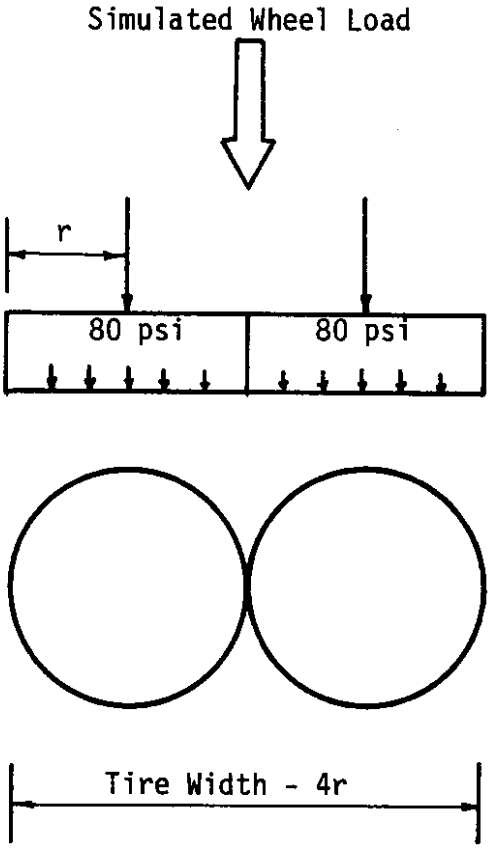

Figure 40. Simulated Single Tires Using Adjacent Circular Loads

inches. The resulting relationships are shown for the three pavement sections in Figures 41, 42 and 43.

Single Circle - Constant Pressure

This method is similar to the double circle method. In this case, the diameter of the circle was chosen to equal the width of the tire to be simulated. The wheel load was equal to the area of the circle times the contact pressure, which was held constant at 80 psi. The maximum horizontal strain at the bottom of the asphalt pavement section was calculated and repetitions to failure determined. A fatigue curve was then fit through the point using the same fatigue curve slopes as those in the double circle method. Fatigue curves were developed for 10, 12, 14, 16 and 18 inch tires. The curves are shown in Figures 44, 45 and 46.

Single Versus Dual Tire Equivalency

For each method and pavement thickness, the percent of dual tire axle load that axles with single tires could carry and have an equivalent fatigue life was determined. These equivalencies were determined graphically using the fatigue curves in Figures 41 through 46. The equivalency relationships for 9.5, 6 and 3 inch asphalt concrete pavements are shown in Figures 47 - 49. Because of the wide range between the double circle and two single circle methods, actual measurements of the effects of single versus dual tires were needed.

There have been only a limited number of investigations to measure the actual effects of dual tires versus single tires on pavement performance. At the AASHO Road Test an investigation was conducted to determine the performance and deflections for a number of pavement sections under the loadings of several pieces of specialized units of military highway and off-highway equipment [9]. These included the study of the use of low pressure - low Silhouette (LPLS) tires on tractor and semi-trailer units and the effects of the use of the GOER a self-propelled cargo or fluid transporter resembling a conventional two axle tractor scraper.

The LPLS tire was designed for a 6,000 lb wheel load at a 35 psi inflation pressure. The contact print for the LPLS tire is

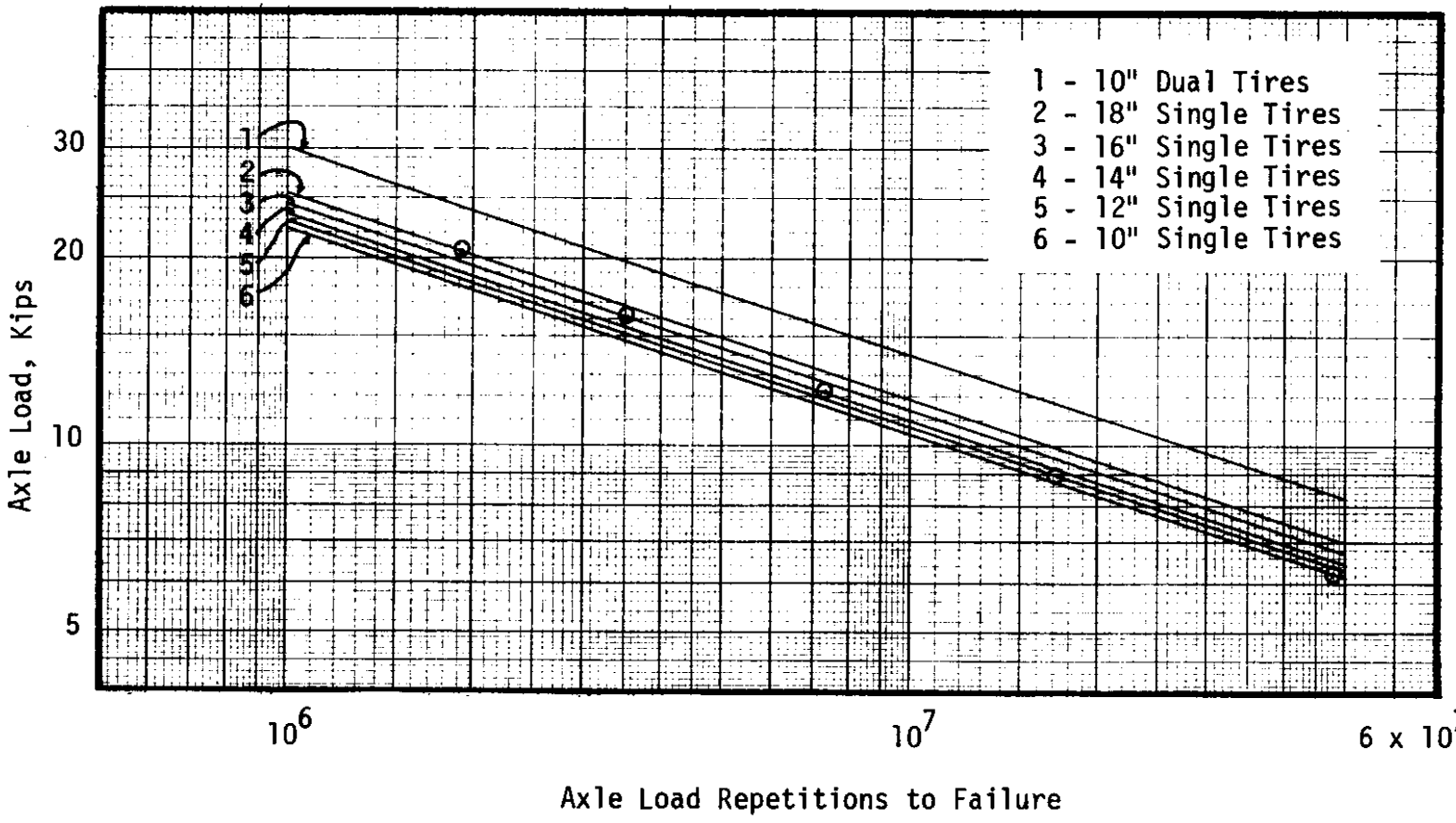

Figure 41. Axle Load Repetitions to Failure for Single Axles on a 9.5-inch Asphalt Concrete Pavement over an 8-inch Crushed Aggregate Base. Double Circle Method.

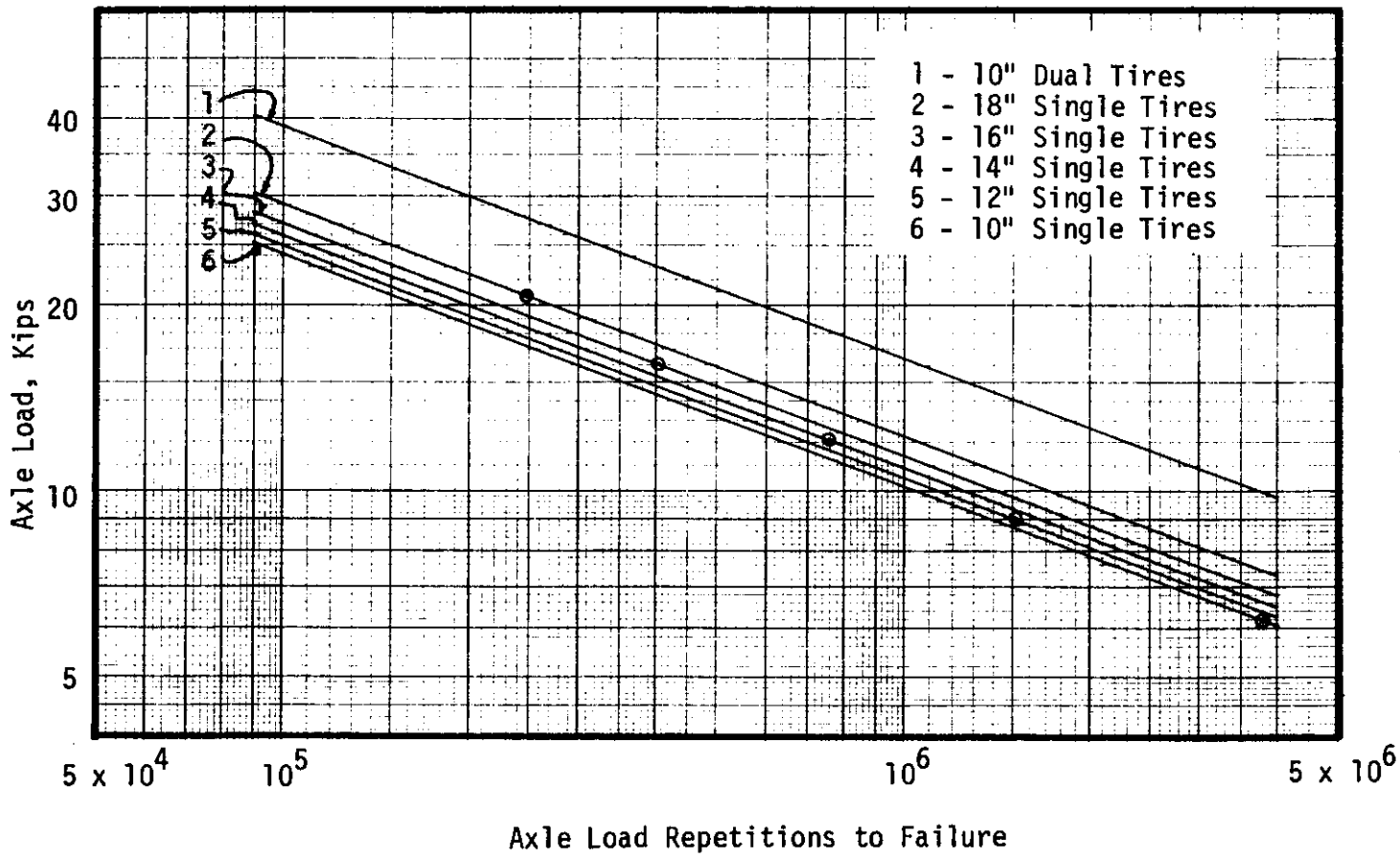

Figure 42. Axle Load Repetitions to Failure for Single Axles on a 6-inch Asphalt Concrete Pavement over an 8-inch Crushed Aggregate Base. Double Circle Method.

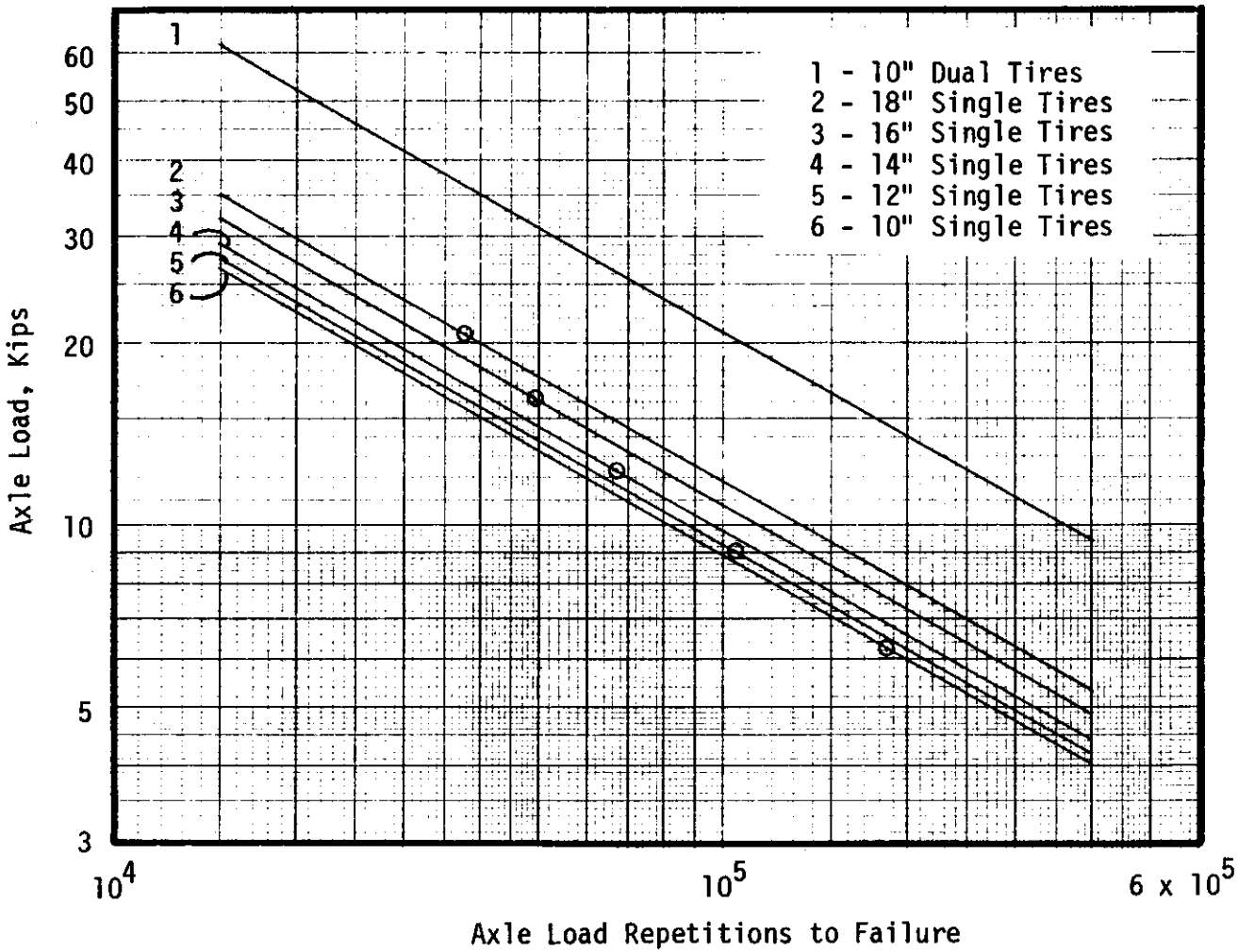

Figure 43. Axle Load Repetitions to Failure for Single Axles on a 3-inch Asphalt Concrete Pavement over an 8-inch Crushed Aggregate Base. Double Circle Method.

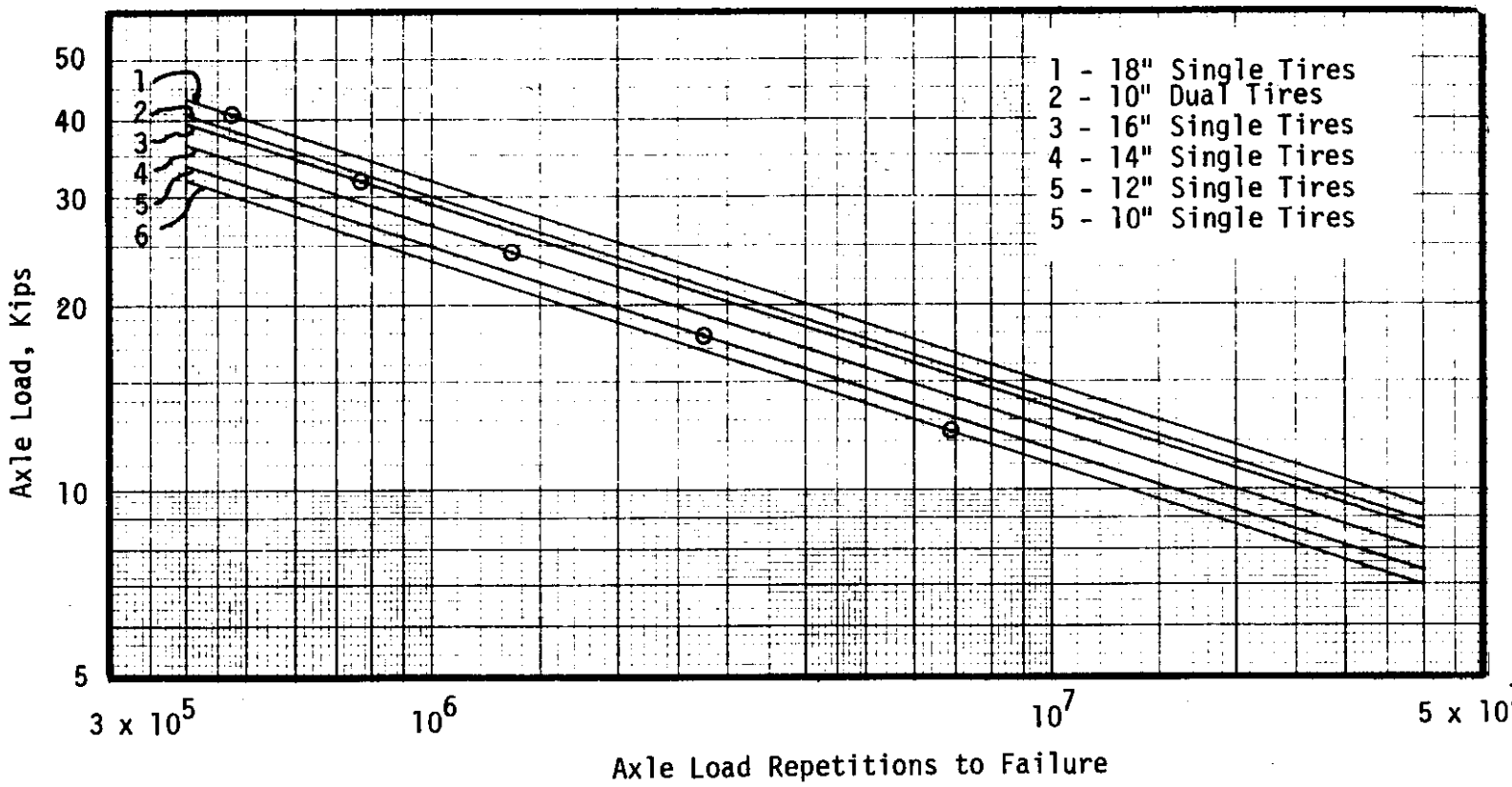

Figure 44. Axle Load Repetitions to Failure for Single Axles on a 9.5-inch Asphalt Concrete Pavement over an 8-inch Crushed Aggregate Base. Single - Constant Pressure Method

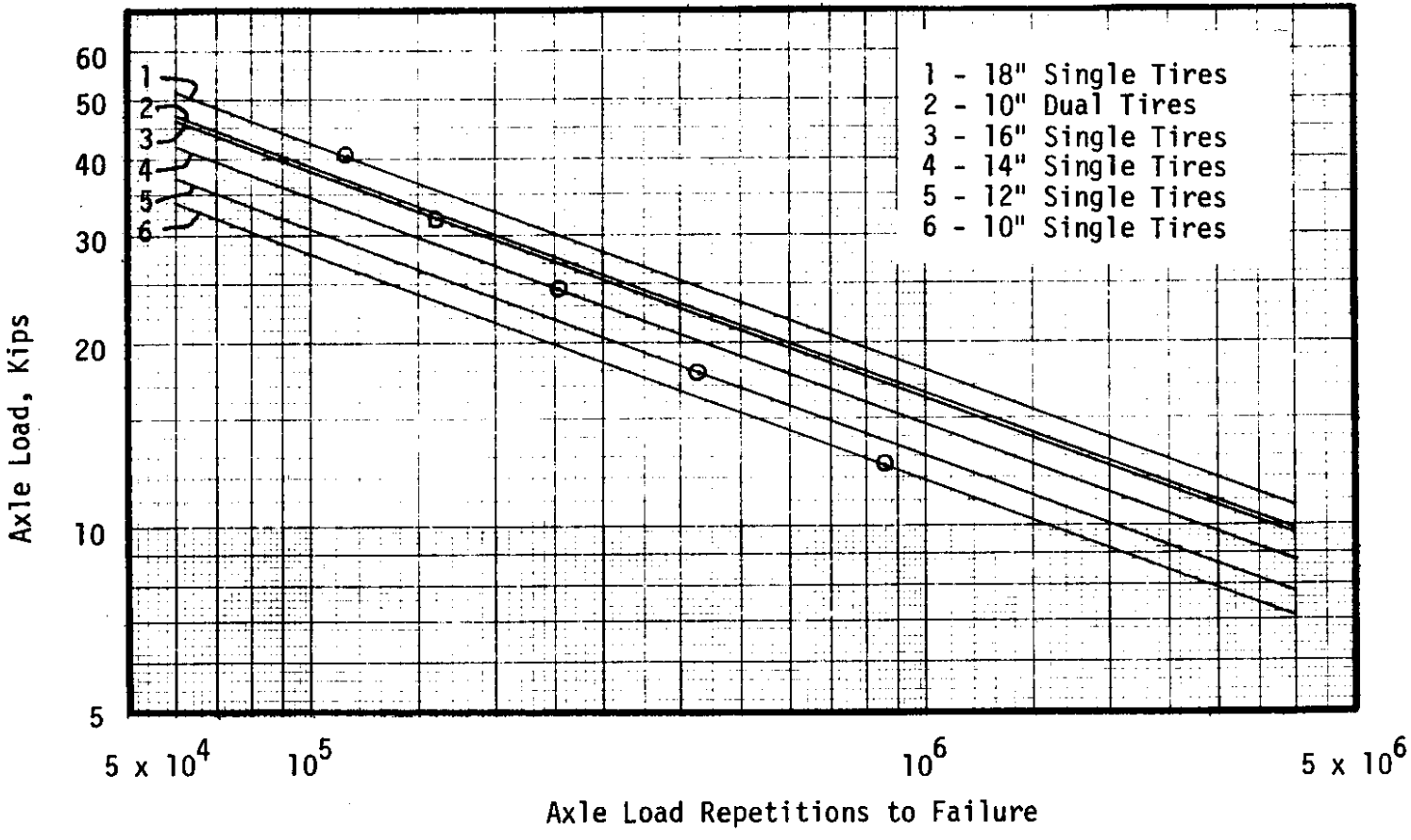

Figure 45. Axle Load Repetitions to Failure for Single Axles on a 6-inch Asphalt Concrete Pavement over an 8-inch Crushed Aggregate Base. Single Circle - Constant Pressure Method

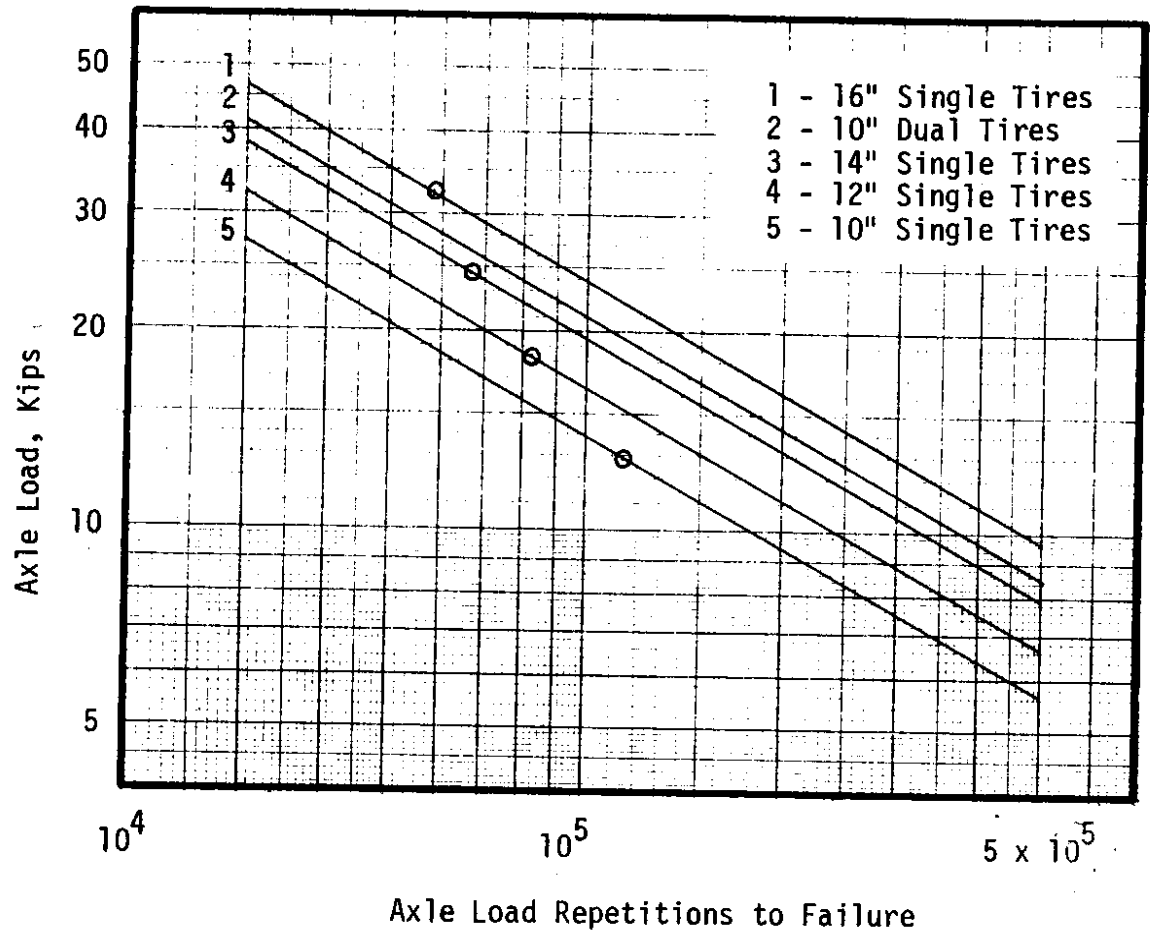

Figure 46. Axle Load Repetitions to Failure for Single Axles on a 3-inch Asphalt Concrete Pavement over an 8-inch Crushed Aggregate Base. Single Circle - Constant Pressure Method.

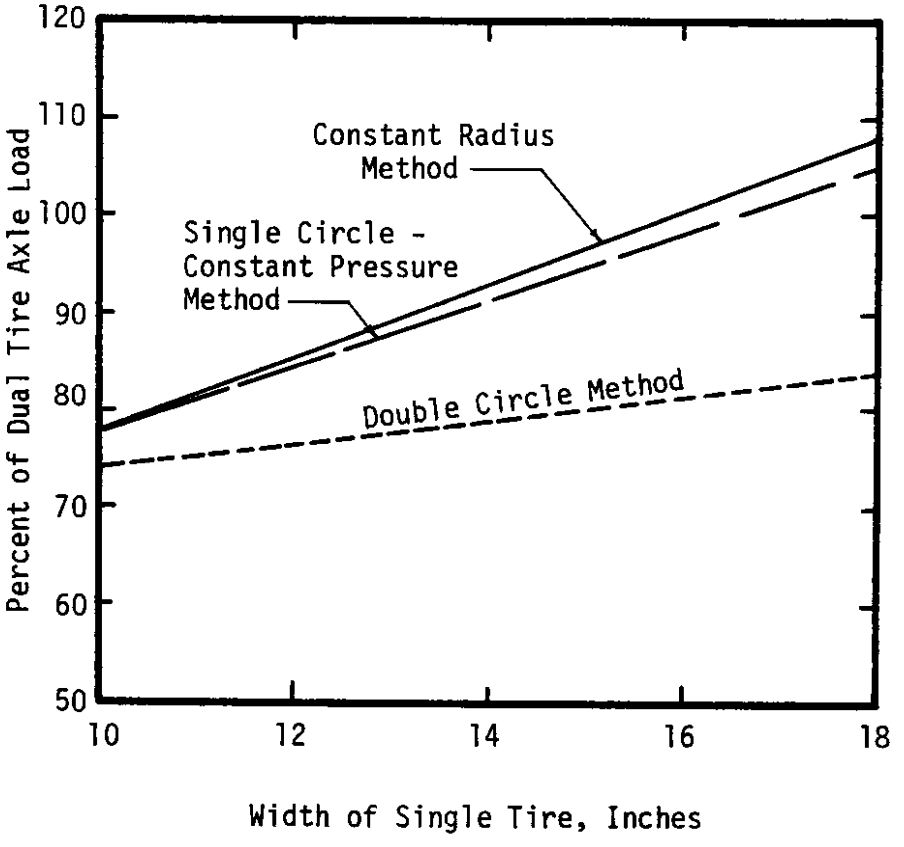

Figure 47. Percent of Dual Tire Axle Load Which an Axle with Single Tires Can Carry for Equivalent Fatigue Life. 9.5-inch Asphalt Concrete Pavement.

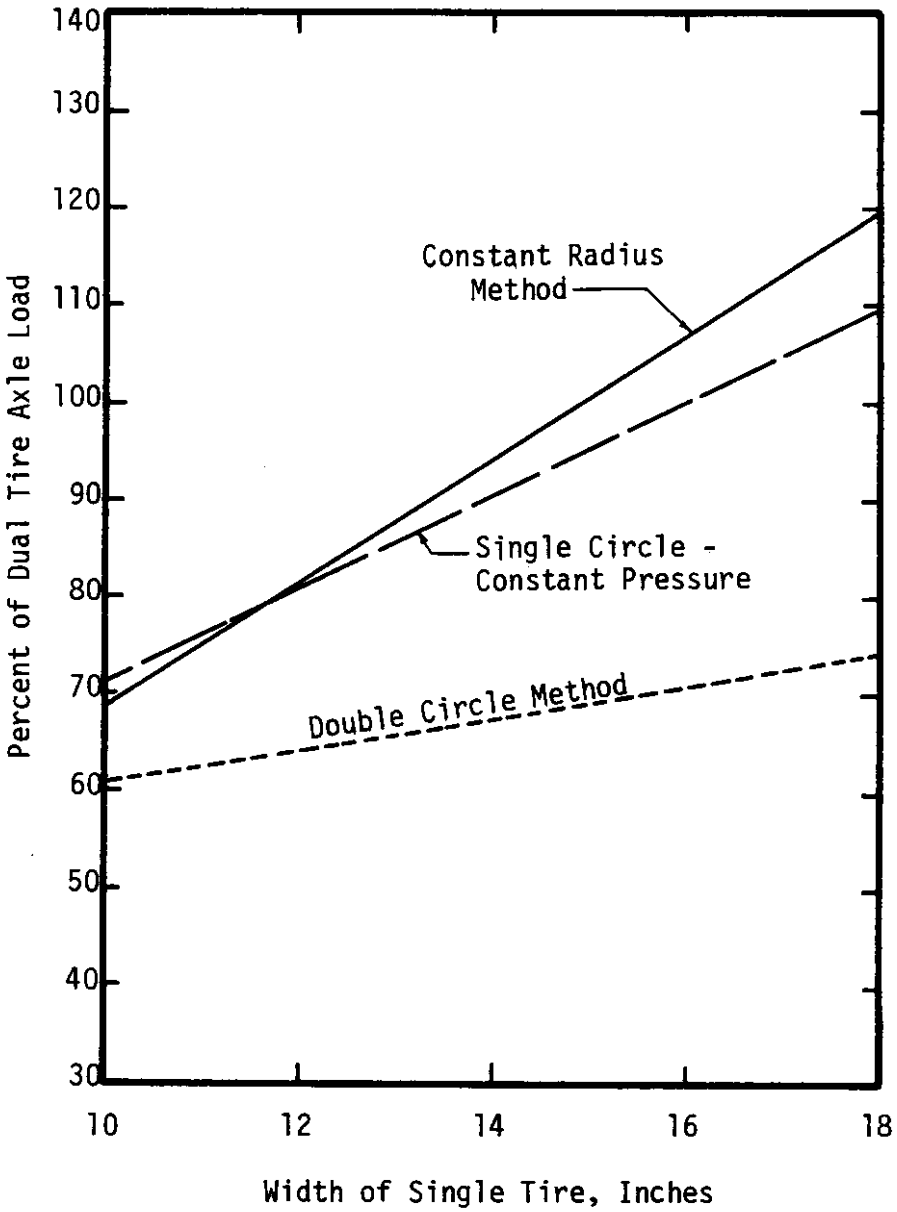

Figure 48. Percent of Dual Tire Axle Load Which an Axle with Single Tires Can Carry for Equivalent Fatigue Life. 6-inch Asphalt Concrete Pavement.

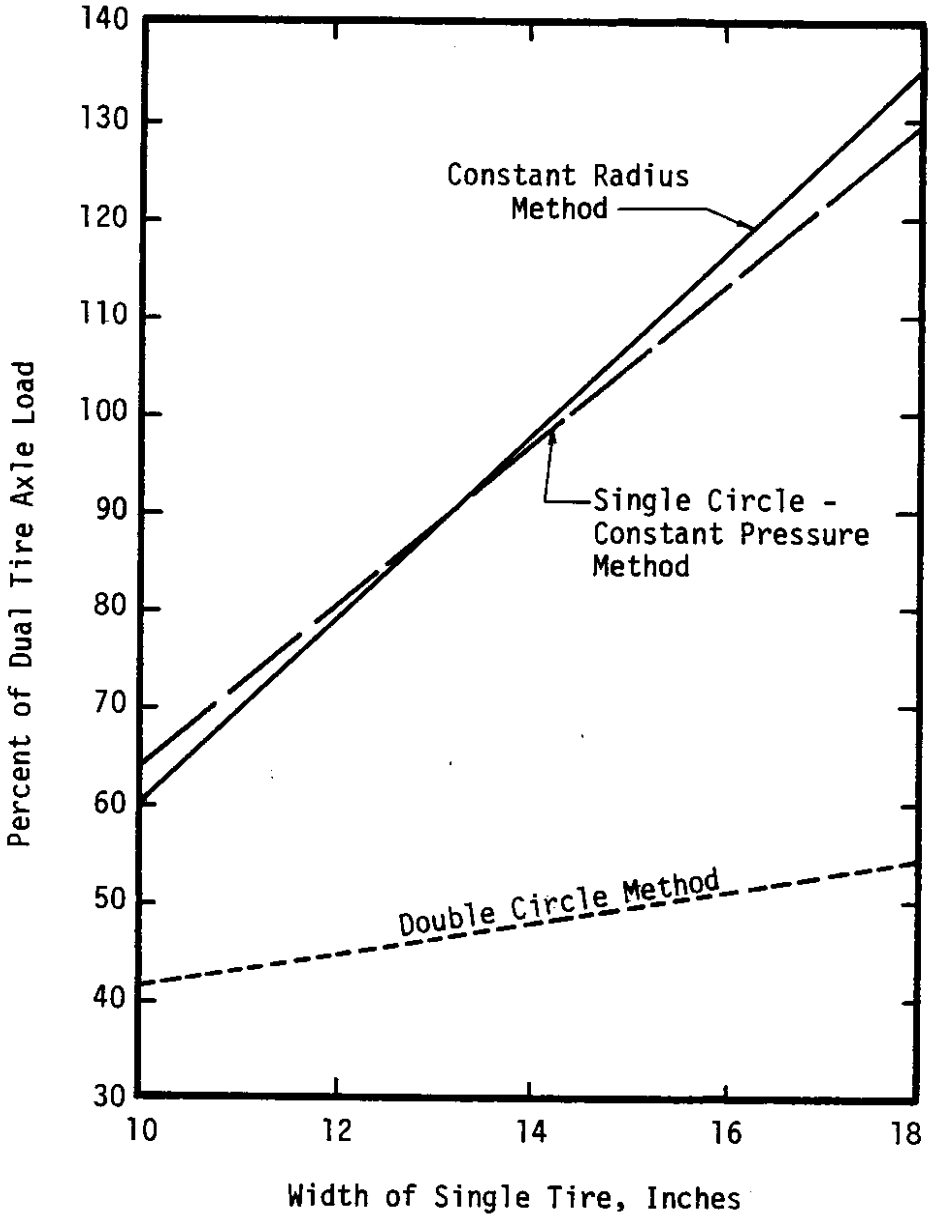

Figure 49. Percent of Dual Tire Axle Load Which an Axle with Single Tires Can Carry for Equivalent Fatigue Life. 3-inch Asphalt Concrete Pavement.

approximately rectangular with a width of approximately 21 inches. The width of the LPLS tire was comparable to the width of military tread dual tires used for comparison, Figure 50.

Comparison studies were made on Loop 2 of the AASHO Road Test between tractor and semi-trailer units equiped with LPLS tires and units with conventional dual (standard military tread) tires. For both flexible and rigid pavements, the loss in serviceability for the sections subjected to the LPLS tires was generally less than for sections subjected to conventional tires.

Figure 51 shows the serviceability trends for a section with 3 inches of asphalt concrete pavement, 6 inches of aggregate base and 4 inches of subbase. This section had the thickest flexible pavement section in this study and is close to the 3 inch ACP section used in the elastic layer analysis. The plot of serviceability trends indicates approximately 1.25 more applications of the LPLS tire axles than the conventional tires were required to reach, a present serviceability index of 2.5. Based on the fatigue curve for a 3 inch asphalt concrete pavement, the LPLS axle could carry 115 percent of a dual tire axle and achieve the same repetitions to a psi of 2.5. However, prior to these studies Lane 1 of Loop 2 had been subjected to over one million 2 kip axle loads and Lane 2 to an equal number of 6 kip axle loads. The influence of this traffic is not known. Since the LPLS tired vehicles were operated in Lane 1, it probably influenced the results in favor of the LPLS tires.

The GOER was equiped with 29.5 x 25/16 inch tires inflated between 25 and 35 psi. The contact width of these tires is approximately 25 inches. Relationships were developed for flexible pavement deflection and axle load for conventional dual tires and GOER tires. This relationship for a section with 5 inches ACP over 9 inches base and 16 inches of subbase is shown in Figure 52. This figure indicates that a wheel load on the GOER tire equals approximately 125 percent of a dual tire load which would cause a similar deflection for a 10 kip wheel load (20-kip axle load).

Based on the studies of the LPLS and GOER tires, it appears

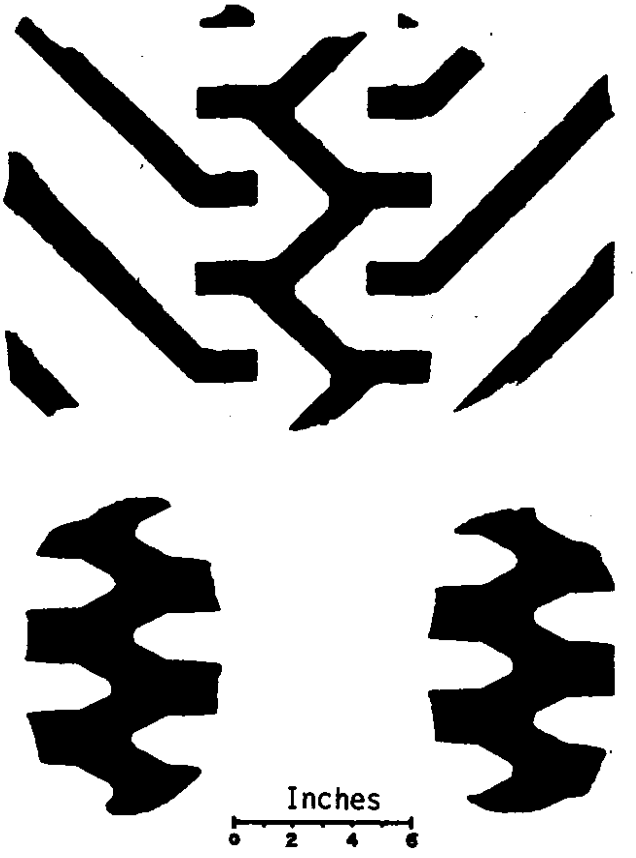

Figure 50. Contact Prints for LPLS (top and Conventional Tires (bottom) [From Reference 9]

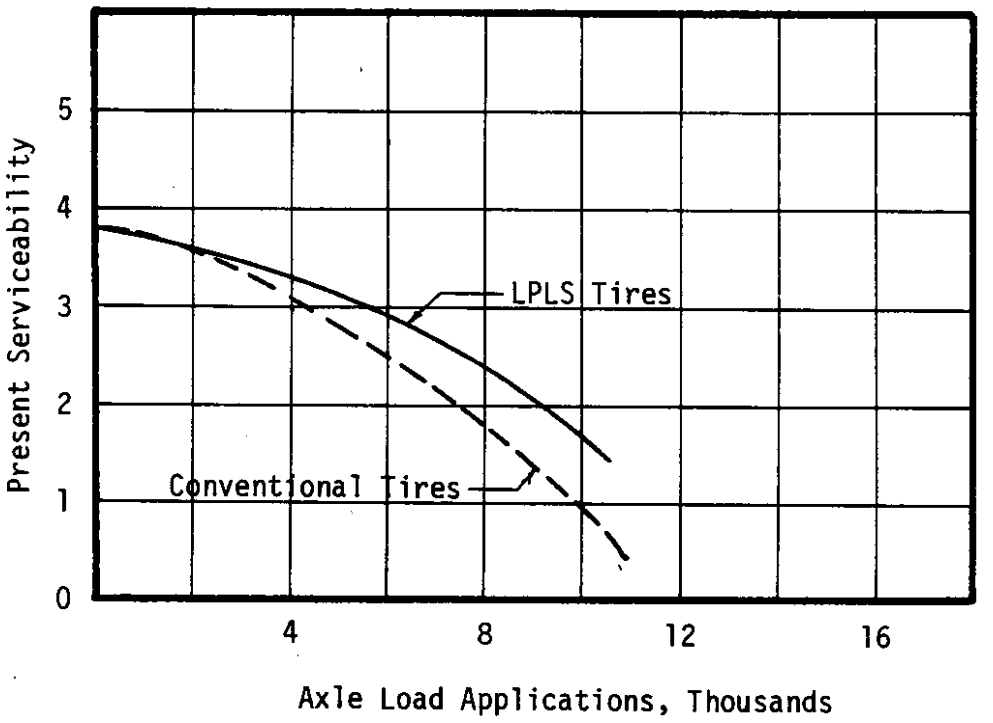

Figure 51. Comparison of Serviceability Trends for LPLS and Conventional Tires [9]

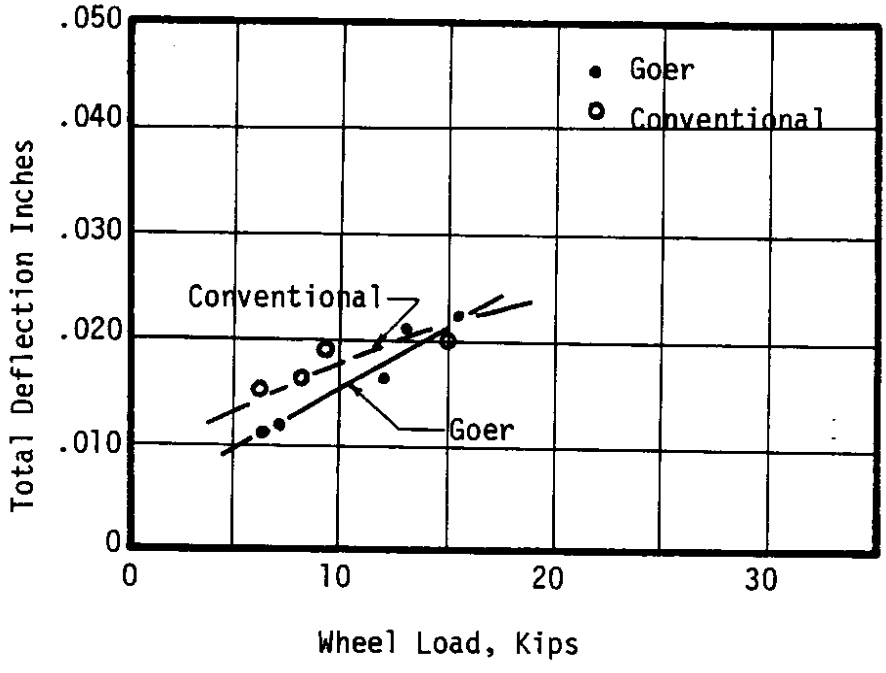

Figure 52. Relationship Between Deflection and Wheel Load, Section 265 of the AASHTO Road Test [9]

realistic to assume that an axle with single flotation tires with a width equal to a set of dual tires (approximately 25 inches) should be able to carry a load equal to 120 percent of the dual tire axle load to give an equal fatigue life.

Zube and Forsyth [30] reported on a study made by the California Division of Highways in 1963 to determine the single wheel - single axle loading which would produce the same destructive effect as a dual wheel single axle loading of 18,000 lb. The size of single tire evaluated was an 18.00 - 19.5 tire with a 16 ply wide base casing inflated to 75 psi. The approximate contact width for this tire was 12 inches. They concluded that based on pavement deflections as a criterion, the destructive effect of a flotation tire with a single-axle loading of 12,000 lb equals or exceeds that of a dual-wheel configuration at an axle loading of 18,000 lb.

At one test site, it was possible for them to obtain both transverse and longitudinal strain measurements from the bottom of the asphalt surfacing. They found that the longitudinal strain was higher than the transverse strain. The longitudinal strains measured are shown in Figure 53. There is very little information on the thickness of a pavement section or its material properties. They do indicate that the section consisted of 3 inches of new ACP over 2 inches of old ACP over a variable asphalt treated base. Based on the measured strain of 380 micro inches/inch for dual tires, structurally the section would lie close to the 3 inch ACP sections used in the elastic layer analysis for this study.

The measured strains were used in a fatigue analysis. This analysis indicated that the 12 inch flotation tire could carry 62 percent of the dual tire axle load and have an equivalent destructive effect.

Based on the AASHO Road Test data, an axle with 25 inch wide tires on a 3 inch asphalt concrete pavement should be able to carry 120 percent of a dual tire axle load and have an equivalent destructive effect in fatigue. The California study indicates that an axle with 12 inch wide tires, on a pavement with a section equivalent to 3 to 4 inches of asphalt concrete on an 8 inch aggregate base, should be able to carry

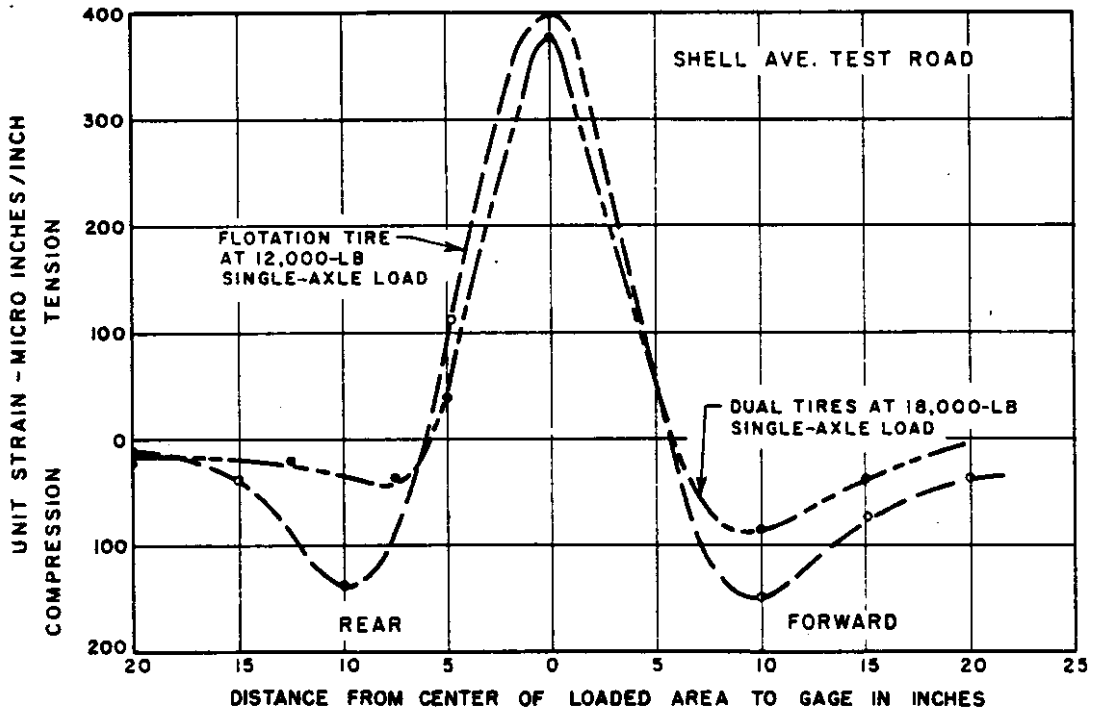

Figure 53. Longitudinal Strain Measured at the Bottom of a 3-inch Asphalt Concrete Pavement by Zube and Forsyth [from Ref. 30]

62 percent of a dual tire axle load. Figure 54 shows these points on a plot of the equivalency relationships developed for single versus dual tires on a 3 inch pavement. Connecting these points indicates that the field data falls approximately midway between the lines developed using single circles and the line developed using double circles. Therefore, an average relationship was developed between the single circle methods and the double circle method. This was accomplished by first developing an average single circle relationship and then combining this with the double circle relationship. The results are shown in Figure 55. Figure 55 indicates that the average single tire to dual tire equivalency is very close to the equivalency developed using field data. For this reason, it was decided to use an average between the single circle and double circle equivalencies for all three pavement sections. These are shown in Figure 56.

Equivalent Wheel Load Factors

The average fatigue curves for dual tires, Figures 37, 38 and 39 were used to develop traffic equivalence factors for single axles with dual tires. For single axles with single tires, fatigue relationships were developed by applying the dual tire equivalencies in Figure 56 to the dual tire fatigue curves. For example, if the single axle with single tires could carry 80 percent of the dual tire axle load and have an equivalent fatigue life, the axle with single tires would have the same fatigue life at a 16 kip axle load as an axle with dual tires and an axle load of 20 kips. Equivalency factors were developed for sections with approximate AASHO structural numbers (SN) of 2, 4 and 6 [1]. The equivalency factors represent 18-kip single axle dual tired axle repetitions where:

$$F_i = \frac{N_{18}}{Ni}$$

F_i = equivalency factor

N_{18} = repetitions to failure for an 18-kip single axle dual tire load

Ni = repetitions to failure for the axle load and tire configuration in question

The equivalency factors are listed in Tables 16, 17, 18 and 19.

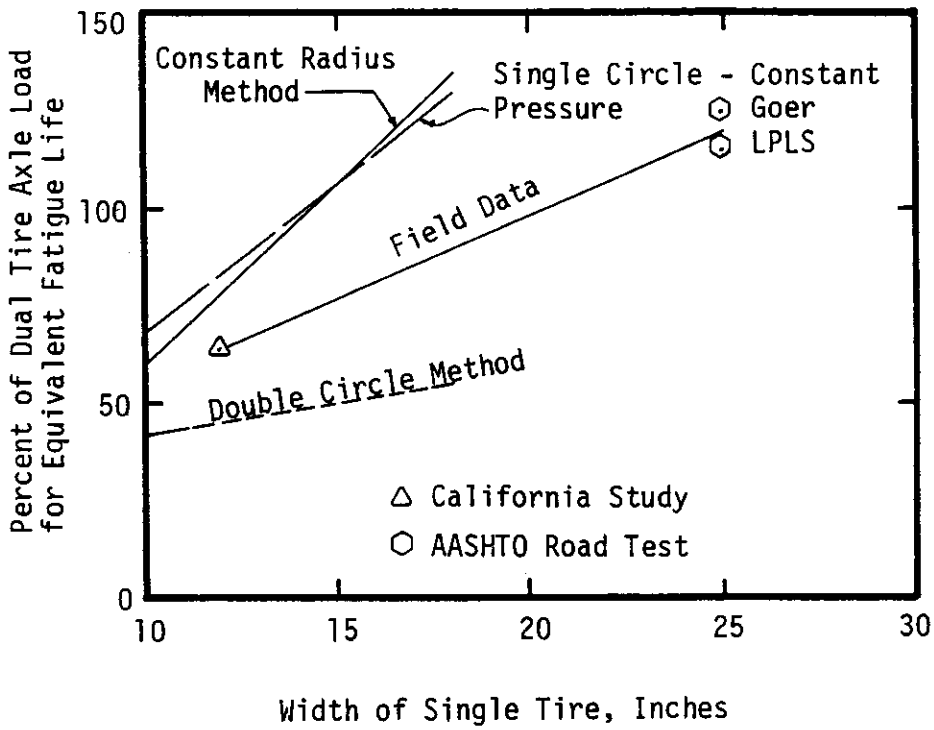

Figure 54. Comparison of Methods for Computing the Equivalency of Single Tires to Dual Tires with Field Data, for a 3-inch Asphalt Concrete Pavement

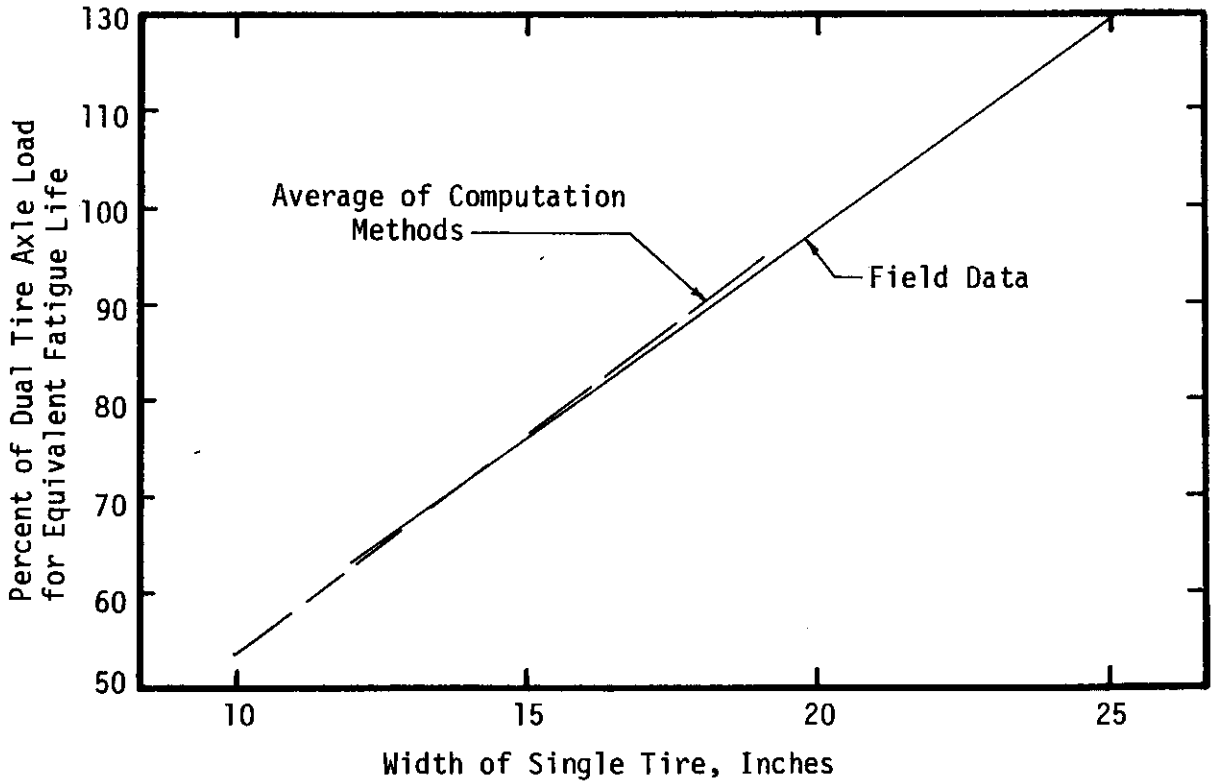

Figure 55. Comparison of the Average Between the Single Circle and Double Circle Computation Methods and Available Field Data for 3-inch Asphalt Concrete Pavement

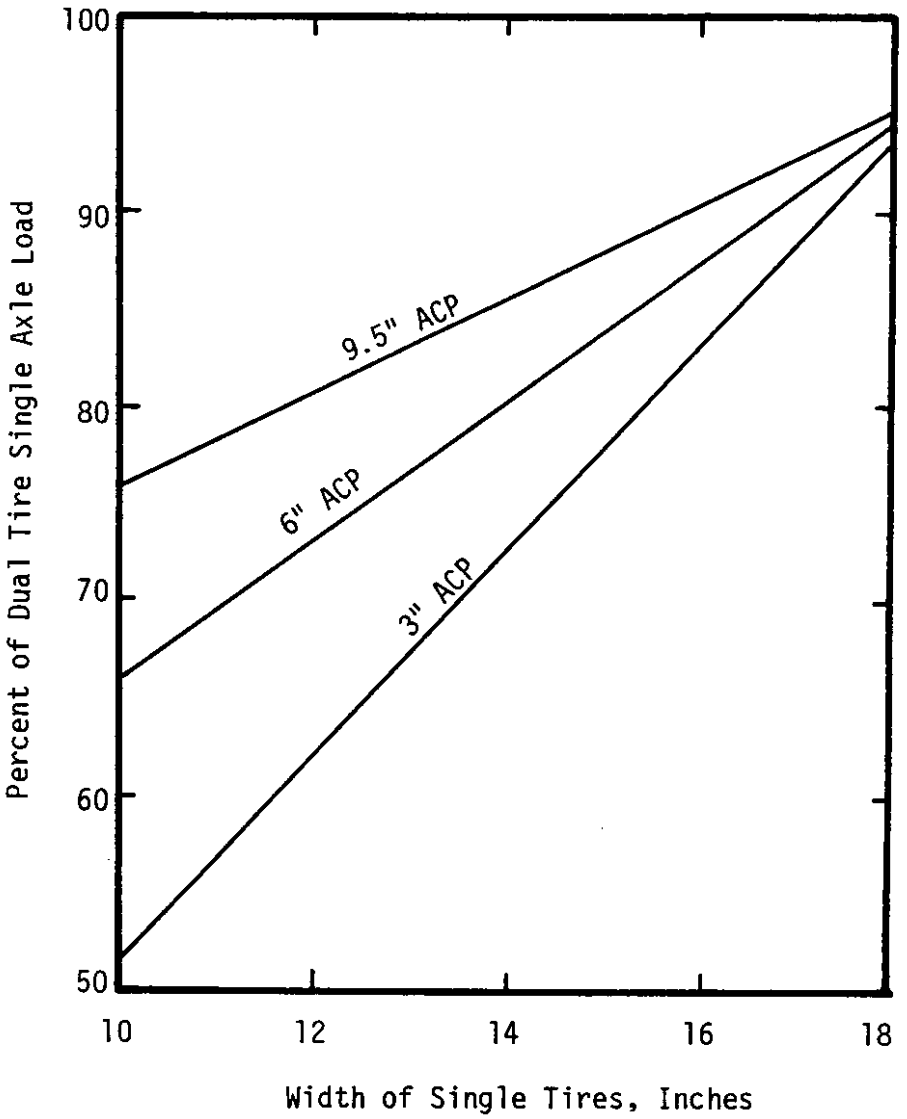

Figure 56. Average Equivalency of Single Axles with Single Tires to Single Axles with Dual Tires for 9.5, 6 and 3 Inch Asphalt Concrete Pavements

Table 16. Traffic Equivalence Factors for Single Axles with Dual Tires - Asphalt Concrete Pavement

Single Axles - Dual Tires Traffic Equivalence Factors (18-kip single axles dual tires)

Axle Load	Approximate Structural Number 2*	4*	6*
10.	.35301	.20683	.1711
12.	.48759	.33721	.2958
14.	.64069	.50978	.4700
16.	.81168	.72922	.7020
18.	1.00000	1.00000	1.0000
20.	1.20520	1.32640	1.3723
22.	1.42687	1.71257	1.8272
24.	1.66467	2.16252	2.3730
26.	1.91827	2.68014	3.0180
28.	2.18738	3.26923	3.7705
30.	2.47175	3.93348	4.6388
32.	2.77113	4.67651	5.6312
34.	3.08531	5.50186	6.7560
36.	3.41408	6.41300	8.0215
38.	3.75725	7.41334	9.4361
40.	4.11465	8.50623	11.0080

*where SN = 2 represents 2 to 4 inches of ACP over aggregate base
SN = 4 represents 5 to 8 inches of ACP over aggregate base
SN = 6 represents 9 inches or more of ACP over aggregate base.

Table 17. Traffic Equivalence Factors for Single Axle with Single - Asphalt Concrete Pavement, SN = 2

ACP SN = 2*

Single Axles - Single Tires Traffic Equivalence Factors (18 kip single axle dual tires)

Axle Load	Tire Width 10"	12"	14"	16"	18"
10.	1.2437	.8656	.64083	.49635	.39599
12.	1.7179	1.1956	.88514	.68557	.54696
14.	2.2573	1.5711	1.16308	.90084	.71870
16.	2.8597	1.9904	1.47347	1.14125	.91051
18.	3.5232	2.4522	1.81535	1.40604	1.12176
20.	4.2462	2.9553	2.18786	1.69457	1.35194
22.	5.0272	3.4989	2.59027	2.00625	1.60061
24.	5.8650	4.0820	3.02196	2.34061	1.86736
26.	6.7585	4.7039	3.48232	2.69718	2.15184
28.	7.7066	5.3638	3.97086	3.07556	2.45372
30.	8.7085	6.0611	4.48708	3.47540	2.77271
32.	9.7633	6.7953	5.03057	3.89634	3.10854
34.	10.8702	7.5657	5.60091	4.33809	3.46098
36.	12.0286	8.3719	6.19775	4.80036	3.82978
38.	13.2376	9.2134	6.82073	5.28288	4.21474
40.	14.4968	10.0898	7.46953	5.78540	4.61565

*where SN = 2 represents 2 to 4 inches of ACP over aggregate base.

Table 18. Traffic Equivalence Factors for Single Axles with Single Tires - Asphalt Concrete Pavement, SN - 4

ACP SN = 4*

Single Axles - Single Tires Traffic Equivalence Factors (18 kip single axle dual tires)

Axle Load	Tire Width 10"	12"	14"	16"	18"
10.	.6309	.4790	.3731	.2969	.24050
12.	1.0286	.7809	.6082	.4840	.39210
14.	1.5549	1.1805	.9195	.7317	.59277
16.	2.2243	1.6887	1.3153	1.0466	.84793
18.	3.0502	2.3157	1.8038	1.4353	1.16279
20.	4.0458	3.0715	2.3925	1.9038	1.54232
22.	5.2237	3.9658	3.0891	2.4580	1.99136
24.	6.5962	5.0077	3.9007	3.1038	2.51455
26.	8.1750	6.2064	4.8343	3.8468	3.11643
28.	9.9718	7.5705	5.8969	4.6923	3.80141
30.	11.9979	9.1087	7.0951	5.6457	4.57379
32.	14.2643	10.8293	8.4353	6.7121	5.43778
34.	16.7818	12.7406	9.9241	7.8968	6.39749
36.	19.5610	14.8505	11.5675	9.2045	7.45695
38.	22.6123	17.1670	13.3719	10.6403	8.62014
40.	25.9458	19.6978	15.3432	12.2089	9.89093

*where SN = 4 represents 5 to 8 inches of ACP over aggregate base

Table 19. Traffic Equivalence Factors for Single Axles with Single Tires - Asphalt Concrete Pavement, SN = 6

ACP SN = 6*

Single Axles - Single Tires Traffic Equivalence Factors (18 kip single axle dual tires)

Axle Load	Tire Width 10"	12"	14"	16"	18"
10.	.3014	.2696	.2420	.2183	.1974
12.	.5211	.4662	.4185	.3774	.3413
14.	.8280	.7407	.6650	.5997	.5423
16.	1.2366	1.1062	.9932	.8956	.8099
18.	1.7615	1.5758	1.4148	1.2758	1.1537
20.	2.4174	2.1624	1.9415	1.7508	1.5832
22.	3.2187	2.8793	2.5851	2.3312	2.1081
24.	4.1802	3.7394	3.3574	3.0276	2.7378
26.	5.3164	4.7558	4.2699	3.8505	3.4819
28.	6.6420	5.9415	5.3346	4.8106	4.3501
30.	8.1716	7.3098	6.5630	5.9184	5.3519
32.	9.9198	8.8736	7.9671	7.1846	6.4968
34.	11.9012	10.6461	9.5585	8.6197	7.7945
36.	14.1305	12.6403	11.3490	10.2343	9.2546
38.	16.6224	14.8694	13.3504	12.0391	10.8866
40.	19.3914	17.3464	15.5743	14.0446	12.7002

*where SN = 6 represents 9 inches or more of ACP over aggregate base

Tandem Axles with Single Tires

An analysis was made to determine if it was reasonable to model a tandem axle with single wheels as two single axles with single wheels. The BISAR (Bitumen Structures Analysis in Roads) elastic layer analysis program, developed by Koninklijke/Shell-Laboratorium, Amsterdam, was used for this analysis [16]. Three cases were considered: Case 1, 4.2 inches of asphalt concrete over 12 inches of aggregate base; Case 2, 8.4 inches of asphalt concrete over 8.4 inches of aggregate base; and Case 3, 9.6 inches of asphalt concrete over 8.4 inches of aggregate base. These cases are based on several pavement sections constructed by the Washington Department of Transportation which were being analyzed in a related study.

The maximum strain was determined for a 17-kip single axle load and a 34-kip tandem axle load. The repetitions to failure were then calculated using Equation (16). In all cases for the tandem axles, the maximum strain occurred under the wheel. Therefore, it was assumed that each pass of a tandem axle resulted in two applications of this strain. The results of this analysis are given in Table 20.

These results indicate that the damage effect of tandem axles would be underestimated by using two single axles to model tandem axles. However, the traffic equivalency factors for tandem dual tires on flexible pavements developed from the AASHO Road Test data [1] indicate that the damage resulting from a tandem axle is less than that caused by two single axles.

Barker, Brabston and Chou [3] noted that for tandem aircraft gear the strain-time curve has two peaks. At shallow depths the ratio of the peak strain to the strain between peaks is large, but approaches unity as the depth increases. They concluded that in estimating strain repetitions for the asphalt pavement a tandem gear would result in two repetitions. However, when considering subgrade strain criteria a tandem gear would result in one strain repetition.

Table 20. Relationship of Tandem Axles to Single Axles

Case	Maximum Strains	Axle Repetitions to Failure	Ratio of Single/Tandem
1 - Single	391.5	140,759	2.1
1 - Tandem	396.0	67,500	
2 - Single	155.1	2,497,047	2.6
2 - Tandem	168.0	959,859	
3 - Single	124.8	5,106.085	2.8
3 - Tandem	139.0	1,790,764	

CHAPTER 3

FIELD VERIFICATION

Introduction

A method of assessing the relative destructive effects of traffic loadings involves analysis of pavement structures in terms of traffic induced stresses, strains, or deflections. Utilizing this approach, the magnitude of these pavement response variables under different loading conditions are compared to those caused by standard load. From these comparisons and appropriate pavement distress criteria, destructive effects of loads are expressed in terms of an equivalent number of applications of the standard load, or load equivalency factors. Field measurements of the response of pavements to moving traffic loads have been limited and therefore, the majority of these analyses have been based on theoretically determined parameters.

As part of this study, field measurements were made to enhance the theoretical development presented in Chapter 1 and 2. The field study was divided in three parts: 1) truck survey at the weigh stations, 2) deflection measurements under actual truck loads at the weigh station, and 3) utilization of field data from Transportation and Surface Water Engineering Division of Alberta Research Council.

Truck Survey

A truck survey was conducted at a weigh station near Fife (I-5 northbound) with the purpose of determining axle loads, tire sizes, tire pressures, contact areas, and to observe the frequency of use of single axle single tires. Appendix C contains the data for each truck type surveyed. Axle loads were measured on the scale at the weigh station in the static mode. Tire sizes were obtained from the manufacturer's designation on the side wall of the tire. Tire pressures were measured with a heavy duty pressure gage, and tire width and contact length on the road was measured by a tape.

Analysis of the truck survey showed that:

1. Total trucks in the sample was 80.
2. There were only six percent of trucks with single tires on single and tandem axles (axles other than steering axles).
3. There was one truck which exceeded the criteria of 550 lb/in. (the tires were 10 in. wide). However, there were at least 15 percent of trucks which had one of the dual tires flat or had a very low tire pressure.
4. There were only two trucks with single tires of 16.5 and 18 inches width.
5. From Figure 57, it appears that the actual contact area is generally more than the assumed contact area (when calculated as a circular area). The assumed contact area was calculated by use of a circular contact area and knowledge of the tire pressure and load.
6. From Figure 58, one can see that the average tire pressure on the highway is about 95 psi compared to the generally accepted assumption of 80 psi. There appears to be no correlation between higher axle load and higher tire pressure.

In Situ Deflection Measurements at Fife (I-5)

In order to verify theoretically derived load equivalency factors, it was necessary to measure in situ deflections for actual truck loadings and tire sizes and to calculate load equivalency factors based on measured deflections. The concept used to calculate load equivalency factors from field data was to measure deflections due to a standard 18 kip single axle dual tire load and compare with those for other axle loads and tire sizes.

Field Instrumentation. To obtain pavement surface measurements, an extensometer was designed to measure in situ deflections. The extensometer is six feet long and consists of two one inch diameter bison coils placed parallel to each other in a PVC tube (shown in Figure 59). The change in voltage between the coils was measured. This voltage change is related to the actual movement through a

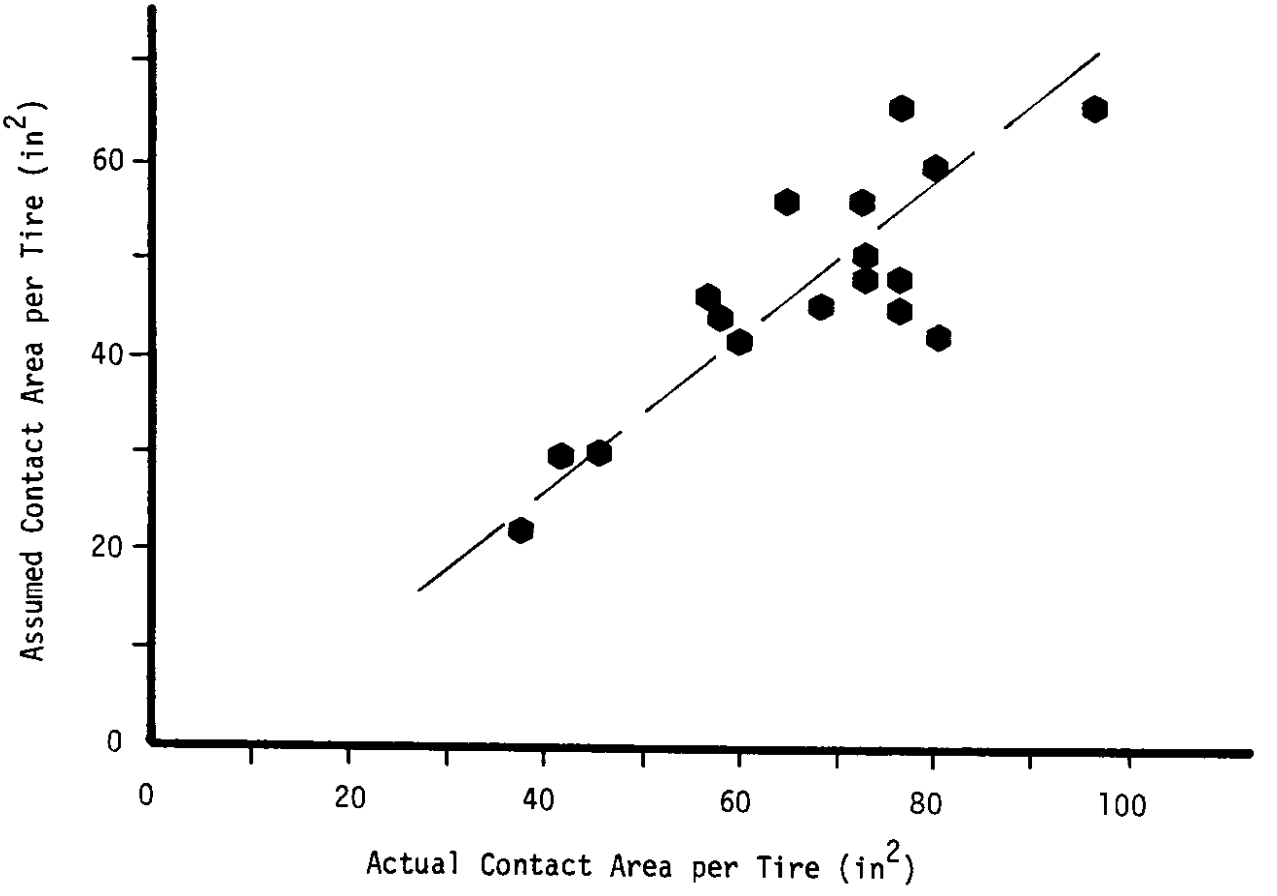

Figure 57. Assumed Contact Area vs. Actual Contact Area for each Tire.

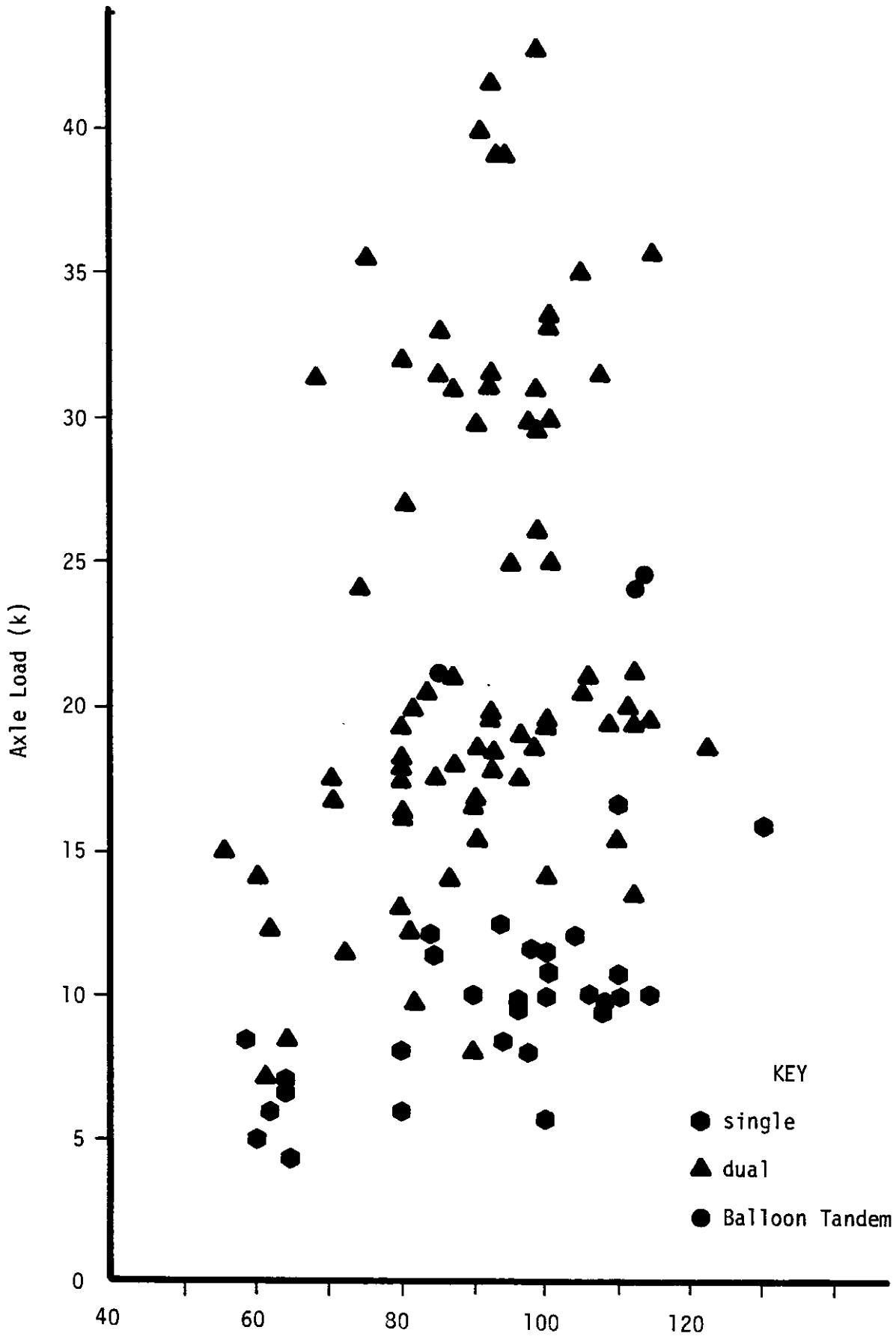

Figure 58. Axle Load vs. Tire Pressure

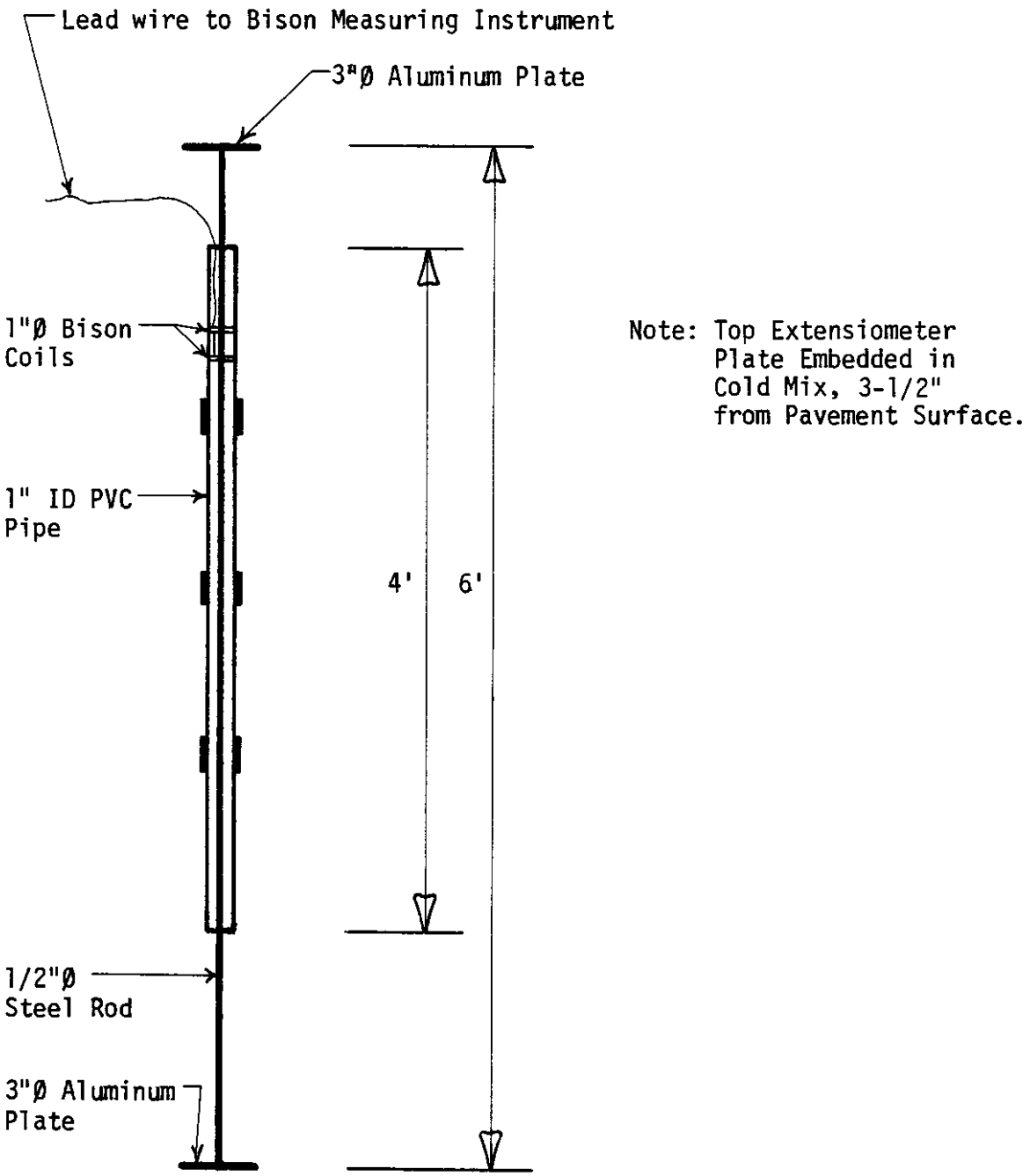

Figure 59. Schematic Drawing of Extensometer

calibration process. Calibration was achieved by using a fixture shown in Figure 60, where two coils are mounted parallel to each other and one of the coils is moved with a micrometer. Curves are developed relating micrometer readings to the change in the voltage. Those curves are then used to interpret the voltage measured in the field to determine actual deflections. Refer to Reference 31 for a complete description of the original calibration process.

Site Location. The weigh station near Fife (I-5 northbound) was chosen for the extensometer location. The deflections were measured just after the axle loads were measured on the scales. The location of the extensometer relative to the test site is shown in Figure 61 and photographs of the extensometer in Figure 62. The drilling required for installation was done by the WSDOT Office of Maintenance, District 1, with a six inch auger (shown in Figure 63). The pavement section consisted of eight inches of dense asphalt concrete, 12 inches of gravel base and at least 12 feet of glacial gravel till.

The fill material appeared to be dry of optimum moisture content. There were no surface cracks visible at the time of installation. The boring was backfilled with the same material with the addition of portland cement. This was done to preclude settling of the extensometer under repeated truck loads.

Data Collection and Analysis. The objective of the data collection was to find a relationship between axle load, tire size and deflection. Hence, each axle of a given truck was weighed, tire sizes noted and deflection readings recorded. A sample of the data is shown in Appendix C. Of the 150 trucks weighed, only 60 were considered in the development of the load deflection relationship as not all trucks passed over the extensometer. Next the load-deflection relationship was established for front axles with single tires, single axles with dual tires, and tandem axles with dual tires. There were only four trucks that had tandem axles with single tires and hence not considered.

Figure 64 illustrates the three relationships. The coefficient of determination (R^2) for single axle dual tire and tandem axle with

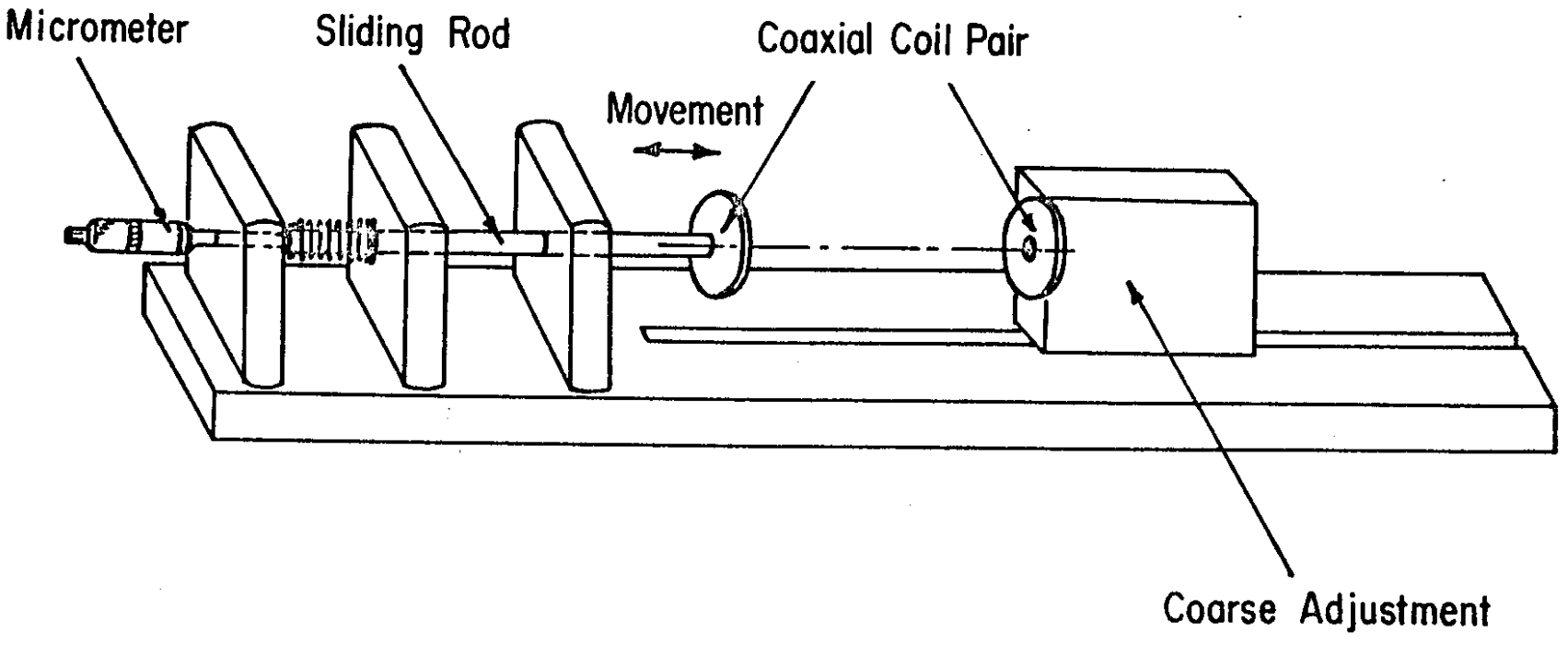

Figure 60. Calibration Fixture for Sensors

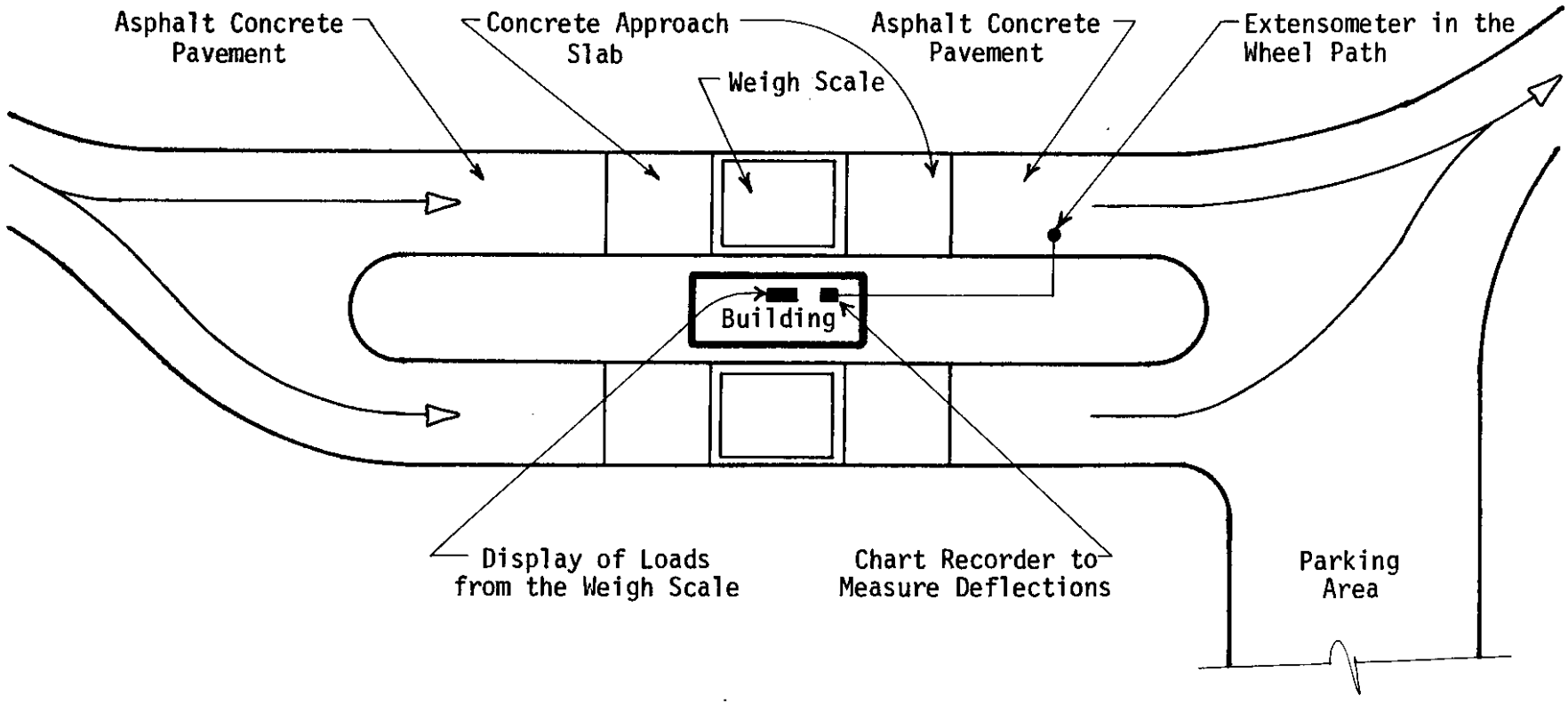

Figure 61. Weigh Station at Fife (I-5)

Figure 62. Two Extensometers (12 ft. and 6 ft. long) and Bison Instrument to Measure Amplitude.

Figure 63. Location of Drill Hole in the Wheel Path for the Extensometer.

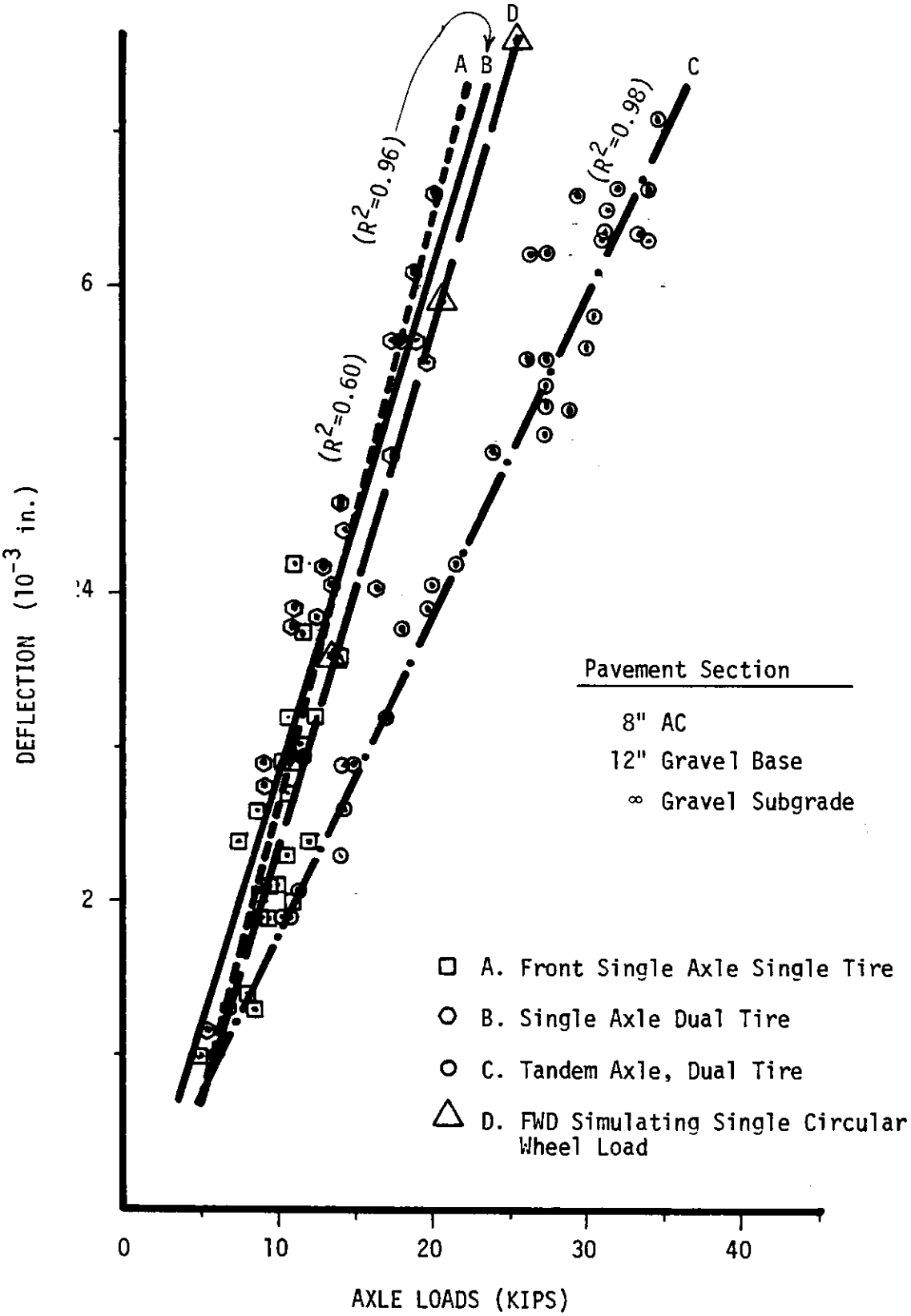

Figure 64. Load Deflection Relationship

dual tires exceeded 0.96 which is considered excellent. The coefficient determination for front axles with single tires is only 0.60. One reason for this low R^2 is that most of the loads measured ranged between 8,000 to 12,00 lbs, which is not a large range. Also, the single tire did not always center directly over the extensometer giving rise to a large variation in deflections.

In addition, falling weight deflectometer (FWD) deflections were measured at four locations near the extensometer. The purpose of the FWD deflections was to correlate deflections with the extensometer and to determine the elastic material properties of the pavement layers. The material properties were determined by using FWD deflection basins and a layered elastic computer program, (BISDEF) [32] the results of which are shown in Figure 65. These material properties were then used to calculate surface deflection and maximum horizontal tensile strains for loads ranging from 6,000 to 22,000 lbs for single axles with dual tires (summarized in Table 21). The calculated and measured deflections were then plotted are shown in Figure 66.

Discussion. The data collection and analysis presented above supported the fact that calculated and observed deflections can be made to agree with each other within statistical bounds for single and tandem axle dual tire loads. However, for single axles with single tires more data was needed for the development of significant relationships between tire size, axle load, and tire pressures. As the objective of this study was to determine the effects of single tires on pavement structures in comparison with standard dual tire loads, it became necessary to find a location to generate such data. From a literature search, it was determined that the Alberta Research Council had developed large amounts of data from field instrumentation and this data was used to verify the theoretical findings and is presented in the next section.

Utilization of Field Data from Alberta

The data from three reports published by the Transportation and Surface Water Engineering Division of the Alberta Research Council [33, 34, 35] were used to present results in this section. In 1973

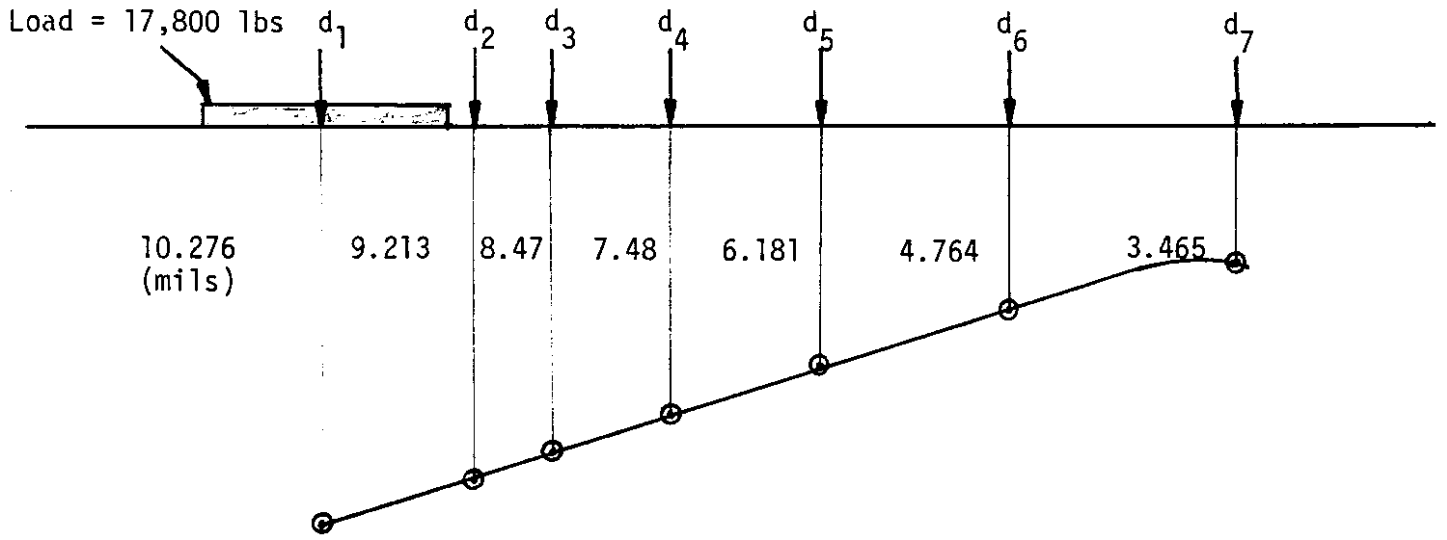

Asphalt Concrete	H_1 = 8"	$E_1 = 2.5 \times 10^6$ psi	ν = 0.15 (Temp.=32°F)
Gravel Base	H_2 = 12"	E_2 = 31,000 psi	ν = 0.35
Subgrade Gravel (glacial till)	$H_3 = \infty$	E_3 = 25,000 psi	ν = 0.35

Figure 65. FWD Deflection Basin and Derived E-values from BISDEF Program

Table 21. Calculation of Surface Deflection and Horizontal Tensile Strain for the Fife Test Site

Axle Load (kips)	Surface Deflection x 10^{-3} in.		Calculated Maximum Horizontal Tensile Strain (x 10^{-6})
Single Axle Dual Tire	Calculated	Measured	
6	1.97	1.60	17.6
8	2.57	2.24	22.3
10	3.17	2.90	26.7
12	3.75	3.56	30.7
14	4.32	4.20	41.0
16	4.89	4.80	38.1
18	5.45	5.50	41.5
20	6.00	6.14	44.7
22	6.54	6.70	47.8
Tandem Axle Dual Tire			
8	1.86	1.42	11.3
12	2.73	2.25	15.9
16	3.58	3.086	20.1
20	4.42	3.90	23.9
24	5.25	4.73	27.4
28	6.07	5.568	30.7
32	6.89	6.38	33.8
36	7.69	7.21	36.6
40	8.49	8.04	39.3

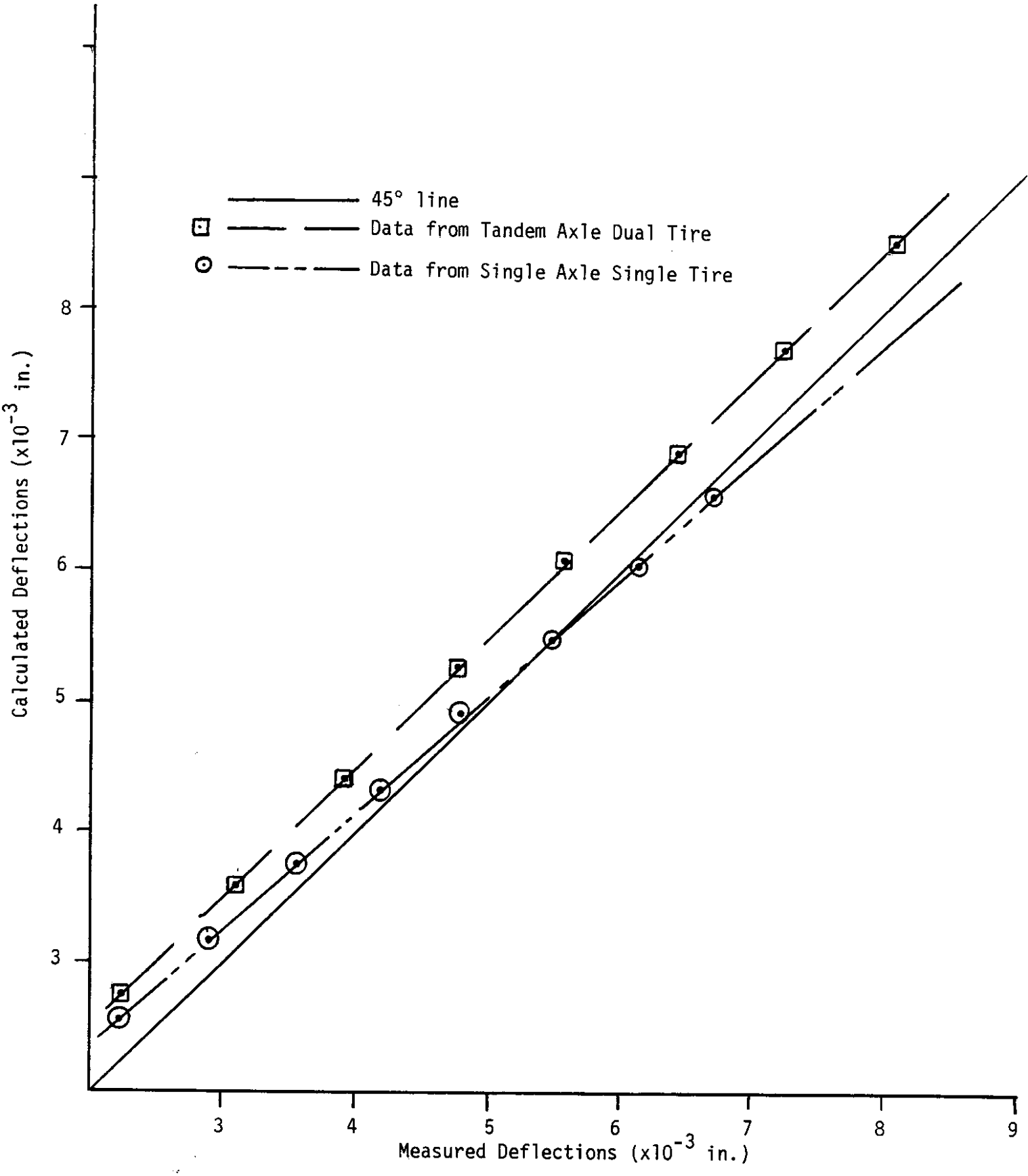

Figure 66. Fit of Calculated and Field Measured Deflections

a test facility capable of recording stresses, strains, and deflections under static and moving traffic loads was incorporated in two full-depth asphalt pavements. Later a third site was instrumeted in the thinner section. Since completion, pavement-subgrade interfacial strains and surface deflections have been recorded under moving wheel loads ranging from 1,000 to 33,000 lbs and various loading configurations. All three test sites are located near Edmonton, Alberta. The pavement structure at these sites consist of:

1. Three inches asphalt concrete, 12 in. gravel base, subgrade.
2. Four inches asphalt concrete overlay over 7.7 in. asphaltic concrete, subgrade.
3. Four inches asphalt concrete overlay over 11 in. asphaltic concrete, subgrade.

Material Properties at the Test Sections. To determine material properties at the three test sites, FWD deflection basins were obtained at four stress levels and every 50 feet for a 500 feet total length. The test sites with corresponding instrumentation can be seen in photographs shown in Figure 67. The deflection data is shown in Table 22.

Resilient modulus of the layers for each pavement section were then calculated with the use of the BISDEF Computer Program. This program is a reverse elastic layered BISAR Program which back calculates elastic moduli for flexible pavements with a maximum of four layers by satisfying observed and calculated deflection basins. The resilient modulus values so calculated are shown in Table 23.

In order to facilitate calculations of tensile strain and surface deflections at these sections for various loads and tire configurations, stress sensitive material properties were derived and are shown in Table 24. In all cases, the subgrade materials exhibit a negative slope indicating a clay type material.

Method of Analysis. The main objective in this section is to compare theoretically derived load equivalency factors for 10, 12, 16.5 and 18 inch wide tires on single axles to those measured in the field at the Alberta test sites. The method to do this is briefly summarized below.

Figure 67a. Instrumentation on the Alberta 3-Inch Section.

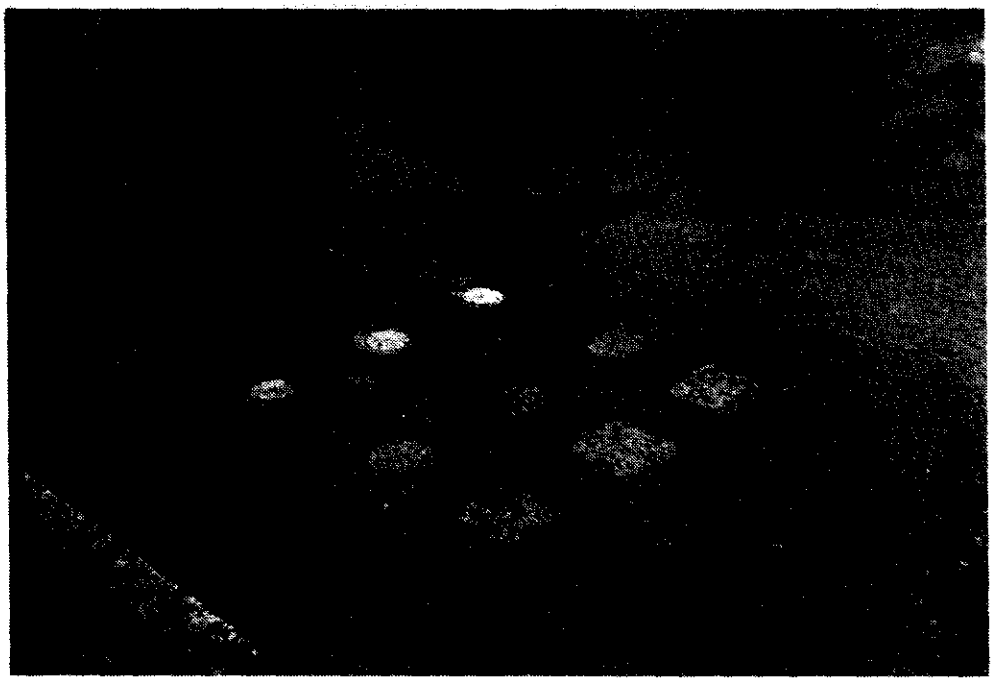

Figure 67b. Instrumentation on the Alberta 3-Inch Section.

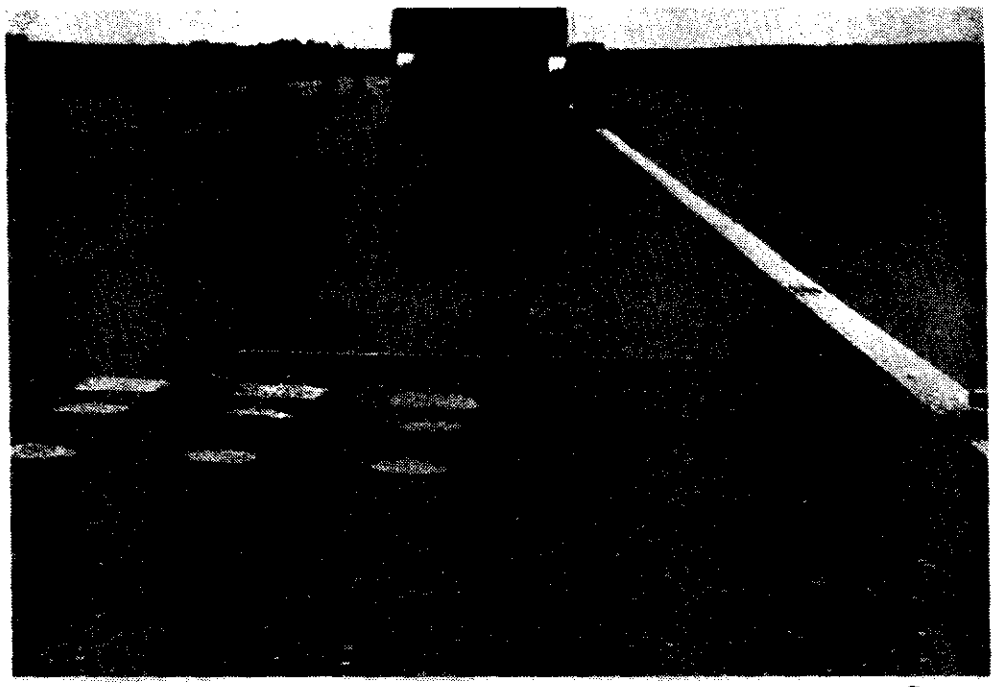

Figure 67c. Instrumentation and Rutting on the Alberta 15-Inch Test Section.

Figure 67d. Truck Used for the Measurement Standard Single Axle, Dual Tire 18,000 lb. Load.

Table 22. FWD Deflection Data at Alberta Test Section

Section	Plate Diameter (mm)	Average Stress (kPa)	Average Deflections (micrometers)[1]						
			δ_1	δ_2	δ_3	δ_4	δ_5	δ_6	δ_7
3 inch	300	317.29 [3.99][2]	475.57 [41.99]	366.71 [24.50]	276.57 [15.80]		106.86		54.43 [4.28]
		603.57 [20.83]	871.14 [56.04]	666.14 [30.07]	518.29 [29.26]		214.00 [30.52]		105.86 [10.82]
		786.86 [21.28]	1139.00 [76.24]	870.43 [36.33]	680.86 [28.47]		287.00 [40.14]		143.00 [12.99]
		966.00 [4.36]	1411.57 [135.45]	1078.29 [71.16]	844.86 [38.61]		356.86 [35.61]		176.57 [12.38]
	450[3]	139.41 [4.15]	411.86 [37.66]	284.86 [8.07]	231.14 [8.65]		104.57 [11.57]		52.29 [4.23]
		272.42 [4.90]	801.43 [61.09]	559.57 [22.57]	469.00 [15.81]		220.00 [20.54]		107.71 [7.93]
		354.95	1044.71 [77.63]	736.00 [33.33]	618.86 [20.82]		293.14 [25.22]		145.29 [10.39]
		428.27 [2.63]	1261.43 [96.84]	892.00 [43.21]	752.14 [26.52]		359.43 [29.61]		177.00 [12.6]
11.7 inch	300[4]	308.33 [11.06]	321.33 [62.24]	213.56 [27.07]	167.44 [18.39]		86.00 [6.58]		45.9 [2.76]
		607.78 [10.39]	676.78 [124.33]	454.89 [65.16]	363.11 [49.84]		183.78 [14.89]		90.44 [4.77]
		784.33 [9.00]	892.56 [160.50]	614.33 [90.39]	494.22 [67.27]		247.89 [20.31]		120.11 [6.41]
		942.33 [7.12]	1079.22 [189.35]	753.44 [110.53]	609.67 [79.66]		303.89 [24.27]		145.67 [6.71]
	450[5]	140.97 [8.26]	255.22 [49.22]	174.44 [19.21]	146.11 [16.57]		86.44 [6.04]		45.56 [2.19]
		273.31 [7.21]	531.22 [90.46]	368.56 [42.68]	307.87 [90.05]		184.11 [13.07]		91.56 [3.40]
		352.41 [6.04]	707.00 [114.36]	499.00 [57.81]	416.63 [40.28]		247.11 [17.37]		120.89 [5.78]
		423.91 [6.45]	856.67 [136.32]	610.22 [71.09]	518.89 [53.48]		301.56 [20.53]		145.67 [6.38]

Table 22. Continued

Section	Plate Diameter (mm)	Average Stress (kPa)	Average Deflections (micrometers)						
			δ_1	δ_2	δ_3	δ_4	δ_5	δ_6	δ_7
15 inch	300	317.56	209.33	139.67	115.00		76.67		46.11
		[13.12]	[31.46]	[13.16]	[12.84]		[5.79]		[3.48]
		622.00	424.22	280.11	237.56		156.11		85.11
		[4.77]	[49.62]	[26.76]	[21.63]		[12.59]		[3.33]
		798.67	554.56	372.11	316.00		206.33		111.11
		[5.66]	[57.40]	[35.47]	[28.59]		[16.87]		[3.02]
		957.44	657.22	452.78	382.78		248.67		133.33
		[6.98]	[66.41]	[38.71]	[36.20]		[20.06]		[4.33]
	450(6)	139.1	162.89	119.11	105.44		75.44		44.78
		[10.20]	[20.43]	[11.52]	[10.25]		[5.88]		[2.82]
		279.13	332.00	242.22	218.44		154.00		85.44
		[4.68]	[35.62]	[25.23]	[22.25]		[12.40]		[3.05]
		320.26	435.89	321.56	290.44		202.78		110.89
		[8.29]	[43.86]	[33.12]	[29.50]		[16.54]		[3.52]
		432.55	522.78	387.67	351.00		243.78		132.67
		[8.67]	[49.72]	[39.68]	[35.47]		[19.72]		[3.74]

(1) δ_1, δ_2, δ_3, δ_4, δ_5, δ_6 and δ_7 were at distances from the load of 0, 200, 300, 450, 650, 900 and 1200 mm, respectively, except as noted
(2) bracketed values are standard deviations
(3) δ_2 is 280 mm and δ_3 is 343 mm from the load
(4) δ_3 is 360 mm from the load
(5) δ_2 is 260 mm and δ_3 is 360 mm from the load
(6) δ_2 is 280 mm and δ_3 is 343 mm from the load

Table 23. Resilient Modulus Calculated from FWD Deflection Basins for Alberta Test Section.

Section	Stress (psi)	Resilient Modulus ACP (psi)	Resilient Modulus Base (psi)	Resilient Modulus Subgrade (psi)	Base Bulk Stress (psi)	Subgrade Bulk Stress (psi)
3 inch	46.02	541,806	13,932	10,089	9.150	5.896
	87.54	595,701	15,190	9,945	17.596	10.682
	114.12	596,520	15,559	9,606	23.332	13.600
	140.10	596,631	15,285	9,908	28.246	17.030
	20.22	360,181	16,224	10,209	8.400	5.534
	39.51	447,950	16,090	9,736	15.634	10.290
	51.41	494,486	15,613	9,910	19.484	13.430
	62.11	472,094	16,345	9,486	24.530	15.770
11.7 inch	44.72	75,405		12,887		8.163
	88.15	70,780		11,822		15.932
	113.76	68,209		11,862		20.926
	136.67	67,826		11,837		25.178
	20.44	81,247		13,128		7.346
	39.64	78,230		12,685		14.270
	51.11	75,746		12,521		18.530
	61.48	75,683		12,438		22.250
15 inch	46.06	136,481		13,499		4.130
	90.21	123,739		13,360		8.433
	115.83	122,633		13,444		10.906
	138.86	125,042		13,427		12.946
	20.17	159,128		13,447		3.552
	40.48	147,434		13,613		7.426
	52.25	150,000		13,500		9.474
	62.74	126,319		13,506		12.305

Table 24. Material Properties Derived from FWD Deflection Basin at Alberta Test Sections.

Section	Base of Subgrade	M_R Versus Θ Regression Equation	r^2
3 inch	Base	$M_R = 11{,}449\ \Theta^{0.093}$	0.86
	Subgrade	$M_R = 10{,}826\ \Theta^{-0.042}$	0.55
11.7 inch	Subgrade	$M_R = 14{,}855\ \Theta^{-0.074}$	0.71
15 inch	Subgrade	$M_R = 13{,}550\ \Theta^{-0.005}$	0.29

Theoretical and Field Approaches. As described in Chapter 2 of this report, three analytical modeling methods are used to calculate tensile strain at the bottom of asphalt concrete and surface deflection. The three modeling methods are 1) constant radius - variable pressure, 2) double circle - constant pressure, and 3) constant pressure - radius equal to the width of the tire. As stated in Chapter 2, the average of the values of the constant radius and double circle methods were used to generate load equivalency factors. These average values were calculated for the Alberta test sections using the material properties described above and the PSAD2A Computer Program. The results of the calculations are shown in Table 25, 26, 27 and 28.

Longitudinal interfacial strains and surface deflections caused by each loading condition in the field were recorded at vehicle velocities ranging from 2 to 25 miles per hour. The pavement response variables caused by 18,000 lb single axle-dual tire load of a standard Benkelman Beam test vehicle were recorded immediately prior to/or following each test series. Employing this test procedure, comparisons between the magnitude of the response variables measured under the various loadings to those caused by the standard load were made at similar vehicle velocities and pavement temperatures.

After calculating the strains and deflection ratios from measured strains and deflections, load equivalency factors were calculated. The approach to calculate load equivalency factors involved the use of established asphalt concrete fatigue life tensile and limiting pavement surface deflection - anticipated traffic relationships. These relationships indicate that pavement life (expressed in terms of equivalent standard load applications, N) can be approximated by the expression:

$$N = \left(\frac{1}{\varepsilon_i}\right)^C \quad \text{and} \quad N = \left(\frac{1}{\delta_i}\right)^C$$

where ε_i and δ_i equal the magnitude of the induced tensile strain and deflection, respectively. Combining these expressions with the definition of a load equivalency factor, the factors, F for

Table 25. Surface Deflection and Tensile Strains Calculated for Single Axle Single Tire Loads for PSAD2A Computer Program for 16:50 x 22.5 and 18:00 x 22.5 Tires Using Three Models.

Section	Model	Axle Load (lbs)	Tire Pressure (psi)	Tire Radius (in.)	Surface Deflection ($\times 10^{-2}$ in.)	Tensile Strain ($\times 10^{-6}$ in/in)
3 inch ACP	constant pressure for 16:50 tire	11,700	80		2.312	393.3
		17,000	80		3.149	455.2
		20,600	80		3.675	485.1
	constant radius for 16:50 tire	11,700		8.25	1.922	195.9
		17,000		8.25	2.765	280.5
		20,600		8.25	3.333	337.3
	constant pressure for 18:00 tire	15,600	80		2.936	441.3
		18,000	80		3.298	464.3
		21,800	80		3.844	493.5
	constant radius for 18:00 tire	15,600		9.00	2.450	224.5
		18,000		9.00	2.816	257.5
		21,800		9.00	3.392	309.4
	double circle	17,106	80	8.25	3,078	529.0
		20,357	80	9.00	3,532	568.5
11.7 inch ACP	constant pressure for 16:50 tire	11,700	80		1.629	242.3
		17,000	80		2,108	324.7
		20,600	80		2,406	373.7
	constant radius for 16:50 tire	11,700		8.25	1,173	178.0
		17,000		8.25	1,704	258.7
		20,600		8.25	2,065	313.5
	constant pressure for 18:00 tire	15,600	80		1.987	304.2
		18,000	80		2.192	338.9
		21,800	80		2.503	389.0
	constant radius for 18:00 tire	15,600		9.00	1.487	220.1
		18,000		9.00	1.715	254.0
		21,800		9.00	2.077	307.6
	double circle	17,106	80	8.25	2.026	331.5
		20,357	80	9.00	2.296	378.2

Table 25. Continued

Section	Model	Axle Load (lbs)	Tire Pressure (psi)	Tire Radius (in.)	Surface Deflection ($\times 10^{-2}$ in.)	Tensile Strain ($\times 10^{-6}$ in/in)
15 inch	constant pressure for 16:50 tire	11,700	80		1.031	108.8
		17,000	80		1.351	151.3
		20,600	80		1.522	177.7
	constant radius for 16:50 tire	11,700		8.25	0.7702	90.3
		17,000		8.25	1.119	131.3
		20,600		8.25	1.356	159.0
	constant pressure for 18:00 tire	15,600	80		1.269	140.5
		18,000	80		1.408	158.8
		21,800	80		1.618	186.2
	constant radius for 18:00 tire	15,600		9.00	0.9832	114.7
		18,000		9.00	1.134	132.3
		21,800		9.00	1.374	160.3
	double circle	17,106	80	8.25	1.327	151.0
		20,357	80	9.00	1.511	176.0

Table 26. Theoretical Average Strain and Deflection Ratios Calculated for Single Axle Single Tire Loads from Constant Radius and Double Circle Methods.

Section	Axle Load (lbs)	Tire Diameter (in.)	Strain[3] Ratio	Average[4] Strain Ratio	Deflection[5] Ratio
3 inch ACP	11,700 CR[1]	16.50	0.490	0.800	0.745
	17,000 CR	16.50	0.701	1.005	1.072
	20,600 CR	16.50	0.843	1.150	1.292
	15,600 CR	18.00	0.561	0.905	0.950
	18,000 CR	18.00	0.644	0.990	1.091
	21,800 CR	18.00	0.724	1.120	1.315
	17,106 DC[2]	16.50	1.322	1.012	1.193
	20,357 DC	18.00	1.421	1.068	1.369
11.7 inch ACP	11,700 CR	16.50	0.627	0.746	0.800
	17,000 CR	16.50	0.911	1.039	1.162
	20,600 CR	16.50	1.104	1.232	1.408
	15,600 CR	18.00	0.775	0.933	1.104
	18,000 CR	18.00	0.894	1.049	1.169
	21,800 CR	18.00	1.083	1.236	1.416
	17,106 DC	16.50	1.167	1.042	1.381
	20,357 DC	18.00	1.332	1.180	1.565
15 inch ACP	11,700 CR	16.50	0.638	0.699	0.757
	17,000 CR	16.50	0.927	0.989	1.100
	20,600 CR	16.50	1.123	1.186	1.333
	15,600 CR	18.00	0.810	0.904	0.966
	18,000 CR	18.00	0.934	1.024	1.115
	21,800 CR	18.00	1.132	1.222	1.350
	17,106 DC	16.50	1.066	0.996	1.304
	20,357 DC	18.00	1.243	1.144	1.485

Note: (1) CR: constant radius

(2) DC: double circle

(3) Strain ratio is defined as $\frac{\varepsilon(L)}{\varepsilon(18)}$

(4) Average strain ratio is average of strain ratio for constant radius and double circle models

(5) Deflection ratio is defined as $\frac{\delta(L)}{\delta(18)}$

Table 27. Theoretical Strain Ratios for Constant Pressure - Single Axle Single Tire Loads.

Section	Axle Load (lbs)	Tire Pressure (psi)	Strain Ratio (3)
3 inch ACP	11,700 CP (1)	80	0.983
	17,000 CP	80	1.138
	20,600 CP	80	1.213
	15,600 CP	80	1.103
	18,000 CP	80	1.161
	21,800 CP	80	1.234
	17,106 DC (2)	80	1.012
	20,357 DC	80	1.068
11.7 inch ACP	11,700 CP	80	0.853
	17,000 CP	80	1.143
	20,600 CP	80	1.316
	15,600 CP	80	1.071
	18,000 CP	80	1.193
	21,800 CP	80	1.370
	17,106 DC	80	1.042
	20,357 DC	80	1.180
15 inch ACP	11,700 CP	80	0.768
	17,000 CP	80	1.068
	20,600 CP	80	1.255
	15,600 CP	80	0.992
	18,000 CP	80	1.121
	21,800 CP	80	1.315
	17,106 DC	80	0.996
	20,357 DC	80	1.144

(1) CP: constant pressure

(2) DC: double circle

(3) Strain ratio = $\frac{\varepsilon(L)}{\varepsilon(18)}$ where

$\varepsilon(L)$ = tensile strain at axle load with single tire.
$\varepsilon(18)$ = tensile strain at standard axle with dual tire.

Table 28. Single Axle Single Tire - Comparison of Field and Theoretical Load Equivalency Factors.

Section	Axle Load (lbs)	Tire Diameter (in.)	Theoretical F	Field F $(F^{3.219})(1,3)$
3 inch ACP	11,700	16.50	0.488	0.332
	17,000	16.50	1.016	1.399
	20,600	16.50	1.568	2.270
	15,600	18.00	0.725	0.593
	18,000	18.00	0.968	1.032
	21,800	18.00	1.440	1.998
11.7 inch ACP	11,700	16.50	0.389	0.332
	17,000	16.50	1.131	1.399
	20,600	16.50	1.957	2.270
	15,600	18.00	0.800	0.593
	18,000	18.00	1.166	1.032
	21,800	18.00	1.978	1.998
15 inch ACP	11,700	16.50	0.316	0.332
	17,000	16.50	0.965	1.399
	20,600	16.50	1.732	2.270
	15,600	18.00	0.723	0.593
	18,000	18.00	1.079	1.032
	21,800	18.00	1.907	1.998

(1) F = Load Equivalency Factor = $\frac{\varepsilon(L)}{\varepsilon(18)}$

(2) Theoretical F calculated by combining constant radius and double circle strain ratios.

(3) Field F calculated by measured horizontal strain from Alberta test sites.

single axle loads were predicted using the expressions:

$$F = \left(\frac{\varepsilon_i}{\varepsilon_b}\right)^c \quad \text{and} \quad \left(\frac{\delta_i}{\delta_b}\right)^c$$

where ε_i and δ_i are the tensile strains and deflections measured under the various single axle loads and ε_b and δ_b equal those caused by the standard 18,000 lbs single axle dual tire load. In Chapter 2, the exponent c was assumed equal to 3.219 and hence this value was used for comparison. Refer to Table 28 for a comparison of the theoretical and field derived load equivalency factors.

Discussion of Results. The following summarizes the further analyses related to defining changes in the magnitude of the measured interfacial tensile strains and surface deflections with respect to axle load variations. From these results, predicted load equivalency factors are presented and the relative potential damaging effect of single tire loadings are assessed and compared.

Single Axle Loads on Dual Tires. In Table 29 are presented calculated surface deflections and tensile strains for the standard 10:00 x 20 dual tires on single axle. The axle loads shown are the same as those used for the field measurements. Theoretical and field strain and deflection ratios are shown in Table 30. It appears that for single axle loads on dual tires the simulation using the constant radius method is adequate to predict field results. Hence, the strain values calculated for 3, 11.7 and 15 inch sections under a standard load of 18,000 lbs are considered accurate for use in comparing results with other axle loads on single tires, which are presented next.

Single Axle Loads on Single Tires. In Figures 68 through 70 are presented tensile strain versus axle loads measured and calculated from the three test sections in Alberta. The single tire sizes reported are 10, 12, 16.5 and 18 inches wide tires. Effects of each tire size is discussed:

1. Tire Size 10:00 x 20. In Figures 68, 69 and 70 are plotted lines of calculated tensile strains for constant radius - variable pressure double circle constant pressure. Measured

Table 29. Single Axle Dual Tire Loads - Surface Deflection and Tensile Strain Calculated from Alberta Test Sections.

Section	Axle Load (lbs)	Tire Pressure (psi)	Tire Radius (in.)	Surface Deflection ($\times 10^{-2}$ in.)	Tensile Strain ($\times 10^{-6}$ in/in.)
3 inch ACP	18,000	80	4.23	2.580	400.0
	14,900	66.22	4.23	2.146	333.0
	22,400	99.56	4.23	3.190	494.5
	24,000	106.67	4.23	3.412	528.7
11.7 inch ACP	18,000	80	4.23	1.467	284.0
	14,900	66.22	4.23	1.214	235.1
	22,400	99.56	4.23	1.825	353.4
	24,000	106.67	4.23	1.956	378.6
15 inch ACP	18,000	80	4.23	1.017	141.6
	14,900	66.22	4.23	0.842	117.2
	22,400	99.56	4.23	1.266	176.2
	24,000	106.67	4.23	1.357	188.8

Table 30. Single Axle Dual Tire, Comparison of Theoretical and Field Strain and Deflection Ratios.

Section	Axle Load (lbs)	Theoretical Strain Ratio	Field Strain Ratio	Theoretical Deflection Ratio	Field Deflection Ratio
3 Inch ACP	14,900	0.83	0.82	0.83	0.88
	18,000	1.00	1.00	1.00	1.00
	22,400	1.24	1.24	1.24	1.14
	24,000	1.32	1.27	1.32	1.17
11.7 Inch ACP	14,900	0.83	0.82	0.83	0.88
	18,000	1.00	1.00	1.00	1.00
	22,400	1.24	1.24	1.24	1.14
	24,000	1.33	1.27	1.33	1.17
15 Inch ACP	14,900	0.83	0.82	0.83	0.88
	18,000	1.00	1.00	1.00	1.00
	22,400	1.24	1.24	1.24	1.14
	24,000	1.33	1.27	1.33	1.17

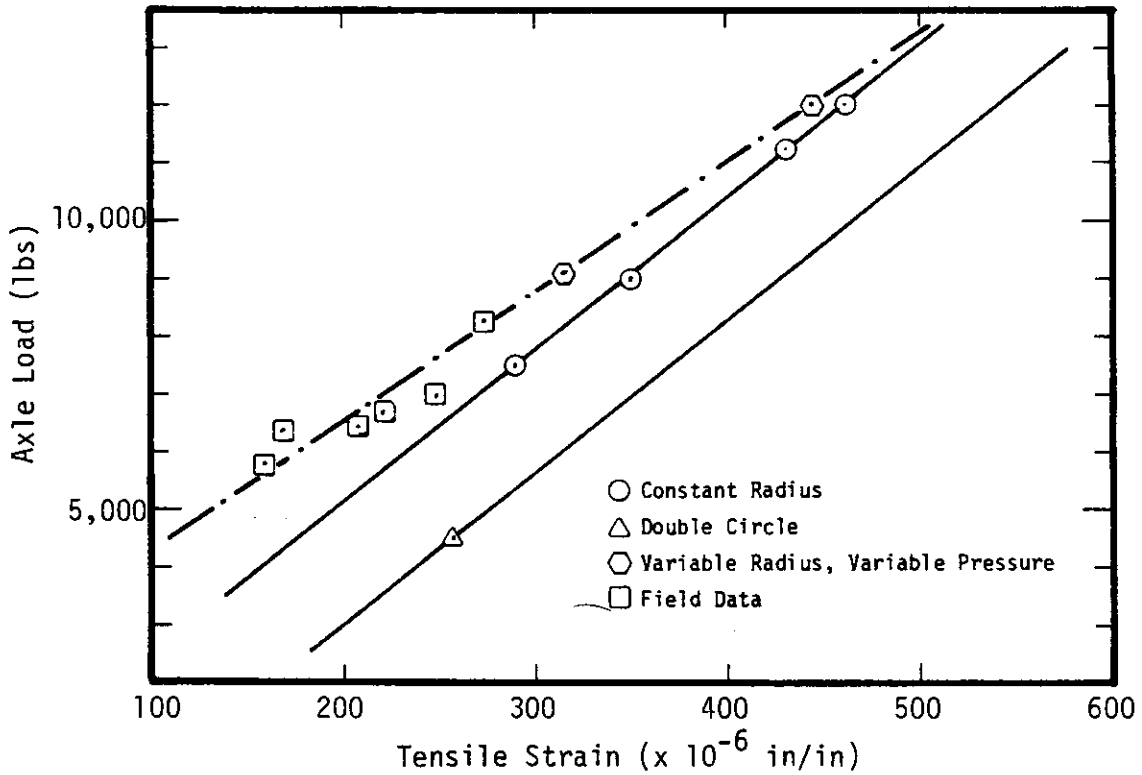

Figure 68. 10:00 x 20 Tire Size, 3 Inch ACP Section.

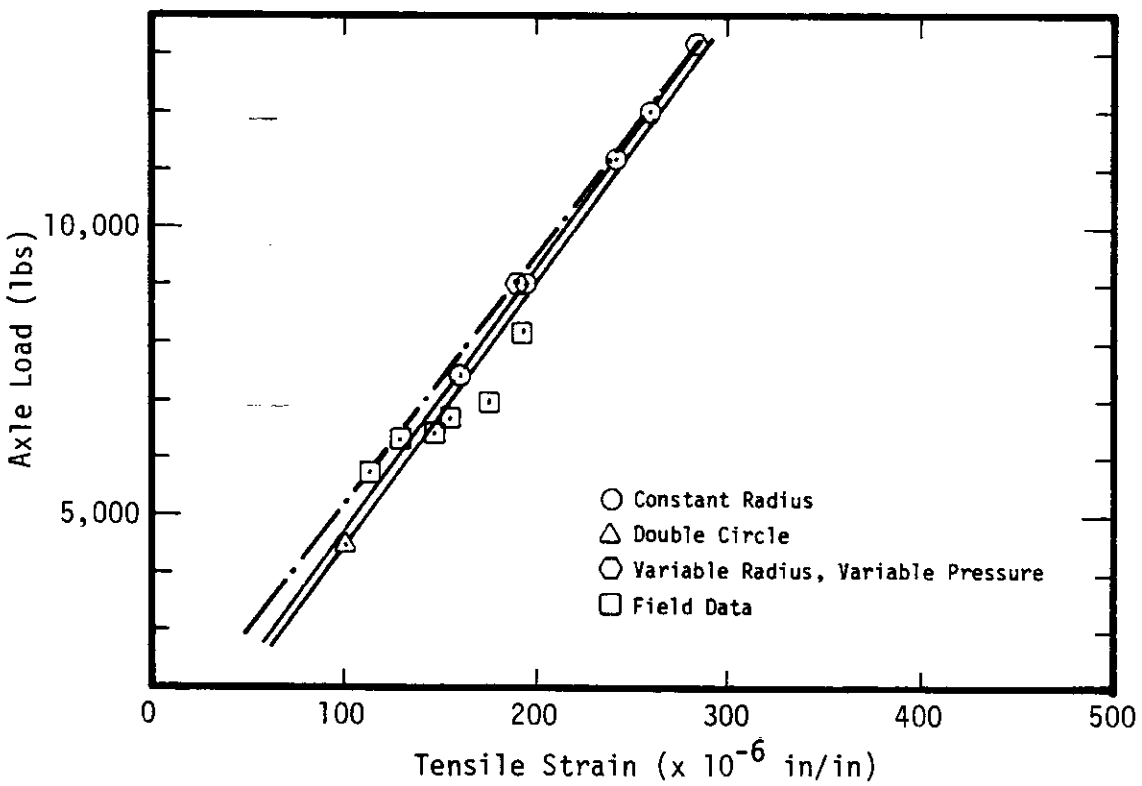

Figure 69. 10:00 x 20 Tire Size, 11.7 Inch ACP Section.

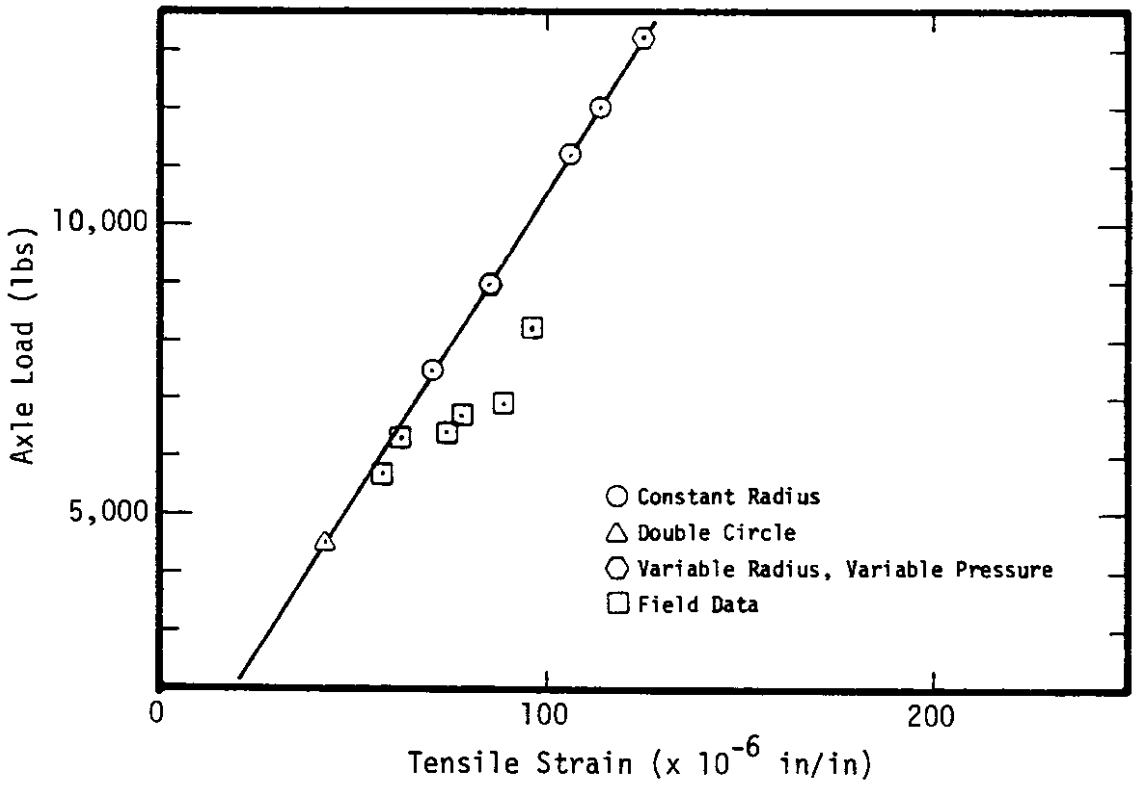

Figure 70. 10:00 x 20 Tire Size, 15 Inch ACP Section.

strains in the field are also plotted and as one can see that for a 3 inch asphalt concrete section (Figure 68), the modeling techniques correlate poorly with the field data. However, for thicker sections (i.e. 11.7 and 15 inches (Figure 69 and 70)), the theoretical models fit the field data well.

In order to improve upon the models discussed thus far, yet another model was considered. The model uses a variable radius and variable pressure. This model makes use of manufacturer's recommendations of tire pressure and load for single tires (Reference 35) and is shown in Tables 31 and 32. The radius was calculated for each tire pressure and the suggested load limit for that tire at that pressure. Tensile strains were calculated using this method are shown in Table 33 and plotted in Figures 68 and 79. Overall, this model fits the field data better for the thin ACP section than the thicker sections.

2. Tire Size 12:00 x 22.5. Figure 71, 72 and 73 are used to present results for the 12 inch wide tire. Variable radius and variable pressure models are presented in these figures and as can be seen for the limited data available for this size tire, for thin sections the fit is excellent while for the thicker sections the variations are greater.
3. Tire Size 16:50 x 22.5 and 18:00 x 22.5. Figures 74 through 79 show results for wide tires. In these figures, no one method appears to work well although it seems that the variable radius and variable pressure model better fits the 16.5 inch wide tires for all three of the ACP sections. While the average strain model (mean of the double circle and constant radius models), as described earlier seems to better fit the 18 inch wide tire.

Alberta Data Summary. Effects of single tires were studied and the modeling techniques were compared with those measured in the field. The four models studied were 1) constant radius variable pressure. 2) double circle constant pressure, 3) constant pressure and radius equal to the width of the tire and 4) variable presssure variable radius as per manufacturer's recommendations. Comparing the four

Table 31. DIAGONAL (BIAS) PLY
TIRES FOR TRUCKS, BUSSES AND TRAILERS USED IN NORMAL HIGHWAY SERVICE
TIRES MOUNTED ON 15° DROP CENTER RIMS

TIRE AND RIM ASSOCIATION STANDARD

TABLE TTB-1B
DUAL (D) SINGLE (S)

TIRE SIZE DESIGNATION		TIRE LOAD LIMITS (LBS.) AT VARIOUS COLD INFLATION PRESSURES (PSI) (The pressure is minimum for the load)												
		55	60	65	70	75	80	85	90	95	100	105	110	115
8-19.5	D	2230	2350	**2460**(D)	2570	2680	**2780**(E)	2880	2980	**3070**(F)				
	S	2270	2410	2540	2680	**2800**(D)	2930	3060	**3170**(E)	3280	3400	**3500**(F)		
8-22.5	D	2490	2620	**2750**(D)	2870	2990	**3100**(E)	3210	3320	**3430**(F)				
	S	2530	2680	2840	2990	**3140**(D)	3270	3410	**3530**(E)	3660	3780	**3910**(F)		
9-22.5	D	2960	3120	3270	3410	**3550**(E)	3690	3820	**3950**(F)	4070	4200	**4320**(G)		
	S	3010	3190	3370	3560	3730	3890	**4050**(E)	4210	4350	**4500**(F)	4640	**4790**	**4920**(G)
10-22.5	D	3510	3690	3870	**4040**(E)	4200	4360	**4520**(F)	4670	4820	**4970**(G)			
	S	3560	3770	4000	4210	4410	**4610**(E)	4790	4970	**5150**(F)	5320	5490	**5670**(G)	
11-22.5	D			4380	4580	**4760**(F)	4950	5120	**5300**(G)	5470	5630	**5800**(H)		
	S			4530	4770	4990	5220	**5430**(F)	5640	5840	**6040**(G)	6240	6430	**6610**(H)
11-24.5	D			4660	4870	**5070**(F)	5260	5450	**5640**(G)	5820	6000	**6170**(H)		
	S			4820	5070	5310	5550	**5780**(F)	6000	6210	**6430**(G)	6630	6840	**7030**(H)
12-22.5	D			4780	4990	**5190**(F)	5390	5590	**5780**(G)	5960	6150	**6320**(H)		
	S			4940	5200	5450	5690	**5920**(F)	6140	6370	**6590**(G)	6790	7010	**7200**(H)
12-24.5	D			5080	5300	**5520**(F)	5730	5940	**6140**(G)	6330	6530	**6720**(H)		
	S			5240	5520	5790	6040	**6290**(F)	6530	6770	**7000**(G)	7220	7440	**7660**(H)

NOTE: Letters in parentheses denote Load Range for which Bold Face Loads are maximum.
IMPORTANT: For speed limitations, inflation requirements, and rim and wheel load restrictions, see pages **2**-04 and **2**-05.
GENERAL DATA SHOWN ON PAGE **2**-26.
CAUTION — ALWAYS USE APPROVED TIRE AND RIM COMBINATIONS FOR DIAMETERS AND CONTOURS. SEE PAGE **2**-29 FOR APPROVED TIRE AND RIM COMBINATIONS.

Table 32. **DIAGONAL (BIAS) PLY**

WIDE BASE TIRES FOR TRUCKS, BUSSES AND TRAILERS USED IN NORMAL HIGHWAY SERVICE

TIRES MOUNTED ON 15° DROP CENTER RIMS

TIRE AND RIM ASSOCIATION STANDARD

TABLE WBTB-1B

DUAL (D) SINGLE (S)

TIRE SIZE DESIGNATION		TIRE LOAD LIMITS (LBS.) AT VARIOUS COLD INFLATION PRESSURES (PSI) (The pressure is minimum for the load)														
		30	35	40	45	50	55	60	65	70	75	80	85	90	95	100
14-17.5	D	2820	3080	3340	**3570**(D)	3800	4020	**4220**(E)	4430	4620	**4810**(F)	5000	5180	**5360**(G)		
	S			3210	3500	3790	**4060**(D)	4320	4570	**4800**(E)	5030	5255	**5470**(F)	5680	**5890**	**6090**(G)
15-19.5	D	**3600**(D)	3930	4250	**4560**(E)	4850	5120	**5390**(F)	5650	5900	**6150**(G)					
	S			**4090**(D)	4470	4830	**5180**(E)	5510	5820	**6130**(F)	6420	6710	**6980**(G)			
15-22.5	D				**5000**(E)	5320	5620	**5910**(F)	6200	6480	**6740**(G)	7000	7250	**7500**(H)		
	S						**5680**(E)	6040	6390	**6720**(F)	7040	7360	**7660**(G)	7950	8240	**8520**(H)
16.5-19.5	D				5310	5640	5970	6270	6580	6870	7150	**7430**(H)				
	S						6030	6410	6780	7130	7480	7810	8130	**8440**(H)		
16.5-22.5	D				5800	6170	6520	6860	7190	7520	7820	**8120**(H)				
	S						6590	7010	7410	7790	8170	8540	8890	**9230**(H)		
18-19.5	D				5900	6270	6640	**6980**(G)	7310	7640	**7960**(H)	8260	8560	**8850**(J)		
	S						6700	7130	7540	**7930**(G)	8310	8680	**9040**(H)	9390	**9730**	**10060**(J)
18-22.5	D				6430	6850	7230	**7610**(G)	7980	8330	**8680**(H)	9010	9340	**9650**(J)		
	S						7310	7780	8220	**8650**(G)	9070	9470	**9860**(H)	10240	**10610**	**10970**(J)
19.5-19.5	D				6950	7390	7820	8230	8620	9010	**9370**(J)					
	S						7900	8400	8890	9350	9800	10240	**10650**(J)			

NOTE: Letters in parentheses denote Load Range for which Bold Face Loads are maximum.

IMPORTANT: For speed limitations, inflation requirements, and rim and wheel load restrictions, see pages **2**-04 and **2**-05.

GENERAL DATA SHOWN ON PAGE **2**-27.

CAUTION — ALWAYS USE APPROVED TIRE AND RIM COMBINATIONS FOR DIAMETERS AND CONTOURS. SEE PAGE **2**-29 FOR APPROVED TIRE AND RIM COMBINATIONS.

Table 33. Single Axle, Single Tire Loads - Variable Radius, Variable Pressure as per Manufacturer's Designation.

Section	Axle Load (lbs)	Tire Size	Tire Pressure (psi)	Deflection ($\times 10^{-2}$ in)	Tensile Strain (10^{-6} in/in)	Strain Ratio (1)
3 inch	4,530	10:20	65	1.809	314.0	0.785
	5,430		85	2.182	392.1	0.980
	6,040		100	2.436	447.7	1.119
	6,610		115	2.675	501.2	1.253
	4,940	12:22.5	65	1.946	325.9	0.815
	5,920		85	2.348	407.4	1.018
	6,590		100	2.624	465.6	1.164
	7,200		115	2.878	521.2	1.303
	7,410	16.5:22.5	65	2.717	380.4	0.951
	9,230		90	3.423	502.1	1.255
	8,220	18:22.5	65	2.953	393.5	0.984
	10,970		100	4.005	569.2	1.423
11.7 inch	4,530	10:20	65	1.281	189.3	0.666
	6,610		115	1.985	285.2	1.004
	4,940	12:22.5	65	1.360	203.2	0.715
	7,200		115	2.105	306.5	1.079
	7,410	16.5:22.5	65	1.798	278.0	0.979
	9,230		90	2.314	355.7	1.252
	8,220	18:22.5	65	1.931	299.8	1.056
	10,970		100	2.693	415.7	1.464
15 inch	4,530	10:20	65	0.809	84.62	0.598
	6,610		115	1.247	125.2	0.884
	4,940	12:22.5	65	0.861	91.57	0.647
	7,200		115	1.326	135.6	0.958
	7,410	16.5:22.5	65	1.155	130.5	0.922
	9,230		90	1.481	165.1	1.166
	8,220	18:22.5	65	1.245	142.3	1.005
	10,970		100	1.728	194.3	1.372

(1) Strain Ratio = $\frac{\varepsilon(L)}{\varepsilon(18)}$

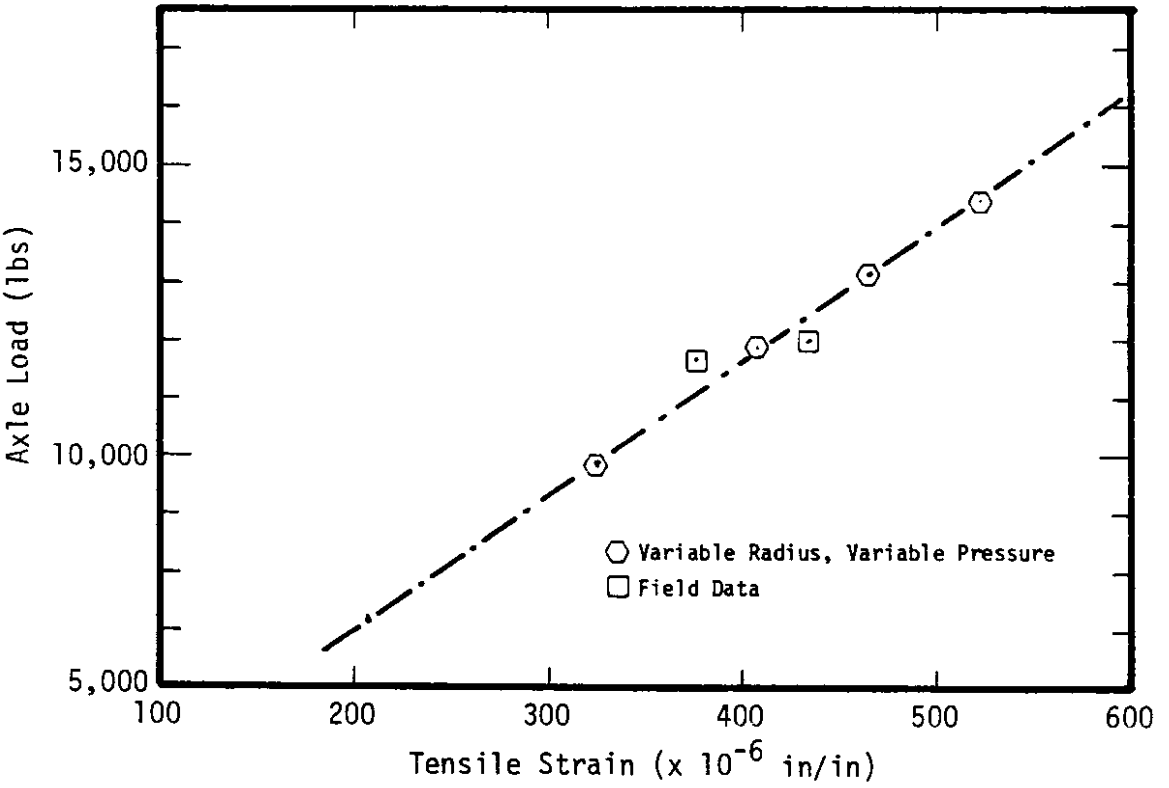

Figure 71. 12:00 x 22.5 Tire Size, 3 Inch ACP Section.

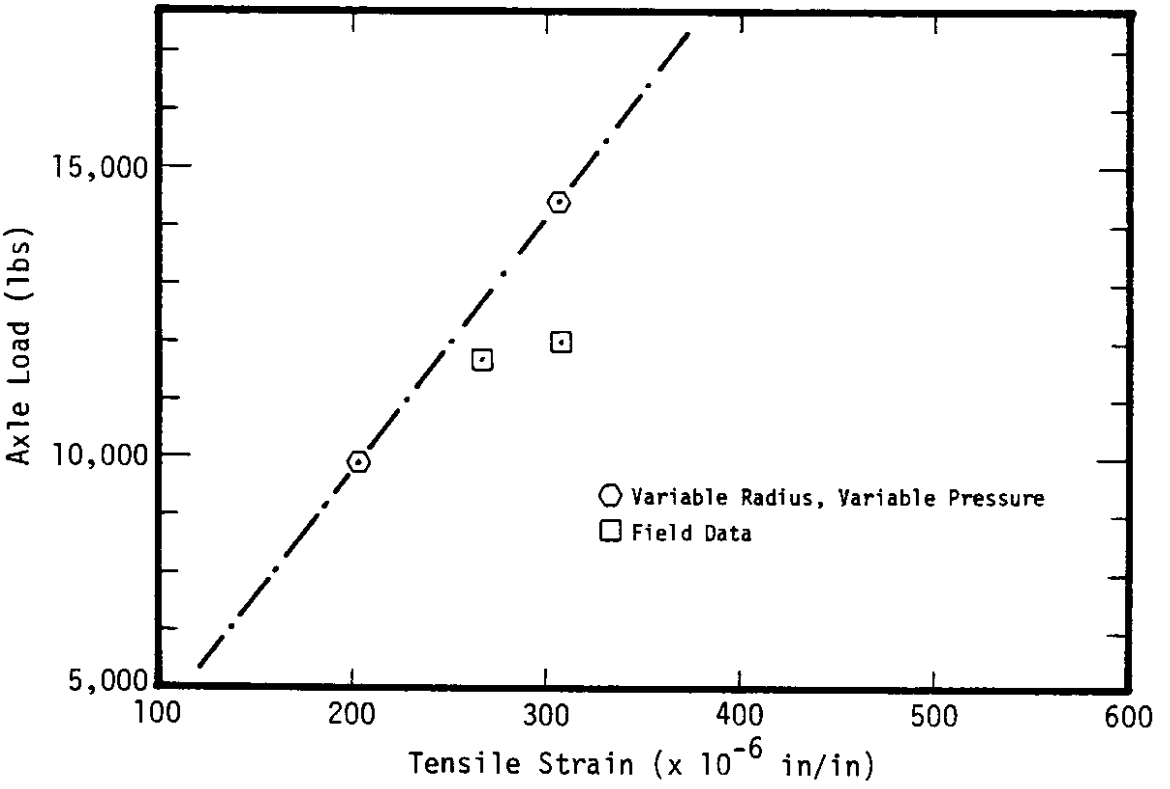

Figure 72. 12:00 x 22.5 Tire Size, 11.7 Inch ACP Section.

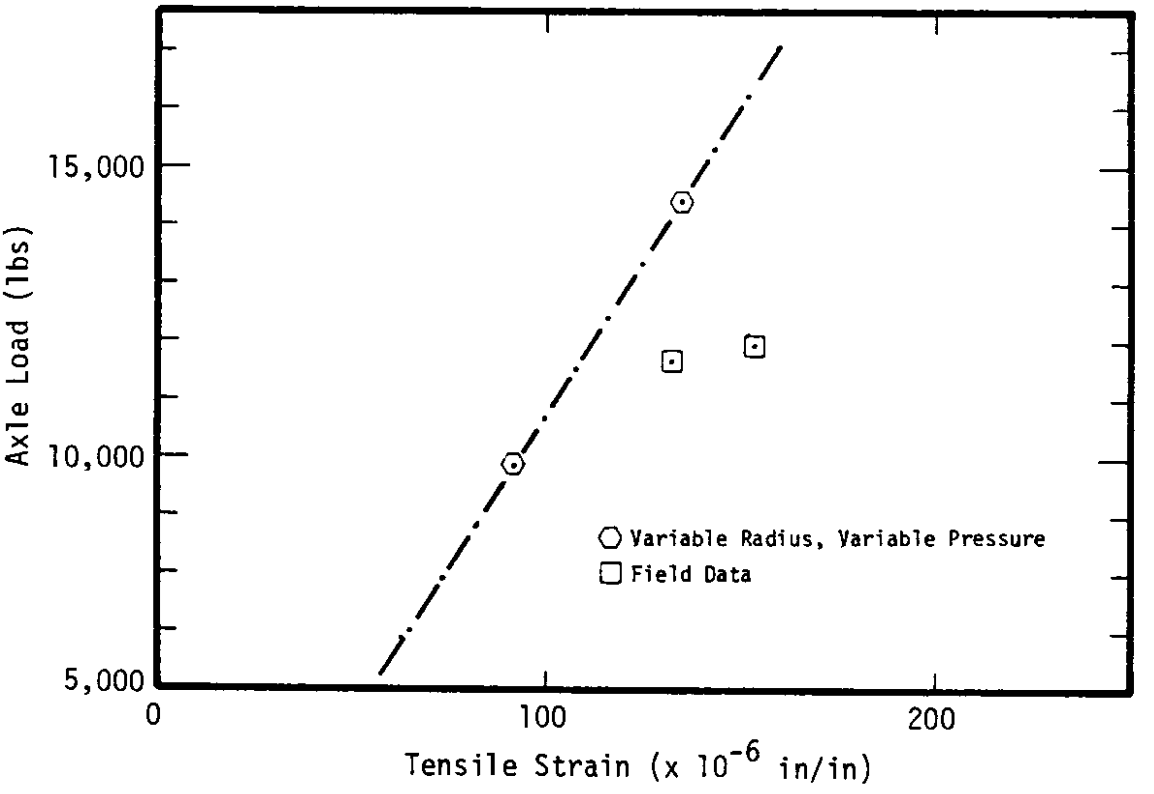

Figure 73. 12:00 x 22.5 Tire Size, 15 Inch ACP Section.

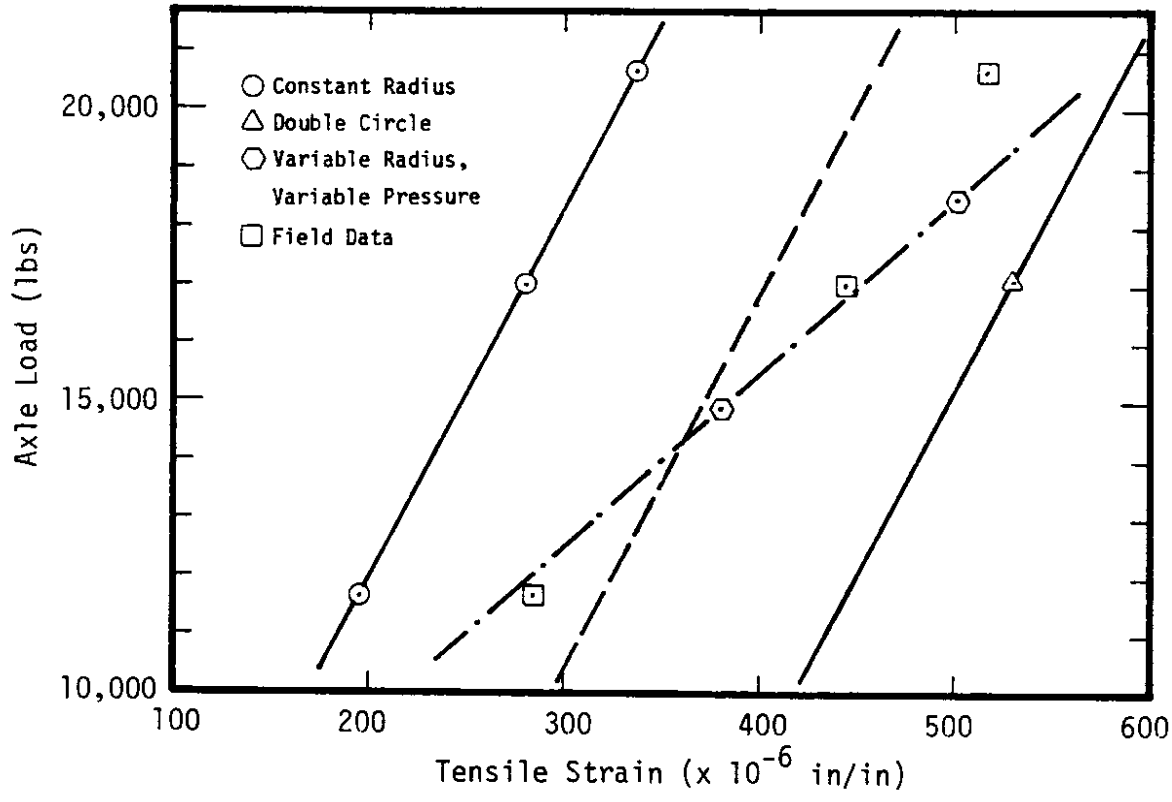

Figure 74. 16:50 x 22.5 Tire Size, 3 Inch ACP Section.

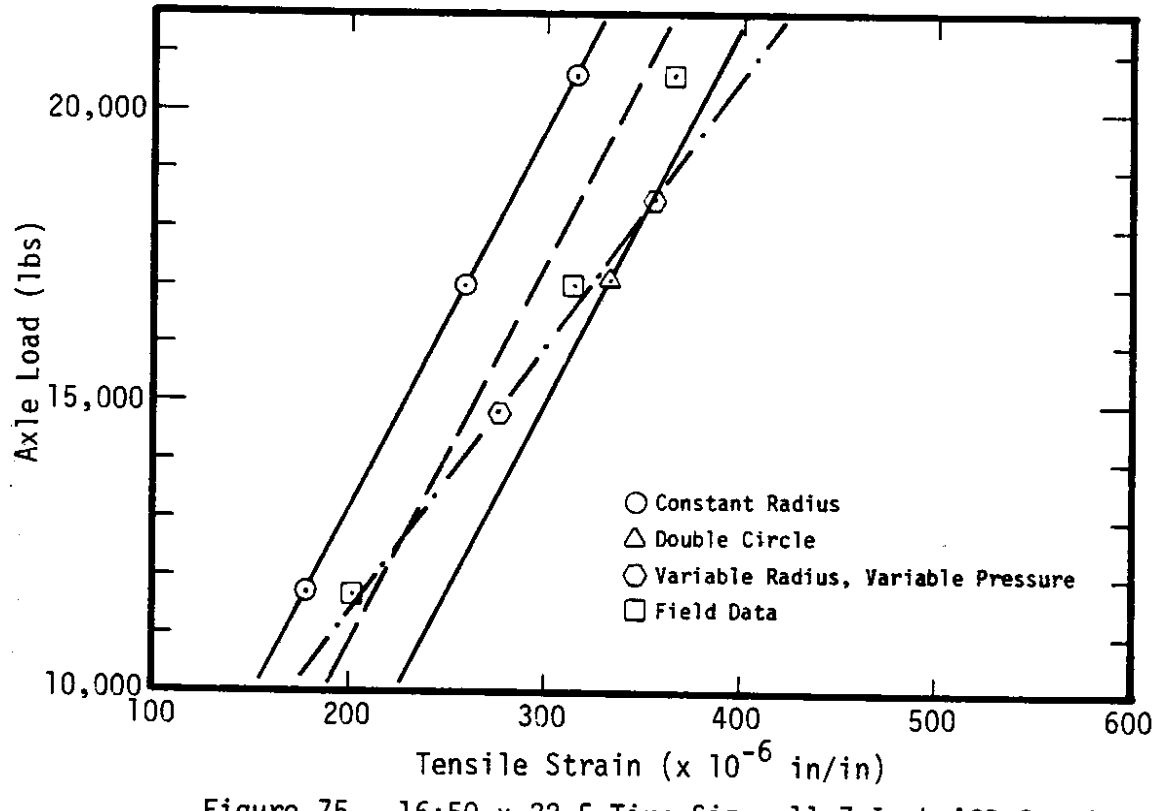

Figure 75. 16:50 x 22.5 Tire Size, 11.7 Inch ACP Section.

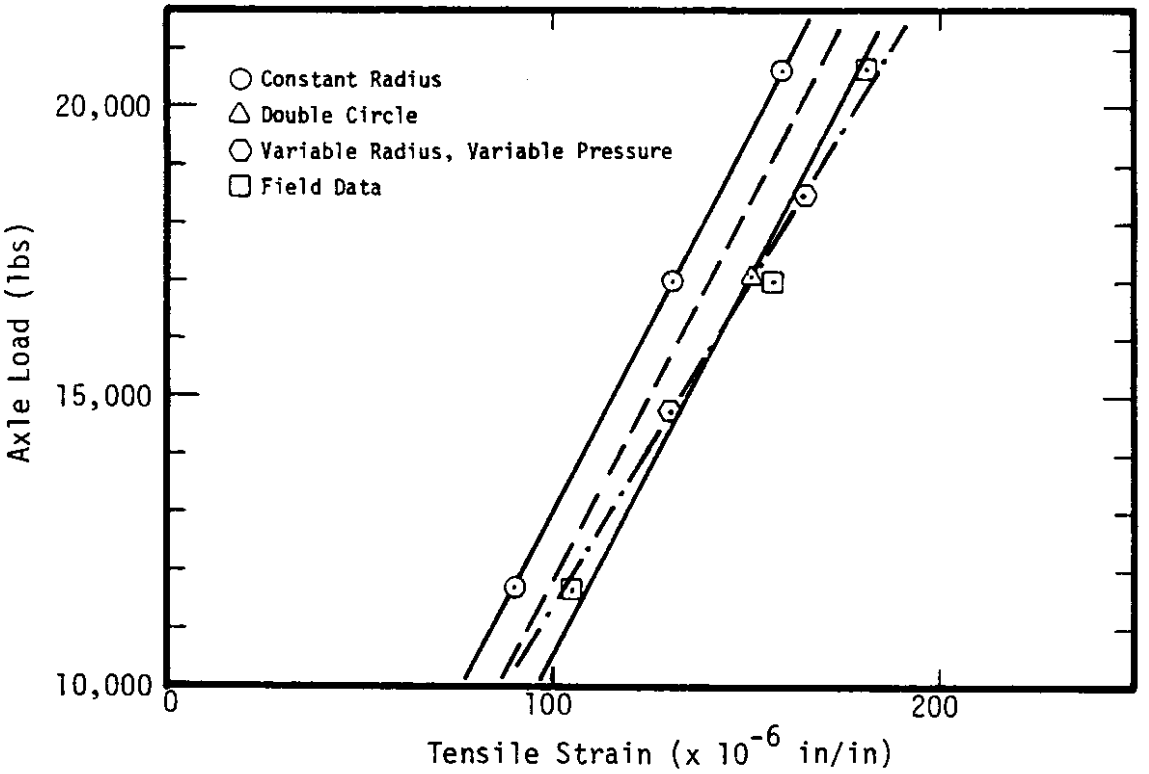

Figure 76. 16:50 x 22.5 Tire Size, 15 Inch ACP Section.

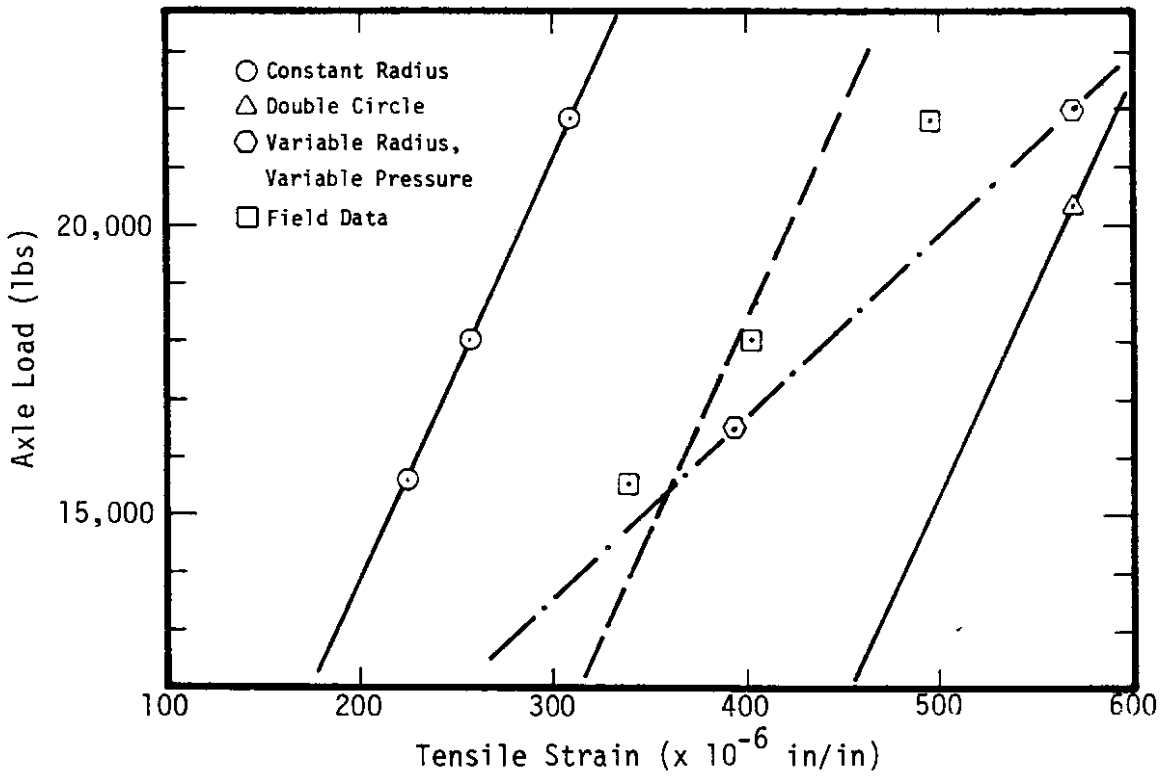

Figure 77. 18:00 x 22.5 Tire Size, 3 Inch ACP Section.

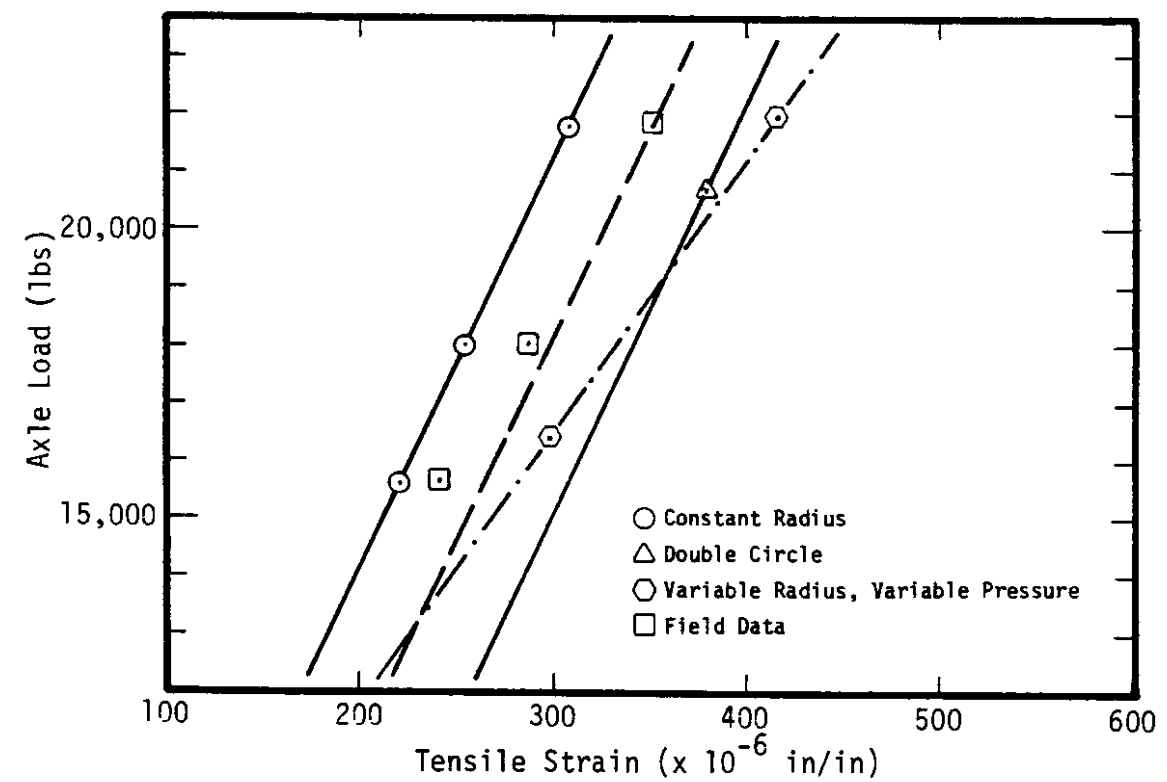

Figure 78. 18:00 x 22.5 Tire Size, 11.7 Inch ACP Section.

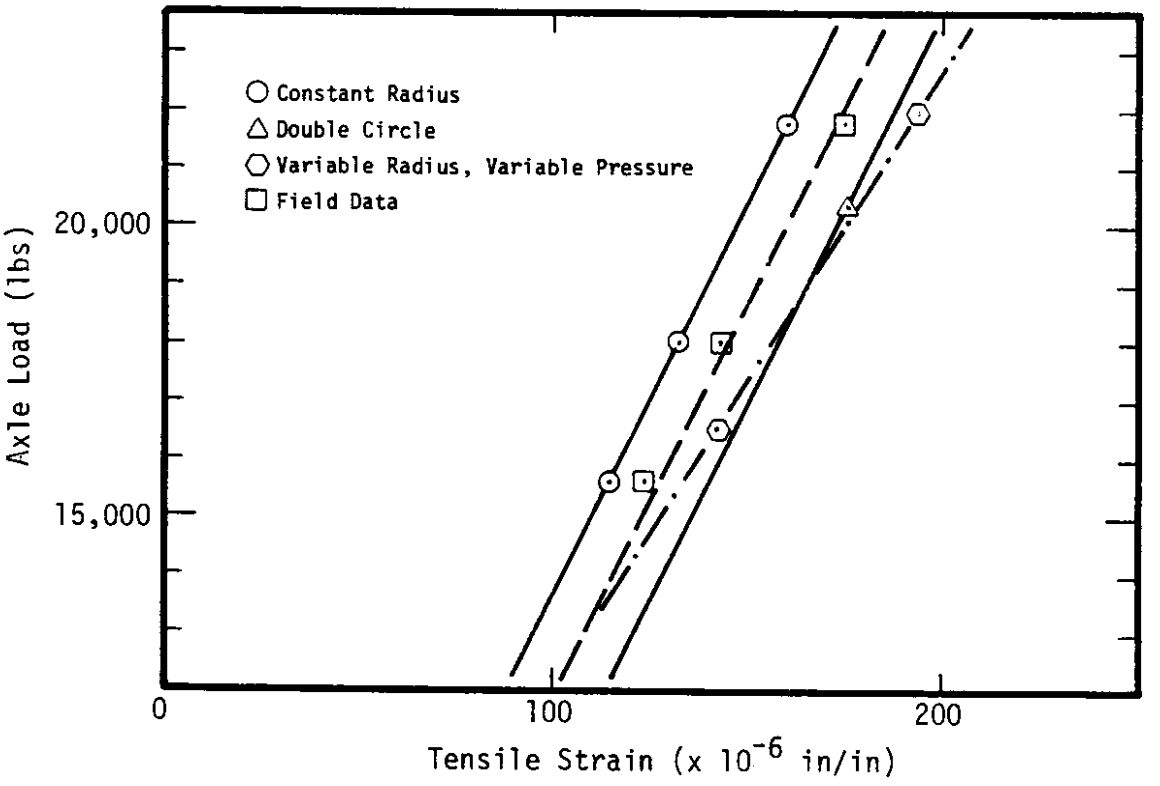

Figure 79. 18:00 x 22.5 Tire Size, 15 Inch ACP Section.

models, it appears that there are two models which describe the field behaviour adequately and those two models are:

1. Variable pressure variable radius as per manufacturer's recommendations.
2. Average values of strain for constant radius and double circle.

Of these two methods it appears that the variable pressure variable radius method works well for tire sizes ranging from 19 to 16:5 inches wide and for thin and thick ACP pavements, while the average value method works well for 18 inch wide tires and thicker ACP sections.

Other Factors. The other factors which are of interest to this study are results reported by the Alberta Research Council for effects of bias ply and radials on the load equivalency factors. Such differences in the tire types are difficult to model analytically; however, it is possible to measure field strain and deflections under actual loading conditions. Figure 80 shows such differences. Equivalency factors for single axle - 10:00 x 20 radial and bias ply dual tire loads indicate that, at comparable loads, one application of the bias ply tire configuration is approximately equivalent in destructive effect to 1.25 applications of the radial tire load. The Alberta authors warn that more tests are necessary to verify apparent differences in the magnitude of the strains and deflections measured under these two tire types.

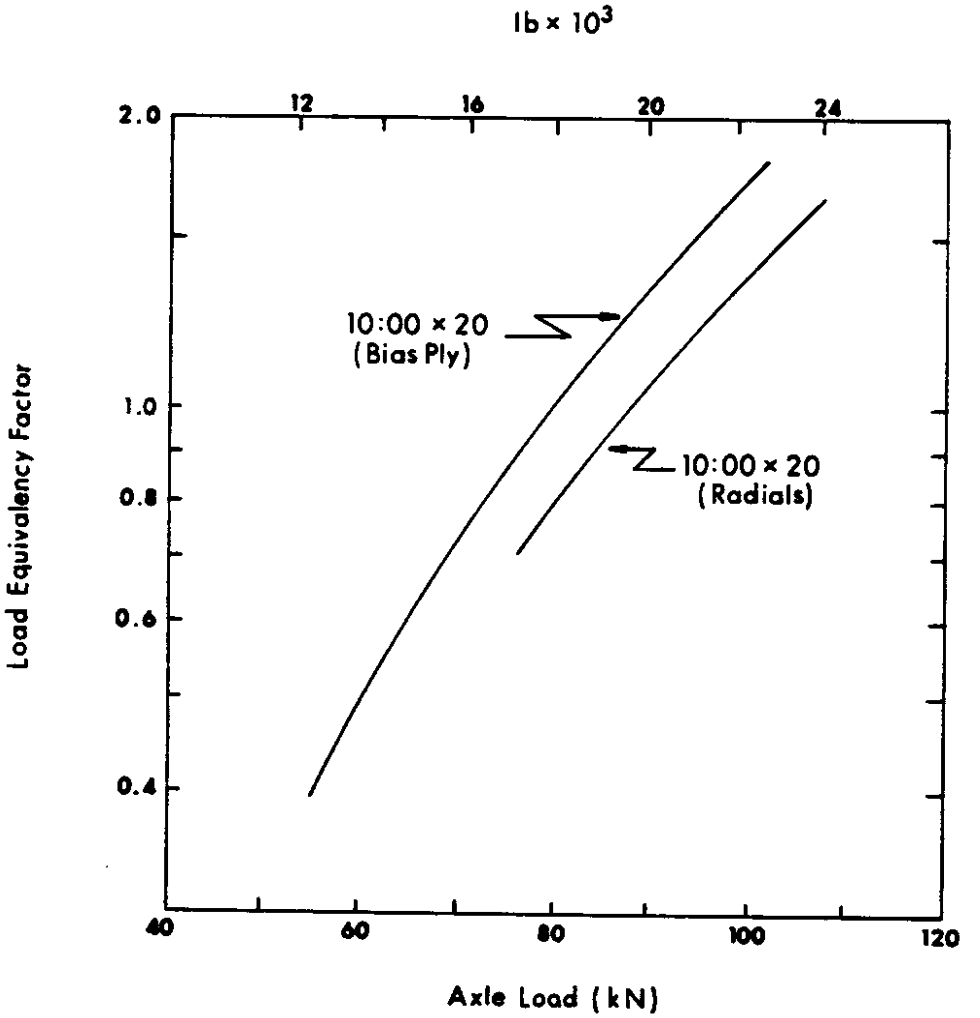

Figure 80. Load Equivalency Factors for Single Axle Loads on Dual Tires (after Ref. 34).

CHAPTER 4

CONCLUSIONS AND RECOMMENDATIONS

Conclusions

The traffic equivalence factors, Tables 4, 5, 6, 7, 8, 9, 10, 12, 13, 16, 17, 18 and 19, developed in this research study can be used to determine the effects of axles, with dual tires and various widths of single tires on both rigid and flexible pavements. These factors can be used to evaluate regulations relating to tire and axle loading configurations. They also permit conversion of mixed traffic, including axles with single tires, to equivalent 18 kip single axle load applications, for use in pavement design and evaluation. Appendix B contains an example analysis using the traffic equivalence factors developed for flexible pavements. This example also demonstrates the complexities of the analysis of axle configurations with single and dual tires.

The fatigue curves, Figures 22 to 27, also can be used to design the thickness of concrete pavements in Washington State. Figure 81 is a comparison between pavement thickness and repetitions of an 18 kip single axle with dual tires calculated using Equation D-15 in the AASHTO Interim Guide for Design of Pavement Structures, 1972 [1] and the results in Figures 22, 23 and 24. This comparison indicates that the analysis procedure used in this study results in predicted pavement thicknesses within 1/2 inch of the AASHTO method. The advantage of using the fatigue curves is that non-standard axle loadings can be evaluated. Since these curves were developed using warping stresses calculated for Washington, use in other geographic areas is possible only if the warping stresses are approximately equal.

Recommendations

1. Single tires with widths of 10 to 18 inches were analyzed in this study. It was found that for equivalent axle loads, the predicted damage to pavements was greater for axles with single tires than axles with dual tires. Also, the relative damage effects of single tires was dependent on the width of the tire. The relative damage effects of single versus dual tires were

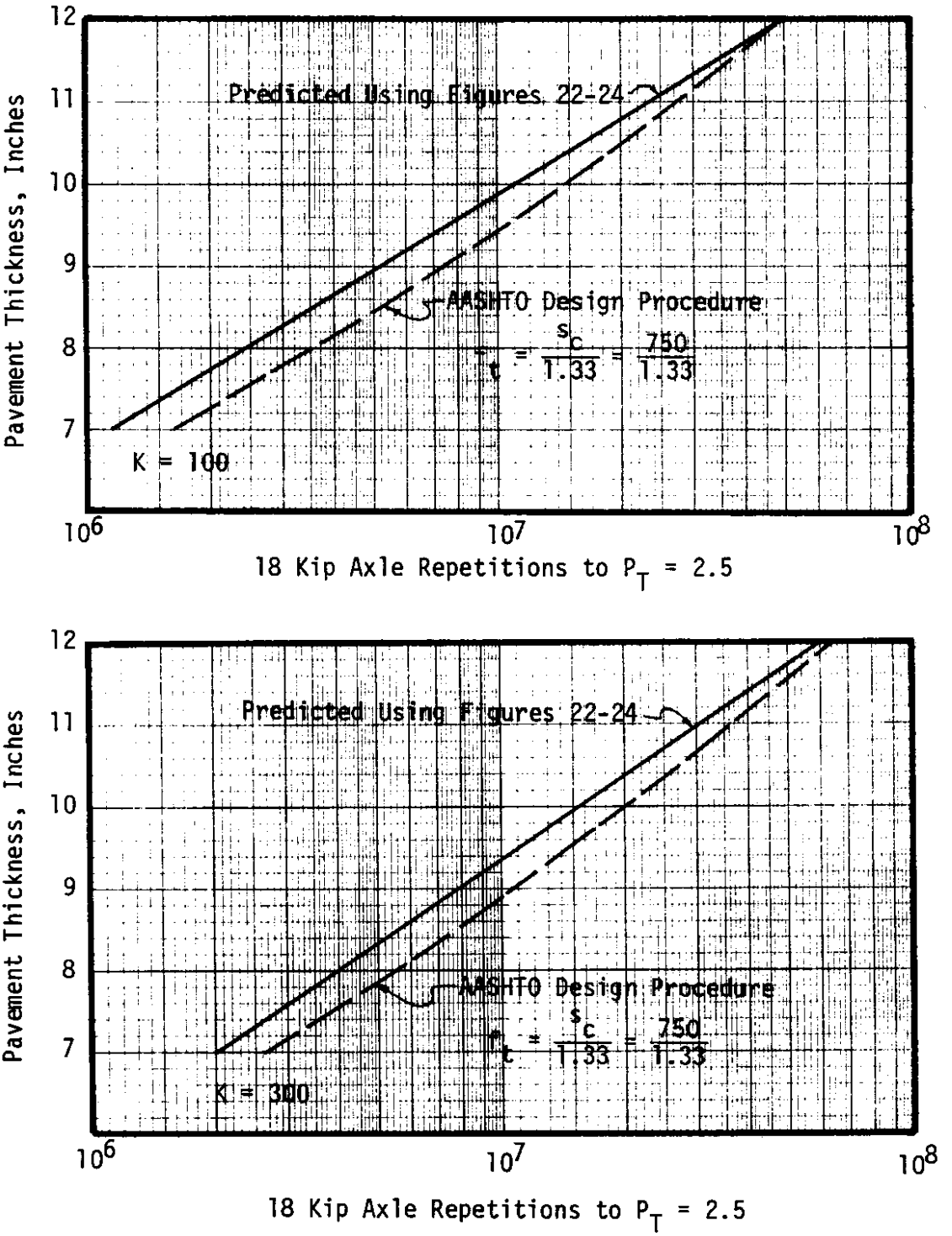

Figure 81. Comparison of the Analysis Procedure For Rigid Pavement Used in this Study with the AASHTO Design Procedure

Table 34. Comparison of Tire Width Regulations for Various States.

States	Tire Size Factor (lb/in)
Alaska	500
Connecticut	600
Florida	550
Idaho	800
Indiana	800
Kentucky	600
Louisiana	450
Maine	600
Massachusetts	800
Michigan	700
New Hampshire	600
New Jersey	800
New Mexico	600
New York	800
North Carolina	600
North Dakota	550
Ohio	650
Oregon	550
Pennsylvania	800
South Dakota	600
Texas	650
Vermont	600
Virginia	650
Washington	550
average =	642

compared with the requirements of the revised code of Washington (RCW) 46.44.042 for a 20,000 lb dual tire, single axle load. RCW 46.44.042 specifies that the maximum gross weight upon a tire will be 550 lbs per inch width of tire for tires less than 12 inches, with a 20 percent tolerance above 550 lb per inch width (660 lbs) for a tire having a width of 12 inches or more. This comparison supported the code requirement of a maximum gross tire load of 550 lbs per inch width of tire. However, as illustrated in Figure 82, the 20 percent tolerance for tires having a width of 12 inches or more was not supported. For example, an axle with 14 inch single tires on a 9 inch concrete pavement with a subgrade K - 100 pci can carry approximately 82 percent of a dual tire axle load (16,400 lbs when the dual tire axle load is 20,000 lbs) for an equivalent fatigue life. While the regulations permit 660 lbs per inch width of tire or a maximum axle load of 18,400 lbs which equals 92 percent of the maximum allowable dual tire load. These results indicate that applying this tolerance will result in single tires causing more pavement damage than dual tires for all classes of highways, particularly as the tire widths increase.

However, the truck survey conducted during this study revealed no significant evidence that the trucking industry is taking advantage of the 20 percent tolerance. Even in the example of SR 542 presented in Appendix B, Lynden Transport Co. could not take advantage of the 660 lb/inch width allowance as the gross weight requirements and number of axle requirements governed the allowable wheel loads.

Also presented in Table 34 is the summary of state that use tire width regulations. The range of tire size factors are from 450 lb/in used by Maine to 800 lb/in used by Pennsylvania, New Jersey, New york, Michigan, Indiana and Idaho. The average value used by all states is about 640 lb/in, which is close to the upper limit allowable in Washington.

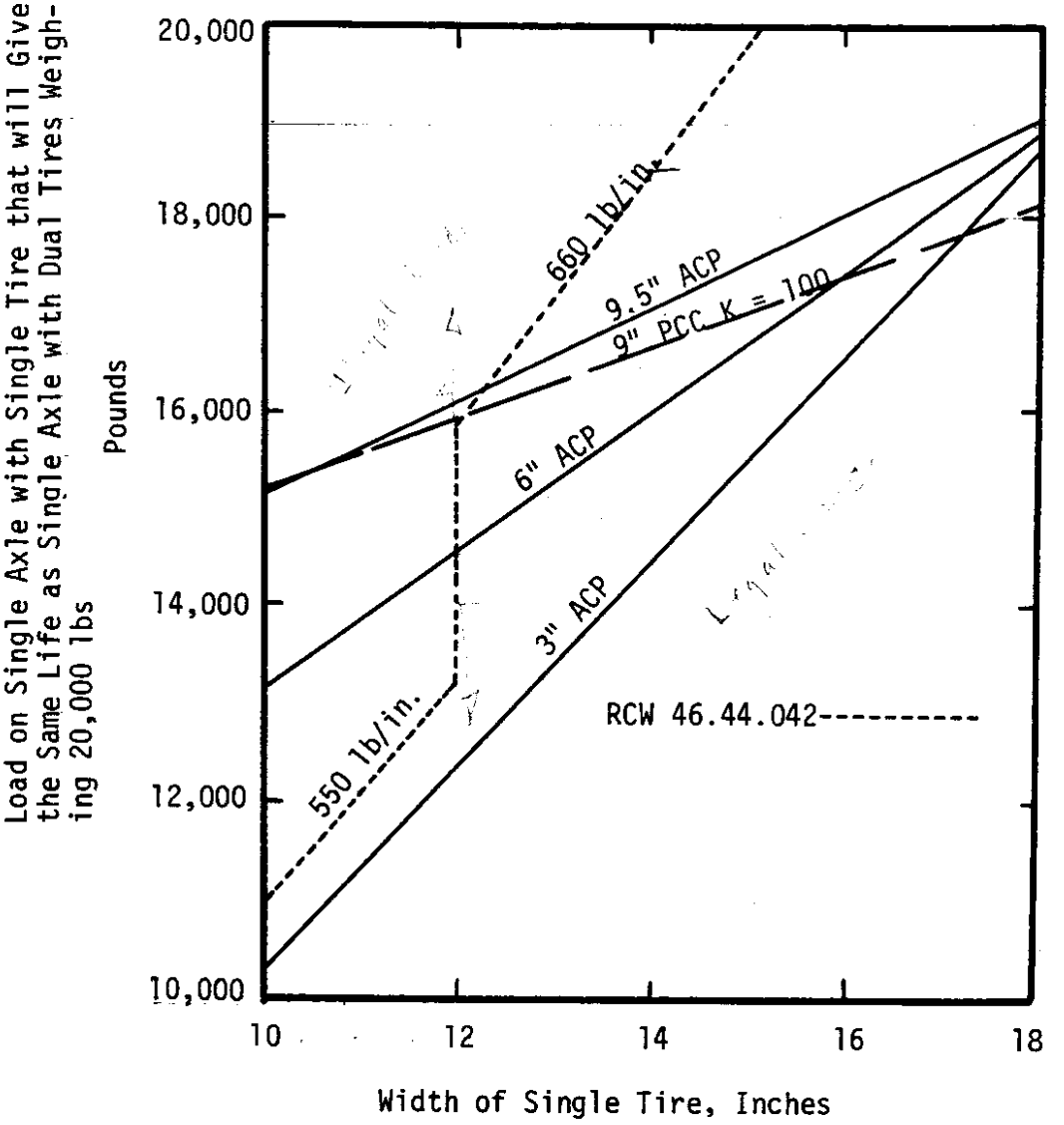

Figure 82. Comparison of the Regulation Requirements for Maximum Tire Loads with the Dual and Single Tire Relationships for Equivalent Fatigue Life. Dual Tire Axle Load Equals 20,000 lb

Recommendations: Consideration should be given to checking tire pressure on dual tires as the resulting tire pressures can violate the current, existing RCW and result in adverse pavement loading conditions.

2. Washington State RCW 46.44.095 provides for issuing permits which increase the maximum gross weight of vehicles from 80,000 to 105,500 lbs. The vehicle must comply with axle load and spacing requirements and tire load regulations. However, as illustrated by the analysis contained in Appendix B, there may be several tire axle configurations which meet the regulations, but which have very different effects on pavement performance.

   Recommendations: RCW 46.44.095 should be revised to require the proposed tire and axle configurations be submitted with the permit application for review and approval prior to receiving an extra tonnage permit. A comparison of the cost of pavmeent damage versus cost to the carrier should serve as a basis for determining a satisfactory tire-axle configuration. However, in no case should the maximum axle loads of 20,000 lbs for a single axle and 34,000 lbs for a tandem axle be exceeded.

3. The analysis of rigid pavements indicated that the combined load and temperature warping edge stresses may exceed the tensile strength of concrete in 7 inch or thinner slabs as shown in Figure 83. This is an important factor to consider when designing low volume urban streets, farm to market roads and parking lots with thin slabs. It may take a relatively few passes of heavily loaded garbage trucks, transit vehicles or devlivery trucks to initiate cracking, particularly if these vehicles travel near the pavement edge.

   Recommendations: Design procedures should incorporate a complete load and temperature-stress analysis when concrete pavements of less than 8 inches are designed. The ILLI-SLAB program and the procedure used in this study to calculate warping stresses would be suitable for such an analysis.

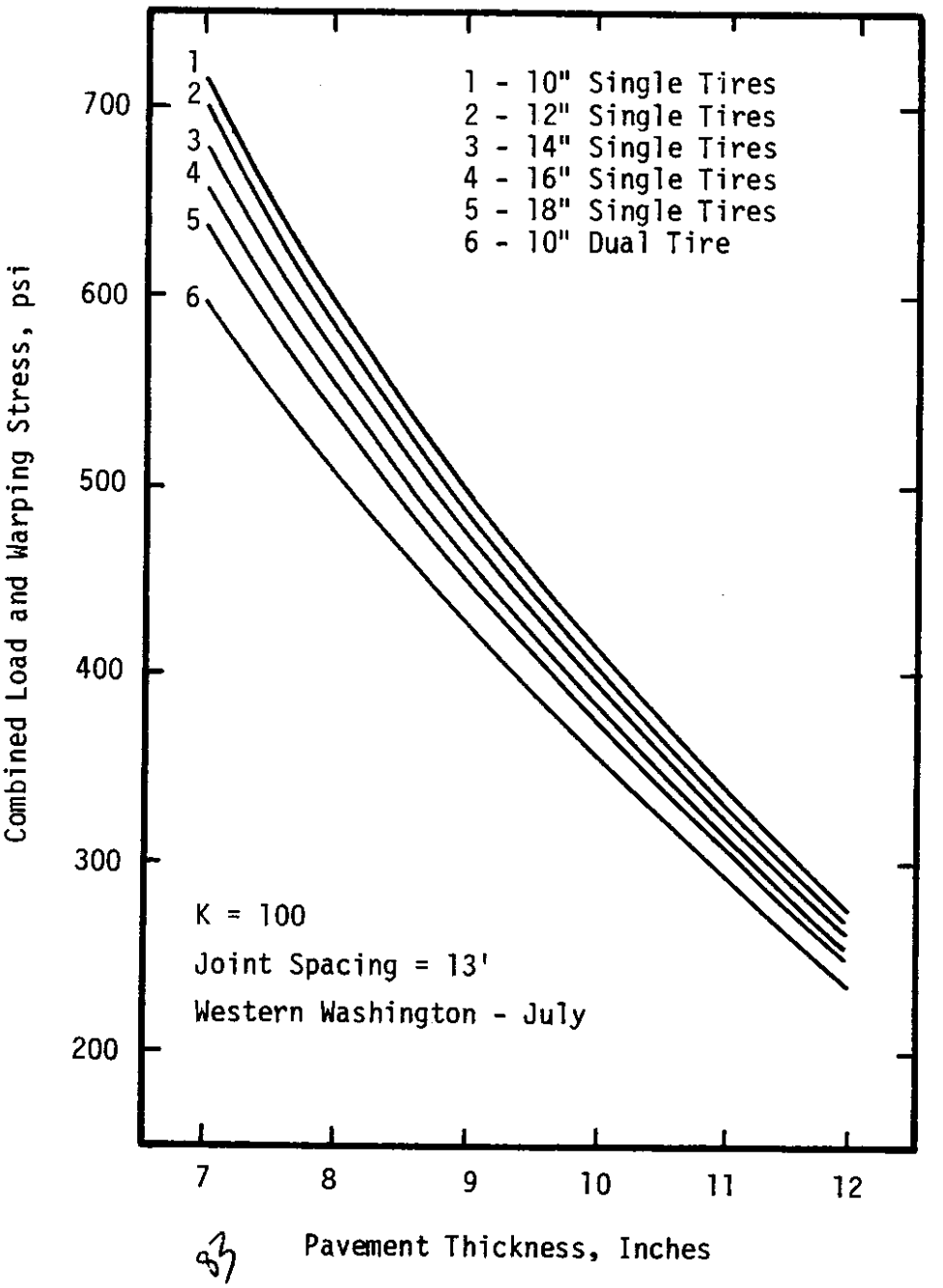

Figure ~~67~~ 93. Total Load and Warping Edge Stress During Month with Maximum Thermal Gradient in Western Washington

4. Previous studies have found that the use of uniformly loaded circles for elastic layer analysis is satisfactory for normal width single and dual tires. However, the analysis performed for this study with the inclusion of field data from the Fife weigh station and three sites near Edmonton, Alberta indicates that the use of uniformly loaded circles may not be entirely satisfactory for modeling wide single tires. The analysis showed that the model consisting of circles calculated from increasing load with increasing pressure as recommended in the tables provided by the tire manufacturer fits the field measured strains the best for tires up to 16.5 inch width. For tires greater than this width, the average value of constant radius and double circle fits the data best.

REFERENCES

1. American Association of State Highway and Transportation Officials, "AASHTO Interim Guide for Design of Pavement Structures, 1972," American Association of State Highway and Transportation Officials, Washington, D.C., 1981.

2. Barber, E.S., "Calculation of Maximum Pavement Temperature from Weather Reports," Bulletin 168, Highway Research Board, Washington, D.C., 1957.

3. Barker, W.R., Bradston, W.N. and Chou, Y.T., "A General System for the Structural Design of Flexible Pavements," Fourth International Conference - Structural Design of Asphalt Pavements, University of Michigan, 1977.

4. Bradbury, R.D., "Reinforced Concrete Pavements," Wire Reinforcement Institute, Washington, D.C., 1938.

5. Darter, Michael I., "Design of Zero Maintenance Plain Jointed Concrete Pavement Vol. 1 - Development of Design Procedures," Report No. FHWA-RD-77-111, Federal Highway Administration, Washington, D.C. 1977.

6. Deacon, John A., "Load Equivalency in Flexible Pavements," Proceedings of the Association of Asphalt Paving Technologists, Vol. 38, 1969.

7. Finn, F. Saraf, C., Kulkarni, R., Nair, K., Smith, W. and Abdullah, A., "The Use of Distress Prediction Subsystems for the Design of Pavement Structures," Fourth International Conference - Structural Design of Asphalt Pavements, University of Michigan, 1977.

8. Hicks, R.G., Swait, J.D., Jr. and Chastian, E.O., "Use of Layered Theory in the Design and Evaluation of Pavement Systems," 3rd Edition, Department of Civil Engineering, Oregon State University, 1978.

9. Highway Research Board, "The AASHTO Road Test, Report 6: Special Studies," Highway Research Board Special Report 61F, Highway Research Board, Washington, D.C., 1962.

10. Hoecher, W. H., Lotton, G.F. and Hass, W.A., "Solar Radiation and Climate Data for Quasi-Homogeneous Climate Regions of the U.S.," National Oceanographic and Atmospheric Administration, 1979.

11. MacLeod, D.R. and Monismith, C.L., "A Cracking Model for Plain Jointed Portland Cement Concrete Pavement," Proceedings, Second International Conference on Concrete Pavement Design, Purdue University, West Lafayette, Indiana, April, 1981.

REFERENCES (Cont.)

12. Majidzadeh, K., Ilves, G.J. and McComb, R., "Mechanistic Design of Rigid Pavements," Proceedings, Second International Conference on Concrete Pavement Design Purdue University, West Lafayette, Indianna, April 1981.

13. McHenry, A.E., "Preliminary Report on SR-542 Excessive Roadway Wear," Interdepartmental Communication, Washington Department of Transportation, 1981.

14. Miller, L.C., "The Washington Highway Department Rigid Pavement Design Procedure," Proceedings, 1969 Northwest Roads and Streets Conference, University of Washington, Seattle, 1969.

15. Ruffner, J.A., "Climate of the States, Vol. 2," Gale Research Company, Book Tower, Detroit, 1975.

16. Shell-Labroatorium, "Bitumen Structures Analysis in Roads (BISAR), Abbreviated Version," Shell-Laboratorium, Amsterdam, Netherlands, July, 1979.

17. Tabatabaie, A.M. and Barenberg, E.J., "Finite-Element Analysis of Jointed or Cracked Concrete Pavements", Transportation Research Record 671, Transportation Research Board, Washington, D.C., 1978.

18. Tabatabaie, A.M. and Barenberg, E.J., "Longitudinal Joint Systems in Slip-formed Rigid Pavements, Vol. III - User's Manual," Report No. FAA-RD-79-4-III, Federal Aviation Administration, 1979.

19. Teller, L.W. and Southerland, E.C., "The Structural Design of Concrete Pavements, Part 1 - A Description of the Investigation," Public Roads, Vol. 16, No. 8, 1935.

20. Teller, L.W. and Southerland, E.C., "The Structural Design of Concrete Pavements, Part 2 - Observed Effects of Variations in Temperature and Moisture on the Size, Shape and Stress Resistance of Concrete Pavement Slabs," Public Roads, Vol. 16, No. 9, 1935.

21. Teller, L.W. and Southerland, E.C., "The Structural Design of Concrete Pavements, Part 3 - A Study of Concrete Pavement Cross Sections, Public Roads, Vol. 16, No. 10, 1935.

22. Teller, L.W. and Southerland, E.C., "The Structural Design of Concrete Pavements, Part 5 - An Experimental Study of the Westergaard Analysis of Stress Conditions in Concrete Pavement Slabs of Uniform Thickness," Public Roads, Vol. 23, No. 8, 1943.

23. Terrel, R.L., "Examples of Approach and Field Evaluation: Research Applications," Structural Design of Asphalt Concrete Pavements to Prevent Fatigue Cracking, Special Report 140, Highway Research Board, Washington, D.C., 1973.

24. Terrel, R.L. and Krukor, M., "Evaluation of Test Track Pavements," Proceedings, Association of Asphalt Paving Technologists, 1970.

25. Terrel, R.L. and Rimsritong, S., "Pavement Response and Equivalencies for Various Truck Axle Tire Configurations," Research Report 17.1, Washington State Highway Commission, Olympia, Washington, 1974.

26. Vesic, A.S. and Saxena, S.K., "Analysis of Structural Behavior of AASHTO Road Test Rigid Pavements," NCHRP Report 97, Highway Research Board, Washington, D.C., 1970.

27. Washington State Department of Transportation, "1979 Final Pavement Condition," Washington State Department of Transportation, Olympia, Washington, 1979.

28. Westergaard, H.M., "Analysis of Stresses in Concrete Pavements Due to Variations of Temperature," Proceedings, Sixth Annual Meeting, Highway Research Board, Washington, D.C., 1927.

29. Yoder, E.J. and Witczak, M.W., Principles of Pavement Design, 2nd Edition, John Wiley and Sons, Inc., New York, 1975.

30. Zube, E. and Forsyth, R., "An Investigation of the Destructive Effect of Flotation Tires on Flexible Pavement," Highway Research Record No. 71, Highway Research Board, Washington, D.C., 1965.

31. Mahoney, J.P., et al., "Sulfur Extended Asphalt Pavement Evaluation in the State of Washington: Design and Construction Report," Final Report, Washington State Department of Transportation, Agreement Y-2004, Olympia, Washington, September, 1981.

32. Bush, A.J., "Non-Destructive Testing for Light Aircraft Pavements, Development of the Non-Destructive Evaluation Methodology," USAEWES Report Number FAA-RD-80-9-11, November, 1980.

33. Christison, J.T., "Evaluation of the Relative Damaging Effects of Wide Base Tire Loads on Pavements," Report HTE 79/01, Alberta Research Council, April 1979.

34. Christison, J.T., "Evaluation of the Effects of Axle Loads on Pavements For Insitu Strain and Deflection Measurements," Report HTE-78/02, Alberta Research Council, June 1978.

35. Christison, J.T., "Strain and Deflections in Pavements Under Moving Single Axle Dual Tire Loads," Report HTE/75/03, Alberta Research Council, August 1975.

APPENDIX A

Calculated Warping Stress for 7, 9, 10 and 12 Inch Pavements in Washington State

Table A.1. Calculated Warping Stresses.

Pavement Depth - 7 Inches

Joint Spacing - 13 Feet

Modulus of Subgrade Reaction	Month	Temperature Stress, psi Eastern Washington	Western Washington
50	January	31.3	34.2
	February	46.7	48.4
	March	70.6	69.5
	April	96.2	90.5
	May	116.5	111.4
	June	123.8	118.1
	July	142.7	131.5
	August	124.2	111.4
	September	100.5	90.5
	October	67.7	62.6
	November	36.5	34.2
	December	26.3	34.2
100	January	39.7	43.4
	February	59.4	61.5
	March	90.1	88.7
	April	123.6	116.1
	May	150.3	143.5
	June	160.1	152.4
	July	185.2	170.2
	August	160.5	143.5
	September	129.1	116.0
	October	86.4	79.8
	November	46.2	43.4
	December	33.2	43.4
200	January	42.2	46.2
	February	63.3	65.6
	March	96.6	95.1
	April	133.2	124.9
	May	162.7	155.2
	June	173.5	165.1
	July	201.6	184.9
	August	174.0	155.2
	September	139.3	124.9
	October	92.6	85.4
	November	49.2	46.2
	December	35.3	46.2

Table A.2. Calculated Warping Stresses.

Pavement Depth - 7 Inches

Joint Spacing - 15 Feet

Modulus of Subgrade Reaction	Month	Temperature Stresses, psi Eastern Washington	Western Washington
50	January	35.3	38.6
	February	52.7	54.6
	March	79.7	78.5
	April	108.9	102.4
	May	132.1	126.2
	June	140.5	133.9
	July	162.1	149.3
	August	140.9	126.2
	September	113.8	102.4
	October	76.5	70.7
	November	41.1	38.6
	December	29.6	38.6
100	January	42.6	46.6
	February	63.7	66.1
	March	96.8	95.3
	April	132.8	124.7
	May	161.5	154.2
	June	172.0	163.8
	July	199.0	182.9
	August	172.5	154.2
	September	138.8	124.7
	October	92.8	85.7
	November	49.7	46.6
	December	35.7	46.6
200	January	43.9	48.0
	February	65.9	68.3
	March	100.3	98.7
	April	138.1	129.6
	May	168.4	160.7
	June	179.6	170.9
	July	208.4	191.2
	August	180.1	160.7
	September	144.4	129.6
	October	96.1	88.7
	November	51.2	48.0
	December	36.7	48.0

Table A.3. Calculated Warping Stresses.

Pavement Depth - 7 Inches

Joint Spacing - 20 Feet

Modulus of Subgrade Reaction	Month	Temperature Stresses, psi Eastern Washington	Western Washington
50	January	45.0	49.2
	February	67.4	69.8
	March	102.4	100.8
	April	140.6	132.0
	May	171.1	163.4
	June	182.3	173.6
	July	211.2	194.0
	August	182.9	163.4
	September	147.0	132.0
	October	98.2	90.7
	November	52.5	49.2
	December	37.7	49.2
100	January	49.7	54.4
	February	74.5	77.2
	March	113.1	111.3
	April	155.1	145.7
	May	188.7	180.2
	June	201.0	191.4
	July	232.6	213.7
	August	201.5	180.2
	September	162.1	145.7
	October	108.4	100.1
	November	58.0	54.4
	December	41.7	54.4
200	January	48.0	52.5
	February	71.9	74.5
	March	109.1	107.3
	April	149.4	140.3
	May	181.6	173.4
	June	193.4	184.2
	July	223.6	205.6
	August	193.9	173.4
	September	156.1	140.3
	October	104.5	96.6
	November	56.0	52.5
	December	40.2	52.5

Table A.4. Calculated Warping Stresses.

Pavement Depth - 9 Inches

Joint Spacing - 13 Feet

Modulus of Subgrade Reaction	Month	Temperature Stresses, psi Eastern Washington	Western Washington
50	January	21.3	20.9
	February	31.9	33.5
	March	48.3	46.3
	April	66.3	63.8
	May	80.6	76.7
	June	85.8	81.0
	July	99.4	93.9
	August	86.1	76.7
	September	69.2	63.8
	October	46.3	42.0
	November	24.8	25.1
	December	17.9	20.6
100	January	30.0	29.5
	February	45.0	47.4
	March	68.6	65.6
	April	94.5	90.8
	May	115.3	109.6
	June	123.0	115.8
	July	142.9	134.7
	August	123.3	109.6
	September	98.7	90.8
	October	65.7	59.5
	November	35.0	35.4
	December	25.2	29.0
200	January	32.9	32.3
	February	49.5	52.1
	March	75.6	72.4
	April	104.7	100.6
	May	128.1	121.7
	June	136.9	128.8
	July	159.6	150.2
	August	137.3	121.7
	September	109.4	100.6
	October	72.5	65.6
	November	38.4	38.9
	December	27.6	31.7

Table A.5. Calculated Warping Stresses.

Pavement Depth - 9 Inches

Joint Spacing - 15 Feet

Modulus of Subgrade Reaction	Month	Temperature Stresses, psi Eastern Washington	Western Washington
50	January	27.1	26.7
	February	40.6	42.8
	March	61.7	59.1
	April	84.8	81.6
	May	103.3	98.2
	June	110.0	103.7
	July	127.6	120.4
	August	110.3	98.2
	September	88.5	81.6
	October	59.2	53.6
	November	31.6	32.0
	December	22.7	26.2
100	January	35.3	34.7
	February	53.0	55.8
	March	80.7	77.2
	April	111.2	106.9
	May	135.7	128.9
	June	144.7	136.3
	July	168.2	158.6
	August	145.1	128.9
	September	116.2	106.9
	October	77.3	70.0
	November	41.2	41.7
	December	29.6	34.1
200	January	37.5	36.9
	February	56.4	59.4
	March	86.1	82.4
	April	119.0	114.4
	May	145.5	138.2
	June	155.4	146.3
	July	181.0	170.4
	August	155.8	138.2
	September	124.4	114.4
	October	82.5	74.7
	November	43.8	44.3
	December	31.4	36.2

Table A.6. Calculated Warping Stresses.

Pavement Depth - 9 Inches

Joint Spacing - 20 Feet

Modulus of Subgrade Reaction	Month	Temperature Stresses, psi Eastern Washington	Western Washington
50	January	41.4	40.7
	February	62.2	65.4
	March	94.8	90.7
	April	130.8	125.8
	May	159.8	151.8
	June	170.5	160.6
	July	198.3	186.9
	August	171.0	151.8
	September	136.7	125.8
	October	90.9	82.2
	November	48.3	48.9
	December	34.7	39.9
100	January	48.1	47.4
	February	72.3	76.1
	March	110.1	105.4
	April	151.8	146.0
	May	185.3	176.1
	June	197.7	186.2
	July	229.8	216.6
	August	198.3	176.1
	September	158.6	146.0
	October	105.6	95.6
	November	56.2	56.9
	December	40.4	46.5
200	January	48.7	47.9
	February	73.1	76.9
	March	111.2	106.4
	April	163.1	147.2
	May	186.7	177.5
	June	199.1	187.6
	July	231.3	218.1
	August	199.7	177.5
	September	159.9	147.2
	October	106.6	96.5
	November	56.8	57.5
	December	40.8	47.0

Table A.7. Calculated Warping Stresses.

Pavement Depth - 10 Inches

Joint Spacing - 13 Feet

Modulus of Subgrade Reaction	Month	Temperature Stresses, psi Eastern Washington	Western Washington
50	January	15.7	17.7
	February	23.5	23.7
	March	35.7	35.9
	April	49.0	45.2
	May	59.7	57.7
	June	63.7	60.8
	July	73.9	67.0
	August	63.9	57.7
	September	51.2	45.2
	October	34.2	32.9
	November	18.3	17.7
	December	13.2	14.7
100	January	24.3	27.4
	February	36.5	36.8
	March	55.6	55.9
	April	76.6	70.6
	May	93.7	90.4
	June	100.0	95.4
	July	116.4	105.4
	August	100.3	90.4
	September	80.1	70.6
	October	53.3	51.1
	November	28.3	27.4
	December	20.3	22.7
200	January	27.0	30.6
	February	40.7	41.1
	March	62.3	62.7
	April	86.2	79.3
	May	105.7	101.9
	June	113.0	107.6
	July	131.8	119.1
	August	113.2	101.9
	September	90.2	79.3
	October	59.7	57.3
	November	31.6	30.6
	December	22.6	25.3

Table A.8. Calculated Warping Stresses.

Pavement Depth - 10 Inches

Joint Spacing - 15 Feet

Modulus of Subgrade Reaction	Month	Temperature Stress, psi Eastern Washington	Western Washington
50	January	22.1	24.9
	February	33.1	33.4
	March	50.3	50.7
	April	69.2	63.8
	May	84.4	81.5
	June	90.1	86.0
	July	104.6	94.9
	August	90.3	81.5
	September	72.4	63.8
	October	48.2	46.3
	November	25.7	24.9
	December	18.5	20.7
100	January	30.3	34.2
	February	45.6	46.0
	March	69.4	69.9
	April	95.8	88.2
	May	117.0	112.9
	June	125.0	119.2
	July	145.4	131.7
	August	125.3	112.9
	September	100.1	88.2
	October	66.5	63.9
	November	35.4	34.2
	December	25.4	28.4
200	January	32.7	36.9
	February	49.2	49.6
	March	75.1	75.6
	April	103.9	95.6
	May	127.2	122.7
	June	135.9	129.5
	July	158.4	143.3
	August	136.2	122.7
	September	108.7	95.6
	October	72.0	69.1
	November	38.2	36.9
	December	27.4	30.6

Table A.9. Calculated Warping Stresses.

Pavement Depth - 10 Inches

Joint Spacing - 20 Feet

Modulus of Subgrade Reaction	Month	Temperature Stresses, psi Eastern Washington	Western Washington
50	January	37.7	42.5
	February	56.7	57.2
	March	86.5	87.1
	April	119.4	110.0
	May	146.1	141.0
	June	156.1	148.8
	July	181.8	164.5
	August	156.5	141.0
	September	124.9	110.0
	October	82.9	79.5
	November	44.0	42.5
	December	31.6	35.3
100	January	45.0	50.8
	February	67.7	68.3
	March	103.2	103.9
	April	142.3	131.1
	May	174.0	167.9
	June	185.8	177.1
	July	216.2	195.7
	August	186.2	167.9
	September	148.8	131.1
	October	98.9	94.9
	November	52.6	50.8
	December	37.7	42.2
200	January	46.3	52.3
	February	69.5	70.2
	March	105.9	106.6
	April	145.9	134.4
	May	178.2	172.0
	June	190.3	181.5
	July	221.3	200.5
	August	190.8	172.0
	September	152.6	134.4
	October	101.5	97.4
	November	54.0	52.3
	December	38.8	43.4

Table A.10. Calculated Warping Stresses.

Pavement Depth - 12 Inches

Joint Spacing - 13 Feet

Modulus of Subgrade Reaction	Month	Temperature Stresses, psi Eastern Washington	Western Washington
50	January	5.0	5.3
	February	7.5	8.0
	March	11.4	11.6
	April	15.7	14.4
	May	19.1	18.3
	June	20.4	20.1
	July	23.7	22.1
	August	20.5	18.3
	September	16.4	13.5
	October	10.9	9.9
	November	5.8	6.1
	December	4.2	5.3
100	January	13.2	13.9
	February	19.8	21.1
	March	30.2	30.8
	April	41.7	38.3
	May	51.0	48.7
	June	54.5	53.7
	July	63.5	58.9
	August	54.6	48.7
	September	43.6	35.9
	October	28.9	26.1
	November	15.4	16.2
	December	11.0	13.9
200	January	15.5	16.4
	February	23.4	25.0
	March	35.8	36.6
	April	49.5	45.5
	May	60.8	58.0
	June	64.9	64.0
	July	75.9	70.4
	August	65.1	58.0
	September	51.8	42.6
	October	34.2	30.9
	November	18.1	19.1
	December	13.0	16.4

Table A.11. Calculated Warping Stresses.

Pavement Depth - 12 Inches

Joint Spacing - 15 Feet

Modulus of Subgrade Reaction	Month	Temperature Stresses, psi Eastern Washington	Western Washington
50	January	12.1	12.8
	February	18.2	19.4
	March	27.7	28.3
	April	38.2	35.2
	May	46.7	44.6
	June	49.8	49.1
	July	58.0	53.9
	August	50.0	44.6
	September	40.0	33.0
	October	26.6	24.0
	November	14.1	14.9
	December	10.1	12.8
100	January	20.3	21.5
	February	30.5	32.6
	March	46.6	47.6
	April	64.3	59.1
	May	78.7	75.2
	June	84.0	82.8
	July	97.9	90.9
	August	84.3	75.2
	September	67.3	55.4
	October	44.6	40.3
	November	23.7	25.0
	December	17.0	21.5
200	January	22.7	24.0
	February	34.1	36.4
	March	52.1	53.3
	April	72.1	66.3
	May	88.4	84.4
	June	94.5	93.0
	July	110.3	102.3
	August	94.7	84.4
	September	75.5	62.1
	October	49.9	45.1
	November	26.5	27.9
	December	18.9	24.0

Table A.12. Calculated Warping Stresses.

Pavement Depth - 12 Inches

Joint Spacing - 20 Feet

Modulus of Subgrade Reaction	Month	Temperature Stresses, psi Eastern Washington	Western Washington
50	January	29.6	31.3
	Feburary	44.5	47.5
	March	68.0	69.5
	April	94.1	86.5
	May	115.2	110.0
	June	123.1	121.3
	July	143.7	133.3
	August	123.5	110.0
	September	98.4	81.0
	October	65.1	58.8
	November	34.5	36.5
	December	24.7	31.3
100	January	37.7	39.9
	February	56.6	60.5
	March	86.5	88.3
	April	119.4	109.8
	May	146.1	139.6
	June	156.1	153.8
	July	182.0	169.0
	August	156.5	139.6
	September	124.9	102.9
	October	82.8	74.7
	November	44.0	46.4
	December	31.5	39.9
200	January	40.0	42.3
	February	60.0	64.1
	March	91.5	93.5
	April	126.3	116.2
	May	154.4	147.5
	June	164.9	162.5
	July	192.1	178.4
	August	165.4	147.5
	September	132.1	108.9
	October	87.7	79.2
	November	46.6	49.2
	December	33.4	42.2

APPENDIX B

Analysis of Lime Rock Haul On Washington Route 542, Mt. Baker Highway

Analysis of Lime Rock Haul on Washington Route 542, Mt. Baker Higher

This is an analysis of a pavement deterioration problem in Washington State, which illustrates the complexities of the analysis of axle configurations with single and dual tires. In 1979, as a result of the bankruptcy of the Milwaukee Railroad, transportation of lime rock between a quarry near Kendall, Washington and a cement plant near Bellingham shifted to trucks. A major portion of this haul is made over State Route (SR) 542.

Based on discussions with State DOT maintenance personnel, it appears that SR 542 was a dirt road which over the years received various oil and asphalt treatements and thin asphalt concrete overlays. An average section assumed for analysis was 3" of asphalt concrete pavement on a subgrade with an AASHTO soil support value of 4.

The trucking contractor is using a truck trailer combination in which he can haul 105,500 pounds gross weight. The maximum axle loads permitted are 20,000 pounds for single axles and 34,000 pounds for tandem axles. The maximum tire loads are 550 pounds per inch of width for tires less than 12 inches wide and 660 pounds per inch of width for tires 12 inches wide or greater. The tire and axle configuration selected by the contractor is shown in Figure B.1. The contractor elected to use tandem axles with single tires rather than single axles with dual tires because this permitted him to have up to 31,680 pounds on four tires. This loading was controlled by the 660 pounds per inch of tire. If he had used single axles with dual tires, the maximum load on four tires would have been 20,000 pounds as controlled by the maximum single axle load regulation. Using dual wheel tandem axles would have reduced the payload that could be hauled by the weight of the 8 additional tires and wheels without providing any advantage to the contractor.

The trucks are making approximately 95 to 105 trips per day. The results of this hauling operation has been to increase the pavement

and shoulder maintenance costs for this section of highway from an average of approximately $28,000 per year for the years 1977 - 1979 to approximately $51,000 per year for the years 1980 and 1981. [13]

The 18-kip dual tire equivalent axle loads per truck were calculated for the tire and axle load configuration currently being used. In addition, 3 other potential tire axle configurations were analyzed. These are described in Figure B.1. The equivalency factors used for axles with single tires and single axles with dual tires were those developed as part of this report, Tables 16 - 19. The equivalency factors for dual tire tandem axles are those contained in Table C2 - 4, "AASHTO Interim Guide for Design of Pavement Structure," 1972 [1]. Tandem axles with single tires were treated as two single axles.

The initial calculation of 18 kip EQAL repetitions for each truck was made using the factors for a pavement with an AASHTO Structural Number (SN) of 2 to simulate the existing pavement section, Table B.1. The 18 kip EQAL repetitions for the existing pavement section were calculated for a 10 year period for the four tire/axle configurations. They are listed in Table B.2. Using the design chart for flexible pavements, P_t = 2.0, Figure II-2, "AASHTO Interim Guide for Design of pavement Structures," 1972 [1], it is obvious that any of the configurations would cause severe distress. To evaluate the effects of increased pavement depth, the 18 kip EQAL repetitions for each tire/axle configuration were calculated for a pavement SN of 4, Table B.3., and a pavement SN of 6, Table B.4. These are summarized in Table B.5. A review of this table indicates the complexity of the analysis of tire/axle configurations. The table indicates that changing the single tire tandems to dual tire tandem would result in the least damage for all thicknesses of pavement studied. However, the existing axle configuration would be the worst case only for the condition of a thin pavement as now exists.

To illustrate the effects of a tire/axle configuration on a thicker pavement the 18 kip EQAL repetitions over 10 years were calculated for an SN = 4, which would represent the approximate pavement thickness required. The 10 year 18 kip EQAL repetition are shown in Table B.6. This illustrates how reducing the gross truck loading can actually

result in an increase in 18 kip EQAL repetitions. Case D represents a maximum gross of 97,000 pounds with dual tire single axle replacing the single tire axle loads. This results in a lower 18 kip EQAL per truck, however, an increased number of trucks would be required to move the same amount of rock per day.

Table B.7, shows the approximate overlay that would be required for each of the tire axle configurations. As can be seen, a substantial overlay is required for any of the configurations. If the contractor replaced the single tandems with dual tandems, this would result in a reduction in the required overlay thickness by 20 percent or a savings of approximately $27,000 per mile over a 10 year period.

CONCLUSIONS

1. The contractor is permitted to increase his gross load from 80,000 pounds to 105,500 only by a permit issued by the State Department of Transportation. Ideally, as part of this permit process the state should be able to evaluate the tire configurations which could reasonably be used and specify the configuration which would result in the least damage to the highways.

2. The pavement section on SR 542 is grossly substandard for the truck traffic it is carrying. Thus, it is doubtful if any axle configuration would result in a reduction in the maintenance effort required on this section.

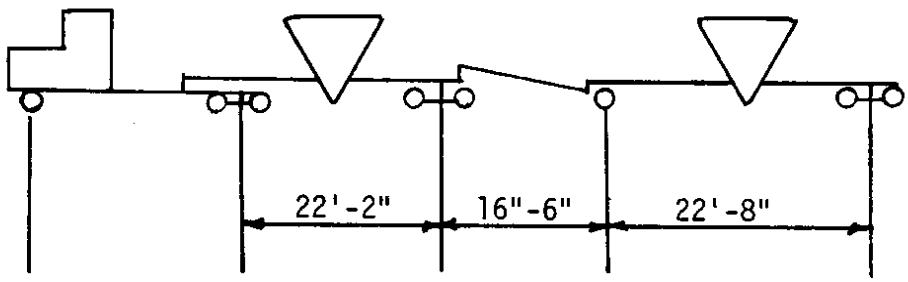

Axle No.	1	2	3	4	5
Tire Size	11.00 x 22.5	11.00 x 22.5	12.00 x 22.5	11.00 x 22.5	12.00 x 22.5
Approx. Axle Load (Kips)	10	27	24	20	24

Configuration

TIRE / AXLE

A. (Existing)

SINGLE / SINGLE — DUAL / TANDEM — SINGLE / TANDEM — DUAL / SINGLE — SINGLE / TANDEM

B. (All single tandems converted to dual tandem)

SINGLE / SINGLE — DUAL / TANDEM — DUAL / TANDEM — DUAL / SINGLE — DUAL / TANDEM

C. (All single tandems converted to dual singles and 20,000 lb axle load exceeded)

SINGLE / SINGLE — DUAL / TANDEM — DUAL / TANDEM — DUAL / SINGLE — DUAL / TANDEM

D. (Single tandems converted to dual singles and 20,000 lb axle load no exceeded) Gross = 97,000 lb

SINGLE / SINGLE — DUAL / TANDEM — DUAL / SINGLE — DUAL / SINGLE — DUAL / SINGLE

Figure B.1. Tire Axle Configuration of the Limerock Trucks

Table B.1. Analysis of 18 Kip Equivalent Axle Repetitions Per Truck Pavement SN = 2 (existing pavement section)

18 Kip Equivalent Axles

Axle Configuration	Axle Number					Truck Total
	1	2	3	4	5	
A	1.05 [1]	.43 [2]	2@1.20 [1]	1.21 [3]	2@1.20 [1]	7.49
B	1.05	.43	.27 [2]	1.21	.27 [2]	3.23
C	1.05	.43	1.66 [3]	1.21	1.66 [3]	6.01
D	1.05	.43	1.21 [3]	1.21	1.21 [3]	5.11

[1] Table 17

[2] Table C2-4 "AASHTO Interim Guide for Design of Pavement Structure"

[3] Table 16

Table B.2. 18 Kip Equivalent Axle Loads Over Ten Years as a Result of Limerock Haul on Existing Pavement, SN ≈ 2

Tire Configuration		18 Kip EQAL in 10 Years
A	90 trucks/day x 5 days/week x 50 weeks/year x 7.49 18 kip EQAL/truck x 10 years	1,685,250
B	90 x 5 x 50 x 3.23 x 10	726,750
C	90 x 5 x 50 x 6.01 x 10	1,352,250
D	100* x 5 x 50 x 5.11 x 10	1,277,500

*Lower gross load/truck

Table B.3. Analysis of 18 Kip Equivalent Axle Repetitions Per Truck Pavement SN = 4

18 Kip Equivalent Axles Per Axle

Axle Configuration	Axle Number					Truck Total
	1	2	3	4	5	
A	.55 [1]	.47 [2]	2@.78 [1]	1.33 [3]	2@.78 [1]	5.47
B	.55	.47	.29 [2]	1.33	.29 [2]	2.93
C	.55	.47	2.16 [3]	1.33	2.16 [3]	6.67
D	.55	.47	1.33 [3]	1.33	1.33 [3]	5.01

[1] Table 18

[2] Table C2-4, "AASHTO Interim Guide for Design of Pavement Structures"

[3] Table 16

Table B.4. Analysis of 18 Kip Equivalent Axle Repetitions Per Truck, Pavement SN ≃ 6

18 Kip Equivalent Axles Per Axle

Axle Configuration	Axle Number					Truck Total
	1	2	3	4	5	
A	.28 [1]	.40 [2]	2@.47 [1]	1.37 [3]	2@.47 [1]	3.93
B	.28	.40	.24 [2]	1.37	.24 [2]	2.53
C	.28	.40	2.37 [3]	1.37	2.37 [3]	6.79
D	.28	.40	1.37 [3]	1.37	1.37 [3]	4.79

[1] Table 19

[2] Table C2-4, "AASHTO Interim Guide for Design of Pavement Structures"

[3] Table 16

Table B.5. 18 Kip EQAL Repetitions Per Truck for Various Tire Configurations and Pavement Structural Numbers

18 Kip EQAL Repetitions Per Truck

Tire Configuration	Pavement Structural Number		
	2	4	6
A	7.49	5.47	3.93
B	3.23	2.93	2.53
C	6.01	6.67	6.79
D	5.11	5.01	4.79

Table B.6. 18 Kip Equivalent Axle Loads for Pavement Rehabilitation, SN ≃ 4

Tire Configuration		18 Kip EQAL in 10 Years
A	90 trucks/day x 5 days/week x 50 weeks/year x 10 x 5.47	1,230,750
B	90 x 5 x 50 x 10 x 2.93	659,250
C	90 x 5 x 50 x 10 x 6.67	1,500,750
D	100* x 5 x 50 x 10 x 5.01	1,252,500

*Additional trucks per day as a result of the lower gross load

Table B.7. Approximate Overlay Required

Tire Configuration	Weighted [1] SN	Pavement Sections [1] ACP		Cost/Mile [2]
		Total Required	Overlay Required	
A	3.8	8.6"	5.6"	$166,320
B	3.4	7.7"	4.7"	139,590
C	3.9	8.9	5.9	175,230
D	3.8	8.6	5.6"	166,320

1 "AASHTO Interim Guide for Design of Pavement Structures" - Regional Factor = 2, P_t = 2.0. Assume: soil support = 4 existing pavement = 3 ACP.

2 Assume: ACP @ $30/ton roadway width = 30'

APPENDIX C

Truck Survey Data

Table C-1. Results of Truck Survey at Weigh Station Near Fife on I-5.

Type	Sample	Axle Load (k)	Tire Size	Tire Pressure (psi)	Tire Width (in)	Contact Length (in)
1	1	5.9 8.4	8.25-20 8.25-20	62 65D	7	
	2	4+ 7+	8.25-20	65 60D		
	3	10 16.3	11-22.5 11-22.5	92 40, 90D	8 1/2	
2	1	6.9 16.8 16.7	10-20 10-20 9x20	80 70D 90D	7 1/2	7 1/2
	2	8.3 12.1 7	10-20 10-20 in 10-20 out 10-22	94 94D (in) 70D (out) 70D	9 8 8	6 1/2
		24 8.3	825-20 9-20 9.5-16.5 9.5-16.5 9.5-16.5	64 74 70 42 63	7 1/4	(#2 w/trailer 0 0 0 0 } trailer 0 0)
3	1	9.5 19.6 15.0	10R20 10R20 11-24.8 11-24.5	96 92D 70D 45D	8 1/2 8 1/4 8 7 1/2	
	2	10 13 17.3	10R20 10R20 11-22.5 11-22.5	106 80D 84D,(80 inside) 60,(no pressure inside) (90 outside / 70 inside \ other side)	8 1/2	
	3	5 14 24	10-20 10-20 10-20 10-20	60 60D 74D 74D	8 1/2	7
6	1	6.5 11.4	10-20 10-20 10-20	64 64D 80D	8 1/2	4 1/2
	2	17.8 27.8	18-22.5	92		
	3		16.5-22.5 10x20	72 80	(concrete mixer 12 1/2 w)	

Note: D = dual tire

Table C-1. Continued

Type	Sample	Axle Load (k)	Tire Size	Tire Pressure (psi)	Tire Width (in)	Contact Length (in)
8	1	11.6	11R22.5	100		9
		31.4	11R22.5	90D		
		31.4	11R22.5	80D		
			11R22.5	94D		
			11R22.5	90D		
	2	5.7	11R24.5	100		
		35.9	11R24.5	70D		
		21.0	11R24.5	80D	8	
			10R22	80D	8	
			10R22	94D	8	
	3	10	10-22ML	110	9 1/2	8
		31.4	10-22ML	95D	9 1/2	8
		41.7	10-22ML	90D		
			10-22	95D	8	8
			10-22	90D	8	9
	4	11.2	11-24.5	85	9	8 1/2
		32.8	11-24.5	80D	8	9
		31.0	11-24.5	90D	8	9
			11R24.5	95D	8 1/2	7
			11R24.5	80D	8 1/2	
	5	12.4	11R24.5	94	8	12
		29.4		D		
		31.2	11R24.5	90D		
			10R22	96D	8	
				(94 inside)		
			10R22	100D		
	6	8	11-22.5	80		
		32	11-22.5	90D	7	9
		31+	11-22.5	70D		
			10-15TR	70D	8	6 1/2
			10-15TR	65D		
	7	7.9	11-22.5	98S		
		29.8	10-20 radial	88D		
		20.7	10R20	106D		
			9R22.5	82D		
			9R22.5	85D		
	8	11.9	11R24.5	104		
		35.6	11R24.5	108D		
		35.1	11R24.5	120D	(lumber truck)	
			11R24.5	100D		
			11R24.5	108D		

Table C-1. Continued

Type	Sample	Axle Load (k)	Tire Size	Tire Pressure (psi)	Tire Width (in)	Contact Length (in)
9	1	9.8	10R22	108	8 1/2	8
		30	10R22	100D		
		19.6	10R22	100D	8 1/2	9
		19.9	10-22	92D		
			10-22	82D	8 1/2	9
	2	10	11R24.5	100	8	9
		33.5	11R24.5	100D	8	
		19.2	11R24.5	100D	8	
		19	11R24.5	100D	8 1/2	
			11R24.5	96D	8 1/2	7
	3	10	11R22.5	114		
		31.8	11R22.5	104D		
		18.5	11R22.5	110D		
		18.1	11R22.5	122D		
			11R22.5	70D (90 other side)		
	4	11.5	12R22.5	98		
		33.1	10R22.5	100D		
		18.4	10R22.5	100D		
		17.3	10R22.5	98D		
			10R22.5	96D		
11	1	10.6	11R24.5	110	8 1/2	9
		15.2	11R24.5	110D	8 1/2	
		14	11R24.5	100D	7 1/2	
		8	11R24.5	90D	7 1/2	5
		9.8	11R24.5	82D	7 1/2	5 1/2
	2	9.8	10-22	96		
		18.5	10-22	90D		
		16.8	10-22	90D		
		16.3	10-22	80D		
		15.4	10-22	90D		
	3	10.3	10-20		8 1/2	9
		19.7	10-20	100D		
		17.9	10-20	80D		
		16.1	10-20	80D		
		17.5	10-20	80D		
	4	9.2	11R22.5	108	(grain truck tandem trailer)	
		20.5	11R22.5	105D		
		21.1	11R22.5	112D		
		19.4	11R22.5	108D		
		20.0	11R22.5	110D		
	12	11	11R22.5	100		
		29.6	11R22.5			
		24.4	11R22.5	98D		
		16.5	12R22.5	112 balloon		
		20.7	12R22.5	114 balloon		
			11R22.5	110 balloon		
			12R22.5	110 balloon		
			12R22.5	60 balloon		

Table C-1. Continued

Type	Sample	Axle Load (k)	Tire Size	Tire Pressure (psi)	Tire Width (in)	Contact Length (in)
16	1	15.4	12R20	130	10	8
		42.8	10-20	96D	8	8
		39.7	10-20	100D		
		17.7	10-20	80D		
			10-20	100D		
			10-20	85D		
	2	12	18-195x	84	14	
		39	11-22	92D		
		27	11R22	94D	8	
		14	10R15	80D	7	
			10x15			
			10x15	86D		
17	1	10.9	11R24.5	100		
		24.9	11R24.5	100D	8	
		20.8	11R24.5	90D	8	
		12.3	11R24.5	104D	7 1/2	6
		13.5	11R24.5	106D	9	
			11-24.5x	62D	7 1/2	
			11R24.5x	112D	9	
	2	11	12R22.5	100		
		25	12R22.5	100D	8	9 1/2
		24	12R22.5	102D	8 1/2	
		19.4	12R22.5	110 balloon		
		19.2	12R22.5	112 balloon	8 1/2	
			10R20	112D		
			10R20	114D	8	10
B train (Canada)	1	10	11R24.5	90		
		26	11R24.5	92		
		19.3	11R24.5	102		
		18.1	11R24.5	76		
			11R24.5	84		
			11R24.5	90		
			11R24.5	88		

Table C-2. Assumed Contact Area and Actual Contact Area Calculation

Load (lbs)	Tire Pressure (psi)	Assumed Contact Area per Tire (in^2)	Actual Tire Width (in.)	Contact Length (in)	Actual Contact Area Per Tire (in^2)
16,700	90D	46.39	7.5	7.5	56.25
8.300	94	44.15	9	6.5	58.5
5,000	60	41.67	8.5	7	59.5
10,000	110	45.46	9.5	8	76
	95D	56.3	8	8	64
41,700	90D	56.35	8	9	72
11,200	85	65.88	9	8.5	76.5
32,800	80D	48.2	8	9	72
	90D	48.2	8	9	72
12,400	94	65.96	8	12	96
9,800	108	45.37	8.5	8	68
10,000	100	50	8	9	72
10,600	110	48.18	8.5	9	76.5
8,000	90D	22.22	7.5	5	37.5
9,800	82D	29.88	7.5	5.5	41.25
15,400	130	59.23	10	8	80
12,300	104D	29.57	7.5	6	45
19,200	114D	42.11	8	10	80

Assumed contact = load/tire pressure
Actual contact area = actual tire width x contact length

Table C-3. Data from I-5 Weigh Station

Truck Type	Axle Load (lbs)	Tire Size	Axle Type	Volts	Deflection ($x10^{-3}$ in.)
1	9,200	11	FS	0.8	1.158
	18,400	11	SD	2.3	3.328
	15,900	10	SD	1.65	2.388
	11,700	10	SD	1.4	2.026
	6,800	10	SD	0.55	0.796
2	9,000	11	FS	1.3	1.880
	14,700	11	TD	2.0	2.894
	11,200	11	TD	1.4	2.026
3	7,400	10	FS	1.65	2.388
	11,500	10	SD	2.05	2.966
4	9,000	11	FS	1.4	2.026
	28,900	11	TD	3.6	5.208
	13,900	11	TD	1.6	2.314
5	11,000	11	FS	2.9	4.196
	27,500	11	TD	3.7	5.354
	14,300	11	TD	2.0	2.894
6	12,000	11	FS	1.2	1.736
	34,200	11	TD	3.3	4.774
	25,800	11	TD	2.3	3.328
7	9,500	11	FS	4.6	6.656
	17,500	11	SD	3.9	5.642
	17,900	11	SD	3.9	5.642
	14,100	11	SD	3.2	4.630
	14,100	11	SD	3.0	4.34
8	8,700	10	FS	1.1	1.592
	8,600	10	SD	1.7	2.46
	8,800	10	TD	0.8	1.158

FS: Front single axle with single tire

SD: Single axle with dual tire

TD: Tandem axle with dual tire

Table C-3. Continued

Truck Type	Axle Load (lbs)	Axle Type	Tire Size	Volts	Deflecting ($x10^{-3}$ in.)
10	11,700	FS	10	2.1	3.038
	34,000	TD	11	4.6	6.656
	32,000	TD	11	4.6	6.656
12	10,700	FS	11	2.2	3.184
	31,900	TD	11	4.6	6.656
	28,100	TD	11	3.6	5.208
	28,100	TD	11	3.5	5.064
	10,600	FS	11	2.0	2.894
	29,900	TD	11	3.9	5.642
	30,200	TD	11	4.0	5.788
	28,800	TD	11	3.6	5.208
14	12,500	FS	11	1.6	2.304
	33,400	TD	11	4.4	6.366
	19,200	SD	11	4.2	6.076
	18,900	SD	11	3.9	5.642
15	9,400	FS	10	1.5	2.170
	17,000	TD	10	2.2	3.184
	10,300	TD	8.25	1.3	1.880
	8,000	FS		1.0	1.446
	12,800	SD	8.25	2.65	3.836
19	8,800	FS	10	1.8	2.604
	14,300	TD	10	1.8	2.604
	19,700	TD	10	2.7	3.906
	11,100	SD	10	2.7	3.906
	17,900	TD	10	2.6	3.762
20	9,200	FS	11	1.3	1.880
	31,300	TD	10 11	4.4	6.366
	23,800	TD	11	3.4	4.920
21	14,100	FS	15	2.5	3.618
	28,700	TD	10	4.3	6.222
	16,200	SD	11	2.8	4.052

Table C-3. Continued

Truck Type	Axle Load (lbs)	Tire Size	Axle Type	Volts	Deflecting ($x10^{-3}$ in.)
22	11,300	11	FS	1.9	2.750
	17,600	11	SD	3.4	4.920
23	11,000	11	FS	4.1	5.932
	33,900	11	TD	4.35	6.294
	31,200	11	TD	4.35	6.294
26	5,100	10	FS	0.7	1.012
	11,100	8.25	SD	2.6	3.762
27	11,600	11	FS	4.0	5.788
	27,600	11	TD	3.85	5.570
	26,300	11	TD	3.85	5.570
29	12,000	11	FS	1.7	2.460
	33,500	11	TD	4.4	6.366
	20,200	11	SD	4.6	6.656
	19,800	11	SD	3.8	5.498
30	10,300	11	FS	2.0	2.894
	28,200	11	TD	4.3	6.222
	19,900	11	TD	2.8	4.052
31	10,600	11	FS	1.9	2.750
	34,400	11	TD	4.9	7.088
	31,600	11	TD	4.5	6.510
33	10,900	12	FS	1.4	2.026
	29,300	11	TD	4.6	6.656
	9,000	11	SD	1.9	2.750
	9,000	11	SD	2.0	2.894
34	8,500	11	FS	0.9	1.302
	10,500	11	TD	1.3	1.880
	5,500	11	SD	0.8	1.158
	5,300	11	SD	0.8	1.158
	6,400	11	SD	0.9	1.302
35	10,400	11	FS	1.6	2.314
	21,300	11	TD	2.9	4.196
	12,500	11	SD	2.9	4.196

Table C-3. Continued

Truck Type	Axle Load (lbs)	Axle Type	Tire Size	Volts	Deflecting ($x10^{-3}$ in.)
35	13,300	SD	11	2.8	4.052
36	9,600	FS	11	1.5	2.170
	21,800	TD	11	2.9	4.196
	17,200	TD	11	2.1	3.038
	7,600	SD	11	1.6	2.314
	11,700	TS	11	1.75	2.532
37	9,700	FS	11	1.4	2.026
	27,000	TD	10	3.9	5.642
	13,000	SD	10	2.25	3.256
	15,500	SD	10	3.4	4.920
38	11,400	FS	13	1.8	2.604

Figure C-1. Truck Types Used in the Truck Survey.

1.

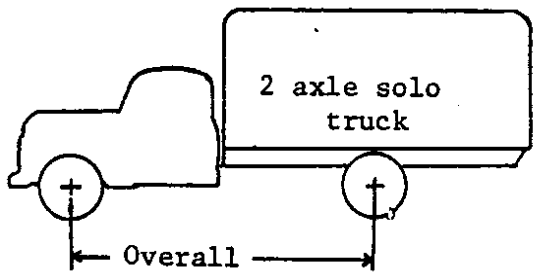

2.

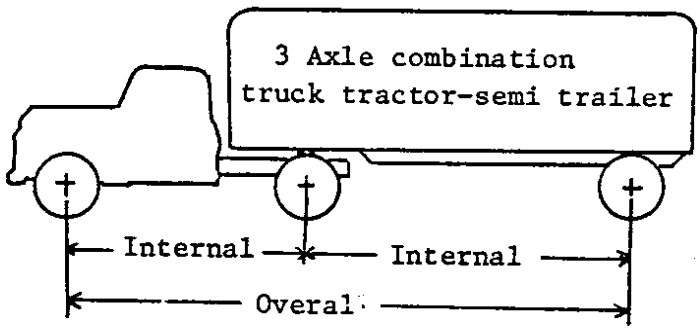

3.

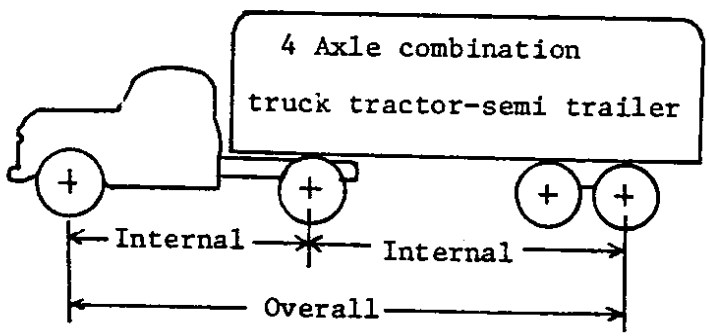

4.

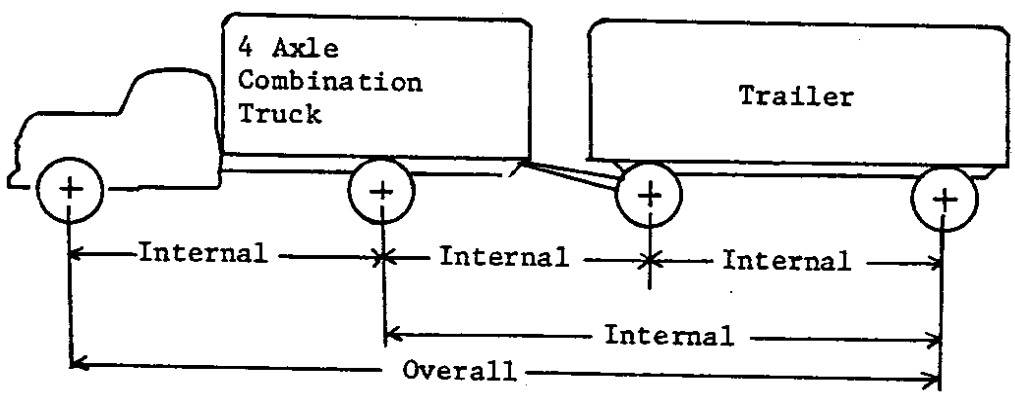

5.

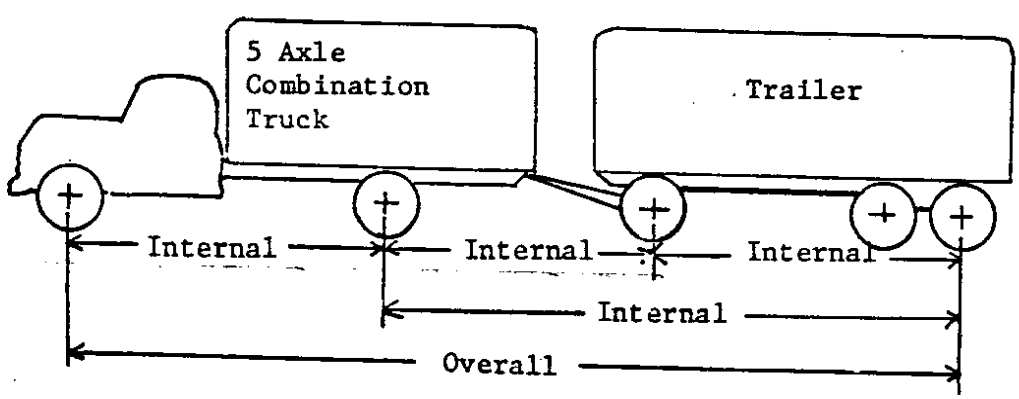

Figure C-1. Continued

6.

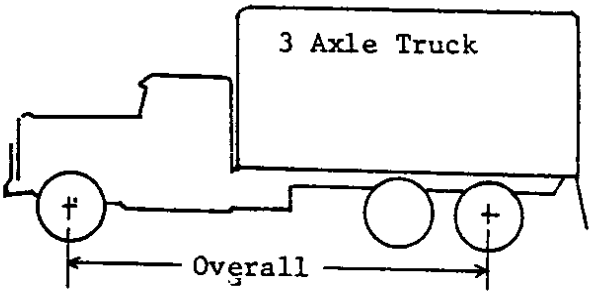

7.

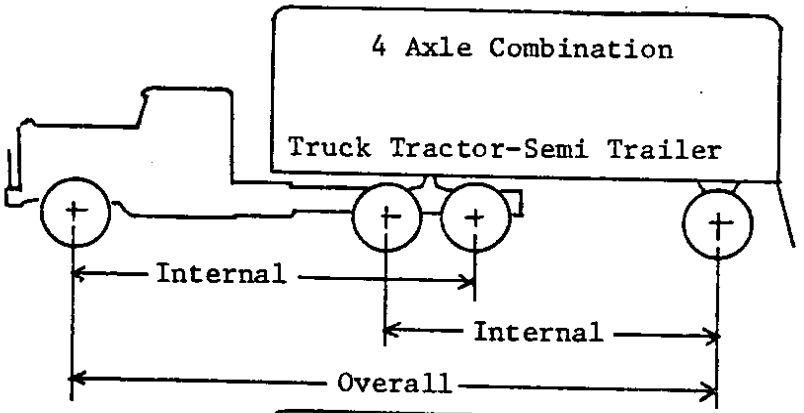

8.

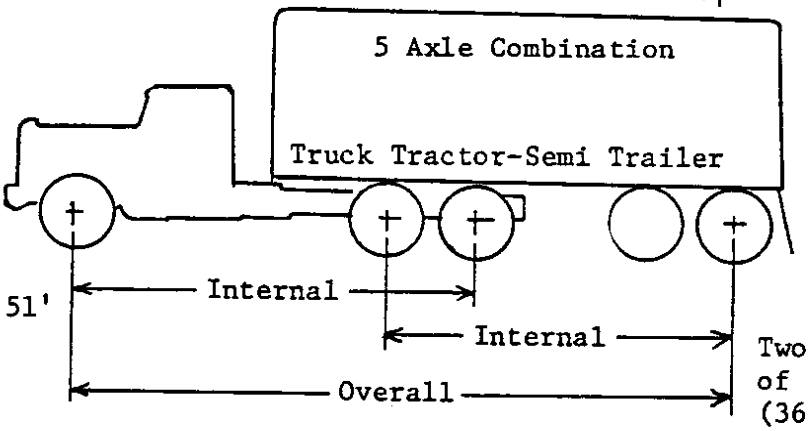

Overall wheelbase of 51' allows 80,000 lbs determined by tire size steering axle

Two consecutive groups of tandem axles (36' allows 68,000 lbs)

9.

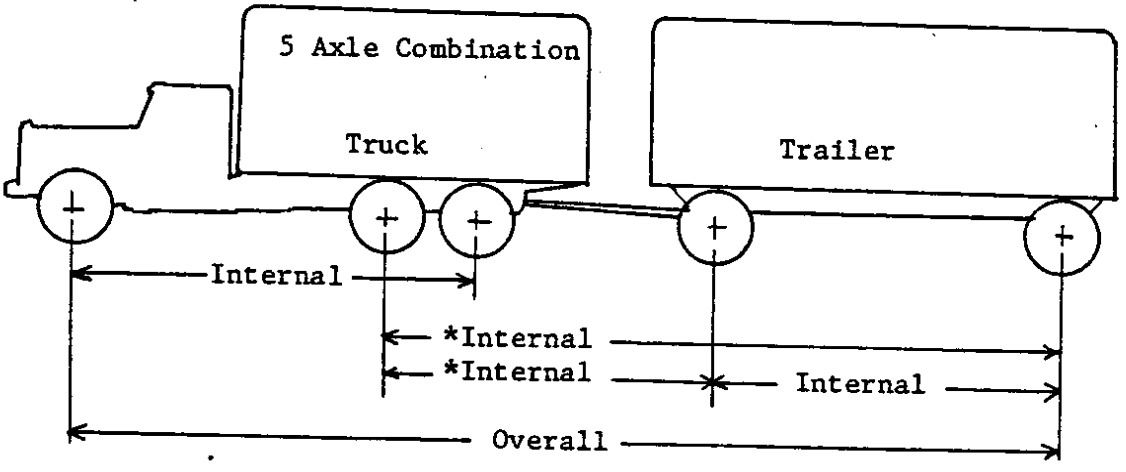

Figure C-1. Continued

10.

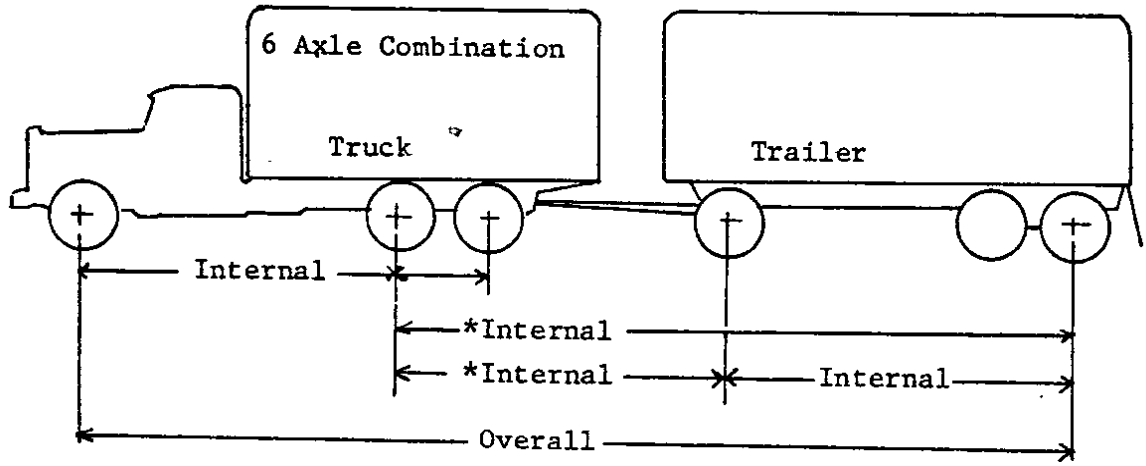

*Indicates the critical measurements

11.

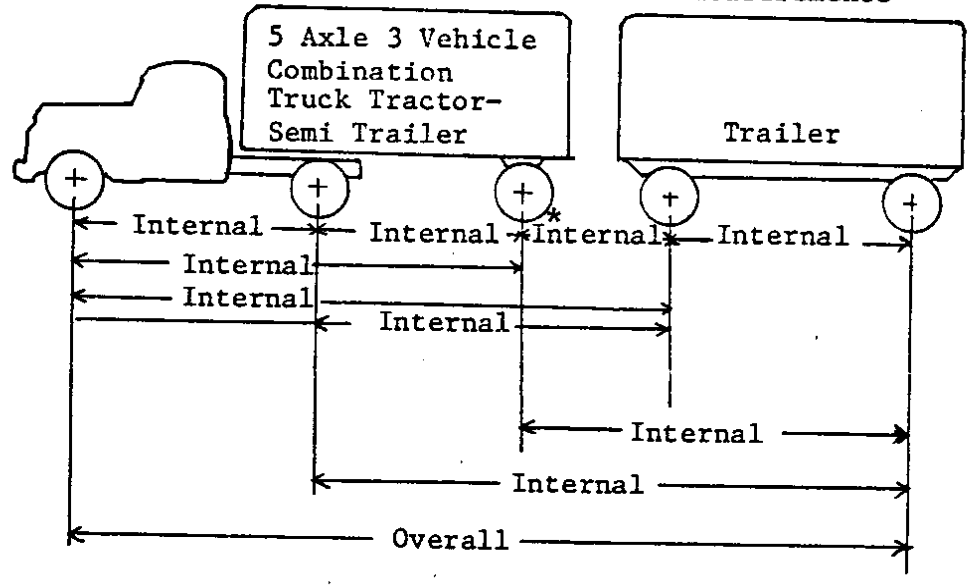

*Indicates the critical measurement

12.

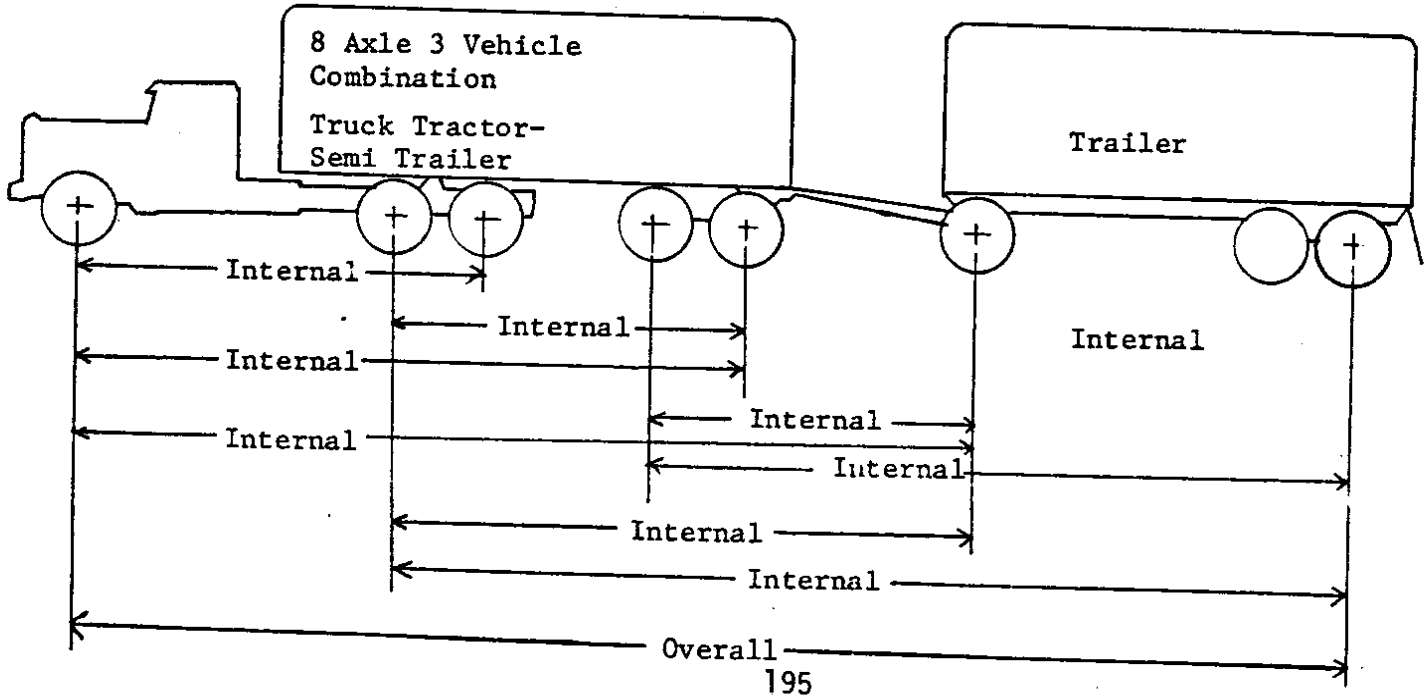

Figure C-1. Continued

13.

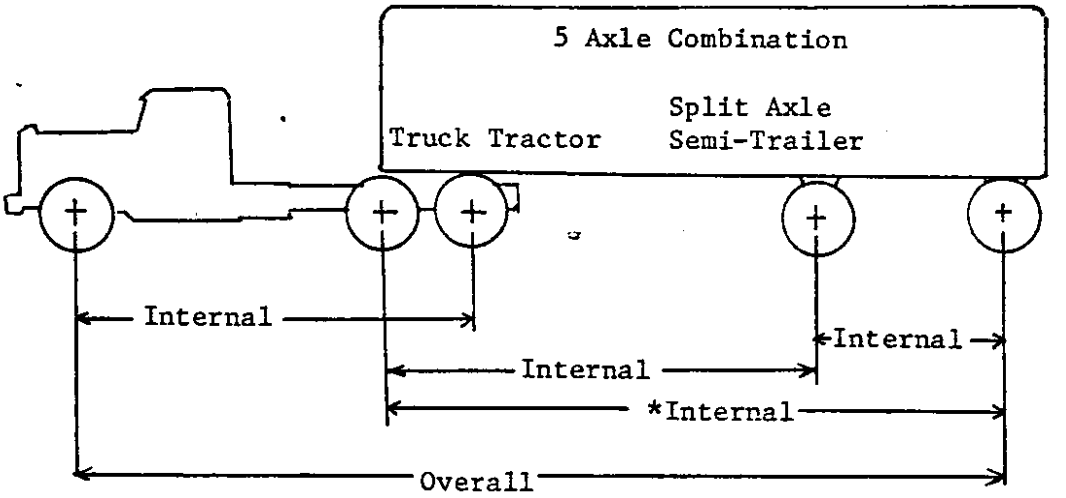

* Indicates the critical measurement

14.

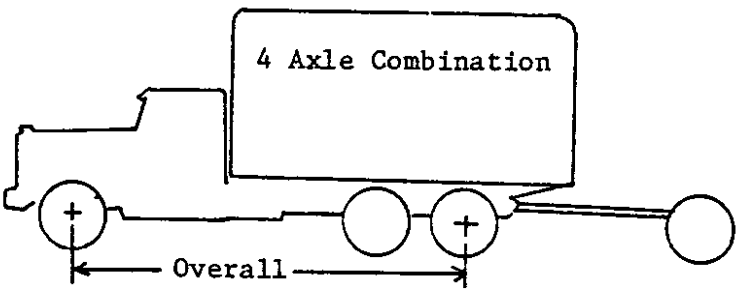

15.

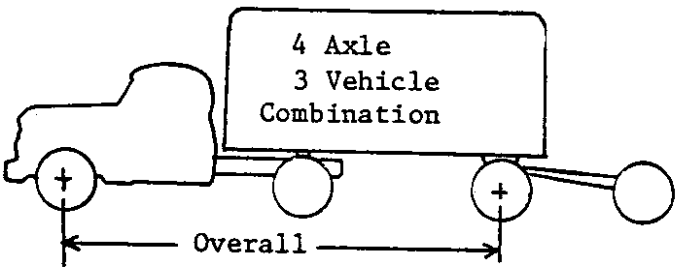

Vehicles towing a dolly axle not designed to support an appreciable part of the load will not be included in the wheelbase measurement for gross combination weight purposes.